UNIVERSITY OF UDINE

DOCTORATE COURSE IN

CIVIL AND ENVIRONMENTAL ENGINEERING AND ARCHITECTURE

XXVIII Cycle

PH.D. THESIS

CONTRIBUTION OF GEOMATIC MODELS TO STRUCTURAL ENGINEERING

Ph.D. Candidate

Ing. ANNA SPANGHER

Tutor

Prof. DOMENICO VISINTINI

Academic Year 2014/2015

To Giulio

INDEX

INTRODUCTION

The main purpose of this PhD thesis can be summarized with the sentence "which could be the possible contribution of *geomatic models* to *Structural Engineering*". It results that, beyond mechanical and costitutive characteristic of the object, the knowledge of *geometry* is as well necessary for the definition of the structural parameters required for analysis. However, contrary to what it could be expected, most of geometric models used for structural analysis are really simple, since are often developed starting from existing plants and sections, obtained from direct surveying, and therefore poor of details. This simplification is acceptable for the largest part of modern constructions, because of their regularity and symmetry, but is not recommended for buildings and objects belonging to cultural heritage, which present much more complex geometries. As well known, for this kind of structures, it is possible to operate by means of *geomatic* surveying, so obtaining realistic 3D models that reproduce geometry in high accuracy and detail. These techniques are nowadays used in many fields, but are not so frequently applied for Structural Engineering. Probably, this lack of connection between the two disciplines is due to the fact that as much Geomatics seeks precision as much Structural Analysis tries to simplify. The goal of this research is therefore trying to find a meeting point between models realized through Geomatics and that ones used for Structural Analysis.

Once declared that Geomatics can supply to Structural Analysis, with its geometric models, it will be necessary to find a method to make these models usable for that purpose, since generally they need indeed further elaborations, before being used in structures software. In order to define the best way to obtain this scope, three sizes of structural elements, along with their surveying and modeling issues, will be examined. In particular, small objects will be represented by statues, medium objects by an arch and large objects by a building.

These three classes have completely different own characteristics for surveying and data elaborations: therefore, first and foremost, it will be necessary to define an *operative procedure*, common for all the situations, even if slightly differently developed for each case, since a complete standardization is hard to achieve.

Second goal will be therefore to obtain models that can be "much more possible directly" analysed by structural software: from the topological point of view this possibility is guaranteed only with closed *3D solid models*. All the procedures for transforming surface models to solid ones were thus analysed and used, focalizing particularly on reverse engineering methodologies.

Following challenge will consist in finding the correct *Level of Detail* of the models, in order to represent faithfully the object, without loosing important information, but also in a way that could be adapt for structural purposes.

Final goal is the performing of the Structural Analysis on so built models and the interpretation of the obtained results.

Besides the models achieved by means of Geomatics, also simplified and hypothetical models were created, in order to investigate the existing differences from the geometrical, and consequently structural point of view.

Concluding, the thesis is developed in a first theoretical and general part, a central practical part on the case of study and, finally, in a summarizing part where all the results are compared and analysed.

The structure of the thesis is the following:

Chapter 1 Introduces the concept of *data recording*, referred to cultural heritage, highlighting its importance for the correct design of its *preservation*. Among all the data useful for documenting, this thesis is focalised on *geometrical data*, and, especially, to those ones obtained by Geomatics, that could contribute to the structural analysis of the objects. Therefore, main documents and resolutions concerning geometrical data recording are listed and quickly examined. Afterwards, current trends of 3D geomatic techniques are described, focusing on laser scanning surveying, which is the methodology used in this research. The pipeline for processing data, from point clouds to 3D models, is defined and then followed throughout the thesis, as *operating procedure*. A quick view is given on the software used for data modeling and to their main functions. Finally some example on current trends of Geomatics surveying and modeling, specifically devoted to cultural heritage, are reported.

Chapter 2 Deals with main notions on structural engineering referred to *masonry buildings*, or stone artefacts, belonging to cultural heritage. The legislative scenario in force in Italy is outlined, with particular attention to the necessity of correctly defining geometry, since from it depends the consistency of the so called "confidence factor" of the analysed structures. The behaviour of masonry buildings is therefore explained, as well as the problematic in its structural modeling, in order to understand which computational approach could be adopted for the structural analysis onto the geometrical models. *Finite Elements Method* resulted the most convenient for the purposes of this research and, therefore, was shortly described, together with the Finite Elements Analysis software used in this thesis and some practical examples.

Chapters 3 Along with the following two chapters, it deals with practical experimentation carried out. First and foremost the small size objects were afforded: main characteristic of the problems and specific standards for these case are examined, as well as the current geomatic trends on this specific problematic, through some example found in literature. Two cases are then considered: the first one relates to the Statue of Emperor Claudio, preserved in Aquileia, and surveyed by *Terrestrial Laser Scanner*, the second one is the Statue of St. John Baptist, preserved in the Bargello Museum in Florence, and surveyed with a particular system called "*Close Range Laser Scanner*". The procedures adopted for obtaining 3D solid models, mandatory for structural analysis, are minutely described, as well as the

obtained results. Two virtual models of the statue of Emperor Claudio were also constructed, in order to define which could have been the structural analysis results with other geometry statue conditions.

Chapter 4 Deals with the medium size object case. After an introduction focusing on general problematic of these typologies of objects, some examples are described. Bollani Arch, realized in Udine by Palladio, represents the practical case. Among all the studied cases, this was the simplest geometrical model, because of the rather regular shape, if compared to the statues, and the limited dimension, if compared to the building. The modeling process was described, according to the pipeline defined in chapter 1. Another model was realized, starting instead from the geometrical data of a direct surveying. Both the models obtained were analysed and compared with two different software. The problem of the geometrical and structural *Level of Detail* is presented and deeply analysed.

Chapter 5 Last practical case is given by the large size object. Also in this thesis part, some existing examples are described, before dealing with the structural analysis of the building, which is the Baptistery of Aquileia. Similarly to the two previous chapters, the procedure for obtaining the 3D solid model was described, following the same pipeline defined in the first chapter. Also in this case, a 3D simple model of the building was realized starting from the measures obtainable by direct surveying. The two different detailed models were firstly compared in geometry and subsequently structurally analysed.

Chapter 6 This last chapter collects and compares all the results and the analysis obtained from the study of the four objects described in chapter 3, 4 and 5. Starting from the data on geometry and following the same pipeline, all the most important values are listed, referring to surveying characteristic for data acquisition, procedures for data elaborations and meshing and, finally, meshing refinement, in order to obtain 3D surfaces models. Data on structural analysis are therefore summarized, highlightening the difference obtained using different models.

Conclusions of this work relates with some final considerations on the research, outlining the open questions and the future goals to achieve with upcoming work.

At the end of each chapter, the bibliographic references, referring exclusively to the same chapter, and therefore related to the specific aspects of each one are outlined.

1. 3D RECORDING FOR CULTURAL HERITAGE

1.1. Introduction

The importance of documenting and, subsequently, recording data, referred to cultural and natural heritage, is well internationally recognized and has been argument of discussions and researches since the *theory of restoration and conservation* has begun to take hold. This concept of "*data recording*" implies, of course, a preliminary study of the object of interest, in the broadest sense of the term: hence the study of all aspects affecting the object itself, such as geometry, materials, history, interactions with the outside world, events that interested it, etc.

As a prerequisite for a conscious conservation, recording is a prime responsibility of everybody involved in conservation processes. All those interested in the understanding, the care, and the management of a heritage place must have access to existing data and, consequently, will generate further information, which must be preserved and made available to others. It is the task of heritage managers and decision makers to establish policies and programs for the correct recording and effective management of conservation-related information (Letellier, 2007);

The six phases of the *Built Heritage Conservation* process revolves, as logical, around the concept of *recording* (*Figure 1.1*) and are defined in the so-called "Guiding Principles of Letellier" as follow:

1. Initiation — This phase involves understanding the situation in which the work will take place and clearly defining the problem. The types of documents gathered during this phase include past project files, reports of previous surveys or conservation interventions, existing representations and site models, current heritage listing or designation, real estate and zoning information, newspaper clippings and so on.

2. Assessment — It is usually divided into three major activities:
   - assessing the significance of the place;
   - assessing its physical condition;
   - assessing the current management system.

   The types of records produced during this phase include more accurate drawings and photographs, thematic maps, condition reports, and "topographic" measures (as defined by the author in this encrypted way), scientific investigation data, historical and archaeological analysis, environmental conditions, analysis of samples, reports on tests for security, safety, and conservation materials or systems.

3. Options — It is the phase when fundamental choices for conservation are taken. The types of records generated during this phase may include

	"detailed drawings" and photographs, recording the as-found condition, 3D models, experts' reports, cost estimates, work schedules, videos, and notes from public participation sessions.
4. Project development	During this phase, professionals "prepare drawings", specifications, detailed budgets and work schedules, and other legal documents for the conservation project according to the selected option. These documents usually become the contract basis for tendering the work and for borrowing or committing the financial resources necessary.
5. Implementation	It is the step at which the project activities are actually carried out. The types of records generated during this phase include on-going recording, as-built records and drawings, photographs documenting different treatment stages, photos of new discoveries, project diaries, work progress reports, maintenance manuals, deficiencies lists, electronic data of all kinds, and samples of conservation materials.
6. Operation	It is the phase in which the object turns to life: a life cycle maintenance program is set in place. This phase generates on-going operational, monitoring, and maintenance activities.

The reported definitions are generalized since they are referred to all those branches of knowledge involved in preservations and, therefore, are not really specific, but play the role of heritage information up.

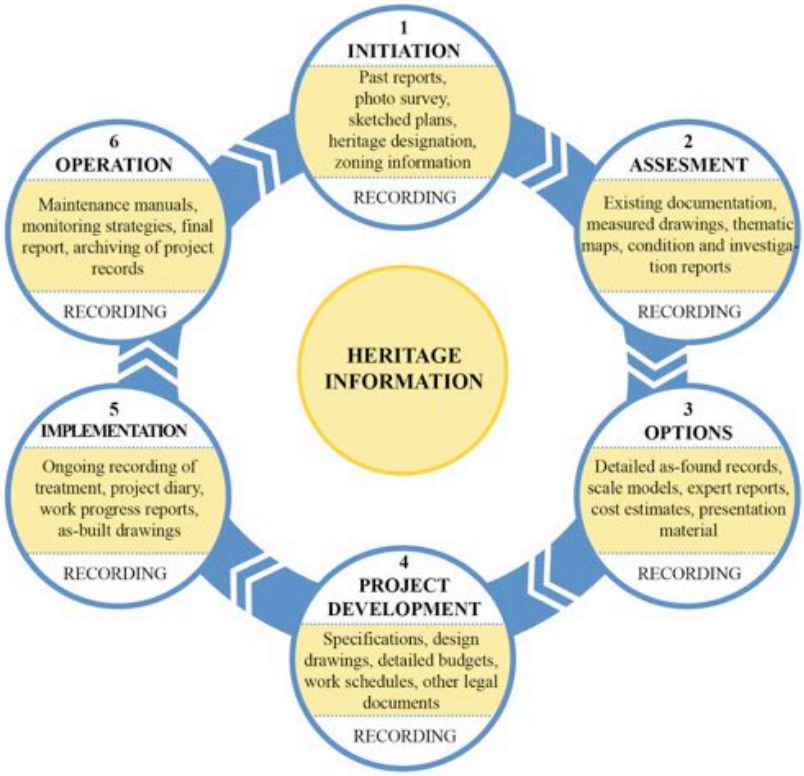

Figure 1.1 - Diagram showing the conservation process and related project information activities (Letellier, 2007).

As already specified in the introduction, the main interest of this thesis is related to the *geometric recording* of the objects, carried out with the most modern techniques offered by Geomatics, and its contribution to the definition of a geometrical level of detail, adopted for structural analysis purposes. Surveying technologies have evolved over time starting from the direct surveying, realized with manual measurements, and arriving to the most modern techniques of automatic 3D data acquisition. Beside the level of technology achieved, surveying always had close synergy with archaeology, architecture and all those disciplines related to the study and preservation of cultural heritage. Therefore, as techniques got more advanced, also rose an increasing pressure to document and preserve heritage digitally. The continuous development of new sensors, data capture methodologies, and multi-resolution 3D representations, and the improvement of existing ones, can contribute significantly to the 3D documentation, conservation, and digital presentation of heritages and to the growth of the research in this field (Remondino & Rizzi, 2010).

In this first chapter of the thesis, it is therefore intended to give, first of all, a quick view over the documents, the conventions and the Italian laws related to the concept of preservation of cultural heritage. To this goal, paragraph 1.2 deals especially on the connection between these writings and data recording, and principally to geometric data. Hence, paragraph 1.3 will be dedicated on the geomatic surveying techniques used for the case of studies of this thesis. Paragraph 1.4 will give a first quick glance to the software used, remanding for a specific description of the commands and algorithm used to the following chapters and specific cases. Finally, paragraph 1.5 will be concerted on some case of application of geomatic surveying of cultural heritage present in literature.

The chapter is therefore structured as follows:

- the importance of surveying for cultural heritage (1.2);
- current trends of 3D geomatic surveying techniques (1.3);
- the 3D modeling and the software used (1.4);
- the recording with 3D geomatic surveying techniques: some example (1.5).

1.2. Importance of surveying for cultural heritage

1.2.1. Basic concepts about preserving cultural heritage

Preservation of cultural heritage is a relatively young discipline, which has its roots, as much in modern historical research, as in traditional maintenance practices, aimed to preserve an object, to which it is recognized a *Value*, be it artistic, economical or of memory loss.

The respect towards cultural heritage has its origins back in the era of the Renaissance, even if the matter was not treated scientifically. It is only from the eighteenth century that, from the first conceptions of a restoration, it rose the relevance of the aspects related to the historical and material characterization of the works. This interest produced even some innovative intervention, like the ones on the southern buttress of the Coliseum in Rome, by Raffaele Stern in 1806, and the one on the Arch of Titus in Rome, by Giuseppe Valadier in 1819. In the second half of the century started a dispute on the methods and concepts of restoration, whose principal exponent were the French architect Eugene Viollet-Le-Duc and the English intellectual John

Ruskin. The first theorized the so-called "stylistic restoration", which aims to bring a building to a stylistic unity, giving it an appearance that could never had in the past ("*restore a building means to restore it in a state of integrity which could never existed*"). The second theorist was instead completely against the idea to re-built or invent part of the ruins and therefore promoted the "romantic restoration", which actually aimed the conservation of the ruins in the same state they reached in that moment, hence a mere consolidation. At the end of the same century, the Italian Luca Beltrami proposed a new theory based on the ideas of Viollet-Le-Duc, as it concerns the integration on the object to restore, but with the commitment that any addiction would respect the history and the research done on the object. The idea of a previous survey and recording of data starts to appear in the studies about restoration.

A "revolutionary" position was proposed, some decades later, by the Italian Camillo Boito, who, as a theoretical, gave importance to the documentary value of the works and therefore, to the respect of the existing state of the object, thinking it important to minimize the rebuilding, which, moreover, must always be recognizable. This theory is famous as "philological restoration" and was proposed at the Congress of Italian engineers and architects held in Rome in 1883. Such views represent the beginnings of critical restoration, later sanctioned by Cesare Brandi, who were established in the Italian Chart of Restoration of 1932.

Over the decades, international organizations and agencies have passed resolutions concerning the obligation for protection, conservation and restoration of monuments. The first main documents and resolutions in which the need for documentation of the monuments is also stressed, as part of their protection, study and conservation are:

- the Athens Convention of 1931 (1.2.2);
- the Hague Convention of 1954 (1.2.3);
- the Chart of Venice of 1964 (1.2.4);
- the Italian Chart of Restoration of 1972 (1.2.5).

UNESCO (United Nations Educational, Scientific and Cultural Organization), which Constitution date back to November 4th, 1946, and the Council of Europe have formed specialized organizations in order to reach this goal, the most important of them is ICOMOS (International Council for Monuments and Sites) but also CIPA (International Committee for Architectural Photogrammetry), ISPRS (International Society for Photogrammetry & Remote Sensing), ICOM (International Council for Museums), ICCROM (International Centre for the Conservation and Restoration of Monuments) and UIA (International Union of Architects) are all involved in this task (Georgopoulos & Charalambos, 2004).

The mission of ICOMOS is to promote the conservation, protection, use and enhancement of monuments, building complexes and sites. Its creation in 1965 is the logical outcome of the first interviews as architects, historians and international experts have begun early in the twentieth century and that had materialized in the adoption of the Chart of Venice in 1964. In light of numerous studies, conferences, symposia and discussions led by its National Committees and International Scientific Committees, ICOMOS has gradually built through philosophical and doctrinal heritage internationally (ICOMOS, 2015).

During the decades the new technologies supplanted the traditional methodologies of recording and starting from the nineties it became increasingly important to create a

standardization of the "recording strategies". This held to the definition of two distinct documents:

- the ICOMOS Principles for the Recording of Monuments, Groups of Buildings and Sites of 1996 (1.2.6);
- the UNESCO Chart on the Preservation of the Digital Heritage of 2003 (1.2.7).

Italy had always been, by virtue of its vast cultural heritage, one of the most advanced countries for what concerns the studies and the theory of preservation and conservation but, as regards the legal field, it is not possible to assume that the current laws are in step with the times. The decree that regulates the field of cultural heritage and landscape in Italy is the so-called "*Urbani Code 42/2004*" (1.2.8), from the Minister that promoted it. On one side it has the merit to be the first organic collection of the numerous laws and articles that regulated this subject before, but, on the other side, it has been fully criticised from the cultural sphere for the centralization of functions related and the liberalization of the management and also because of the long approval process, has failed to implement the latest standards and therefore was born as an outdated law.

1.2.2. The Athens Convention of 1931

The Athens Convention is the first Chart for the Restoration of Historic Monuments and consists in a seven-point manifesto (First International Congress of Architects and Technicians of Historic Monuments, 1931) also called "*Carta del Restauro*":

The seven main resolutions were therefore:

1) international organisations for restoration on operational and advisory levels are to be established;
2) proposed restoration projects are to be subjected to knowledgeable criticism to prevent mistakes which will cause loss of character and historical values to the structures;
3) problems of preservation of historic sites are to be solved by legislation at national level for all countries;
4) excavated sites which are not subject to immediate restoration should be reburied for protection;
5) modern techniques and materials may be used in restoration work;
6) historical sites are to be given strict custodial protection;
7) attention should be given to the protection of areas surrounding historic sites.

1.2.3. The Hague Convention of 1954

The Hague "Convention for the Protection of Cultural Property in the Event of Armed Conflict" is an international treaty that requires its signatories to protect cultural property in war. It was signed at The Hague, Netherlands, on May 14th, 1954, and entered into force in August 7th, 1956. As now, it has been ratified by 126 states (UNESCO, 1954).

The convention defines a protective sign (Article 16) to facilitate the identification of protected cultural property during an armed conflict. Following the Second World War, UNESCO adopted the Hague Convention (1954), which created rules to protect cultural goods

during armed conflicts. This Convention was the first international treaty aimed at protecting cultural heritage in the context of war, and which highlighted the concept of common heritage and led to the creation of the International Committee of the Blue Shield (ICBS). The convention promotes the recording of all the data related to the cultural heritage of the different states and therefore the collection of all the documents and information, also geometrical, of the various objects.

1.2.4. The Venice Chart of 1964

The Venice Chart for the Conservation and Restoration of Monuments and Sites is a code of professional standards that gives an international framework for the conservation and restoration of ancient buildings. The committee aimed to provide principles to guide the preservation of the historic buildings (Erder, 1977).

The Chart is made of sixteen articles, among them, as it regards the concept of recording of data and documenting, the most important is the following:

ARTICLE 16:
In all works of preservation, restoration or excavation, there should always be precise documentation in the form of analytical and critical reports, illustrated with drawings and photographs. Every stage of the work of clearing, consolidation, rearrangement and integration, as well as technical and formal features identified during the course of the work, should be included. This record should be placed in the archives of a public institution and made available to research workers. It is recommended that the report should be published.

1.2.5. The Italian Chart of Restoration of 1972

The Italian Chart of Restoration, was promulgated with Circular No. 117 of April 6th, 1972 by the Ministry of Education, in order to achieve uniform standards in the specific activity of the administration of antiquities and fine arts in the field of conservation of the artistic heritage.

These rules are preceded by a short report and followed by four separate reports containing instructions for:

- Annex a) "The protection and restoration of antiquities";
- Annex b) "The conduct of the architectural restoration";
- Annex c) "The execution of the restoration of painting and sculpture";
- Annex d) "The protection of city centres".

The article more interesting for the scope of this thesis is:

ARTICLE 8:
… any intervention should be previously studied and justified in writing and its progress will be kept a journal, which will be followed by a final report, with photographic documentation before, during and after surgery. All the research and analysis done possibly with the aid of physics, chemistry, microbiology and other sciences will also be documented. Of all these documents will be kept in the archive copy of the Superintendent competent and another copy

sent to the Central Institute of Restoration. In the case of cleaning operations, possibly in a liminal zone made, it must be kept a sample of the stadium prior to the intervention, while in the case of added, removed parts will possibly be stored or documented in a special archive-filing of competent Superintendents.

1.2.6. The ICOMOS Principles for the Recording of Monuments, Groups of Buildings and Sites of 1996

The XI ICOMOS General Assembly in Sofia has ratified the ICOMOS Principles for the Recording of Monuments, Groups of Building and Sites, in October 1996. The aim of the document is *to set out the principal reasons, responsibilities, planning measures, contents, management and sharing considerations for the recording of the cultural heritage* because:

- cultural heritage is an unique expression of human achievement;
- cultural heritage is continuously at risk;
- recording is one of the principal ways available to give meaning, understanding, definition and recognition of the values of the cultural heritage;
- the responsibility for conserving and maintaining the cultural heritage rests not only with the owners, but also with conservation specialists and the professionals, managers, politicians and administrators working at all levels of government, and public;
- article 16 of the Chart of Venice requires it as essential that responsible organisations and individuals record the nature of the cultural heritage.

The document is divided in the six following section, that are here entirely reported since they are the most complete document about recording of data in cultural heritage currently existing:

DEFINITIONS OF WORDS USED IN THIS DOCUMENT:

Cultural Heritage refers to monuments, groups of buildings and sites of heritage value, constituting the historic or built environment.

Recording is the capture of information, which describes the physical configuration, condition and use of monuments, groups of buildings and sites, at points in time, and it is an essential part of the conservation process.

Records of monuments, groups of buildings and sites may include tangible as well as intangible evidence, and constitute a part of the documentation that can contribute to an understanding of the heritage and its related values.

THE REASONS FOR RECORDING

1) the recording of the cultural heritage is essential:
   a. to acquire knowledge in order to advance the understanding of cultural heritage, its values and its evolution;
   b. to promote the interest and involvement of the people in the preservation of the heritage through the dissemination of recorded information;
   c. to permit informed management and control of construction works and of all change to the cultural heritage;

d. to ensure that the maintenance and conservation of the heritage is sensitive to its physical form, its materials, construction, and its historical and cultural significance.

2) recording should be undertaken to an appropriate level of detail in order to:
   a. provide information for the process of identification, understanding interpretation and presentation of the heritage, and to promote the involvement of the public;
   b. provide a permanent record of all monuments, groups of buildings and sites that are to be destroyed or altered in any way, or where at risk from natural events or human activities;
   c. provide information for administrators and planners at national, regional or local levels to make sensitive planning and development control policies and decisions;
   d. provide information upon which appropriate and sustainable use may be identified, and the effective research, management, maintenance programmes and construction works may be planned.
3) recording of the cultural heritage should be seen as a priority, and should be undertaken especially:
   a. when compiling a national, regional, or local inventory;
   b. as a fully integrated part of research and conservation activity;
   c. before, during and after any works of repair, alteration, or other intervention, and when evidence of its history is revealed during such works;
   d. when total or partial demolition, destruction, abandonment or relocation is contemplated, or where the heritage is at risk of damage from human or natural external forces;
   e. during or following accidental or unforeseen disturbance which damages the cultural heritage;
   f. when change of use or responsibility for management or control occurs.

RESPONSIBILITY FOR RECORDING

1) the commitment at the national level to conserve the heritage requires an equal commitment towards the recording process.
2) the complexity of the recording and interpretation processes requires the deployment of individuals with adequate skill, knowledge and awareness for the associated tasks. It may be necessary to initiate training programmes to achieve this.
3) typically the recording process may involve skilled individuals working in collaboration, such as specialist heritage recorders, surveyors, conservators, architects, engineers, researchers, architectural historians, archaeologists above and below ground, and other specialist advisors.
4) all managers of cultural heritage are responsible for ensuring the adequate recording, quality and updating of the records.

PLANNING FOR RECORDING

1) before new records are prepared, existing sources of information should be found and examined for their adequacy.
   a. the type of records containing such information should be searched for in surveys, drawings, photographs, published and unpublished accounts and descriptions, and related documents pertaining to the origins and history of the building, group of buildings or site.

It is important to search out recent as well as old records;

b. existing records should be searched for in locations such as national and local public archives, in professional, institutional or private archives, inventories and collections, in libraries or museums;

c. records should be searched for through consultation with individuals and organisations who have owned, occupied, recorded, constructed, conserved, or carried out research into or who have knowledge of the building, group of buildings or site.

2) arising out of the analysis above, selection of the appropriate scope, level and methods of recording requires that:

a. the methods of recording and type of documentation produced should be appropriate to the nature of the heritage, the purposes of the record, the cultural context, and the funding or other resources available. Limitations of such resources may require a phased approach to recording. Such methods might include written descriptions and analyses, photographs (aerial or terrestrial), rectified photography, photogrammetry, geophysical survey, maps, measured plans, drawings and sketches, replicas or other traditional and modern technologies;

b. recording methodologies should, wherever possible, use non-intrusive techniques, and should not cause damage to the object being recorded;

c. the rationale for the intended scope and the recording method should be clearly stated;

d. the materials used for compiling the finished record must be archivally stable.

CONTENT OF RECORDS

1) any record should be identified by:
   a. the name of the building, group of buildings or
   b. a unique reference number;
   c. the date of compilation of the record;
   d. the name of the recording organisation;
   e. cross-references to related building records and reports, photographic, graphic, textual or bibliographic documentation, archaeological and environmental records.
2) the location and extent of the monument, group of buildings or site must be given accurately - this may be achieved by description, maps, plans or aerial photographs. In rural areas a map reference or triangulation to known points may be the only methods available. In urban areas an address or street reference may be sufficient.
3) new records should note the sources of all information not obtained directly from the monument, group of buildings or site itself.
4) records should include some or all of the following information:
   a. the type, form and dimensions of the building, monument or site;
   b. the interior and exterior characteristics, as appropriate, of the monument, group of buildings or site;
   c. the nature, quality, cultural, artistic and scientific significance of the heritage and its components and the cultural, artistic and scientific significance of:
      - the materials, constituent parts and construction, decoration, ornament or inscriptions

- services, fittings and machinery,
- ancillary structures, the gardens, landscape and the cultural, topographical and natural features of the site;

d. the traditional and modern technology and skills used in construction and maintenance;
e. evidence to establish the date of origin, authorship, ownership, the original design, extent, use and decoration;
f. evidence to establish the subsequent history of its uses, associated events, structural or decorative alterations, and the impact of human or natural external forces;
g. the history of management, maintenance and repairs;
h. representative elements or samples of construction or site materials;
i. an assessment of the current condition of the heritage;
j. an assessment of the visual and functional relationship between the heritage and its setting;
k. an assessment of the conflicts and risks from human or natural causes, and from environmental pollution or adjacent land uses.

5) in considering the different reasons for recording (see Section 1.2 above) different levels of detail will be required. All the above information, even if briefly stated, provides important data for local planning and building control and management. Information in greater detail is generally required for the site or building owner's, manager's or user's purposes for conservation, maintenance and use.

MANAGEMENT, DISSEMINATION AND SHARING OF RECORDS

1. the original records should be preserved in a safe archive, and the archive's environment must ensure permanence of the information and freedom from decay to recognised international standards.
2. a complete back-up copy of such records should be stored in a separate safe location.
3. copies of such records should be accessible to the statutory authorities, to concerned professionals and to the public, where appropriate, for the purposes of research, development controls and other administrative and legal processes.
4. up-dated records should be readily available, if possible on the site, for the purposes of research on the heritage, management, maintenance and disaster relief.
5. the format of the records should be standardised, and records should be indexed wherever possible to facilitate the exchange and retrieval of information at a local, national or international level.
6. the effective assembly, management and distribution of recorded information requires, wherever possible, the understanding and the appropriate use of up-to-date information technology.
7. The location of the records should be made public.
8. a report of the main results of any recording should be disseminated and published, when appropriate.

1.2.7. The UNESCO Chart on the Preservation of the Digital Heritage of 2003.

During its 32nd General Conference in 2003, UNESCO adopted the Chart on the Preservation of the Digital Heritage. Digital heritage consists of "digitally created or digitized resources of human knowledge or expression with lasting value and significance". The Chart draws attention to the risk of loss which digital heritage is exposed to due to the rapid obsolescence of the hardware and software which brings it to life, uncertainties about resources, responsibility and methods for maintenance and preservation, and the lack of supportive legislation. It urges Member States to take legal, economic and technical measures to safeguard this heritage.

As a result of the conference, it was promoted the "*Recording, Documentation, and Information Management (RecorDIM) Initiative*" (*Figure 1.2*) in order to connect *Information Users* and *Information Providers* as long the could take evidence of the existing gaps and proceed to a reviewing and improvement of their recording, documentation, and information management practices and to better integrate them into conservation processes (Letellier, 2007).

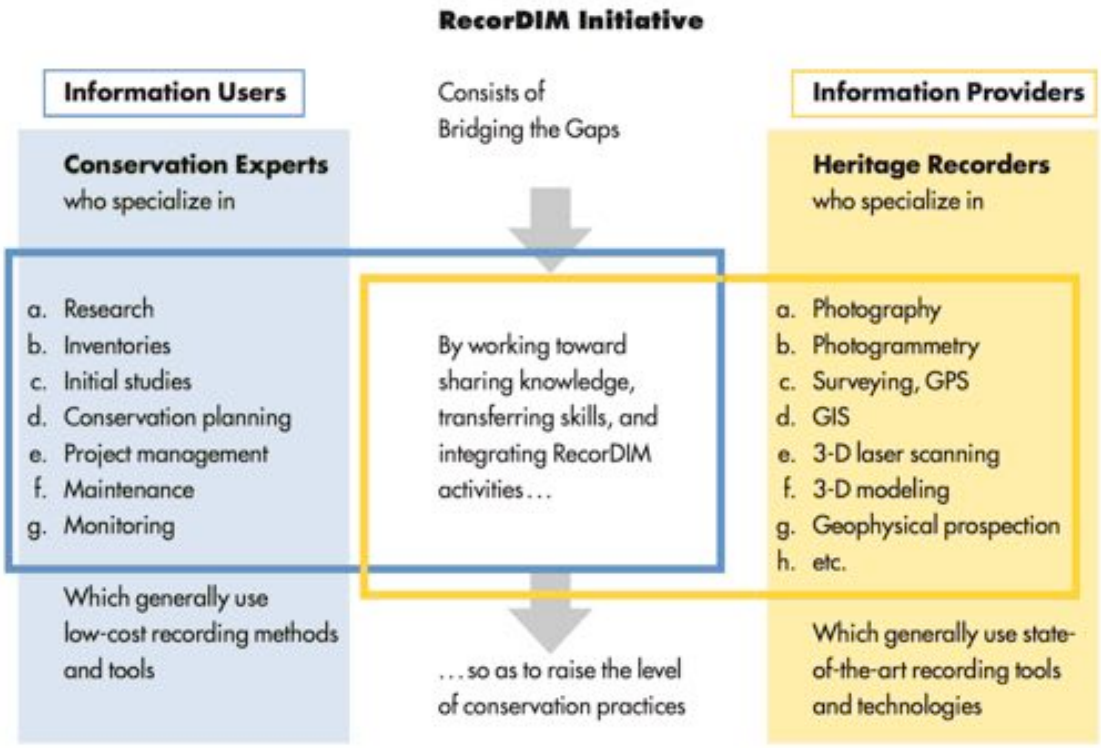

Figure 1.2 - Organizational diagram for the RecorDIM Initiative.

1.2.8. The Italian Urbani Code of 2004

Article 17th of the Code of Cultural Heritage and Landscape, or Code Urbani, governs the act of cataloguing historical and artistic heritage. It is considered essential for the general protection activities, both in terms of knowledge and planning of conservation of the heritage, either because systematically organized knowledge offers valuable support and effective prevention against criminal actions, affecting the artistic and cultural heritage of our country.

It is essential, therefore, for the management, for the enhancement and, in particular, for the protection of cultural heritage, that the scientific act of cataloguing is assumes an organized and systematic method of collecting of more information possible about works of art, being them public or private property.

The decree gives the Ministry, with the participation of the Italian Regions and with the possible collaboration of the University, the task to identify and define common methodologies for the collection, exchange, access and processing of data at a national level. This innovation express a renewed vision of the role of various institutions, working in the field of protection, knowledge and appreciation of the artistic and cultural heritage, and promote the effective cooperation among them, mainly in terms of the agreement programs and cataloguing standards valid throughout the national territory (Nobile, 2012).

1.3. Current trends of 3D geomatic surveying techniques

In the field of Cultural Heritage, according to UNESCO (1972), the geometric documentation can be defined as "*the action of acquiring, processing, representing and registering the data necessary for the determination of the position, shape and size of a monument within a three-dimensional (3D) space and at a given moment in time*". That is, such documentation records the present state of a heritage element, providing the basis for the study of its past (Georgopoulos & Charalambos, 2004).

The disciplines of surveying have improved over time, in step with technological development, from simple methods, based on direct measurements, to those by means of topographic instruments, to other image-based ones exploiting principles analogous of those of descriptive geometry. The technologies recently introduced, and collected in the term "Geomatics", allow surveying, with remarkable accuracy, and representing three-dimensional objects such as, for example, sculptures and archaeological finds, and large objects such as architectural structures (Peloso, 2005).

As obvious, the recording of position, dimensions and/or shape is a necessary part of almost every project related to the conservation of a cultural heritage, forming an important step of the documentation and analysis process. For example, knowing the size and shape of a feature located in a historic landscape can help archaeologists identify its significance; knowing how quickly a stone carving is eroding helps a conservator to determine the appropriate action for its protection. Simply having access to a clear and accurate record of a building façade helps a project manager to schedule the work for its restoration. It is common to represent surveying measurements as plans, sections and/or profiles, plotted on hardcopy for direct use on site. However, with the evolution of new methods of three-dimensional measurement, computer software ubiquity and literacy among users, there is a growing demand for three-dimensional digital information. There are a variety of techniques available to generate three-dimensional surveying models. These techniques can be characterised in different ways, but a useful method is (*Figure 1.3*) by the scale at which they might be used (which is related to the size of the object to measure), and by the number of measurements they might be used to acquire (which is related to the complexity of the object) (Barber & Mills, 2011).

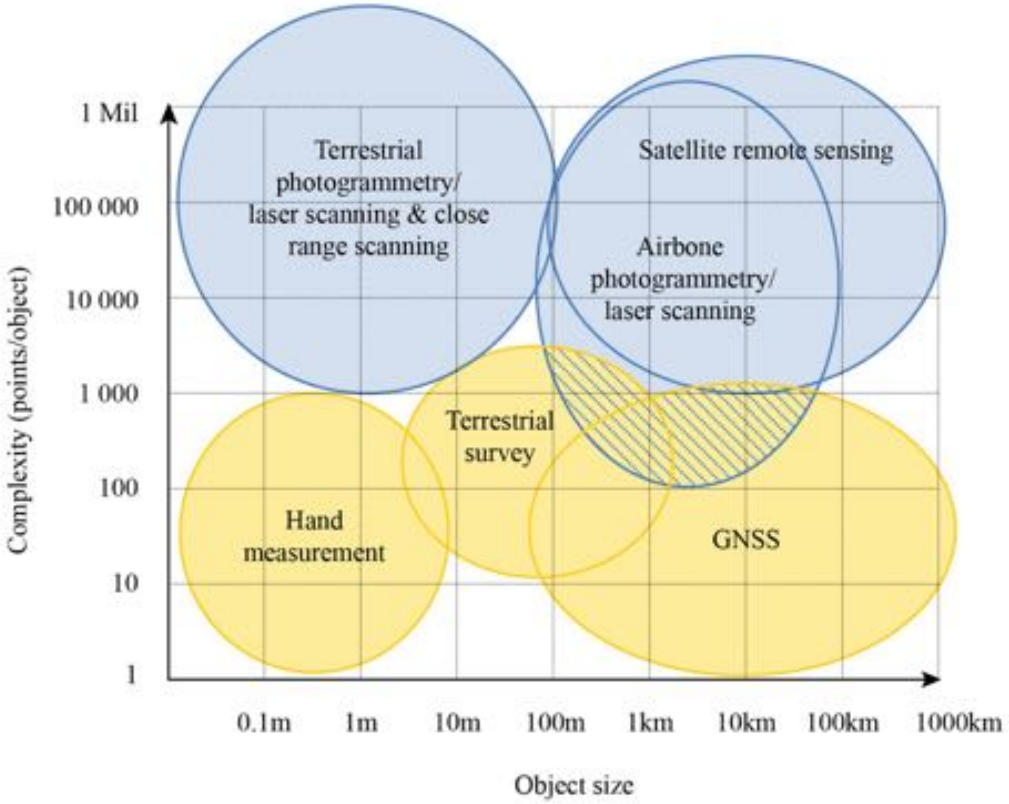

Figure 1.3 - Three-dimensional survey techniques grouped by scale and object size (Barber & Mills, 2011).

The surveying for cultural heritage has own specific features, which, beyond the unquestionable value and "charm" often offered by the recorded objects, make it very interesting and, at the same time, difficult to describe with conventional schemes and standardized methodologies. Every situation is often a "special case", and it is not uncommon that the surveying of an object is a sort of challenge for the operator, forcing him to integrate, with his own experience and sometimes with his own imagination, the lack of suitable tools in situations or environments that were highly unusual and difficult. Therefore, virtually all the "geo-topo-cartographic modern tools" can be adopted in the field of cultural heritage, but certainly some are more adapt to solve the problems mentioned above (Bitelli, 2002).

Among the wide panorama of the existing surveying techniques, this thesis focuses on Terrestrial Laser Scanning (TLS) and Close range scanning, without dealing with photogrammetry, which represent the other contactless surveying technique most used in the field of cultural heritage.

The opportunity to acquire information on the geometry of certain regions of space, or of a specific object, so accurate, fast and non-invasive technology offered by the nowadays laser scanning makes it one of the most appreciated geomatic techniques. The term "laser scanner" is applied to a family of instruments that operate by means of differing principles, in different environments and with different levels of precision and resulting accuracy (Barber & Mills, 2011): a classification of these instruments is reported in the following *Table 1.4*.

scanning system		use	typical accuracy / operating range
triangulation-based artefact scanners	rotation stage	• scanning small objects (that can be removed from site) • to produce data suitable for a replica of the object to be made	50 microns / 0.1m–1m
	arm mounted	• scanning small objects and small surfaces • can be performed on site if required • can be used to produce a replica	50 microns / 0.1m–1m
	mirror/prism	• scanning small object surface areas in situ • can be used to produce a replica	sub-mm / 0.1m–25m
terrestrial time-of-flight laser scanners		• to survey building façades and interiors, resulting in line drawings (with supporting data) and surface models	3–6mm at ranges up to several hundred metres
terrestrial phase-comparison laser scanners		• to survey building façades and interiors resulting in line drawings (with supporting data) and surface models – particularly where rapid data acquisition and high point density are required	*c* 5mm at ranges up to 50–100m
airborne laser scanning		• to map and prospect landscapes (including in forested areas)	0.05m+ (depending on the parameters of the survey) / 100m–3500m
mobile mapping		• to survey highways and railways • for city models • to monitor coastal erosion	10–50mm / 100–200m

Table 1.4 - Laser scanning techniques used in cultural heritage management activities (Barber & Mills, 2011).

In order to provide to the laser scanning surveying of the objects of interest for this thesis, two typologies of instruments have been used, and specifically:

- *Close Range Laser Scanner* - (CRLS) (used only for the case described in paragraph 3.5) which belong to the first family of the "triangulation-based artefact scanner" of *Table 1.4*. It uses very high-resolution scanners to capture smaller areas of data at very high resolutions, right down to tens of microns. This is particularly useful for recording smaller objects or in-situ structures and features requiring very detailed surface analysis. Of course, it requires a lot of time for acquisition and instruments are still very expensive (*Figure 1.5 a)*).
- *Terrestrial Laser Scanner* - (TLS) employs the "time-of-flight" or a "phase-comparison" method to measure distances and it is mainly used for surveying entire buildings and large engineered structures, but can be also used to survey smaller object, as long as they are set over a minimum distance. They are sufficiently diffused and their price is starting to be affordable, considering also the fact that they can be used for different applications (*Figure 1.5 b)*).

Figure 1.5 – a) Close Range Laser Scanner - b) Terrestrial Laser Scanner.

The methodology of utilization of the two families of instruments will be focused on later, among the examples proposed in chapter 3, 4 and 5, anyway it is possible to assume, right off, that the results obtained are the same, albeit with a different precision. Both the typologies, in fact, will generate a *point cloud* as result, which will have to be later opportunely processed to obtain the 3D model.

Therefore, whatever of the technologies previous listed have been used, the surveyed data present some common characteristics (Bonora & Tucci, 2012):

1. Data are always digital (real-world information is converted and stored as binary numeric form), with several advantages regarding flexibility, transmissibility, sharing, possible automatic storage of metadata, etc.;
2. Data are 3D: a metric survey records the position, size and shape of every part of the scanned object; even though the need for plans, sections and profiles plotted on hardcopy is still strong (e.g. for direct use on site), the modern survey techniques always generate three-dimensional survey information;
3. At the moment of acquisition, data are undifferentiated since they come from a sampling carried out directly on the surface of the object;
4. Time required for their on-site acquisition is very short: most recent scanning systems work at a higher and higher speed and it takes only a few minutes to survey a room or the façade of a building. In spite of this acquisition in "near real time", the subsequent processing carried out, to meet various needs, will require pretty long time;
5. Surveying is always carried out without touching the object;
6. Objects are sampled at high resolution. The concept of resolution during acquisition (resolution is "*the smallest change in a quantity being measured that causes a perceptible change in the corresponding indication*" (JCGM, 2012)) is directly linked to the concept of *Level of Detail* (LoD) during restitution: the higher the resolution, the smaller the geometric detail documented by the model. This concept will be furthermore investigated in the following thesis chapters;
7. Geometric data are often associated to information on texture coming from photographic images: raster and vector data can be directly combined in 3D modeling software.

Outlining therefore the process related to the operation of surveying, it must be emphasized that, first and foremost, the design of the entire procedure is a prerequisite for the proper coordination of all the subsequent operations and for controlling the quality of the results. Subsequently, the main phases of a TLS surveying consist in:

- data acquisition,
- data recording,
- data processing.

As it concerns to acquisition, the following aspects may be considered:

Position of scan stations — The positions of the scan stations, as well as the scan resolution have to be designed according to the shape and size of the spaces under investigation. Sometimes in architectural applications, the greatest constraint is given by the necessity to operate in confined

spaces and not by the maximum capacity of the instrument (*Figure 1.6*). It is necessary to have always a sufficient degree of overlap between each scans, and all scans should be enough wide for covering the surrounding areas. The extension of the overlap area is otherwise depending on the morphology of the object. Obviously, a complete documentation must provide, depending on the size of the examined object, acquisitions, not only from below, but possibly at different heights, consistent with the needs related to the poor handling of scanner systems and the stability necessary for the proper performance of the measures.

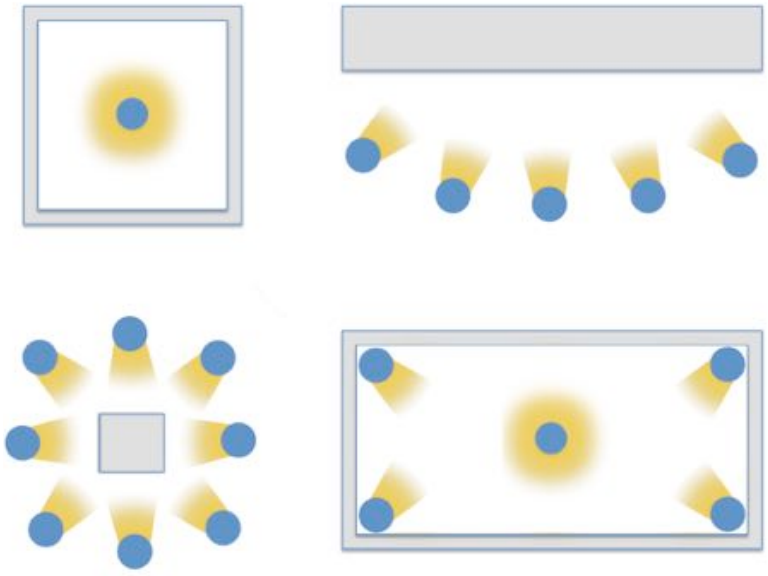

Figure 1.6 – Different possibilities of scan station positioning.

Positioning of target

In order to proceed with the registration and georeferencing of the scans, it is practically needful to chose some points on the scene or to set targets easy to identify by the acquiring systems. The target elements are usually provided with a high reflectance and of suitable shapes and sizes quite variable, particularly in dependence on the distance from the scanner and by the resolution of the scan. The positioning of these target is as much important as the scan stations positioning and have to be designed before the acquisition.

Time of acquisition

As already indicated in the point 4 of the previous list, the time for the acquisition is definitely short, but it is important to remember that, with respect to the mere execution of the scans, the times needed for displacement of the sensor result prevalent.

Resolution

The resolution for the acquisition must be designed as well according to the instrument used and to the object that is going to be acquired (*Figure 1.7*).

feature size	*example feature*	*point density required to give 66% probability that the feature will be visible*	*point density required to give a 95% probability that the feature will be visible*
10m	large earth work	3500mm	500mm
1m	small earth work/ditch	350mm	50mm
100mm	large stone masonry	35mm	5mm
10mm	flint galleting/large tool marks	3.5mm	0.5mm
1mm	weathered masonry	0.35mm	0.05mm

Figure 1.7 – Appropriate point densities (sampling resolutions) for various sizes of cultural heritage feature.

Second step of data recording should include the following (Barber & Mills, 2011):

- file name of the raw data;
- date of capture;
- scanning system used (with manufacturer's serial number);
- company name;
- monument name;
- monument number (if known);
- project reference number (if known);
- scan number (unique scan number for this survey);
- total number of points;
- point density on the object (angular rate or reference distance);
- weather conditions during scanning (outdoor scanning only).

The third phase of processing of the data covers a large amount of procedures: it is actually the most important operation of the TLS surveying in terms of time and in terms of knowledge. The processing needs different software for its accomplishment, which results will depend from many factors. This phase will be analysed more deeply, in a general way, in the following paragraph, juxtaposing its analysis to the software used for the obtaining of the 3D models, and subsequently with the examination of practical cases, in chapters 3, 4 and 5.

1.4. 3D modeling and software used

1.4.1. Introduction

In order to proceed with the 3D modeling of the various TLS point clouds, three different software have been used and experimented in this PhD research. The necessity to test and process data in different environment rose from the various algorithms implemented in each one and to the different results obtained testing each software.

Whichever software it will be used, the pipeline for data processing will be the one shown in the following *Scheme 1.8*:

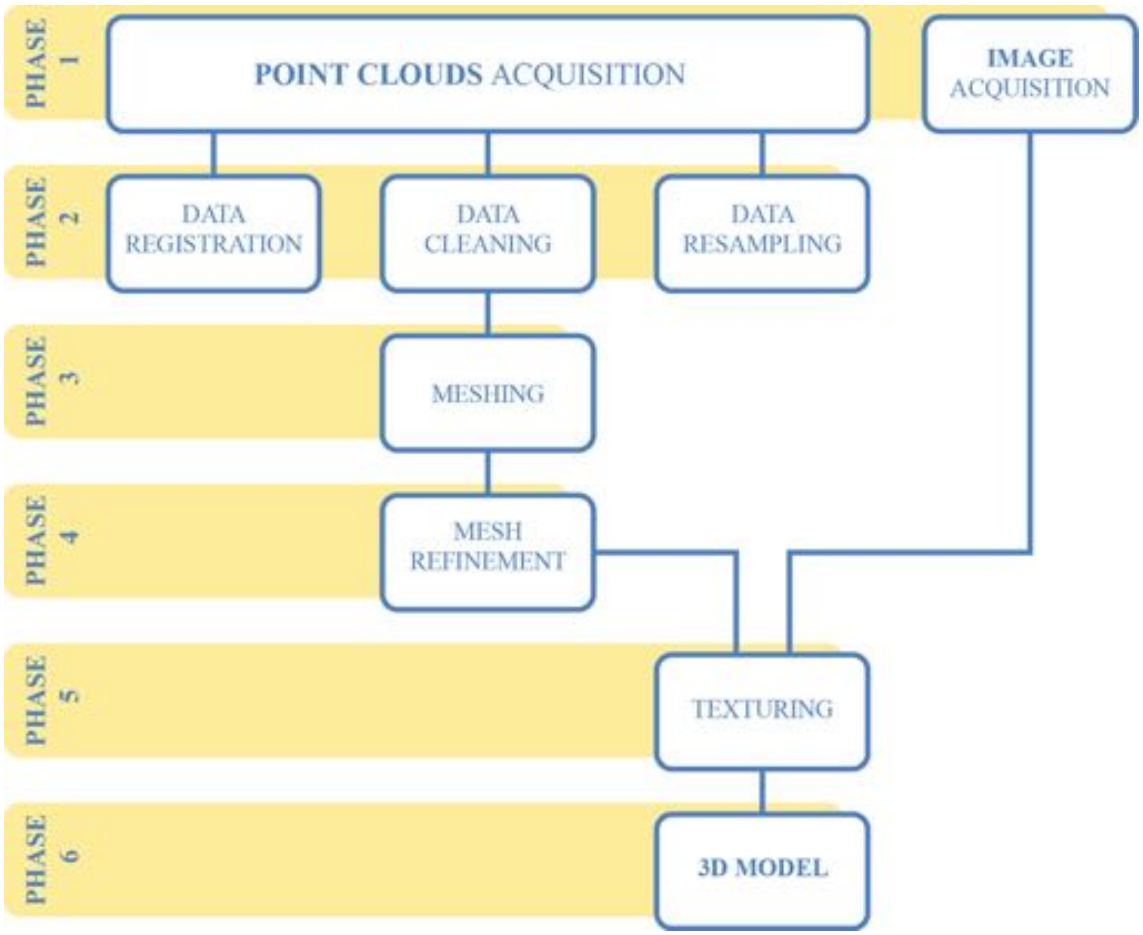

Scheme 1.8 – Flow-chart of TLS data processing.

In this thesis, the investigated procedures were all those included among the "*Point clouds acquisition*" and the "*3D model*", with the only exception of "*Texturing*", which have been excluded since, generally, not useful for Structural Analysis and mainly proper of Photogrammetry, but that was cited for completeness in the processing scheme above reported.

Data registration is the operation that allows the congruent setting of all the point clouds in the same reference system (*Figure 1.9*). This process is also called "alignment" or "matching" and is based essentially on the minimization of the distances between the "same" point belonging to different clouds. Different algorithms have been implemented to reach this goal and consequently applied in the employed software, the most used is Iterative Closest Point.

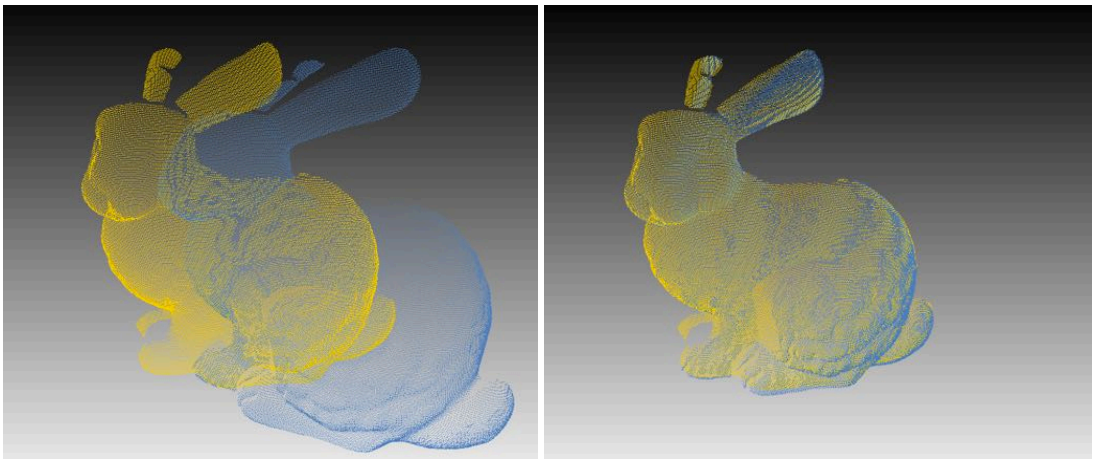

Figure 1.9 – Point clouds registration – an elaboration of the "Stanford Bunny" (Stanford Computer Graphics Laboratory, 1993).

Through *Data Cleaning* it is possible to remove all the furthest points, not belonging to the object of interest but anyway surveyed, all the so-called "double points", or all those points due to noise of data (*Figure 1.10*).

Figure 1.10 – Point clouds cleaning – an elaboration of the "Stanford Bunny" (Stanford Computer Graphics Laboratory, 1993).

Noise of data can be due to (Levoy, et al., 2000):

- systematic bias, usually given by the instruments itself or by the conditions influencing the instruments life, like the condition of illumination or of atmosphere. This typology of noise is usually not really impacting when modeling medium or big size objects because of its little relevance compared to the general measures, while is really influencing on small size objects surveying;
- material capacity of absorbency or reflectivity the laser beam (*Figure 1.11*): this problem is reduced by covering (if possible) the surface with a dust, since it had been proved that if the reflectance of the objects is lowered survey give better results;
- occlusion (and self-occlusion) force grazing scans, which lead to holes (*Figure 1.12*);

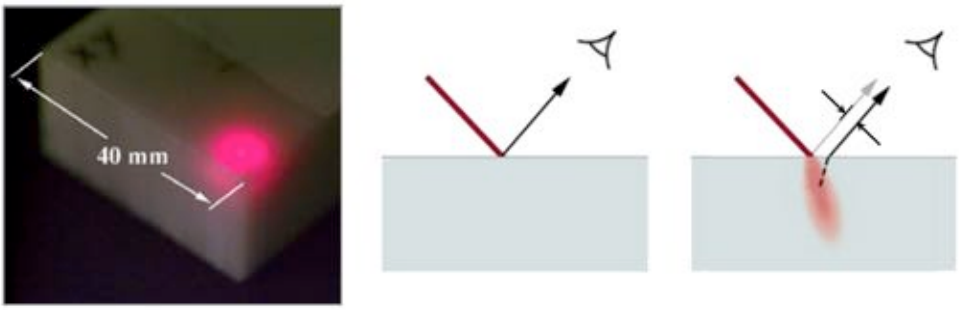

Figure 1.11 – Noise of data due to the material capacity of absorbency or reflectivity the laser beam.

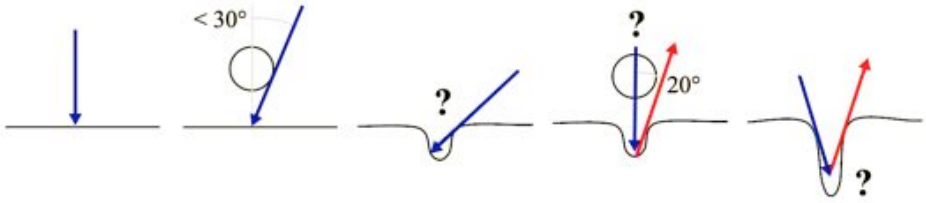

Figure 1.12 – Occlusion in laser scanning.

In order to prevent these problems, the surveying must be previously designed in detail: it must be chosen the most appropriate equipment and, above all, it has to be define, right away, which is the primary purpose of the survey itself. If the main intent is to obtain a model for the structural analysis, it is not necessary to have a high detail model, otherwise if the primary goal is the 3D reprinting of the object, it will be necessary to eliminate of all the problems that could then lead to an incorrect modeling. Also in this case, several algorithms have been implemented in the different software.

Data resampling (*Figure 1.13*) is the operation used for reducing the number of points belonging to the cloud and to suitably reorder them in a defined *grid*. Apparently this operation would lead to think to a data loss: on the contrary, it is fundamental and propaedeutic to the further operations of surfaces reconstruction, because the handling of a huge amount of points would be impossible.

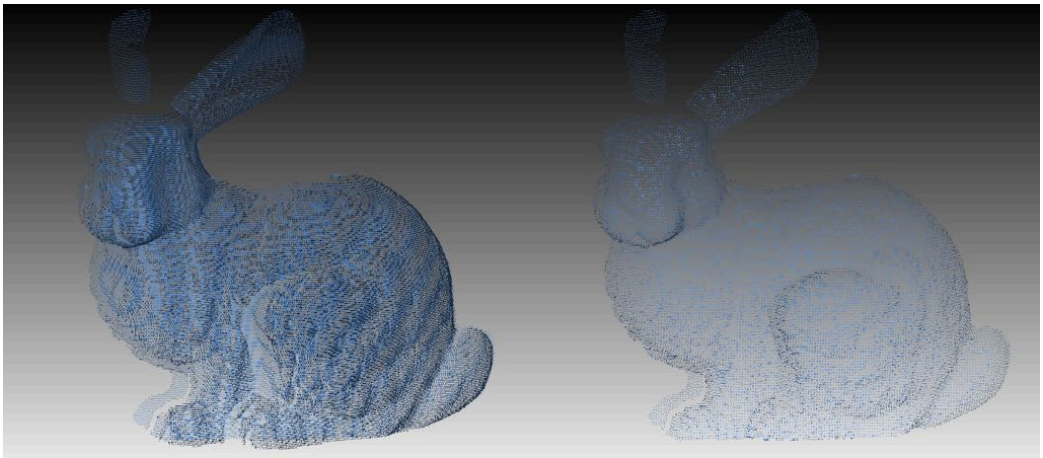

Figure 1.13 – Point clouds resampling – an elaboration of the "Stanford Bunny" (Stanford Computer Graphics Laboratory, 1993).

Meshing is the core processing for the achievement of a 3D model (*Figure 1.14*). In fact, within this definition are represented all those operations necessary for transforming a point cloud to a surface composed by triangles, properly said *mesh*.

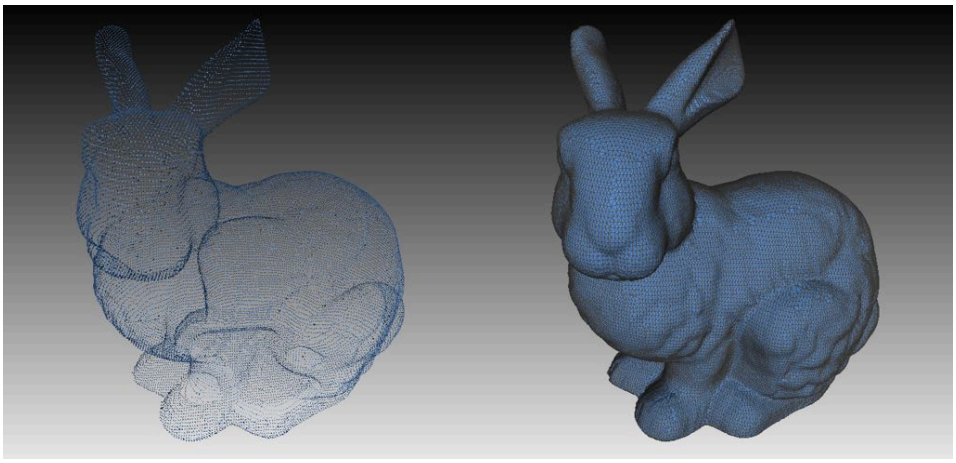

Figure 1.14 – Meshing - an elaboration of the "Stanford Bunny" (Stanford Computer Graphics Laboratory, 1993).

Many various algorithms have been developed for surface reconstruction and most of them have been implemented in the used software. Most of them had been tested, but the best performing resulted the Poisson Surface Reconstruction proposed by Kazhdan, Bolitho, & Hoppe (2006), of Johns Hopkins University, and widely explained in subparagraph 3.3.3.

Meshing refinement includes all those operations necessary for the removal of the incongruences that are often presents after a process of surface reconstruction, and namely (Attene, Campen, & Kobbelt, 2013):

- *isolated vertex*

  vertex which is not on a face or on any other element of the mesh is defined isolated;

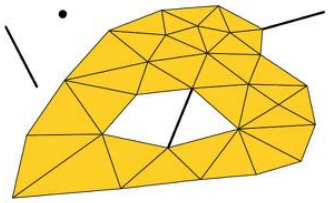

- *dangling edges*

  naked edges, scilicet edges with no incident triangles;

- *singular edges*

  when more than two polygons share a common edge, then such an edge is said to be “singular”, “complex”, or “non-manifold”;

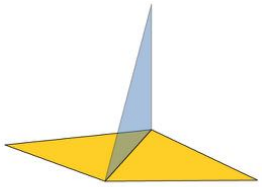

- *singular vertex*

  when a vertex is not manifold in the topology of the abstract simplicial complex, it is called a combinatorially "singular vertex";

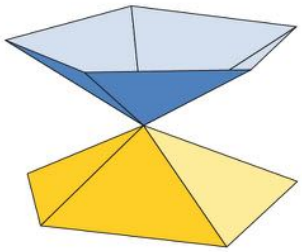

- *topological noise*

  is a problem which arises when the reconstructing implicates the creation of tiny handles or tunnels, not present in the original object, but introduced in the digital model caused by aliasing effects or noise in the data;

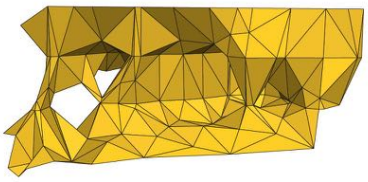

- *orientation inconsistence*

  implies that polygons representing meshes have different sequences of vertex indices, and, therefore the visibility of faces are not congruent, namely the normals are mismatching;

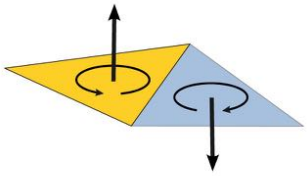

- *surface holes*

  are undesirably missing pieces of surface: the boundary consists of one or more closed edge loops;

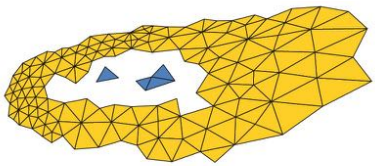

- *surface gaps*

  is defined as the empty region between two triangulated surface patches that should be continuously connected but are not: the boundary, is then made of two (or more) disconnected chains of edges;

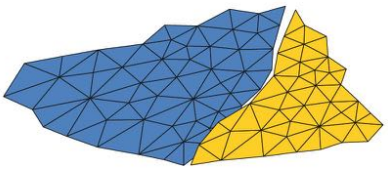

- *self-intersections*

  from the word itself are typically generated by tessellation of multi-patch models, by deformation of mesh models, by composing without care models out of multiple parts;

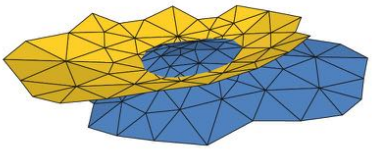

- *degenerate*

  elements degenerate triangles are triangles with zero area: near-degenerate elements are therefore triangles with are proximate to zero;

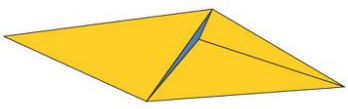

- *data noise*
  due to the lack of precision of the digitization tool and to various sources. It implies that the point cloud present a non-uniformity of the raw data. If not corrected before the processing of the surface, it will result a not smoothed mesh;

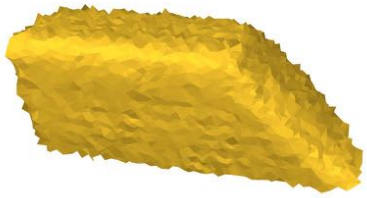

- *sharp feature chamfering*
  it happens when sharp edges and corners are removed by the sampling process and replaced by irregularly triangulated chamfers, which often result in a poor-quality visualization and high distortion.

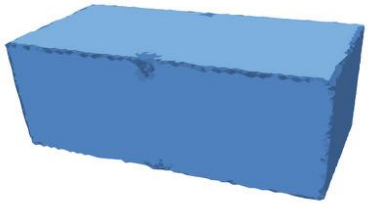

Even for these case, the various software offer different possibilities to operate on these incongruences: most of these commands have been tested, in order to solve the different and peculiar problems of each analysed case; therefore a specific explanation of every dealt procedure is reported in chapter 3, 4 and 5.

The software used and tested within the PhD research are:

- Meshlab version 1.3.3 (Visual Computing Lab - ISTI CNR, 2014);
- CloudCompare version 2.6.0 (Girardeau-Montaut, 2015);
- Geomagic Wrap version 2014 (3DSystem, 2014);

a brief analysis of the characteristic of each one is reported in the following sub paragraphs.

1.4.2. Meshlab

MeshLab is an open source, portable, and extensible system for the processing and editing of unstructured 3D triangular meshes. The system is aimed to help the processing of the unstructured point-clouds and models arising from 3D laser scanning, providing a set of tools for editing, cleaning, healing, inspecting, rendering and converting this kind of meshes. The system is heavily based on the VCG library developed at the Visual Computing Lab of ISTI - CNR, and have been developed starting from 2005 to the latest version, as now dated April 2nd, 2014 (Visual Computing Lab - ISTI CNR, 2014). It is currently compiled on Windows, Linux and Mac OS and for 32 bits and 64 bits architectures.

The mesh processing functionalities that MeshLab currently provide are a lot and a short, incomplete, high level list of MeshLab characteristic have been presented in "*MeshLab: an Open-Source Mesh Processing Tool*" (Cignoni, Callieri, Corsini, Dellepiane, Ganovelli, & Ranzuglia, 2008).

Beside the classical commands of selection, importing/exporting, various colorization and inspection filters, the filters most commonly used and tested in this research have been:

- Mesh Cleaning Filters (many referring to previous explained incongruences):
  - removal of duplicated, unreferenced vertices, null faces, small isolated components;
  - coherent normal unification and flipping;

  - erasing of non manifold faces;
  - automatic filling of holes;
- Remeshing filters:
  - Subdivision surfaces (loop and butterfly);
- Slicing tool, that allows to create and export planar sections of a mesh in SVG (Scalable Vector Graphics) format;
- 3D specific tools:
  - Alignment: ICP (Iterative Closest Point) based registration tool, for putting meshes into the same reference space;
  - Merging of multiple meshes;
  - Poisson Surface Reconstruction.

Most of these commands have been used for the treatment of the point clouds and are not described in this thesis, since they are of very common use in the 3D environments, while some other filters are widely described, especially in subparagraph 3.3.2.

1.4.3. CloudCompare

CloudCompare is an open-source software designed by Daniel Girardeau-Montaut (INRIA/LOIRA), used for 3D point cloud (and triangular mesh) editing and processing. It is developed in C++ and exploits on a specific *octree* data structure that improves the graphic performances. Also this software is currently compiled on Windows, Linux and Mac OS and for 32 bits and 64 bits architectures. The latest version as now is version 2.6.2.

It was originally designed to perform direct comparison between 3D point clouds or between a point cloud and a triangular mesh, but later has been implemented with many other point cloud processing algorithms, like (Girardeau-Montaut, 2015):

- registration;
- resampling;
- managing of colours, normal and vectors/scalar fields;
- statistics computation;
- scanner positioning and orientation management;
- interactive or automatic segmentation;

as well as other display enhanced representation tools like:

- custom colour ramps;
- colour & normal vectors handling;
- calibrated pictures handling;
- openGL shaders;
- plugins for:
  - Hidden Points Removal;
  - Acquisition of coloured point clouds with a Kinect device;
  - Interface for PCL library - normal computation, outliers removal;
  - Ambient Occlusion for mesh or point cloud;
  - Poisson Surface Mesh Reconstruction;
  - Automatic RANSAC Shape Detection;

- Surface of Revolution Analysis;
- Point Cloud Classification;
- Computation of robust signed distances between point clouds;
- Constructive Solid Geometry;
- Animation rendering;
- Structural geology.

Most of its command have been used and tested in this research, with particular regard to the registration algorithm and to the comparing processes, since it resulted the best performing in this particular needs.

1.4.4. Geomagic Wrap

Geomagic Wrap is a free-trial-runs software toolbox design to transform 3D scans data and imported files into 3D models for their immediate use. Since it is not open-source software, its architecture and algorithm are kept reserved and it is not possible to know which algorithms govern its command (3DSystem, 2014).

The main functions offered by the software are:

- point cloud editing and creation of polygonal models based on the 3D scan data;
- remeshing tool for creating *clean* polygon models from *dirty* scan data;
- polygon editing tools for hole filling, smoothing, patching and water-tight model creation;
- surfacing tools that allows patch layout, surface quality, and continuity;
- curves and features extraction from polygon bodies.

The most used commands in this research are the meshing tools and mesh refinement ones, which resulted the best performing among the used software.

1.5. Recording with 3D geomatic surveying techniques: some example

As it concern to the studies held so far in this field, literature is really wide; following the same development of the thesis, as specified in the introduction, example will be examined starting from small size object and arriving to large size ones.

Some of the most famous exempla of "small" size objects recording, namely surveying and 3D modeling include "The Digital Michelangelo Project: 3D Scanning of Large Statues", held by the Stanford University in California, USA (Levoy, et al., 2000) (*Figure 1.15*) and the Reconstruction of the Great Buddha of Bamiyan in Afghanistan (Grün, Remondino, & Zhang, 2004) (*Figure 1.16*), held by the Swiss Federal Institute of Technology (ETH), Zurich. Both of these works have received huge media attention, either for the importance of the object of the survey, either for the problems faced. In the first case, it was used TLS technology, while a photogrammetric surveying supported the second case: in both cases, a cloud of points was the result on which later obtained a digital model. Although surveys have been carried out in two distinct periods, both modeling projects were completed in the early 2000. Since then, laser scanning technology became much more economical and versatile and, therefore, used more and more frequently.

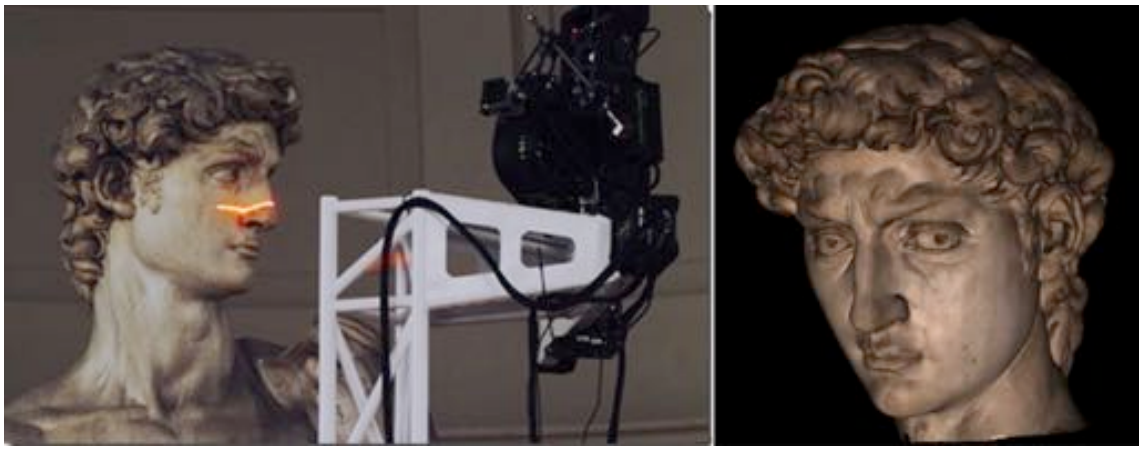

Figure 1.15 – The survey of the David on the left and the 3D model on the right.
A detail of the head. (Levoy, et al., 2000).

Figure 1.16 – The Great Buddha of Bamiyan in Afghanistan. Particulars of two original metric images.
Point cloud generated by automatic matching on the images.
Textured 3D model (Grün, Remondino, & Zhang, 2004)

Other successive interesting studies among the laser scanning surveying of small objects are the ones reported in "Tridimensional digitizing of Donatello's Maddalena", (Guidi, Pieraccini, Ciofi, Damato, Beraldin, & Atzeni, 2001) (*Figure 1.17*), the one of "Building a Digital Model of Michelangelo's Florentine Pieta" (Bernardini, Rushmeier, Martin, Mittleman, & Taubin, 2002) (*Figure 1.18*), as well in "Laser scanning and photogrammetry for the documentation of a large statue-experiences in the combined use" (Ioannidis, 2003) (*Figure 1.19*) and in "Digital Three-Dimensional Modeling of Heritage by Frequency-Modulated Laser Radar: the case of Donatello's "David"" (Cioci, Spinetti, Atzeni, Cassani, & Lupus, 2005) (*Figure 1.20*). All of these studies refer to significant cultural heritage example, carried out through the collaboration of important international research centres: all the publications describe the processes followed for obtaining 3D surface models.

Figure 1.17 – Donatello's Maddalena – a picture of the statue conserved in the Opera of Duomo in Florence (Italy), the point clouds and the 3D Model (Guidi, Pieraccini, Ciofi, Damato, Beraldin, & Atzeni, 2001)

Figure 1.18 – The Michelangelo's Florentine Pieta– on the left a picture of the statue and on the right the 3D mesh model (Bernardini, Rushmeier, Martin, Mittleman, & Taubin, 2002)

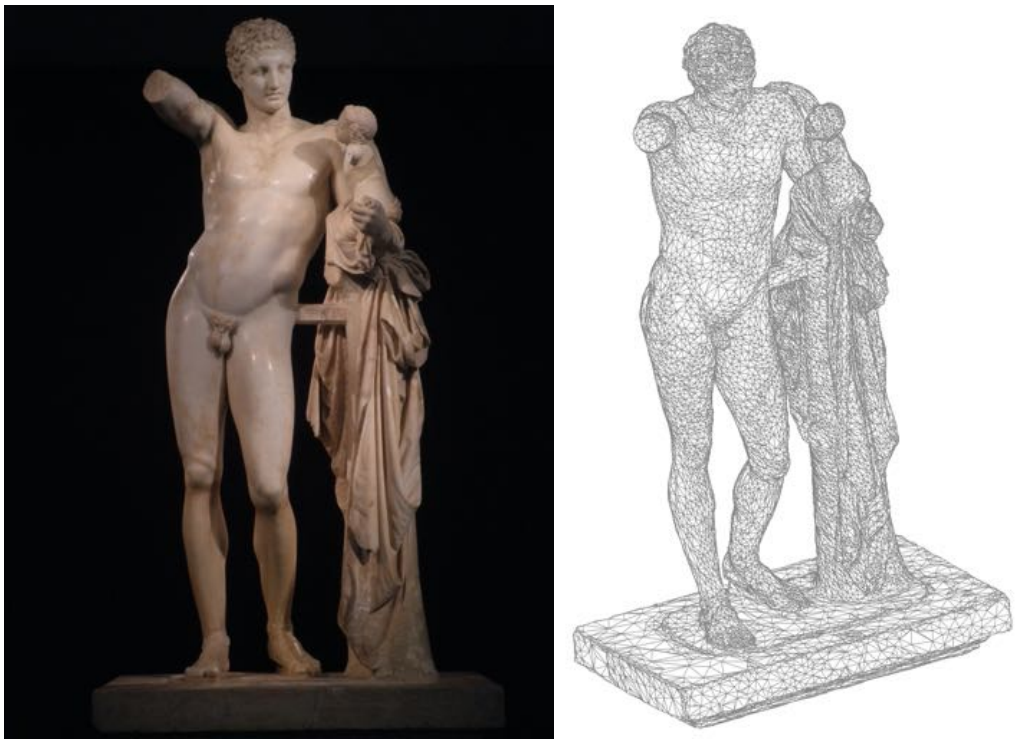

Figure 1.19 – The Hermes of Praxiteles conserved in the Archaeological Museum of Olympia in Greece – on the left a picture of the statue and on the right the mesh model in wireframe mode (Ioannidis, 2003)

Figure 1.20 – The Donatello's David preserved in the Museum of Bargello in Florence – a picture on the left and the 3D model on the right (Cioci, Spinetti, Atzeni, Cassani, & Lupus, 2005)

Referring to medium size objects, there is a wide list of example in literature, since these can be considered the most "*easy*" to survey and to model, because dimensions and complexity do not reach the level of large size object and, at the same time, the LoD does not have to be so defined like in small size object.

Many of the examples refer to archaeology, like the cases illustrated in "Laser scanner survey of an archaeological site – Scala di Furno (Lecce)" of *Figure 1.21* (Costantino, Angelini, & Caprino, 2010), where the surveying regarded the walls contained in a small area as rest of the archaeological site, or in "3D Modeling of Large and Complex Site Using Multi-sensor Integration and Multi-resolution Data" (Guidi, Remondino, Russo, Menna, & Rizzi, 2008), where many medium size object belonging to the rests of Pompei where surveyed and modelled (*Figure 1.22*). Relevant architectural examples are shown in "Geometric documentation of the Almoina door of the cathedral of Valencia" (Stathopoulou, Lerma, & Georgopoulos, 2010) where the abutment of the main door of a church was surveyed and modelled (*Figure 1.23*) or in "Multi-scale 3D metric survey for investigation and architectural representation of the archaeological and environmental area of Susa" (Aicardi, et al., 2014) where, an arch was surveyed and modelled (*Figure 1.24*).

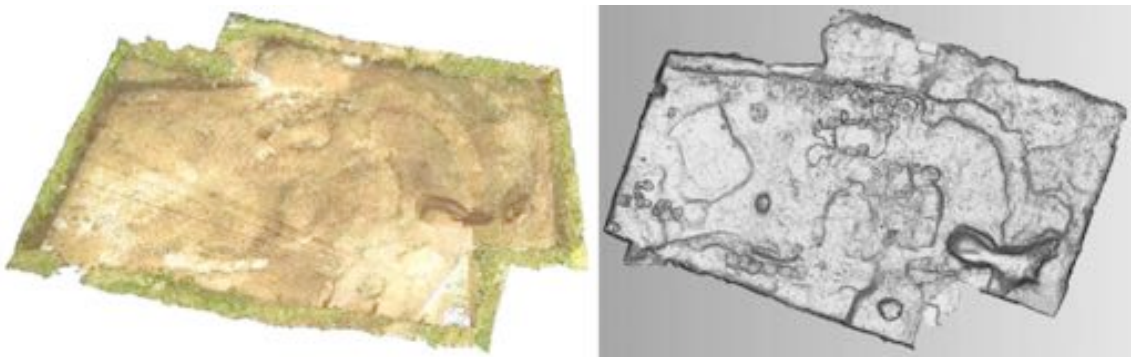

Figure 1.21 - Archaeological area of Scala di Furno (Lecce): on the left the point cloud of the site and on the right the 3D model obtained (Costantino, Angelini, & Caprino, 2010).

Figure 1.22 – 3D models of different elements surveyed in the Pompei area (Guidi, Remondino, Russo, Menna, & Rizzi, 2008).

Figure 1.23 – 3D models of the portal of the Almoina door of the Cathedral of Valencia: on the right the surveying, the 3D point clouds and the model (Stathopoulou, Georgopoulos, & Lerma, 2010).

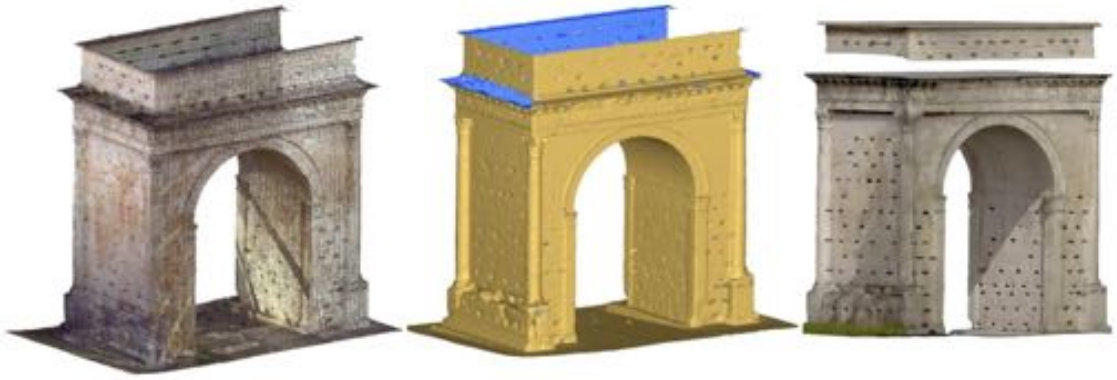

Figure 1.24 – From left: point cloud of Augustus arch in Susa acquired with laser scanners, the mesh surface of the arc and the arc textured mesh (Aicardi, et al., 2014).

Lastly, regarding the studies held on large size object surveying and modeling, for sure a mention is deserved for the following works, because of the obtained results and of the originality in use done of data:

- "The Basilica della Madonna dell'Umiltà in Pistoia: Survey, Analysis and Documentation" (Tucci, Nobile, & Riemma, 2011), describes the surveying and processing of point clouds, and the modeling of some portions of this imposing church of Pistoia (Italy) (*Figure 1.25*);

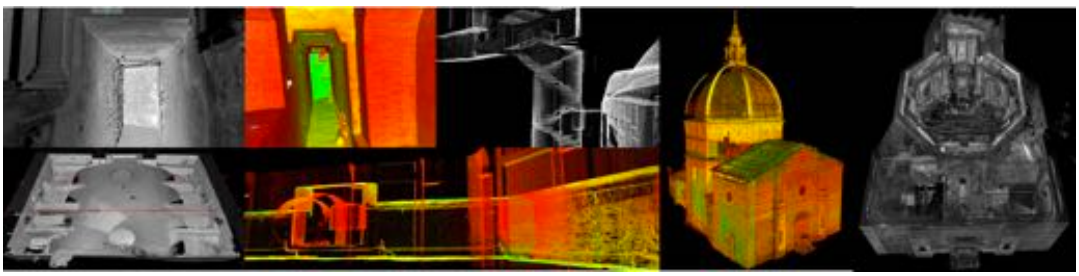

Figure 1.25 – Three-dimensional views of the complete model showing the connections of the chains and the reduced spaces of the horizontal and vertical connections of Basilica (Tucci, Nobile, & Riemma, 2011)

- "Using multiple scanning technologies for the 3D acquisition of Torcello's Basilica." (Balzani, et al.), where the 3D scanning campaign of the ancient Basilica in Torcello (Venice, Italy) (*Figure 1.26*) were carried out by means of different TLS devices: a triangulation scanner for medium scale artefacts, a phase-modulation time-of-flight device

for larger surfaces (mosaics), and a standard time-of-flight system for the overall architecture. All the gathered data have been integrated and fused in a multi-resolution 3D model.

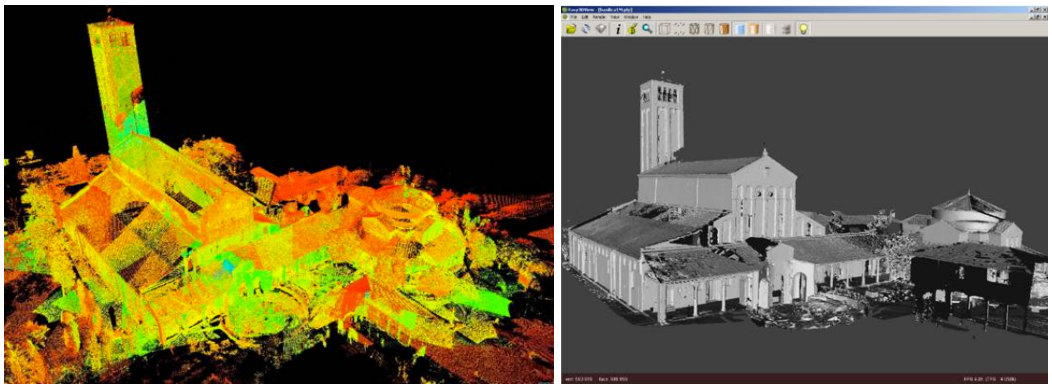

Figure 1.26 – Point clouds of the Basilica of Torcello (Italy) and 3D surface mesh (Balzani, et al.)

- "Tooteko: a Case Study of Augmented Reality for an Accessible Cultural Heritage. Digitization, 3D Printing and Sensors for an Audio-Tactile Experience" (D'Agnano, Balletti, Guerra, & Vernier, 2015), where the results of the surveying were used for a 3D printing, specially devoted to tactile use of blind people (*Figure 1.27*).

Figure 1.27 – The church of S. Michele in Isola (Venice): Point clouds – DSM – The resin model and hotspot for activating audio track (D'Agnano, Balletti, Guerra, & Vernier, 2015).

As a last example, it will be cited the study executed on a large object by University of Udine, in 2005, on the Castle of Gorizia (Italy), presented at the SIFET Conference in the following year: "3D modeling of an urban environment by integration of terrestrial and aerial laser scans: the example of the Castle of Gorizia (Modellazione 3D dell'ambiente urbano mediante integrazione di scansioni laser aeree e terrestri: l'esempio del castello di Gorizia)" (Visintini, Fico, & Spangher, 2006). In this experience, the point cloud (36 millions of points) was processed in order to obtain a large number of numerical products as coloured point clouds, vector sections and profiles, mesh surfaces, and digital image texturing (*Figure 1.28*).

Figure 1.28 – On the left, the coloured point cloud of the gateway to uphill leading to the Castle right, the textured surface of the Court of Lanzi.

1.6. Conclusions

In this first chapter was introduced the concept of data recording, underlining its importance and its connection to cultural heritage. The documents referring to these two concepts and their correlation to Geomatics were therefore highlighted, as well as the most used and advanced techniques for the surveying of cultural heritage, that were illustrated, focusing on the laser scanning method, since it is the one used in this research.

The procedures involved in laser scanning acquisition, recording and processing were shortly described, converging attention on the 3D modeling step, which aims a large part of this thesis. Some noteworthy examples were therefore reported, describing the results obtained so far.

These arguments will be developed with practical applications in the following chapters 4, 5 and 6, where the case of small size, medium size and large size structures will be treated respectively. All the cases of study were developed following *Scheme 1.8*, and using the software described in previous paragraph.

1.7. Bibliography

3DSystem. (2014). *Geomagic*. Based on http://www.geomagic.com/it

Aicardi, I., Boccardo, P., Chiabrando, F., Donadio, E., Lingua, A., Maschio, P., et al. (2014). Rilievo metrico 3D multiscala per l'indagine e la rappresentazione architettonica e ambientale dell'area archeologica di Susa . *Convegno Nazionale ASITA 2014* (p. 27-34). Firenze: ASITA.

Attene, M., Campen, M., & Kobbelt, L. (2013). Polygon mesh repairing: An application perspective. *Journal ACM Computing Survey , 45* (15).

Balzani, M., Callieri, M., Caputo, G., Cignoni, P., Dellepiane, M., Montani, C., et al. Using multiple scanning technologies for the 3d acquisition of torcello's basilica. *In Int. Workshop 3D-ARCH*, (p. 22-24).

Barber, D., & Mills, J. (2011). *3D Laser Scanning for Heritage.* Swindon: English Heritage Publishing.

Bernardini, F., Rushmeier, H., Martin, I., Mittleman, J., & Taubin, G. (2002). Building a Digital Model of Michelangelo's Florentine Pietà. *IEEE Computer Graphics and Applications* , p. 59-67.

Bitelli, G. (2002). Moderne tecniche e strumentazioni per il rilievo dei beni culturali. *Atti 6a Conferenza Nazionale ASITA. IX-XXIV*. Perugia: ASITA.

Bonora, V., & Tucci, G. (2012). New technologies for cultural heritage documentation and conservation: the role of Geomatics. *Iconoarch - I Architectural and Technology International Congress*, (p. 444-451). Konya.

Cignoni, P., Callieri, M., Corsini, M., Dellepiane, M., Ganovelli, F., & Ranzuglia, G. (2008). MeshLab: an Open-Source Mesh Processing Tool . *Eurographics Italian Chapter Conference.* Salerno: V. Scarano, R. De Chiara, and U. Erra (Editors) .

Cioci, A., Spinetti, A., Atzeni, C., Cassani, C., & Lupus, A. (2005). Digital Three-Dimensional Modeling of Heritage by Frequency-Modulated Laser Radar: the case of Donatello's "David". *The 6th International Symposium on Virtual Reality, Archaeology and Cultural Heritage.* Vast: M. Mudge, N. Ryan, R. Scopigno (Editors).

Costantino, D., Angelini, M. G., & Caprino, G. (2010). Laser scanner survey of an archaeological site – Scala di Furno (Lecce, Italy). *ISPRS Commission V, Mid – Term Symposium "Close range image measurements techniques. XXXVIII Part 5.* , p. 178-183. Newcastle upon Tyne, United Kingdom: Editors: Mills, J. P., Barber, D. M., Miller, P.E. and Newton, I.. .

D'Agnano, F., Balletti, C., Guerra, F., & Vernier, P. (2015). Tooteko: a Case Study of Augmented Reality for an Accessible Cultural Heritage. Digitization, 3d Printing and Sensors for an Audio-Tactile Experience . *ISPRS-International Archives of the Photogrammetry, Remote Sensing and Spatial Information Sciences* (1), 207-213.

Erder, C. (1977). The Venice Charter Under Review. Ankara.

First International Congress of Architects and Technicians of Historic Monuments. (1931). The Athens Charter for the Restoration of Historic Monuments. Athens.

Georgopoulos, A., & Charalambos, I. (2004). Photogrammetric and Surveying Methods for the Geometric Recording of Archaeological Monuments . *FIG WORKING WEEK - Workshop - Archaeological Surveys* . Athens: FIG.

Girardeau-Montaut, D. (2015). *CloudCompare*. Based on http://www.cloudcompare.org/

Grün, A., Remondino, F., & Zhang, L. (2004). Photogrammetric Reconstruction of the Great Buddha of Bamiyan, Afghanistan. *The Photogrammetric Record , 19* (107), 177-199.

Guidi, G., Pieraccini, M., Ciofi, S., Damato, V., Beraldin, J. A., & Atzeni, C. (2001). Tridimensional digitizing of Donatello's Maddalena . *Ieee International Conference on Image Processing (ICIP 2001)*, (p. 578-581). Thessaloniki.

Guidi, G., Remondino, F., Russo, M., Menna, F., & Rizzi, A. (2008). 3D Modeling of Large and Complex Site Using Multi-sensor Integration and Multi-resolution Data. *VAST- The 9th International Symposium on Virtual Reality, Archaeology and Cultural Heritage* (p. 85-92). M. Ashley, S. Hermon, A. Proenca, and K. Rodriguez-Echavarria (Editors).

ICOMOS. (2015). *ICOMOS - International Council of Monuments and Sites*. Consulted on November 28, 2015 da www.icomos.org: http://www.icomos.org/

Ioannidis, M. T. (2003). Laser scanning and photogrammetry for the documentation of a large statue-experiences in the combined use. *Proceedings of CIPA XIX International Symposium*, (p. 517-523).

JCGM. (2012). VIM 2012. *International vocabulary of metrology 2012. Basic and general concepts and associated terms* . (J. C. Metrology, A cura di)

Letellier, R. (2007). *Recording, Documentation, and Information Management for the Conservation of Heritage Places - Guiding Principles.* Los Angeles: The Getty Conservation Institute.

Levoy, M., Pulli, K., Curless, B., Rusinkiewicz, S., Koller, D., Pereira, L., et al. (2000). The digital Michelangelo project: 3D scanning of large statues. *Proceedings of the SIGGRAPH '00 - 27th annual conference on Computer graphics and interactive techniques* (p. 131-144). New York: CM Press/Addison-Wesley Publishing Co.

Nobile, A. (2012). I sistemi a Scansione 3D per la documentazione metrica e lo studio diagnostico dei beni culturali. Firenze: Tesi di Dottorato.

Peloso, D. (2005). Tecniche laser scanner per il rilievo dei beni culturali. *Archeologia e Calcolatori , XVI*, 199-224.

Remondino, F., & Rizzi, A. (2010, September). Reality-based 3D documentation of natural and cultural heritage sites—techniques, problems, and examples. *APPLIED GEOMATICS* , 85-100.

Stanford Computer Graphics Laboratory. (1993). 3D Standford Bunny Model. *http://graphics.stanford.edu/data/3Dscanrep/* .

Stathopoulou, E. K., Lerma, J. L., & Georgopoulos, A. (2010). Geometric documentation of the Almoina door of the cathedral of Valencia. *EuroMed2010 - 3rd International Conference dedicated on Digital Heritage* (p. 60-64). Limassol, Cyprus: M. Ioannides, D. Fellner, A. Georgopoulos, D. Hadjimitsis .

Tucci, G., Nobile, A., & Riemma, M. (2011). The Basilica della Madonna dell'Umiltà in Pistoia: Survey, Analysis and Documentation. *Proceedings of XXIII International CIPA Symposium*, (p. 1-8). Prague, Czech Rep.

UNESCO. (1972). Photogrammetry applied to the survey of Historic Monuments, of Sites and to Archaeology. UNESCO Editions.

UNESCO. (1954). *Unesco Portal*. (U. N. Organization, A cura di) Consulted on November 28, 2015 da http://unesdoc.unesco.org/images/0008/000824/082464mb.pdf#page=66

Visintini, D., Fico, B., & Spangher, A. (2006). Modellazione 3D dell'ambiente urbano mediante integrazione di scansioni laser aeree e terrestri: l'esempio del castello di Gorizia. *Proceedings of the Convegno SIFET 2006.*

Visual Computing Lab - ISTI CNR. (2014, April 02). Based on Meshlab: http://meshlab.sourceforge.net/

2. STRUCTURAL ANALYSIS OF MONUMENTS AND HISTORICAL CONSTRUCTIONS

2.1. Aims, challenges and difficulties in modeling and analysis of historical structures

The largest part of the Italian monuments and building heritage, especially the historical and artistic ones, consists of masonry buildings or stone artefacts. For many centuries, history of construction corresponded, in fact, to that one of masonry buildings (*Figure 2.1*) because, although the number of timber construction has been, over time, certainly much higher, nowadays, due to fire, destruction and demolition of these constructions there is little memory. Protection and conservation of such built objects, as reported in chapter 1, represent an issue that has significant economic and social benefits, as recently reiterated by the scientific community: therefore, different systems and methodologies for restoration and preservation have been proposed during the last two centuries. The application of these technologies requires a thorough knowledge of the object, from different points of view, at least both mechanical both geometrical.

Figure 2.1 – a) Giants grave in Olbia Tempio (Sardinia) (II millennium B.C.) – b) Portico of Octavia in Rome (II century B.C) c) Palazzo Vecchio in Florence (XIII century) d) Gallery Vittorio Emanuele II in Milan (XIX century).

The use of steel and then of concrete date back to historically recent times (from the nineteenth century onwards), while most of the wood building have been destroyed during times, as already specified, hence the historic buildings that actually endure are almost entirely of masonry. The forms and construction methods of these buildings are not only very different from the modern ones, but differ also to each other depending to the historical period, location and many other factors.

The structural analysis of masonry structure had not been considered for a long period of time during history since it was supposed that good practice and experience was at the establishment of the art of constructing. The Roman architect Vitruvius in his work "Ten Books on Architecture" compares the quality of stone and wood from various locations and speaks about proportions of various construction elements and structures, but he does not say anything about their computation. A structure that has "right proportions" was considered "structurally adequate" and that way of thinking was kept during the Middle Ages. The trait of this time is strictly keeping knowledge of verified proportions that are passed on from one generation to another. Many impressive structures made in these times, that are still here today, show that the experience and knowledge about stability and distribution of forces within the masonry structure was not negligible. Many of the buildings constructed during the Renaissance, in the fifteenth century, became more slender: this required a proper theoretical basis for their construction (Smoljanović, Živaljić, & Nikolić, 2013).

The *scientific* checks of the resistance of masonry walls began in the '700, with systematic evidence of compressive strength on the stones, as done by Émiland Gauthey (a French mathematician, civil engineer and architect) in 1773 for the Church of Sainte Genevieve in Paris, and then by Jean-Rodolph Perronet (a French architect and structural engineer) in his studies on stone bridges. The first theories on the strength of the arches and vaults date to 1695 and is due to Philippe de la Hire (a French mathematician and astronomer): it was articulated just before the discussions in 1743 on the stability of the Dome of St. Peter in Rome by Giovanni Poleni (an Italian physicist, mathematician and antiquarian) and the three mathematicians Fathers Tommaso Le Seur, Francis Jacquier of the Order of Minimi, and Ruggiero Giuseppe Boscovich of the Society of Jesus (*Figure 2.2*).

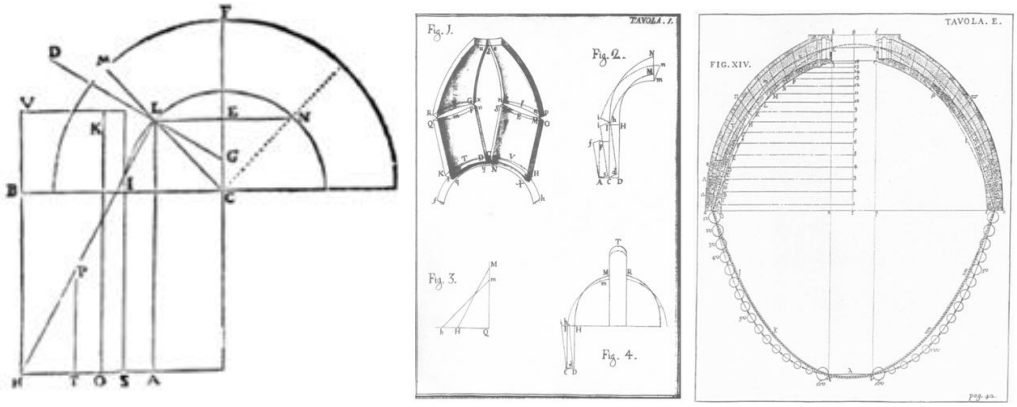

Figure 2.2 – a) de la Hire mechanism to calculate the thickness of the abutments
b) Theory of Le Seur, Jacquier and Boscovich on St. Peter's Dome in Rome
c) Theory of Poleni on St. Peter's Dome in Rome.

Since then the mechanical modeling and the mathematical analysis presented a significant progress. So called "Balancing methods" were firstly introduced by Charles-Augustine de Coulomb (1773) until the most modern versions due to Jacques Heyman, an English engineer (1995). The major step forward was then verified with the compatibility of the deformation to the static balancing, and this was due to various scientists, of whom can be cited Carlo Alberto Castigliano, an Italian engineer and mathematician (1880) (Giangreco, 2002).

The most heated debate began around 1950, when the *finite element method* opened the widest horizons to comprehension and verification of complex constructions of the past: the application of advanced computer methods to the analysis of historical structures was pioneered by the studies of the Brunelleschi Dome in Florence by Chiarugi et al. (1995), the Pisa Tower in Pisa by Macchi et al. (1993) (*Figure 2.3 a)*), the Colosseo in Rome by Croci (1995) (*Figure 2.3 b)*), Mexico City Cathedral by Meli and Sánchez-Ramírez (2007) and San Marco's Basilica in Venice by Mola and Vitaliani (1995), among others. By then, the development of methods for accurate analysis of steel and concrete structures, including non-linear applications, was already at a very advanced stage thanks to the work of Zienkiewicz and Taylor, Ngo and Scordelis and many others. Notwithstanding, analysts attempting to use computer tools for the study historical structures were by then facing overwhelming challenges. Methods then available were not yet prepared to tackle the specific problems of ancient constructions concerning materials, structural arrangements and real preservation condition. In fact, the difficulties posed by historical structures are still very challenging, and still reminiscent of those encountered by the pioneers, in spite of significant progress during the last decades (Roca, Cervera, Gariup, & Pelà, 2010).

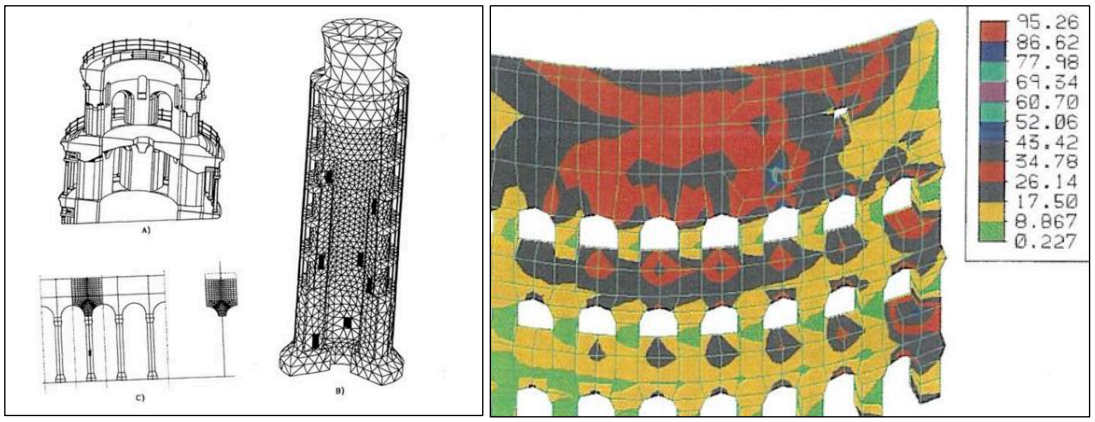

Figure 2.3 – a) Tower of Pisa: FEM model (B) and substructuring of the colonnade system (A and C) (Macchi, Ruggeri, Eusebio, & Moncecchi, 1993) b) Elastic modal analysis of Coliseum in Rome: maximum principal stresses (Croci, D'Ayala, & Liburdi, 1995)

Even if the greatest part of the construction during times has been realized using this technology, the normative that rules the criteria for the design and verification is nowadays not as complete and thorough, as the one that governs other technology such as steel or concrete. This is justified by the fact that it results particularly difficult to idealize the basic behaviours for structural modeling: it is very hard, in fact, to apply to such structures the idealizations of the beam, frame and flat shells typical of structural engineering (Giangreco, 2002).

The analysis of historic masonry structures, considering what has been highlighted so far, is therefore a complex task. First, limited resources have been allocated to the study of the mechanical behaviour of masonry, which includes non-destructive *in situ* testing, adequate laboratory testing and development of reliable numerical tools, since, for a long time, studies of structural analysis have been focusing on new structures rather than existing ones. Second, and even most important, the difficulties in using the existing knowledge are inherent to the analysis of historic structures themselves as specified in the following list.

Usually, salient difficulty aspects related to the analysis are (Lourenċo, 2002):

- geometric data is missing;
- information about the inner core of the structural elements is generally missing;
- characterization of the mechanical properties of the materials used is difficult and expensive to know;
- mechanical properties have large variability, because of workmanship and of use of natural materials;
- significant changes could occurred in the core and constitution of structural elements, associated with long construction periods;
- construction sequence is unknown;
- existing damage in the structure is unknown;
- part of regulations and standards are not applicable.

Summarizing, the structural analysis of historical buildings in masonry, and especially of buildings of monumental character, requires attentions and precautions that are beyond the calculation approaches traditionally applied for the study of the new structures, since the models and the calculation methods normally employed for ordinary buildings can not be uncritically used. Moreover, to add uncertainty about the methods of analysis, and interpretation of the structural behavior, it is also to be considered the fact that very often it is very difficult to identify clearly the nowadays static scheme of a building that has been modified during centuries (Betti, Orlando, & Spinelli, 2015).

In this chapter, the intent is therefore to:

- conduct a brief description of the current legislation on structural analysis in Italy, focusing on the aspects that become important with particular regard to the geometric survey and modeling of objects (2.2);
- examine which are the calculation methods that best fit to the analysis of structures made from brick and stone elements and which one is the method chosen for the exempla analysed in the present thesis (2.3);
- briefly analyse which are the calculation software used in this thesis and its salient features (2.4).

2.2. The Italian legislative framework in the field of structural analysis

2.2.1. Introduction

As it concern to the arguments of this thesis, and namely to the historical masonry building, the general legislative framework seems to be overall fragmented and difficult to consult because

it is to be considered not only a specific regulation but many. In addition to that, what is reported in the different laws it is not always enough and therefore needs to be complemented with addenda or manuals.

In detail, the main rules governing the structural analysis of masonry buildings are the following and the most important will be explained into single points:

- Technical Standards for Construction (Norme tecniche per le costruzioni, 2008) issued by the Ministerial Decree 14th January, 2008;
- Structural Eurocodes published by CEN (Committee European Normalisation - European Committee for Standardization), with specifications listed in the National Appendices or, in lack of that, in the international EN (European Normalization) form – and particular to Eurocode 6 "Design of masonry structures";
- Harmonized UNI EN whose references are published in the Official Gazette of the European Union;
- Standards for testing, materials and products published by UNI (Ente Italiano di Unificazione);
- Instructions of the Superior Council of Public Works;
- Guidelines of the Central Technical Services of the Superior Council of Public Works;
- Guidelines for the evaluation and reduction of seismic risk of the cultural heritage and as amended by the Ministry of Heritage and Culture, as licensed by Superior Council of Public Works (Linee Guida per la valutazione e riduzione del rischio sismico del patrimonio culturale, 2010);
- Operating and technical documents of the National Research Council (CNR).

Specifically, as already explained, this thesis does not even intends to investigate in-depth the analysis of the regulations and calculation methods used for masonry structures, but it rather proposes to analyse thoroughly how much the survey of the geometry, of the structure investigated, and its subsequent modeling affects the results obtained from the structural analysis. Therefore, considering what has been highlighted up to this point, it is meant in this section to focus which, in the current technical Italian laws, regarding the structural analysis of the existing historical buildings in masonry, are the aspects of particular interest within the survey and the modeling.

2.2.2. The Technical Standards for Construction

The Technical Standards for Construction, so on called NCT 2008, is the mandatory text on the *Design of Structures* in Italy. It collects, in a unitary code, the rules issued in Italy during years, which govern design, construction and testing of buildings. The aim of this new regulatory body is to ensure, for certain levels, security and public safety and, incorporating the comments and suggestions of the scientific, professional and productive world, provides to give guidelines for the calculation and evaluation of the structures, as well as instructions for proper planning and execution of the works. The NCT 2008 represent also the adoption and the implementation of the Structural Eurocodes published by CEN. The most innovative and complex topics of NCT 2008 have been explained by the further Circular 617 of 2 February 2009 *(Istruzioni per l'applicazione delle Norme tecniche per le costruzioni di cui al D.M. 14 gennaio 2008, 2009)*

The main goals reached by the NTC 2008 are therefore:

- the collection in a single and organic text of the standards previously distributed in more decrees;
- the introduction of significant changes and issues not previously considered;
- the introduction of the concept of model of performance;
- the foreword, finally, of rules for all the most common building materials (concrete, steel, wood and masonry);
- the introductory to the use and design of innovative materials;
- the adoption of supranational legislation, especially referring to Eurocodes;
- the maintenance of a necessary link with the Italian tradition on construction;
- the mandatory introduction to the seismic analysis, before treated as complementary;
- the strictly regulation of the rules which have to be applied to the drafting of the executive projects of structures.

NCT 2008 are divided into twelve chapters listed as follow:

1. Object of the law
2. Safety and performance expectations
3. Actions on buildings
4. Civil and industrial buildings
5. Bridges
6. Geotechnical
7. Designing in the presence of seismic actions
8. Existing buildings
9. Static test
10. Rules for the drafting of the executive plans and calculation reports
11. Materials and products for structural use
12. Technical Reference

The second and third chapters of NCT 2008 identify basic concepts applicable to all cases both of different kind of structures both of different use of materials.

Chapter 2 - identifies the basic principles for the safety assessment, including:

- the definition of appropriate Ultimate Limit State (ULS - SLU) and Serviceability Limit State (SLS - SLE) beyond which the structure no longer fulfils the relevant design criteria;
- the introduction to the important concepts of “Design Working Life”, “Reliability differentiation” and “Durability”;
- the definition the possible actions working on the buildings and set out which different combinations and checks have to be carried out;

Chapter 3 - encodes the analytical models for the description of the forces acting on civil and industrial structures such as permanent weights and loads, variables overload, seismic, wind, actions of snow, temperature and exceptional actions.

From the forth chapter, NCT 2008 starts to specify more deeply the various arguments:

Chapter 4 - discusses the different types of civil and industrial buildings as a function of the material used (concrete, steel, wood, masonry and other materials).

Chapter 5 - provides the general criteria and technical guidance for the design and the execution of road and rail bridges.

Chapter 6 - deals with the problem of geotechnical design distinguishing, in particular, the design and implementation of foundation works, supporting structures, underground works, works and artefacts of loose natural materials, faces of excavation, improvement and reinforcement of soils and rock masses, consolidation of the ground facing on existing structures, as well as the Safety Assessment of the slopes and the feasibility of works that have reflections on large areas.

Chapter 7 - concerns the design taking into account seismic actions. It introduces also an important paragraph dealing explicitly with the general criteria of design and modeling of structures in relation to the unavoidable use of automatic calculation programs. In paragraph concerning the methods of analysis and verification criteria, it is appropriately treated, the linear and the nonlinear analysis.

Chapter 8 - deals with problems of existing buildings, field of main interest in this PhD thesis. It introduce to general criteria on different types of buildings and the variables that allow to define the status of conservation. It also presents the fundamental distinction of three different types of intervention that can be performed on an existing construction:

- *adaptation measures*, in order to achieve the levels of security required by NTC 2008;
- *improvement measures*, which will increase the existing structural safety without necessarily reach the levels required by the NTC 2008;
- *local interventions or reparations*, which involve isolated elements but however entail an improvement of the existing security conditions.

Another important section deals with the requirements for the design of interventions in the presence of seismic actions in the different types of existing buildings, which differ substantially from the case of new buildings.

The last four chapters, from 9 to 12, assume a general point of view again and respectively refers to:

Chapter 9 - the general requirements for the static testing of the structures and the responsibility of the tester. It sets the rules on the load tests that have to be provided, with special attention to the load tests on prefabricated structures and bridges.

Chapter 10 - deals with the general rules for the arrangement of projects and structural calculation report and on the completeness of the documentation that characterizes a correct executive project. If the structural analysis and verification are conducted along with automated calculation, a specific paragraph indicates to the designer, which checks have to be made on the reliability of software used and on the trustworthiness of the results obtained.

Chapter 11 - completes the technical content of the standards by providing the qualification rules, certification and acceptance of materials and products for structural use, yields consistent with the established procedures of the Central Technical Service and the Higher Council and the European Community provisions.

Chapter 12 - indicates some of the most common technical documents that can be used whenever there are not specific indications in the NCT 2008.

As long as it concern to masonry constructions, NCT 2008 refers to them in section 5 of chapter 4: this section is particularly aimed to new buildings construction but, however, it illustrates all the information necessary to determine the parameters of the material and its mechanical properties. The most important part of the NCT 2008 for the object of the study is chapter 8, which refers to the existing building and has a specific section dedicated to masonry building. This chapter has been introduced in the standards because of the fundamental importance in Italy of the preservation of the existing architectural heritage and there is not yet an equivalent legal reference at European level, which is in fact still in the process of drafting. Just thinking to the urbanization level reached in our cities, it is evident that the need to recover what has already been built is higher than that to provide for new buildings; furthermore, the Italian culture is much more related and strictly connected to its past than other countries and, therefore, this regulatory aspect, although improvable, it is definitely at the forefront in Europe. Considering also that the largest part of the existing architectural heritage in Italy is often protected by the Ministry of Heritage and Culture and Tourism and, therefore, it is subjected to particular constraints, it is necessary to accompany the reading of NCT 2008 to the Guidelines for the evaluation and reduction of seismic risk of the cultural heritage issued by the same Ministry, described in the following section.

2.2.3. The Guidelines for the evaluation and reduction of seismic risk of the cultural heritage

With the introduction of the Ordinance of the President of the Council of Ministers no. 3274, 20th March 2003, which obligated to carry out seismic checks on strategic buildings and establishes relevant standards for the evaluation and adaptation of existing buildings, it rose the need to give practical application to the seismic safety of the cultural heritage, hitherto dealt with discontinuities, also because of the possibility of exceptions and derogation authorized by the laws, or otherwise the lack of laws. In this context, in May 2005, it was defined between the Department of Civil Protection and the Ministry of National Heritage and Culture, an institutional agreement aimed to elaborate guidelines for enforcement technique of the peculiar needs of the cultural heritage, as provided in the ordinance mentioned above. Thus it was formed a multidisciplinary team that released, a few months later, a document containing the “Guidelines for the assessment and mitigation of seismic risk of the cultural heritage”, so on called simply Guidelines. In the time between the approval of the Guidelines by the Board of Public Works and the publication in the Official Gazette, the NCT 2008 was enacted. Although under a methodological point of view the contents of the Directive were perfectly aligned with the addresses of the NCT 2008 it was necessary to provide to a harmonization between the two laws, therefore with the document approved by the Board no. 92 of Public Works in the General Assembly on 23th July 2010, the two standards have been definitely aligned.

The new Directive aims to define a path of knowledge, assessment of the level of security, against seismic loads, and design of any interventions, conceptually similar to that provided for the buildings not protected, but suitably adapted to the needs and peculiarities of the cultural

heritage, in order to formulate, as objectively as possible, the final criteria on the safety and conservation guaranteed by seismic improvement. The document, which refers only to the masonry, is completed with several attachments, insights and examples and it is divided into seven chapters as listed:

1. Object of the Directive
2. Safety and conservation
3. Seismic action
4. Knowledge of the artefact
5. Models for the evaluation of seismic safety
6. Criteria for the seismic improvement and intervention techniques
7. Summary picture of the path of seismic safety evaluation and design of seismic upgrading systems

The chapters of the Directive provides to define the seismic action, in relation to the hazardous nature of the site, to the intended use of the building, and to the capacity of the structure, through a proper understanding and modeling of the construction:

Chapter 2 - shows the safety requirements to be considered for the architectural value of art history;

Chapter 3 - provides guidance for an accurate definition of the seismic action;

Chapter 4 - explains which is the level of knowledge of the building that has to be acquired, taking into account as specified in paragraph C8A Circular, in accordance with the program for monitoring the state of conservation of architectural heritage protected, for the acquisition knowledge of Italian cultural heritage;

Chapter 5 - describes the various ways of modeling the structural behaviour of a historic masonry construction;

Chapter 6 - describes the criteria for the seismic improvement, or a reduction of vulnerability established as a consequence of the knowledge of modeling and observation of damage.

2.2.4. General criteria for the analysis of masonry preserved cultural heritage

According to the Guidelines and to the NCT 2008 for the preserved cultural heritage, in order to decide which kind of intervention has to be carried on it, must be obeyed one of the two following criteria:

- Improvement for enhancing the existing structural safety, while not necessarily reaching the levels of safety required by the NCT 2008;
- Local interventions or repairs involving isolated elements, and that in any case enhance an improvement of existing security level.

For the design of the interventions, two levels of evaluation are therefore introduced:

- LV2 (*repair or local intervention*) - in case of local interventions on limited areas of the construction, which do not alter significantly the ascertained structural behaviour, the evaluations that have to be taken in consideration are the ones for which methods of local analysis can be applied. In this case, the evaluation of the seismic action at SLV (*Stato Limite*

di salvaguardia della Vita – Ultimate State Limit of Safeguarding Life) is still required per the entire artefact, and has to be carried out with tools that allow the evaluation through simplified methods, based on a limited number of geometrical and mechanical parameters or using qualitative data (query visual, reading constructive characters, critical survey and stratigraphic).

- LV3 (*improvement project*) - In case of projects of widespread interventions in the whole construction, which anyway as far as possible should not alter the structural functions, the evaluations that have to be taken in consideration are acquired through the path of knowledge, as described both in NCT 2008 both in Guidelines, referring especially to chapter 4. The assessments must cover the entire artefact, and can use a global structural model, where this can be considered reliable, or methods of analysis provided to the local level LV2, as long as applied in a generalized equilibrium of all the construction elements. The experience acquired, as a result of past seismic events, has in fact shown that, for historical buildings in masonry, the collapse is achieved, in most cases, through the loss of balance of limited portions of the construction, defined as macro-element. The level of assessment LV3 can be used even when, in the absence of an intervention project, it would nonetheless request an accurate assessment of seismic safety of the construction.

The main goal is therefore to avoid superfluous works, supporting the criterion of minimum intervention, but also to highlight the cases when it is appropriate to operate with more incisive actions.

2.2.5. Definition of limit states of reference for cultural heritage

As it concern architectural artefacts, of historical or artistic interest, it is necessary to acquire a level of security and protection, with regard to seismic risk, through the compliance of three limit state: two of them refer to the limit states defined by the NTC 2008, while one is specific for cultural heritage.

The Ultimate State Limits, SLU, are motivated by the desire to protect the building and its occupants in the event of rare and of high intensity earthquakes: they are differentiated in State Limit of Safeguarding Life (SLV), and State Limit of Prevention of Collapse (SLC). The Serviceability Limit States, SLE, are intended to limit the damage for less intense but more frequent earthquakes: for economic and functional reasons they are differentiated into the State Limit of Operability (SLO) and State Limit of Damage (SLD). Limit states to be considered for cultural heritage are normally SLV and SLD, the definitions of which are contained in Section 3.2.1 of the NTC 2008.

There may be also further reasons in order of which it is necessary to protect specific works of art contained in the construction, intended as decorations (paintings, stucco, painted surfaces, etc.), architectural elements (altars, organs, balustrades, flooring, etc.) as well as appurtenant goods and furniture (altar, baptismal fonts, statues, etc.), for the protection of which it is appropriate to introduce a specific State Limit of Damage to artistic property, SLA, defined as follows: following an earthquake of appropriate level (usually the one considered for the SLD), the artistic heritage has to suffer the minor damage possible, such that it can be restored without significant loss of cultural value.

In conclusion:

- the evaluation in respect of the SLV is required for each protected artefact, although not subjected to continue use, as it ensures not only the protection of its occupants but also the preservation of the same artefact;
- the evaluation in respect of the SLD is required only for each protected artefact for which it is substantially necessary to ensure the functionality after the earthquake, in relation to their use;
- the evaluation in respect of the SLA, locally, is required only for each protected artefact, in the parts of the building where there are elements of particular historical and artistic value; the organs of protection may require a differentiated level of seismic protection, in relation to the historical and artistic importance of these elements, taking into account the most significant cases also the seismic action for the SLV.

2.2.6. Main indexes of seismic safety and procedure implementation

In order to define the reference level of seismic safety, the following parameters have to be defined:

V_N Rated life - it has to be defined by the analysis of the construction taking into consideration all the different aspects of its historical and technical life;

C_U Class of use – it refers to Section 2.4.2 of NCT 2008 and it defines the use of the construction in function of the presence of people.

The seismic actions are therefore valued taking into consideration a reference period V_R which is the result of:

$$V_R = V_N C_U$$

Starting from the reference period V_R, and from the considered State Limit, which is associated to an expectancy P_{V_R}, it is possible to compute the return reference period of the seismic action T_R:

$$T_R = \frac{V_R}{ln(1 - P_{V_R})}$$

Taking into consideration the three difference State Limit, as defined before, and their correspondent return reference period, it appears to be particularly significant the one referred to SLV, which represents the index of seismic safety $I_{S,SLV}$:

$$I_{S,SLV} = \frac{T_{SLV}}{T_{R,SLV}}$$

where, if $I_{S,SLV} \geq 1$ the construction can be considered safe in connection to a definite rated life and class of use, otherwise it is necessary to test its safety.

The ideal procedure for the implementation of a project of interventions, for improving the resistance of the buildings to seismic events includes:

1) achieving an adequate knowledge of the structure, through the *path of knowledge*;
2) adopting one or more mechanical models of the structure, or of its parts;
3) defining a reference level of seismic safety;
4) evaluating the rated life in the state of fact;
5) designing the seismic intervention;
6) evaluating the rated life in the state of the project;
7) adopting appropriate rules of detail in the implementation of interventions.

Since the goal of this thesis is to define how, and how much, geomatic techniques can contribute to the path of structural analysis of artefacts belonging to cultural heritage, the points that mostly interest this analysis, and on which it intends to concentrate, are the first two of the previous list.

2.2.7. The path of knowledge

Referring merely to the NTC 2008, to capitol 8, specifically dedicated to existing constructions, it can be clearly deduced how much important it is the phase of "knowledge" of the structure on which there is the intention to intervene. In particular, the standard cited above, defines three different stages leading to any further operation, and namely:

- the historical-critical analysis;
- the survey operations;
- the mechanical characterization of materials.

Once accomplished these steps can be defined the parameters related to the "level of knowledge" of the structure and subsequently to the "confidence factors", which are multiplication coefficients to be applied further to safety coefficients. It follows that the higher it is the level of knowledge of the artefact, the lower it will be the multiplication coefficient to be applied.

In the NTC 2008 these aspects are reduced to a few sections, while they are rather largely descripted in the guidelines, which define a veritable "path of knowledge", well defined and expressed according to specific analytical process.

According to the Guidelines "The knowledge of the historical construction of masonry is a prerequisite both for a reliable assessment of current seismic safety both for the choice of an effective improvement intervention". In fact, if it is clear that the problems affecting the existing buildings are the same as the historic and protected buildings, it is also equally clear that the attention necessary to analyse the characteristics and the types of intervention for the historic building will be more relevant, because it will be problematic to operate with moreover invasive probing surveys or operations.

It was therefore necessary to define different degrees of reliability, even in relation to their impact, and accordingly for every degree different methods of analysis and interpretation of

historical artefacts and a different level of detail, depending on the accuracy of survey operations, historical research, and experimental investigations.

All these operations are called “path of knowledge” and essentially consist in the following phases:

1. The identification of the building, of its location, in relation to particular risk areas, and of the relationship with the surrounding urban context; the analysis comprises schematic surveying of the building and the identification of any elements of value (the fixed decorative assets and the artistic furniture) that may affect the level of risk;
2. The geometric survey of the building in its present state, considered as a full stereometric description of the entire construction, including possible cracking phenomena and deformation;
3. The evolution of the building, as the sequence of the processing steps of construction, by the hypothetical original configuration to the current one;
4. The identification of the elements founding the resistant structural body, both from the material to the constructive point of view, with a strong focus on production techniques, construction details and the connections between elements;
5. The identification of materials, of their degradation and their mechanical properties;
6. The knowledge of subsoil and foundation structures, with reference to the changes that occurred over time and related disruptions.

Although only the second point relates specifically to the geometric survey of the building, to a careful reading it looks evident that the concept of survey is intrinsic to each of the six steps of the path of knowledge, even if it is articulated under different points of view.

The first step includes in fact a first schematic surveying of the building and its surroundings and through this operation it must be able to identify:

- the location of any elements not particularly prone to damage;
- the identification of the valuable elements, from artistic and cultural point of view;
- the identification of the possible expendable elements, when implementing any destructive investigations or locating any necessary reinforcement;
- the relationship of the building with its adjacent structures;
- the hierarchy and constructive relations between the building and the surrounding environment;
- the constituents’ bodies of the building, and namely walls, arches, columns and pillar,… .

At this stage, the analysis of spaces and functions must be accompanied by the historical investigation, since joining this information, it is possible to understand the motivations of the geometric and structural changes that have occurred over time and therefore explain any observable signs of instability on the structure, like cracks or displacements.

The second step of the path of knowledge is completely dedicated to the surveying operations, which are, as well known, devoted to the knowledge of the geometry of the body construction, both to the overall geometry than to that of the construction elements, including also the relations with any buildings in tack.

The stereometric description of the building involves the identification of all the planimetric and elevation characteristics of the building, for each level, from the outside and from the inside of the building, and therefore:

- walls;
- arches and vaults (thickness and profile);
- floors, ceilings and roof (type and warping);
- stairs (structural type);
- niches, cavities, closed openings (and in which way);
- chimneys or other included extraneous elements;
- stucco, decorations and non-structural elements;
- crack pattern and existing damages;
- out of plumb, sags, bulges, bulging, depressions in the vaults;
- type of foundations.

Although nowadays geometric techniques allow 3D representations, NTC 2008 considers traditional graphic output of the surveying as plans, elevations and sections as well as with the detail of the construction elements. Through all these operation it must be possible to correctly define the resistant structural scheme.

Considering that the main difficulties of the geometrical survey are often linked to the accessibility of certain spaces, such as attics, spaces or vaults between false ceilings and roofs, or the excessive height of the elements, as in the case of bell towers, towers, vaults in a nave, it is possible to use diagnostic techniques that through a quick acquisition return accurate results, even in the case of complex elements, like direct investigation techniques (endoscopy) or indirect (thermography, ground penetrating radar, etc.).

There is no mention in the guidelines, however, as regards the modern geometric techniques of photogrammetry and laser scanning “surveying without contact”, that suite very well to tough surveying conditions as well as to the definition of certain parameters, which would be very hardly, if not possible, measureable by direct methods.

The third step combines the historical and functional analysis of the building to the architectural surveying: through the study of the processes that rule the construction, and its subsequent changes during times, and the physical evidences that results from the survey, as well as the direct observation of the building itself.

Through this passage, it is meant to highlight:

- zones of possible discontinuities and non-homogeneities for the used materials, both in plan and elevation (added bodies, super-elevations, substitutions of horizontal elements, etc.);
- signs due to particular natural events (fire, earthquakes, floods ...) or anthropogenic (changes of use of the building, modifications or extensions ...);
- identification of the events suffered, especially those most significant and traumatic, and their corresponding effects, as ascertainable by documentary (written or iconographic sources) or through a direct surveying of the construction;

- nature of the interventions of consolidation already achieved in the past, their localization and the structural elements involved, the period of realization and the verification of their effectiveness over time.

This step of the analysis will be the guide for the subsequent definition of the most critical mechanisms of damage and for the consequent definition of reliable calculation models.

Steps from fourth to sixth are not directly related to the geometric survey and discuss about problems related to:

- definition of materials and of the state of conservation of the building;
- definition of the mechanical parameters related to the materials;
- geotechnical characteristics;

In particular, it will be necessary to integrate the survey with tests and specific mechanical evaluations or, at least, if it is not possible to operate with invasive techniques, with the comparison with almanacs of different construction types, reasoning by analogy, and tables with reference values of the mechanical properties, derived from experiments.

2.2.8. Levels of knowledge and confidence factors

Once the construction has been clearly identified, in relation to the completeness of the geometric survey and of the investigation with regards to the materials of construction, to the mechanical characteristic and to the ground and foundations parameters, the designer hires a confidence factor F_C, which can vary among 1 and 1,35; this allows to grade the reliability of the structural model and to take into account the evaluation of seismic safety index (or the rated life).

Masonry is a material presenting distinct directional properties due to the mortar joints, which act as planes of weakness. In general, the approach towards its numerical representation can focus on the micro modeling of the individual components or the macro-modeling of masonry as a composite material (Lourenċo, 2002) as it will be better described in the following section. According on these two types of representations, for the choice of the seismic safety evaluation it is necessary to value if the model considers:

- deformability and strength of materials and structural elements;
- balance limit of the different elements of the building, by considering the masonry material as rigid and resistant to traction.

For each of these classes it will follow a particular strategy of allocating F_C, regulated by the Circular No. 617 of the Council of Public Works of February 2nd, 2009, which is complementary to NCT 2008. In both cases, the definition of the confidence factor F_C will be referred to the material/type that more penalizes the specific mechanism of damage/collapse under examination. According to the guidelines, the confidence factor F_C is given as:

$$F_C = 1 + \sum_{k=1}^{4} F_{Ck}$$

set on the basis of numerical coefficients reported in *Table 2.4*, to which are associated the four categories of investigations and subsequently the level of knowledge reached, in *Table 2.5*.

Geometric survey	Geometric survey complete.	$F_{C1} = 0$
	Geometric survey complete, with graphic reconstruction of cracks and displacements.	$F_{C1} = 0{,}05$
Historical phases of the building and characteristic of the construction	Hypothetical reconstruction of the construction phases based on a limited material survey and documental analysis.	$F_{C2} = 0{,}12$
	Partial reconstruction of the construction phases based on: a) limited material survey and documental analysis and a complete structural history of the building; b) complete material survey and documental analysis.	$F_{C2} = 0{,}06$
	Complete reconstruction of the construction phases based on a complete material survey and documental analysis and a complete structural history of the building.	$F_{C2} = 0$
Mechanical properties of materials	Mechanical properties derived from available documentation.	$F_{C3} = 0{,}12$
	Limited set of test and survey of materials.	$F_{C3} = 0{,}06$
	Complete set of test and survey of materials.	$F_{C3} = 0$
Ground and foundations	Limited set of test and survey on ground and foundations, in absence of documentation.	$F_{C4} = 0{,}06$
	Limited set of test and survey on ground and foundations, with limited documentation.	$F_{C4} = 0{,}03$
	Complete set of test and survey on ground and foundations.	$F_{C4} = 0$

Table 2.4 – Definition of the confidence factors

Level of knowledge	**Geometry**	**Building details**	**Materials properties**	**Analysis method**	F_C
LC1	Surveying of walls, vaults, horizontal structures, and stairs. Definition of loads on each constructive element. Surveying of cracks and displacements.	Limited in situ test and survey	Limited in situ test and survey	Limited in situ test and survey	1,35
LC2		Complete in situ test and survey	Extended in situ test and survey		1,20
LC3			Complete in situ test and survey		1,00

Table 2.5 – Definition of the confidence factors

In these regulatory steps, the value of the geometric survey, in relationship to other kind of investigations, can be weight according to the Council of Public Works: if the graphical representation of crack patterns and deformation is not produced, the confidence factor worse 5%,

roughly as if a partial knowledge of the construction phases and interpretation of the structural behaviour or only limited investigation of the mechanical parameters of materials (Visintini & Spangher, 2013).

The explaining of the construction phases shall be articulated through specific drawings that allow to relate the different components of the building with its constructive epochs; these sequences, hypothesized, partial or comprehensive, have to be accompanied by a synthetic justification of the proposed historiographical reconstruction, for example from: historical records available, the result of targeted diagnostic tests, readings issues facing the geometry and/or metrology factory, by analysis of the masonry, from stratigraphic investigation, by comparative considerations etc.

In the case of presence of different structural materials, the level of detail and the resulting confidence factor F_{C3} can be related to the material or the materials which are more influential on the determination of the index of safety. In the case where the seismic analysis is based on the evaluation of several distinct local mechanisms, for each of them must be defined different levels of knowledge and partial confidence factors.

2.3. Analysis method for existing buildings

2.3.1. Main characteristic of masonry

In order to introduce the topic on the structural analysis of masonry buildings it is necessary to make some clarifications concerning the main characteristics of this type of construction.

First of all, masonry has the following characteristics relative to the mechanical behaviour:

- *Non-homogeneity*: due to the fact that mortar and bricks have completely different mechanical characteristics, and it is not sufficient to know the mechanical characteristic of each of them, to determine how the performance of the whole complex will evolve, since it often happens that chemical-physical reactions are established between the two composing elements and the final behaviour seems to be different from what expected;
- *Anisotropy*: due to the intrinsic directionality of masonry itself as well as the shape and the proportions of the elements that compose it;
- *Asymmetry of behaviour* as already known masonry has no tensile strength;
- *Non-linearity* of the bond stress-strain.
- Secondly, the behaviour of masonry is given also by (Pinto & Franchin, 2008):
- 1. morphology of the wall;
- 2. level of connection between the various elements that constitute the masonry itself;
- 3. level of connection between the various parts that constitute the building.
- depending, all of these variable elements both on the historical period both on the function of the building both on the location and construction techniques in use.

As concern to the first point, there are several classifications of wall surfaces according to the constructive features, those that are analysed in this context are the ones, which, in some way, affects the modeling of the structural behaviour of the wall (*Figure 2.6 a)*). Often walls have no monolithic behaviour because their structure is made of small pebbles or by two external leaves

even well ordered but not mutually connected, sometimes containing a rubble infill (Binda, Cardani, & Saisi, 2005) so it assumes an evident importance to identify which type of masonry it has to be referred in order to get a realistic model of the structural behaviour, as it is possible to deduce by the following *Figure 2.6 b)*.

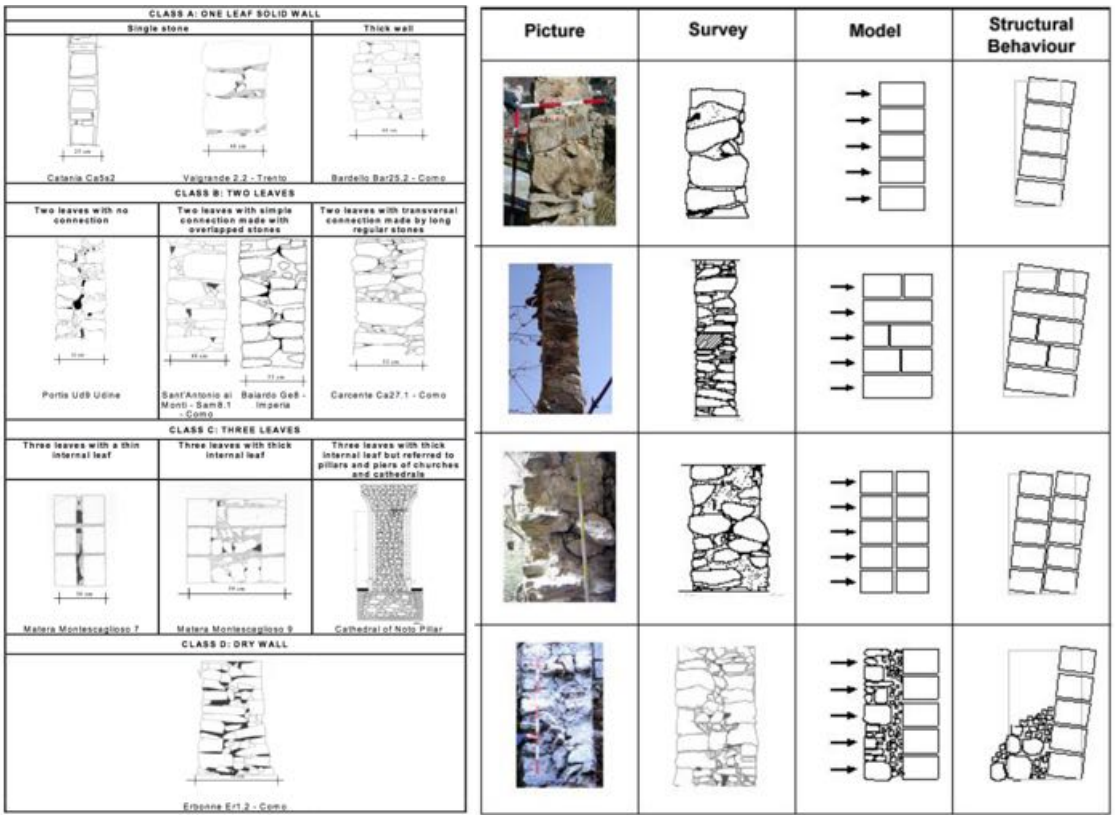

Figure 2.6 – a) Classification of stonework masonry
b) Structural behaviour of different typologies of walls (Binda, Cardani, & Saisi, 2005)

Following the traditional classification of stone masonry held in the Italian territory in the early ninety's by Binda (1999) or by Giuffrè (1991) it is possible therefore to identify four different types of wall section:

a) single leaf or solid;
b) two leaves with or without connection;
c) three leaves;
d) dry walls.

In order to determinate the level of connection between the various elements that constitute the masonry itself, second circumstance that affects the structural behaviour of the structure, it is necessary to know:

- dimension of the elements;
- shape and workability of the stones;
- texture of the wall;
- presence of diatons in the wall section;
- mortar quality and quantity;

- presence of wedges;
- presence of clear horizontal courses.

All of these characteristics depend upon the time and the location of the construction and for this reason during years have been produced different catalogues and databases containing many different masonry sections from various Italian Regions classified by the percentage of mortar, void and stone, the distribution of stones, the texture and so on (*Figure 2.7*).

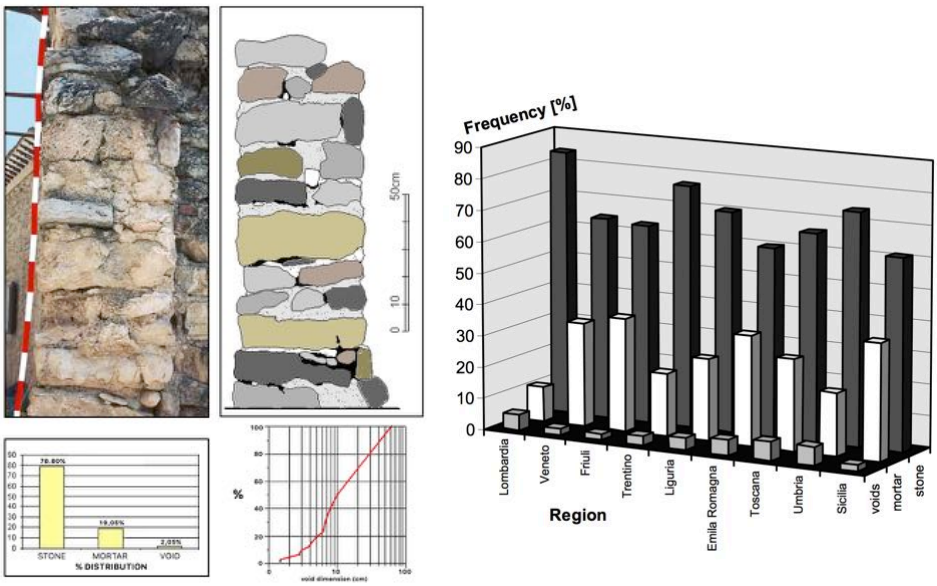

Figure 2.7 – a) Section of the wall with determination of the percentage of void and mortar b) Percentage of void, mortar and stone in different regions of Italy (Binda, Cardani, & Saisi, 2005)

As it concern to the third point of the list, and namely to the level of connection between the various parts of the building, it is necessary to refer to the different typologies of structures which are representative of the building function, and to the mechanisms of damage and failure they are subjected to. Many studies and classification of mechanisms of damage and failure have been held on structures and the most important are reported in the following list:

- *Simple overturning of the wall* - is manifested through the rigid rotation of entire facades or portions of walls with respect to axes mainly horizontal at the base of them and that run through the wall structure stressed by actions outside the plane;

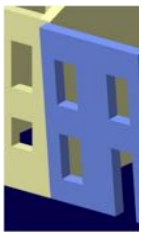
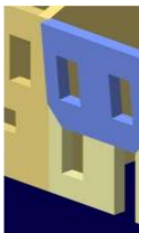

- *Complex overturning of the wall* - is appears when there is a rigid rotation of entire facades or portions of walls than horizontal axes mostly accompanied by dragging parts of the walls belonging to the shear walls.


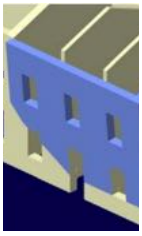

- *Vertical bending of the wall* - is manifested by the formation of a horizontal cylindrical hinge that divides the wall into two blocks and is described by the mutual rotation of the same about said axis for actions outside the plane.

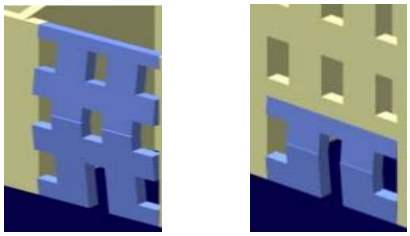

- *Horizontal bending of the wall* - is manifested by the ejection of material from the summit area of the wall and with the detachment of cuneiform bodies accompanied by the formation of plastic hinges oblique and vertical actions out of the plane.

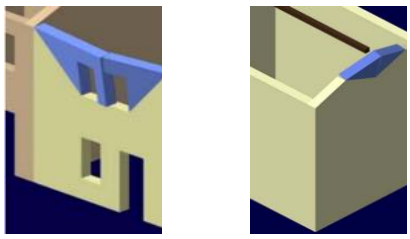

It has been proved in fact that frequently the same typologies suffer from structural damages similar of the special typology, or, otherwise, to the same combination of mechanisms, and therefore have been defined the typologies of *Figure 2.8* (Binda, Cardani, & Saisi, 2005).

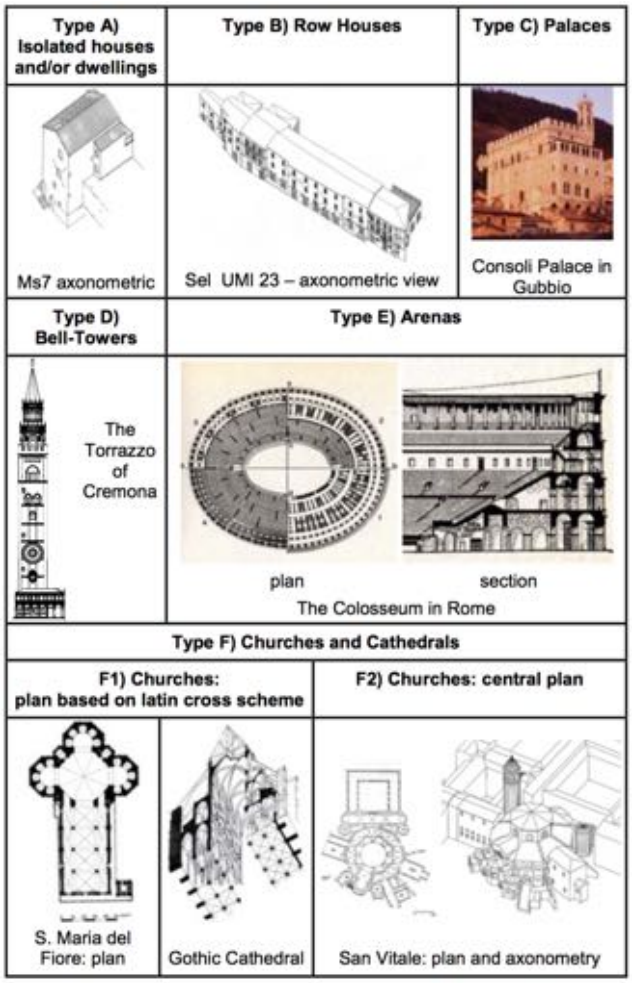

Figure 2.8 – Building typologies (Binda, Cardani, & Saisi, 2005)

2.3.2. Modeling masonry

In the assessment of an existing building, accuracy of the method of analysis has a crucial importance, since by an accurate analysis a conservative method may indicate unnecessary expensive interventions while a non-conservative one may leave the building exposed to an excessive risk *(Pinto & Franchin, 2008)*. In contrast, from the above evaluation, it is clear that the numerical modeling of a masonry structure is complex and, above all, involves the adoption of significant simplifications.

In the last decades, various methods for the resolution of this problem have been proposed based on the degree of complexity, size of input data, and required accuracy and which take into account that the composite nature of masonry is the main cause of its non-linear and complex behaviour. The best method to use is determined each time in function of the object that is going to be analysed, comparing results and choosing the one that minimize the error.

Generally, two basic approaches are used in numerical modeling of masonry structures and namely idealization using the continuum or discontinuum, and, as second step, it has to be taken into consideration also the level of simplicity and accuracy, and, explicitly micro-modeling, simplified micro-modeling, and macro-modeling *(Smoljanović, Živaljić, & Nikolić, 2013)*.

Continuum hypothesis assumes that strains and deformations across the observed structure are described by continuous functions, and this method refers to the *Finite Element Method* (FEM) in order to find an adequate numerical solution. On the other hand, in discontinuum hypothesis, the structure is supposed to be composed by discrete elements, which are analysed separately, and then combined in a mutually dynamic interaction. Numerical models that use this approach are included in *Discrete Element Methods* (DEM).

Regardless the assumed hypothesis the levels of simplicity, as before listed, are:

macro-modeling	equal characteristics are assumed for all the points of the structure, according a homogenization factor for the materials, and masonry is treated as a homogeneous anisotropic continuum. This approach is appropriate when analysing larger structures because the calculation is numerical less demanding (*Figure 2.9 a)*);
micro-modeling	blocks and mortar are modelled separately, each one with its constitutive law, with finite elements, while the connection between the block and mortar is presented with contact elements. This approach is appropriate for modeling smaller structures because of big calculation demands (*Figure 2.9 b)*);
simplified micro-modeling	blocks are modelled with finite elements while the mortar is described with contact elements that also represent potential cracking points. The constitutive law of mortar, which greatly affects the compressive strength, is not taken in consideration (*Figure 2.9 c)*).

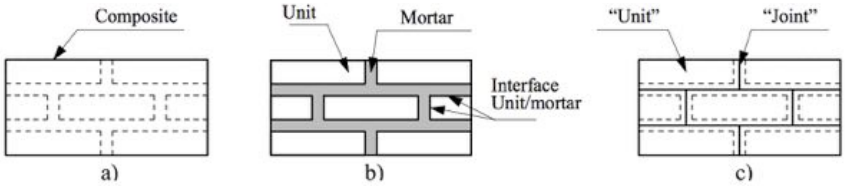

Figure 2.9 - Levels of modeling of masonry structures:
a) macro-modeling; b) micro-modeling; c) simplified micro-modeling; d)

A wide set of possibilities have been developed to describe masonry structures to different levels of accuracy, from rough (but useful) *engineering approaches* to very detailed modeling taking into account the distinct response of the individual components. A very significant effort is undertaken at present to produce homogenization criteria allowing a better interconnection between the micro- and macro-analysis levels. At the present time, micro-modeling and simplified micro-modeling are still requiring high computer effort and, in practice, can only be used to analyse small individual structures such as solid or hollow walls. Moreover, sophisticated methods often require complex material properties, which can only be determined through costly and sophisticate laboratory experiments. In the case of the study of real buildings, such properties are not normally available and need to be indirectly estimated on more common and available evidence *(Roca, Cervera, Gariup, & Pelà, 2010)*.

As it concerns to the numerical method used for compute the structural analysis, as reported before, the most used are the finite elements method and the discrete element method, widely described in scientific literature, and not reported here. Since the goal of this thesis is to verify how a 3D model, obtained through geomatic techniques, can be used for structural analysis, the chosen method is the simplest FEM, because of its adaptability to the needs of the considered problem.

2.3.3. Finite Element Analysis Method

The *Finite Element Analysis* (FEA) is a numerical method oriented to seek approximate solutions to problems described by differential equations, reducing them to an approximate system of algebraic equations. As anticipated in paragraph 2.1, it was born around 1950, as a branch of Solid Mechanics but it is nowadays commonly used for multiphysics problems, such as:

- structure analysis;
- solid mechanics;
- dynamics;
- thermal analysis;
- electrical analysis;
- biomaterials.

The FEA method involves therefore the application of algebraic equations and simplified conditions on the discretization of the continuous body that is going to be analysed, and the sub sequential recombination of the results, in order to represent them on the total body.

The greater is the number of the elements used to describe the body, the better definition is reachable for shape and dimension. In the continuum, each finite element is considered a field of numerical integration of homogeneous characteristics.

The main feature of the finite element method is the discretization by creating a grid (mesh) made up of primitives (finite element) in encrypted form (lines in 1D domains, triangles and quadrangles in the 2D domains, hexahedrons and tetrahedrons for the 3D domains – as represented in *Figure 2.10*). The formulation is based on the fact of creating a correspondence between an element of any shape in the Cartesian system (X, Y, Z) and an element of simple shape in the natural system (ξ, ψ, ζ) by the shape functions.

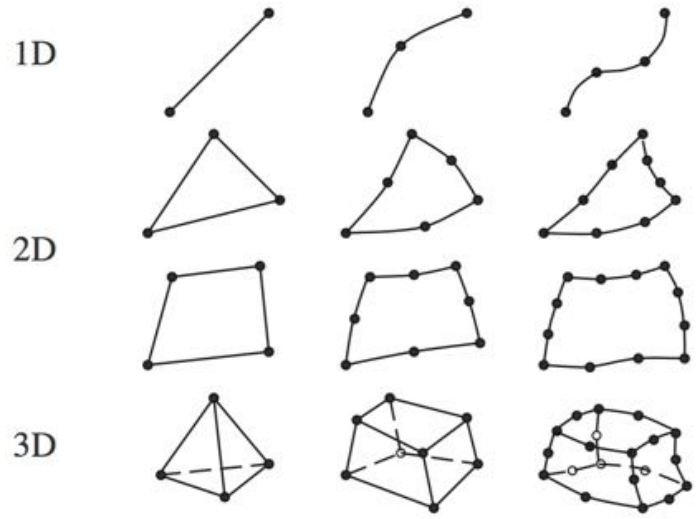

Figure 2.10 – Different types of finite elements: one, two and three-dimensional

Therefore, starting from the structure to analyse, it is necessary to create a model, as much representative of reality as possible and then to adopt the following procedure *(Gugliotta, 2002)*:

1. division of the structure into n-elements;
2. mapping and matching of the equations governing the elements and the equations governing the structure;
3. calculation for each element of the stiffness matrix and of the vector of equivalence of the loads element-structure;
4. setting of the boundary conditions;
5. solution of the system in terms of general displacement;
6. calculation of reaction forces;
7. calculation, starting from the displacements, of forces and stresses of each element.

As it concern with the argument of this thesis, the steps of interest are only the first phases of modeling of the structure and its discretization, as the other successive steps are not involved with Geomatics. In order to verify the results, obtained with the methods of modeling tested, different software for FEA have been used, however, without getting the heart of the matter on the different algorithms that rule them.

In order to define the characteristics considered for the analyses, the following simplifications and criteria were taken:

- strains and deformations across the observed structure have been described by continuous functions;
- linear elastic analysis, considering that this hypothesis is valid within the limits of the effect of the "natural pre-compression", due to gravitational loads (with a clear prevalence of weight) that makes up the strain "request" resulting from bending effects;
- only static analysis, since the purpose was to test the geometric model and not to test how the structural analysis works;
- modeling have been held with three-dimensional elements;
- composite material with mechanical characteristic defined by the combination of characteristic of mortar and blocks.

2.3.4. Algorithms and software used for the structural analysis

During the last decades many commercial software (*Table 2.11*) have been implemented for the specific needs of structural analysis of masonry, and many of these belong to the Italian panorama, because of the large interest set on the existing structures that compose the Italian building heritage. Mainly three different approaches are used for the analysis:

- FEM, as previously defined;
- Simplified Calculation Mode (SCM), is a method that provides the calculations of efforts through the redistribution of forces on each resistant walls, proportionally to their relative stiffness in each direction and the compatibility of the displacements of resulting from the formation of rigid diaphragms formed by the slabs;(Quim, Lima, & Silva, 2012);
- Storey Mechanical Analysis (Storey Mech.), it is a method based on FEM but operate verifying singularly each wall basing on the Equivalent Structure Model.

Program	Country	Code	Approach	Web adress
AEDES	Italy	Italian	FEM and SCM	www.aedes.it
CMT+L	Spain	Eurocode	FEM	www.arktec.com/cmtl.htm
FEDRA	Norway	Eurocode	FEM	www.runet-software.com/FEDRA.htm
WIN-Statik MurDim+	Sweden	?	?	www.strusoft.com
Por 2000	Italy	Italian	SCM	www.newsoft-eng.it/Por2000.htm
TQS CAD/Alvest	Brazil	Brazilian	?	www.tqs.com.br/v13/alvest.htm
Tricalc.13	Spain	Eurocode	FEM	www.arktec.com/new_t13.htm
Tricalc.17	Spain	Spanish	FEM	www.arktec.com/new_t17.htm
WinMason	USA	USA	Storey Mech.	www.archonengineering.com/winmason.html
3DMacro	Italy	Italian	SCM	http://www.3dmacro.it/
3Muri	Italy	Italian	SCM	www.stadata.com
ANDILWall	Italy	Italian	SCM	www.crsoft.it/andilwall
MURATS	Italy	Italian	Storey Mech.	www.softwareparadiso.it/murats.htm
Sismur	Italy	Italian	Storey Mech.	www.franiac.it/sismur.html
TRAVILOG	Italy	Italian	Storey Mech.	www.logical.it/software_travilog.aspx
Tecnobit	Italy	Italian	Storey Mech.	www.tecnobit.info/products/murature.php
CDMaWin	Italy	Italian	FEM and SCM	www.stsweb.net/STSWeb/ITA/homepage.htm

Table 2.11 – List of wide used software for analysing masonry (Marques & Lourenço, 2011)

The software used for the verification of the models, which have been studied in this thesis, don't belong to the above list, but are more general FEM software that can be used also for other materials, and were essentially two:

- Lisa Finite Element Analysis 8.0.0™ (LisaFEA) (Sonnenhof Holdings, 2013), which is a software that allows the modeling of structure through mono-bi-tri-dimensional elements (like the ones of *Figure 2.10*) and once assumed the right loads and constraints proceed with the analysis solving the model with the FEM. It has been used to test the obtained results;
- Scan-and-Solve™ (Intact Solutions, Inc., 2014), which is a plug-in of the 3D modeling software Rhinoceros (Robert McNeel & Associates, 2014). Through a procedure that will be further explained, allows conducting a structural analysis directly on a 3D model, as long as it is a 3D solid model or a closed surface. It has been used to analyse the processed models obtained directly from the laser scanning survey.

While Lisa FEA follows, in terms of algorithms, the classical computational analysis, with the discretization of the model into frame elements, mesh or ashlars and with the calculation of forces and reactions at a nodal level, Scan-and-Solve adopts a completely different principle and suitable for the purpose of the research, that it is therefore considered useful to be summarize in this sub paragraph. The approach, proposed by Scan-and-Solve developers, is a Solution Structure Method (SSM) based on the idea to create separate geometric and physical representation of the model to analyse and to combine them only when it results necessary. This methodology offers the opportunity to use native geometry of the object and therefore the pre-processing phase of structural 3D modeling is unnecessary, with a great saving of time and also with the advantage of preserving from errors due to interpretation of geometry and modeling. The procedure is therefore in the following described (Freytag, Shapiro, & Tsukanov, 2011)

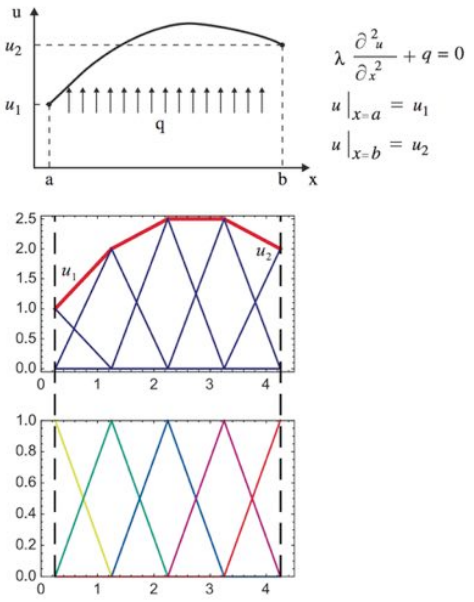

Figure 2.12 a) String in tension. Problem formulation b) Finite element solution with Galerkin formulation

The classic FEM design is usually built upon the Galerkin formulation, which is based on the discretization of the domain into *n*-parts and the application of a shape functions to each single portion. Considering a common one-dimensional example (*Figure 2.12 a)*) of a string subjected to an axial tension λ, fixed at the extremities, and loaded by a vertical force q, it will be demonstrated, via the Galerkin method, what will be the shape of the string by determining the vertical displacement $u(x)$.

In this example the 1D element is divided into smaller segments (*Figure 2.12 b)*) where the first node coincides with point a and the last node to point b, so that the displacements u_1 and u_2 may be enforced at these locations. This condition necessarily means that the finite element meshes have to conform to the domain's boundary.

The vertical displacement is therefore a linear combination of shape functions χ_i so represented:

$$u = \sum_{i=1}^{n} C_i \chi_i$$

where the shape functions takes the value of 1 at the corresponding node of the mesh and 0 in all the other nodes. This represents an approximate solution of the problem and it is therefore necessary to minimize the residuals, operation possible through the weighted residual method, which requires that:

$$\int_a^b \left(\lambda \frac{\partial^2 u}{\partial x^2} + q(x)\right) \chi_j(x) dx = 0 \qquad j = 2, \dots, n-1$$

Therefore, substituting the displacement as explicated before and applying the boundary condition it is possible to obtain the following equation:

$$-\sum_{i=2}^{n-1} C_i \underbrace{\int_a^b \frac{\partial \chi_j}{\partial x} \lambda \frac{\partial \chi_i}{\partial x} dx}_{\text{stiffness coefficient}} = \underbrace{-\int_a^b q(x)\, \chi_j dx}_{\text{load due to force q}} + \underbrace{u_1 \int_a^b \frac{\partial \chi_j}{\partial x} \lambda \frac{\partial \chi_1}{\partial x} dx + u_2 \int_a^b \frac{\partial \chi_j}{\partial x} \lambda \frac{\partial \chi_n}{\partial x} dx}_{\text{load due to applied displacement at the nodes}}$$

which solution allows to obtain the values of C_i to assume in the determination of the displacement.

The SSM of Scan-and-Solve applies instead the concepts of Kantorovich and Rvachev to the classical FEA based on the key idea that the solution of a different equation with homogenous Dirichlet boundary conditions $u|_{\partial\Omega} = 0$ can be represented in the form:

$$u = \omega \Phi$$

where ω is a know function that takes zero values on the boundary of the domain and positive inside the domain, and Φ is an unknown function. Since it is not possible to determine function Φ exactly it will be necessary to approximate it by a finite linearly independent series of basis functions:

$$\Phi = \sum_{i=1}^{n} C_i \chi_i \Rightarrow u = \omega \sum_{i=1}^{n} C_i \chi_i$$

where C_i represent a scalar coefficient and χ_i are some basis functions which do not affect the discretization of the domain.

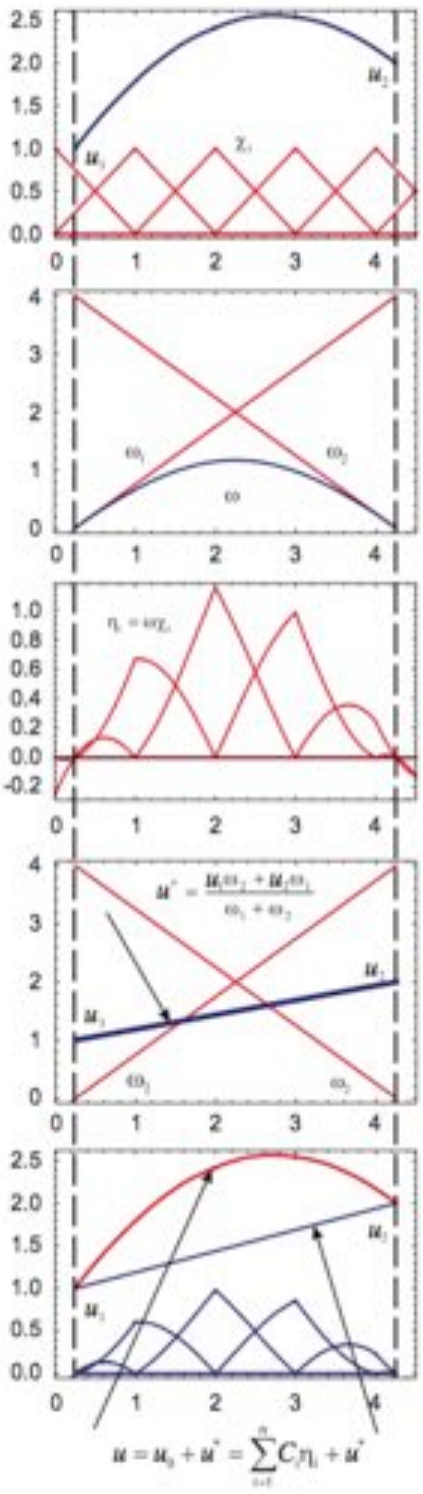

Figure 2.13 – Solution of 1D string through SSM

Applying this method to the same case of 1D element it will be possible to operate differently and instead of meshing the domain it will be associated to the string a uniform grid formed by a regular range on the *x*-axis and a basis function associated with each grid point (*Figure 2.13*). The most noticeable aspect is the separation between the grid and the boundary domain even if there is the assumption of the same basis function of the previous method for shape functions.

The basis functions are therefore created following Kantorovich idea, assuming ω as a smooth function measuring approximate distance to the end points of the segment (0 in points a and b and maximum in the middle of the segment):

$$\eta_i = \omega\chi_i \qquad\qquad i = 1, \dots, n$$

The displacement is therefore:

$$u = u_0 + u^* = \sum_{i=1}^{n} C_i\eta_i + u^*$$

Applying therefore the same weighted residual method it is possible to obtain:

$$\int_a^b \left(\lambda\left(\frac{\partial^2 u_0}{\partial x^2} + \frac{\partial^2 u^*}{\partial x^2}\right) + q(x)\right)\eta_j\,(x)dx = 0$$

and, after expanding u_0 as a linear combination of functions η_i and using the divergence theorem the previous equation becomes:

$$-\sum_{i=1}^{n} C_i \underbrace{\int_a^b \frac{\partial \eta_j}{\partial x}\lambda\frac{\partial \eta_i}{\partial x}dx}_{\textit{stiffness coefficient}} =$$

$$= \underbrace{-\int_a^b q(x)\,\eta_j dx}_{\textit{load due to force q}} + \underbrace{\int_a^b \frac{\partial \eta_j}{\partial x}\lambda\frac{\partial u^*}{\partial x}dx}_{\textit{load due to applied displacement}}$$

which appears to be very similar in its structure to the FEM equation except to the boundary condition, that, in this case, are enforced at every point on the boundary.

Generalizing to the full 3D problem of static elasticity (*Figure 2.14*), starting from the 1D string so far analysed, it is important to refer to the following energy balance statement:

$$\int_{\Omega} \mathcal{E}^T \boldsymbol{\sigma}\, d\Omega = \int_{\Omega} \boldsymbol{u}^T \boldsymbol{F} d\Omega + \int_{\Gamma_t} \boldsymbol{u}^T \boldsymbol{T} d\Gamma_t$$

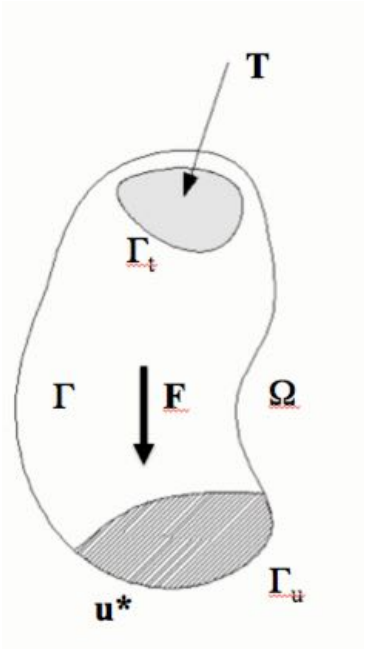

Figure 2.14 – Schematization of a 3D solid domain

where:

Ω	3D solid domain
Γ_t	boundary of the domain where the loads applied
Γ_u	boundary of the domain where displacements are prescribed
Γ	free boundary
$\boldsymbol{T}$	loads (or tractions) applied to the boundary
$\boldsymbol{F}$	forces applied to the body (like gravity)
$\boldsymbol{\sigma}$	stress
$\mathcal{E}$	strain
$\boldsymbol{u}$	resulting displacement, which has the gen form of $\boldsymbol{u} = \sum_{i=1}^{n} \boldsymbol{C}_i \boldsymbol{\eta}_i + \boldsymbol{u}^*$

Applying therefore the appropriate substitutions and taking into account again the weighted residual statement, considering also that $\boldsymbol{B}$ represent the strain-displacement matrix of derivates, so that $\mathcal{E} = \boldsymbol{B}[\boldsymbol{u}]$, and $\boldsymbol{D}$ the stress-strain matrix, so that $\boldsymbol{\sigma} = \boldsymbol{D}\mathcal{E}$, it results the following system of *n* linear equations:

$$-\sum_{i=1}^{n} \mathbf{C}_i \underbrace{\int_{\Omega} \boldsymbol{B}^T[\boldsymbol{\eta}_i]\boldsymbol{D}\boldsymbol{B}[\boldsymbol{\eta}_i] d\Omega}_{\text{stiffness coefficient}} = \underbrace{-\int_{\Omega} \boldsymbol{\eta}_j \mathbf{F} d\Omega}_{\text{load due to force}} + \underbrace{\int_{\Omega} \boldsymbol{B}^T[\boldsymbol{\eta}_i]\boldsymbol{D}\boldsymbol{B}[\boldsymbol{u}^*] d\Omega}_{\text{load due to applied displacement}} - \underbrace{\int_{\Gamma_t} \boldsymbol{\eta}_j \boldsymbol{T} d\Gamma_t}_{load\ due\ to\ applied\ loads}$$

Solving this linear system, it is possible to obtain an approximate solution of $\boldsymbol{u}(x)$ and, consequently, of all the other components needed to define structurally the problem, like stresses and strains and so on.

The functions $\boldsymbol{\omega}$ used by Scan-and-Solve have to comply with the conditions of smoothness and positivity inside the boundary, efficiency and rapidity of differentiability, and of zero value in the boundary conditions, where the displacement is specified. The functions of the Euclidean distance do not fully satisfy these conditions and it is therefore indispensable to simplify them through the use of smooth basis function. The use of these functions excellently

generalizes the problem but makes the computation really onerous and therefore it is necessary to proceed to voxel geometry.

Without getting the heart of the matter, the aspects that regulate this issue $\boldsymbol{\omega}$ functions take this aspect:

$$w(X,Y,Z) = \sum_k \sum_j \sum_i d(i,j,k) \cdot h(X - X_i) \cdot h(Y - Y_i) \cdot h(Z - Z_i)$$

where i, j, k are indices into the neighbourhood of samples around the point (X, Y, Z) and (X_i, Y_i, Z_i) are the coordinates of each sample and where the size of the neighbourhood is determined by the size of the kernel through sinc-functions windowed, which is a type of function with zero value outside of a certain range.

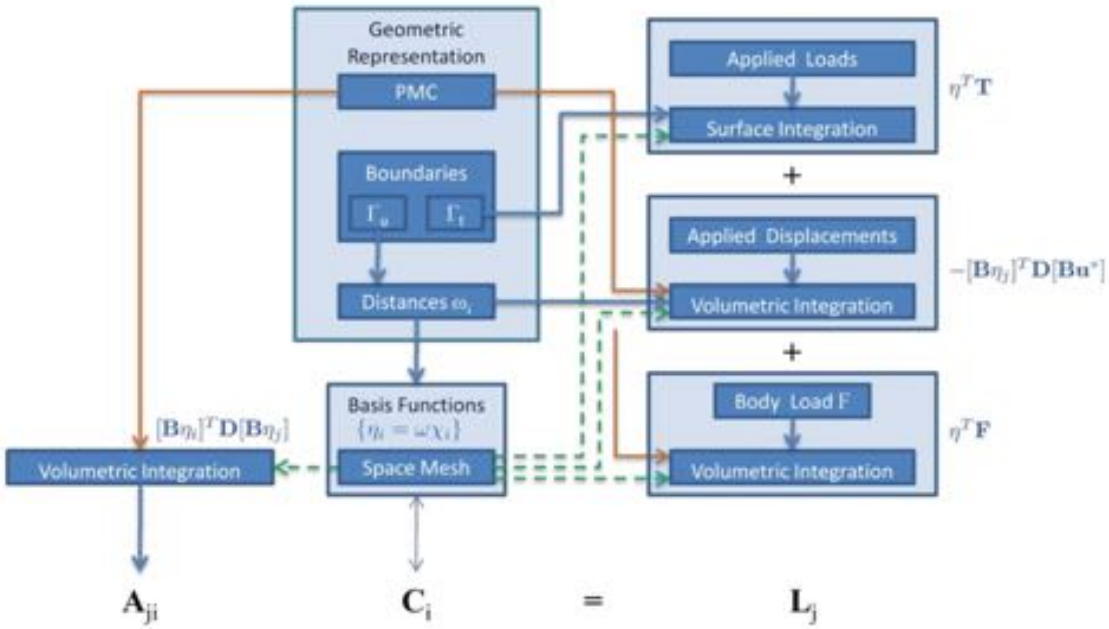

Figure 2.15 – The overall structure of the Scan-and-Solve system

With the equations so far illustrated and with the assumptions made, it is now possible to define the schema that describes the assembly process (*Figure 2.15*) that is solved through processes of sampling.

The most interesting aspect concerns the fact that are created separate physical and geometric representations of the model in question, and that the same are then combined only when necessary.

Therefore, the solution of the linear system is implemented on the physical "fictitious" model and then "projected" on the real geometric model through parameters of adaptation, well argued in *(Luft, Tsukanov, & Shapiro, 2008)*).

2.3.5. Example of analysed structure with Scan-and-Solve

Even if Scan-and-Solve was initially developed for reverse engineering, and therefore more strictly for mechanical simulations, it can be used also for basic structural analysis. So far the existing example refer all to objects modelled, on purpose, on the Rhinoceros environment software and not derived from a TLS surveying.

The most significant available examples are:

- the "Arc de Triomphe" in Paris, which is a model (*Figure 2.16 a)*) modelled in truth in SketchUP (Trimble Navigation, 1999) by (Thrall, 2006) of University of Wisconsin-Madison, made by 280 polygons, then imported into Rhinoceros and finally analysed for its own gravity stress (*Figure 2.16 b)*) (Intact Solutions, Inc., 2014).

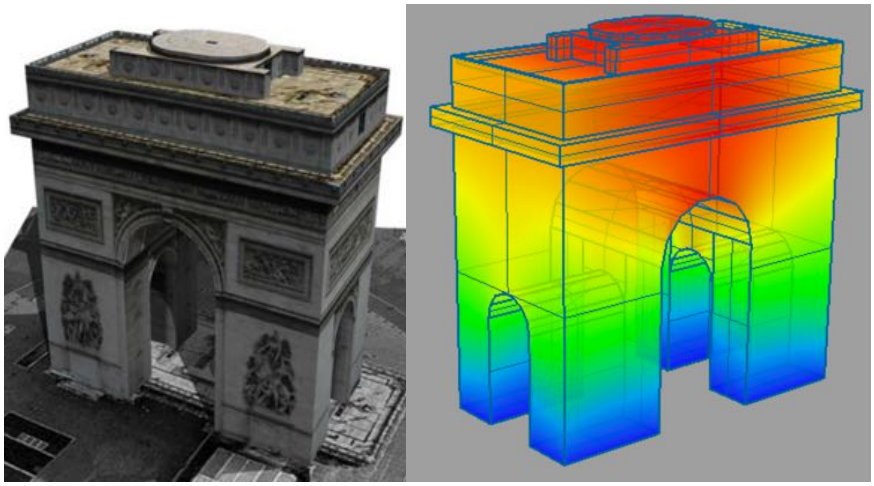

Figure 2.16 – a) Model of the Arc de Triomphe b) Model analysed for gravity stress

- the "*Dome*", which is a model (*Figure 2.17 a)*) designed by Michael Freytag (Intact Solutions, Inc., 2014), made by 212 polygons, realised into Rhinoceros and the analysed for stress analysis under gravity, in case of failure when the foundation disappears under one of the twelve pillars. (*Figure 2.17 b)*).

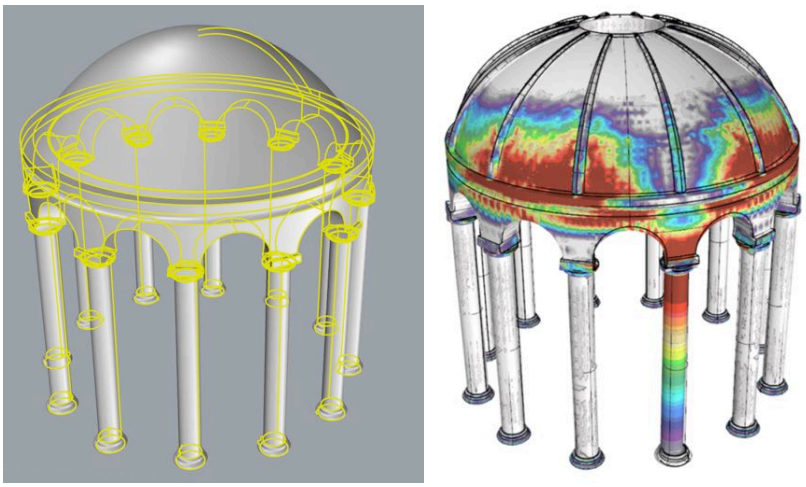

Figure 2.17– a) Model of the dome in Rhinoceros
b) Failure when the foundation disappears under one pillar.

- the model of the "Church of St. Jame's apostolate in Padova": performing seismic analysis on the bell tower. The model designed by Daniele Nale, an Italian engineer, a private user of the software. The model is realised into Rhinoceros but no more information are given about it, except that the bell tower was analysed under the possible seismic forces (Intact Solutions, Inc., 2014). (*Figure 2.18 a) and b)*).

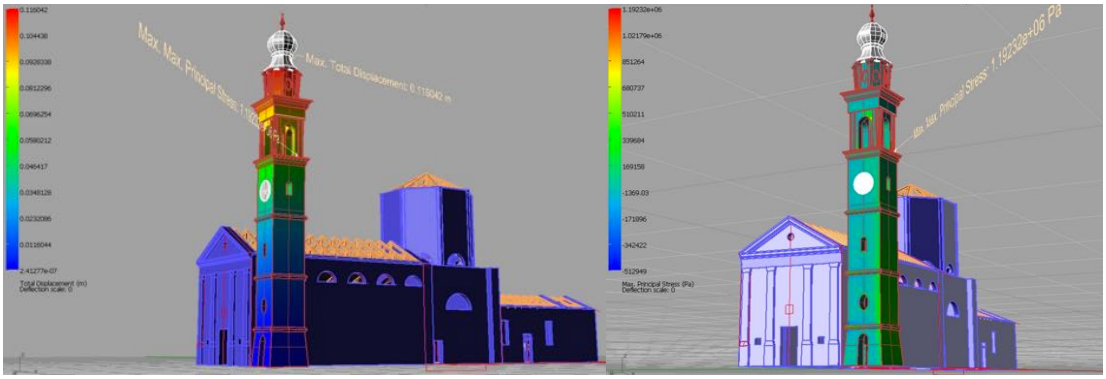

Figure 2.18– a) Maximum displacement resulting from analysis
b) Maximum principal stress resulting from analysis.

2.4. Conclusions

In this second chapter were introduced the basic notions of structural analysis, in particular relation to masonry constructions. After an overview on the specific laws and standards ruling this branch, the difficulty of the analysis of the existing buildings were focused on together with the possible approaches to their solutions. Among the various possibilities of structural calculus, for the analysis of the cases described in the following chapters 3, 4 and 5, it was chosen the FEA method, which was therefore described.

Beside the essential theory, explained in the last two paragraphs, were introduced the software used for FEA, with a short explanation of their characteristic and with the description of some examples.

Concluding, the challenge of this thesis will be the transformation of the 3D models obtained from a TLS surveying into suitable models for FEA, scilicet models with geometric characteristics well defined, continuous and without open edges, holes, non-manifold surfaces or other various discrepancies.

2.5. Bibliography

Betti, M., Orlando, M., & Spinelli, P. (2015). La Rocca Strozzi a Campi Bisenzio: Analisi strutturali e proposte di interventi di consolidamento e miglioramento sismico. *Bollettino Ingegneri* (5), 3-24.

Binda, L., Cardani, G., & Saisi, A. (2005). *A classification of structures and masonries for the adequate choice of repair - International RILEM Workshop on Repair Mortars for Historic Masonry*, (p. 20-34). Delft.

Binda, L., Penazzi, D., & Saisi, A. (2003). Historic Masonry Buidings. Necessity of a Classification of Structures and Masonries for the Adequate Chioce of Analytical Models. *VI International Symposium Computer Methods in Structural Masonry* (p. 22-24). Rome: STRUMAS.

Chiarugi, A., Bartoli, G., & Bavetta, F. (1995). La meccanica della cupola. In *La cupola di Santa Maria del Fiore, il cantiere di restauro 1980-1995* (p. 47-62). Rome: Istituto Poligrafico e Zecca dello Stato.

Croci, G., D'Ayala, D., & Liburdi, R. (1995, 11/2). History, observation and mathematical models in the seismic analysis of the Valadier abutment area in the Colosseum. *Annali di Geofisica , XXXVIII* (5-6), p. 957-970.

Freytag, M., Shapiro, V., & Tsukanov, I. (2011, April 16). Finite element analysis in situ. *Finite element in Analysis and Design* , p. 957-969.

Giangreco, E. (2002). *Ingegneria delle strutture - Progettazione strutturale* (Vol. 3). Torino: UTET.

Gugliotta, A. (2002). *Elementi finiti* (Vol. 2). Torino: Otto Editore.

Intact Solutions, Inc. (2014). *Scan-and-Solve for Rhino*. Based on http://www.scan-and-solve.com/

Istruzioni per l'applicazione delle Norme tecniche per le costruzioni di cui al D.M. 14 gennaio 2008 , Circolare n. 617 (Consiglio Superiore dei Lavori Pubblici febbraio 2, 2009).

Linee Guida per la valutazione e riduzione del rischio sismico del patrimonio culturale, prot. n. 92 (Consiglio Superiore dei Lavori Pubblici luglio 23, 2010).

Lourenċo, P. B. (2002, 7 17). Computations on historic masonry structures. *Progress in Structural Engineering and Materials , 4* (3), p. 301-319.

Luft, B., Tsukanov, I., & Shapiro, V. (2008). Geometrically Adaptive Numerical Integration. *Proceedings of 2008 ACM Symposium on Solid and Physical Modeling* (p. 147-157). New York: Stony Brook.

Macchi, G., Ruggeri, G., Eusebio, M., & Moncecchi, M. (1993). Structural Assessment of the Leaning Tower of Pisa. *IABSE reports of the working commissions , 70* (351), p. 401-408.

Marques , R., & Lourenço, P. B. (2011). Possibilities and comparison of structural component models for the seismic assessment of modern unreinforced masonry buildings. . *Computers & Structures , 89* (21), p. 2079-2091.

Mola, F., & Vitaliani, R. (1995). Analysis, diagnosis and preservation of ancient monuments: the St. Mark's Basilica in Venice. In S. a. I. Barcelona, Spain: CIMNE.

Norme tecniche per le costruzioni (Decreto Ministeriale gennaio 14, 2008).

Pinto, P. E., & Franchin, P. (2008). Assessing existing buildings with Eurocode 8 part 3: a discussion with some proposal. *Eurocodes: background and application Workshop.* Brussels.

Quim, F., Lima, A., & Silva, N. (2012). Comparative analysis through semplified methods, plane frames and space frame for design of structural masonry buildings. *15th International Brick and Block Masonty Conference.* Florianopolis, Brazil.

Robert McNeel & Associates. (2014). *Rhinoceros*. Based on https://www.rhino3d.com/it/

Roca, P., Cervera, M., Gariup, G., & Pelà, L. (2010, 7 22). Structural Analysis of Masonry Historical Constructions. Classical and Advanced Approaches . *Archives of Computational Methods in Engineering* (17), p. 299-325.

Smoljanović, H., Živaljić, N., & Nikolić, Ž. (2013, 7 25). Overview of the methods for the modelling of historical masonry structures. *Građevinar , 65*, p. 603-618.

Sonnenhof Holdings. (2013). *Lisa FEA*. Based on http://lisafea.com/

Thrall, M. (2006). *3DWarehouse*. Based on

https://3dwarehouse.sketchup.com/model.html?id=b9ef29089cc807e5293cf63222c527f5

Trimble Navigation. (1999). (©. 2. Limited, Produttore) Tratto il giorno 2015 da SketchUp: http://www.sketchup.com/it

Visintini, D., & Spangher, A. (2013). Rilevamento laser scanning, modello della superficie (DSM) e modello per il metodo agli elementi finiti (FEM) di una struttura . *Atti 17a Conferenza Nazionale ASITA* (p. 1287-1294). Riva del Garda: ASITA.

3. SMALL SIZE OBJECT

3.1. Introduction

As written in the Introduction, the first class of objects that will be analysed, throughout this thesis, is that one of the "small" size artefacts, like statues or construction elements, where the level of detail has to be the highest. Construction elements can be considered or in their own or as part of a more complex structural system, even without actively contributing to the same and not playing a structural role in the building, but assuming a purely decorative role.

The interest for the study of small objects surveying and modeling has been developing gradually more, especially since arose the awareness that this heritage could be damaged by earthquakes or by events of other kinds. Profile cases are represented by all those sculptures destroyed, or otherwise damaged beyond repair, by the earthquake in Umbria, or by the recent damage suffered by the museum exhibits of the Near and Middle East, as a result of terrorism. It is therefore increasingly clear the need to provide, on the one hand to the study for the safety of these objects, from another side to the storage of digital three-dimensional models able to reproduce exactly the objects.

In Italy, for historical and cultural reasons, the artistic heritage is not, generally, a prerogative study of engineers, but of other professionals and, rarely, teams with different skills are created for the analysis of objects of art under different point of view. This condition implies that modern TLS technologies for surveying have been mostly used, so far, exclusively for the creation of three-dimensional models suitable for studies on the restoration or on the different artistic aspects, but very rarely for the structural characterization of the artefacts themselves.

In this chapter it is therefore intended to highlight how these same models, created for purposes not proper of the engineering field, can be used, with the appropriate transformations, also for the structural analysis.

The chapter is therefore structured as follows:

- existing legal framework;
- analysis of small-size elements: current trends;
- first case of study: the Statue of Emperor Claudius;
- second case of study: the statue of St. John the Baptist.

3.2. Existing legal framework

Differently than the case of buildings and architectural details, which structural aspects have a strict regulation, as described in the second paragraph of Chapter 2, it currently does not exist a specific and similar law for the verification of the small size elements. As it will be explained in this section, the only reference is contained in the "Guidelines for seismic risk assessment of cultural heritage", already described in sub paragraph 2.2.3. The most complete document on this argument is the "Guidelines for the Safeguard of Cultural Heritage against Natural Risk", which is the results of the Programme – Activity B - ENEA-MIUR concluded in

2005 and, unfortunately, not implemented in any specific rule or standards, remaining so far only in the field of academic research.

The "Guidelines for seismic risk assessment of cultural heritage" issued by the Ministry of Heritage and Culture indicates, at chapter 2.3 - " In the event that there are significant artistic goods located only in some parts of the building, the *structural* evaluation, and namely the assessment of the SLA (State Limit of Damage to artistic property), *as defined in the previous chapter*, must be carried out exclusively on those areas, through local models of the structurally autonomous parts (this substructure will be define macro-element and it can correspond both to architectural elements, both, more generally, it will be recognized on the basis of a constructive reading of the historical building). Usually damages to goods of artistic value, such as frescoes and stucco, *but not only these kinds of apparatuses*, become significant and unacceptable in the presence of significant injury to the structural elements (cracking and warping of the bearing walls), the same ones that are taken into referenced to decide about the conformity to standards of the building. In these cases, for verification, SLA can be assimilated to SLD (State Limit of Damage). However, there are situations in which damages to the decorative apparatuses may also occur in absence of a structural damage (for example, stuccos of considerable thickness or insufficiently connected to the structure) or vice versa (apparatuses not fully constrained and therefore advancing lesions and structural deformations), or still, artistic heritage with an independent structural behaviour (pinnacles or other items that can be considered as structural appendages). In these cases it is necessary to develop criteria and assessment tools specific to the SLA". With this last sentence the legislator gives complete freedom to the designer as it regards the criteria and assessment tools to adopt, without giving any specific indication.

As it refers, instead, to the "Guidelines for the Safeguard of Cultural Heritage against Natural Risk" there is a specific section, the third, dedicated to museum goods. The standard proposed through this documents provide to:

- a classification of the objects according to their seismic reaction;
- a valuation of the seismic reaction;
- a proposal of intervention according to the previous valuation.

The museum goods are therefore classified like in *Table 3.1*, and, according to the type of support classified as reported in *Table 3.2*.

Category	Description of the object
T1	small object with flat base
T2	small object with no flat base
T3	statues, sculptures in general and large pots
T4	pictures and paintings in general
T5	chandeliers and hanging objects
T6	other

Table 3.1 – Classification of museum goods.

	A **objects leaning** on a flat surface				**B** **objects fixed** on a flat surface or on a pedestal	**C** **hanging or suspended objects**	
	A1	***A2***	***A3***	***A4***		***C1***	***C2***
	on the floor	***on a pedestal***	***in a showcase***	***on shelves in boards***		***hung on a wall***	***suspended from the ceiling***
T1	**X**	**X**	**X**	**X**	**X**		
T2	**X**	**X**	**X**	**X**	**X**		
T3	**X**	**X**		**X**			
T4						**X**	
T5							**X**
T6	**X**	**X**	**X**	**X**	**X**	**X**	**X**

Table 3.2 – Classification of museum goods according to the support.

The two classifications above proposed are functional to the definition of the possible mechanisms of dynamic reaction and damage mechanisms, which are defined according to the category of support or, otherwise, to the category of the object.

Category	Dynamic reaction	Damage Mechanism	Acronym
A	adherent movement	over stressing	R1
A	slipping movement	over displacements	R2
A	oscillation movement	repeated collision	R3
A	oscillation movement	overturning	R4
B	adherent movement	over stressing	R1
C	oscillation movement	repeated collision	R5/R6

Table 3.3 – Mechanism of dynamic reaction and damage mechanism.

Category	Dynamic reaction
T1	R1 R2 R3 R4
T2	R1 R2 R3 R4
T3	R1 R2 R3 R4
T4	R5
T5	R6
T6	R1 R2 R3 R4 R5 R6

Table 3.4 – Dynamic reaction according to the category of the object.

Where, referring to Figure 3.5, it results (Augusti & Ciampoli, 2000):

- adherent movement — occurs when there is not relative motion. The force applied to an object of mass M is therefore equal to:

$$F = Ma_a = Ma_g$$

being a_a the absolute acceleration of the object and a_g the dragging acceleration.

- slipping movement — starts when the force of inertia Ma_g that the support transmit to the object, in conditions of perfect adherence, exceeds (in absolute value) the frictional resistance of the first detachment, that occurs, when: $a_g > \mu g$

being g the gravity acceleration and μ the friction coefficient between the object and the support/plane surface. The force transmitted to the object during the motion is therefore:

$$F = Ma_g = M\mu g$$

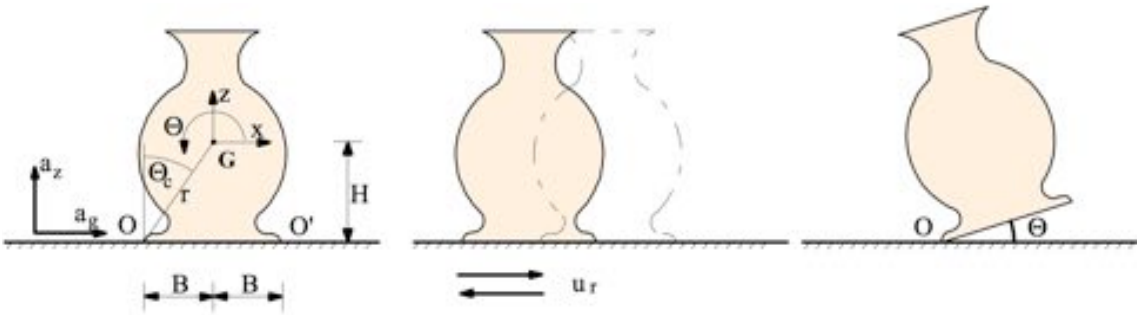

Figure 3.5 – Diagram of the object: (a) motion of oscillation movement; (b) slipping movement.

- oscillation movement — occurs when the slipping movement is, for some reason, prevented. Therefore, according to the formula of West, it results:

$$a_g > \frac{B}{H} g$$

being H the height of the centre of gravity G on the supporting plane (in rest position) and B the distance of the projection of G from the rotation axis, coincident with a tangent to the base (O or O'). In order to overturn the object, it must be applied an acceleration of intensity at least equal to a_g for a time of sufficient duration to ensure that the speed of the object reaches a critical value.

It will results therefore that the condition for having an oscillation movement is:

$$\mu < \frac{B}{H}$$

In order to study the movement that could affect the object, it is convenient to assume simplified criteria, like the ones proposed by Ishiyama (1984), which formulation relates with the overturning of lean rigid bodies through the imposition of conditions in the intensity of acceleration, velocity and displacement. Through the analysis of these impositions it is therefore possible to determinate three domains (*Figure 3.6*):

Domain A — which corresponds to values of ratio $\frac{B}{H} > \frac{a_g}{g}$, and therefore with no relative movement because $\mu > \frac{a_g}{g}$;

Domain B — which corresponds to a condition of oscillatory motion, but at an insufficient speed to determine the overturning;

Domain C — which corresponds to a condition for which it is likely to occur tipping.

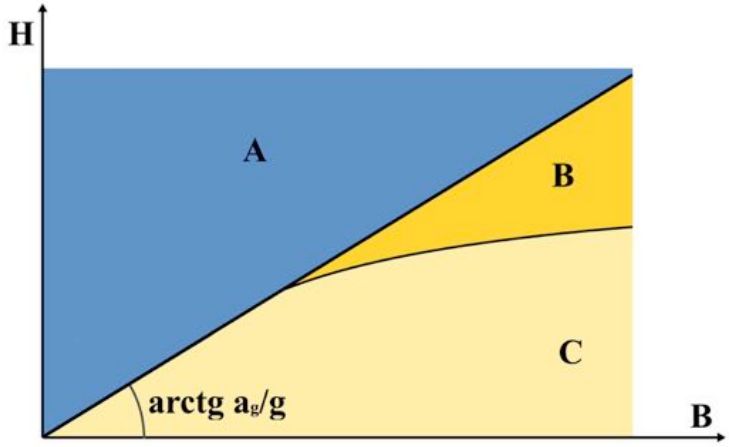

Figure 3.6 – Domains of Ishiyama.

Concluding, in order to fully analyse the aspects that involve structurally a small-size object it is necessary to know:

- the position of its centre of gravity and its geometry,
- the condition relating to its connections with the boundary (leant, fixed, suspended ...),
- the conditions of the resistance of the material composing the object,
- the damages or cracks suffered,
- the forces that might impact on the object.

3.3. Analysis of small-size elements: current trends

Beside the examples quoted in paragraph 1.5, that concern the mere geometric modeling of small size objects, it results interesting to examine the case of 3D models applied in structural analysis.

The most famous and cited example is for sure the analysis of the Michelangelo's David (Borri, et al., 2005), where starting from the 3D model realized by the Standford University (Levoy, et al., 2000), already cited in paragraph 1.5, and importing it in the software Ansys, a

well known FEA software, were performed a static and a seismic analysis, with several different supposed inclinations, in order to define the reason why the back support, called *broncone*, and the left ankle of the statue resulted cracked (*Figure 3.7*).

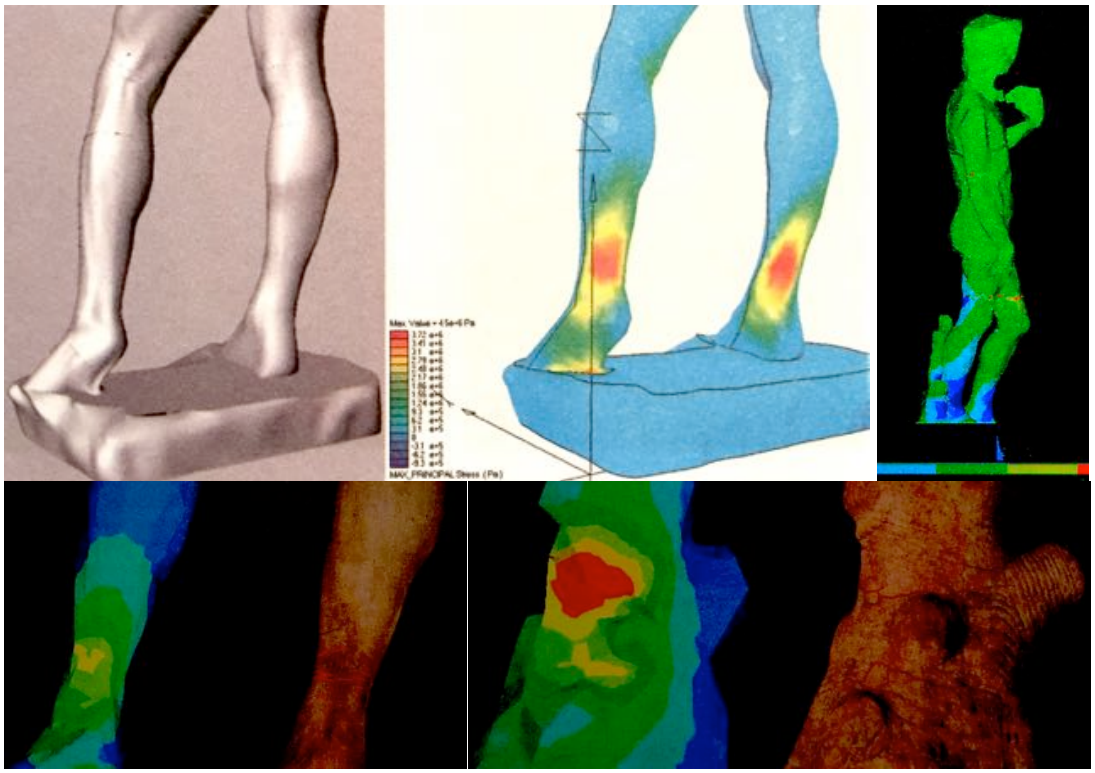

Figure 3.7 – The analysis of (Borri, et al., 2005) on the Michelangelo's David. On the top left the 3D model of the statue seen from the bach. The analysis results of Ansys showing the most stressed area from the back and of the entire sttue. On the bottom the ankle model with stresses and the cracks and the Broncone model with stress along with the cracks.

So far, researches on structural analysis performed on 3D models derived from TLS survey have not been so frequent, also because few models are unrestricted for use, therefore, the possibility to use freely the model of Michelangelo's David of the Standford University, along with the artistic and cultural importance of this statue, made it one of the most studied example. Among all, it deserve to cite the works of (Lolli, 2010), (Pascale, Bastianini, & Carli, 2011) and (Intact Solutions, LLC, 2009).

As logical, the largest part of the published work on this argument relate to the most famous arts object, since it is natural that the major effort for saving and preserving is done on these kind of objects. Therefore another important study is the one held on the Bronzes of Riace statues by (De Canio, 2012). In this case the analysis was dedicated to the possible introduction of seismic base isolations for the statues (*Figure 3.8*).

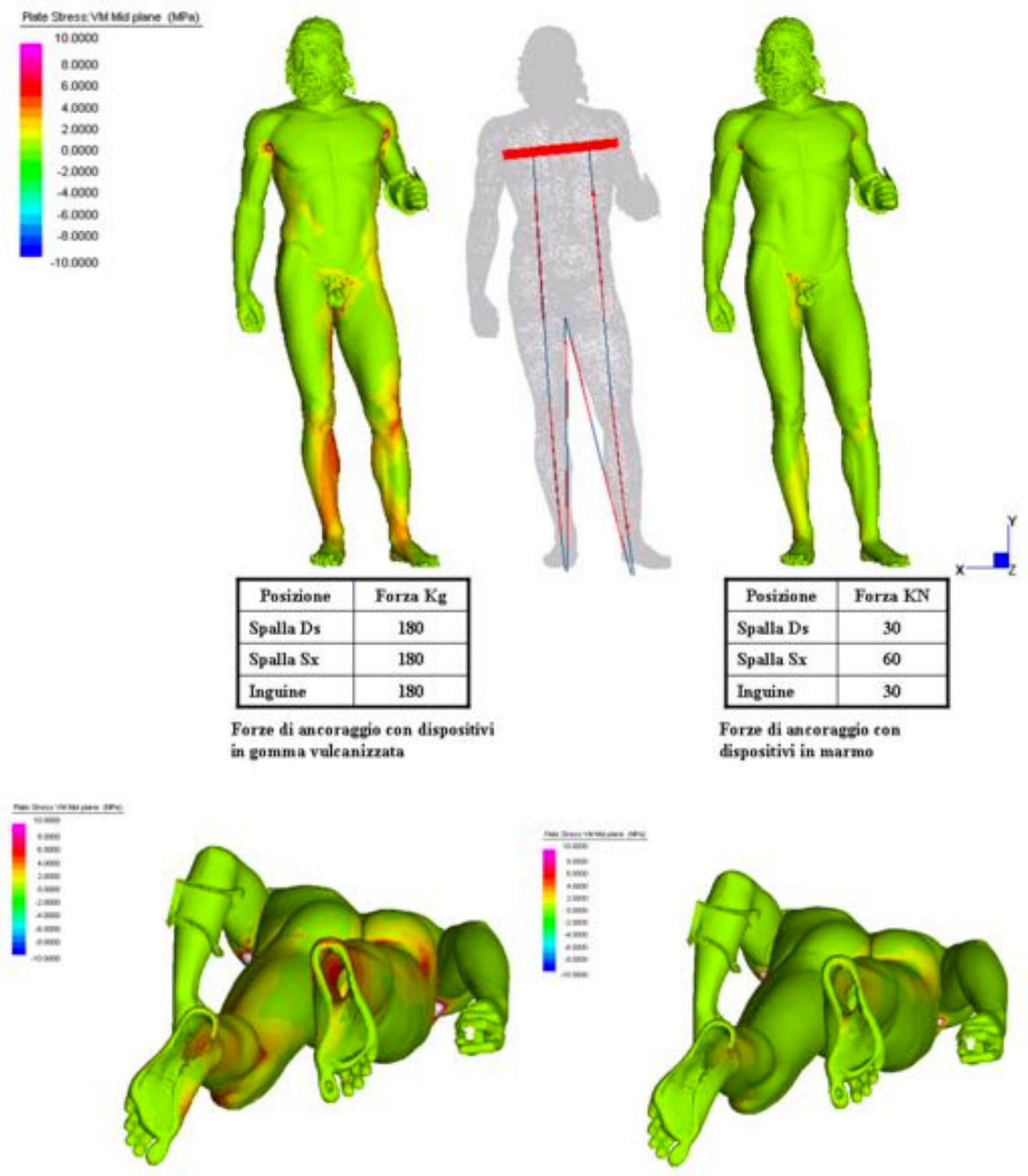

Posizione	Forza Kg
Spalla Ds	180
Spalla Sx	180
Inguine	180

Forze di ancoraggio con dispositivi in gomma vulcanizzata

Posizione	Forza KN
Spalla Ds	30
Spalla Sx	60
Inguine	30

Forze di ancoraggio con dispositivi in marmo

Figure 3.8 – The 3D model of one of the statue textured with the structural analysis results in two different case: with a vulcanized rubber base isolation and with a marble base isoltion (De Canio, 2012).

A particularly interesting work is that one held on the Tullio Lombardo's statue of Adam, preserved in the Metropolitan Museum of Art in New York (USA) (Riccardelli, Soultanian, Morris, Becker, Wheeler, & Street, 2014), which crashed because of the collapse of its pedestal in 2002. In order to design the restoration and with the purpose to find a less invasive and more reversible approach of reconstruction, the conservators decided to preliminary study all the aspect laser scanning the fragments of the statue, virtual reconstructing the model of the statue and finally analysing it with FEM (*Figure 3.9*).

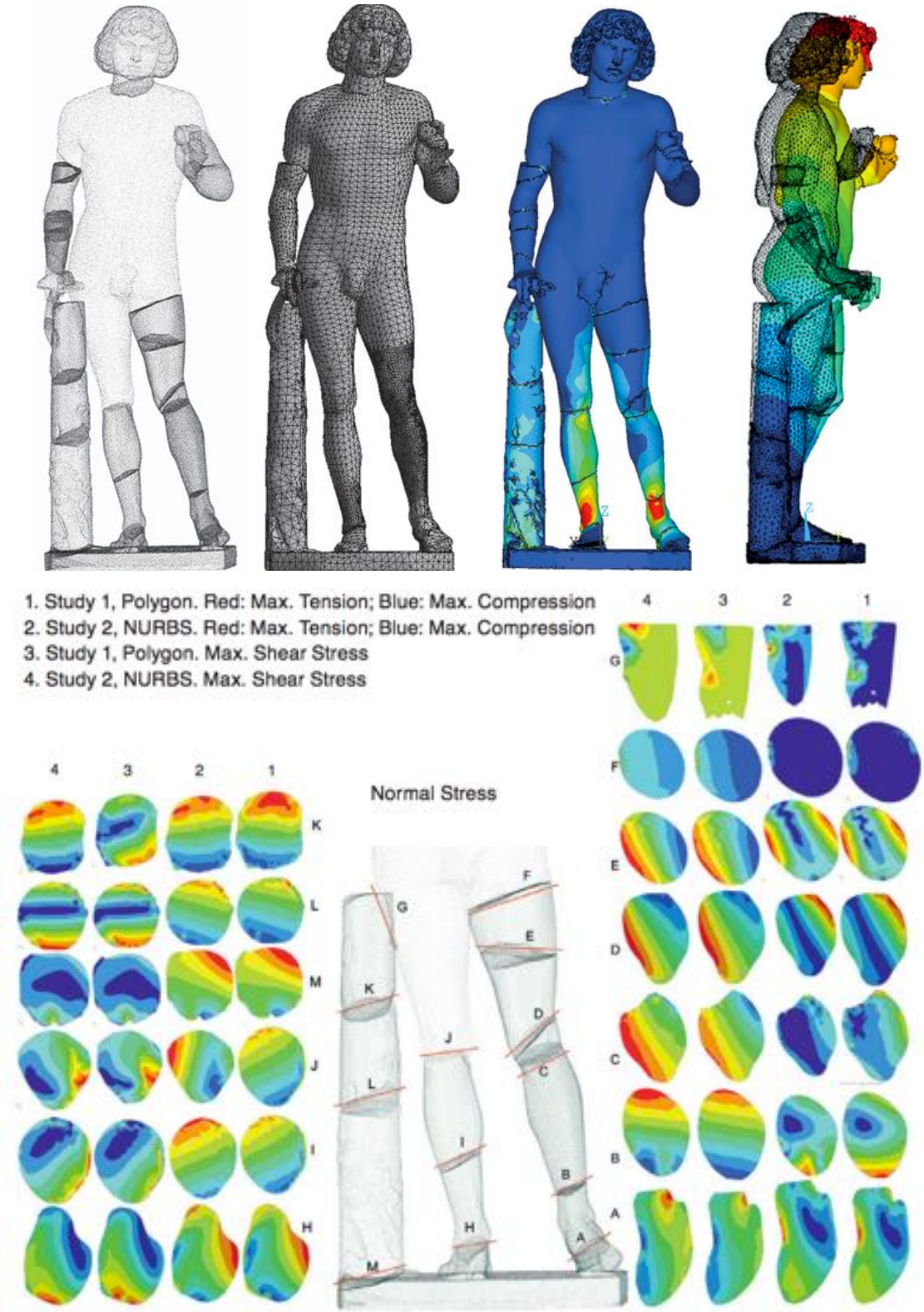

Figure 3.9 – The 3D model of the statue of Adam, obtained from the virtual reconstruction of the scans of the various fragments. The triangulated model and the strcutral analysis results and possible displacements. Trend of stress on the sections corresponding to the cracks. (Riccardelli, Soultanian, Morris, Becker, Wheeler, & Street, 2014).

The last example considered "Seismic performance assessment and base-isolated floor protection of statues exhibited in museum halls" (Sorace & Terenzi, 2015) concerning the evaluation of seismic response of statues exhibited in art museums and base-isolated floor strategy for their enhanced protection. The analysed statue is a marble copy of a Hellenistic sculpture reproducing the Greek philosopher Socrates: in this case the analysed model correspond to a simplification of the original 3D model (*Figure 3.10*).

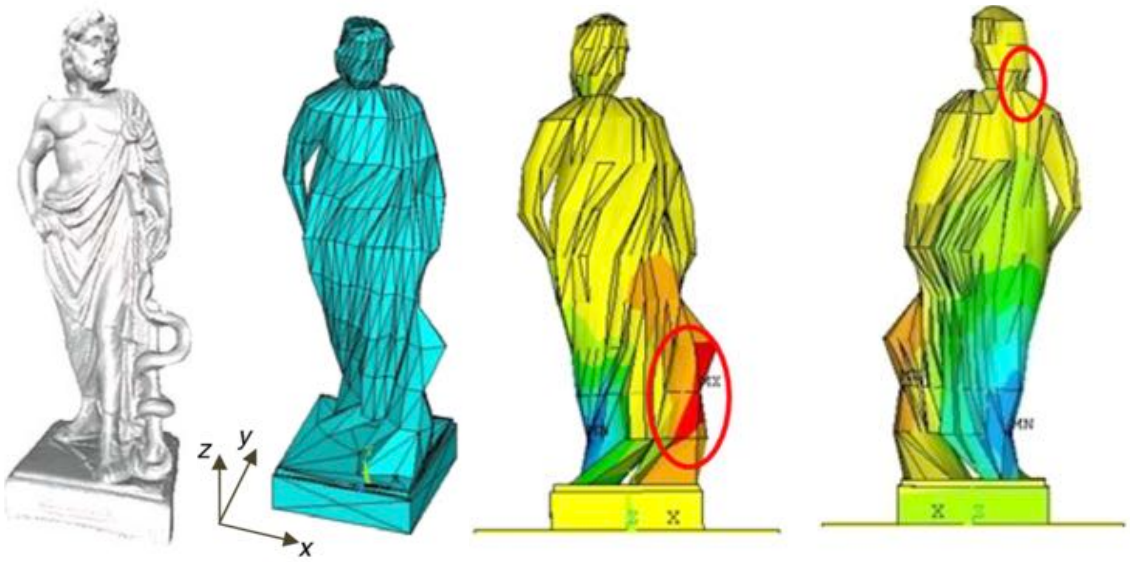

Figure 3.10 – The 3D model of the statue of Socrate and its seemplification, along with the results obtained from its analysis (Sorace & Terenzi, 2015).

From the examination of cited examples, it is evident that, in order to investigate on the structural behaviour of a statue, it is necessary to proceed with a scrupulous modeling of the object. It must be highlighted that if the geometry of the object to survey is too complex and the spatial description cannot be reached through the surveying of few points, it is necessary to use technologies able to sample the spatial trend through a "matrix of dots" with high density, such as an optical instrument or a laser scanner. Therefore, the presence of free-form surfaces and geometric primitives not well defined, suggest the opportunity to recur to other forms of surveying, based on the integration of different techniques.

As written in paragraph 1.3, the use of laser scanners has considerable advantages related to speed and automatisms in the acquisition phase, the possibility of varying the resolution of the acquisition function of the geometry and the ability to detect forms of any level of complexity. The combination of these advantages makes these tools very versatile, justifying their high use.

In the following, two cases are analysed and they belong to two different typologies: the first case is a model obtained from a TLS surveying, and is not characterized by a high level of detail. On the opposite, the second case refers to a model directly obtained with a close range laser scanner, which is able to process the point clouds directly, with a very high level of detail, even exceeding that one required for a structural analysis.

3.4. First case of study: the Statue of Emperor Claudio

3.4.1. Historical description

The first object used as case study of the thesis is the statue of Emperor Claudio (*Figure 3.11 a)*) preserved in the National Archaeological Museum of Aquileia and dating, presumably, to the first century AD, whose sculptor is unknown. The statue represents a military figure portrayed in an upright position as if greeting his soldiers, wrapped in military dress - the *paludamentum* - tied on its shoulder. The body stand on the right leg while the left, slightly bent, is brought back. The figure is mutilated because it lacks much of the left side (shoulder, arm, chest and back) and the right arm that, for consistency with other similar contemporary statues and structure, it is assumed to be facing up. *(Istituto Regionale per il Patrimonio Culturale del Friuli Venezia Giulia, 2008)*. The flattening rear testifies the original accommodation in a niche, like the other two statues preserved in the same "Hall of Sculpture" of the Museum, namely the one of the Emperor Augusto, and the one Antonia the Minor (mother of Claudio), that supposedly formed a cycle representing the family of Claudio, whom was very linked to the city of Aquileia in order to the policy interventions made in its favour.

Nevertheless in truth the white Greek marble statue was initially modelled to represent another authority and only later was accommodated to represent Claudio, through the insertion of the head, worked in a separate block of Italics marble. The face, framed by a fringe of hair, has an expression corrugated and is partially ruined on nose and ears being chipped (*Figure 3.11 b)*).

Figure 3.11– a) The Statue of Emperor Claudio preserved in the Hall of Sculpture of Aquileia b) A detail of the head

The statuary complex is 201,3 cm tall and is set on a concrete pedestal of 70 x 70 h 35 cm. The estimated weight of the statue is set about 5,2 q whereas a specific weight of the marble equal to 2370 kg/m^3. The state of preservation is modest: the statue in fact, besides being mutilated (green areas in *Figure 3.12*) has several fractures (blue areas of the same figure), some of which are grouted (pink areas). In addition the entire surface has dark spots spread as evidence of the action of a past fire. The presence of these fractures and injuries mode this statue interesting for the study proposed in this thesis.

Figure 3.12 – Front and rear of the statue, with evidence of cracks, grouting and lakcs.

3.4.2. The geometric survey by TLS

As before mentioned, the statue is preserved in the Museum Room II, "Hall of Sculpture", and is flanked by other sculptures or "*acroliti*" resting on pedestals, while the walls are draped with heavy curtains, that serve as backdrop for the better enjoyment of the sculptures: therefore, the scene has required careful design of the TLS surveying, since it resulted greatly difficult the positioning of both scans and targets.

Referring to *Scheme 1.8*, phase 1, the statue was scanned with the Faro Focus3D S120 TLS system, from nine different stations, each with an horizontal angular range of 120° and a step angle of 0,044° (*Figure 3.13 b)*), four scans were acquired from four corner positions, at an altitude of 76 cm from the floor (coloured in cyan in the figure), the other four of the same positions but from an altitude of 196 cm (coloured in red in the figure), and the last scan position was frontal at a height of 196 cm (coloured in yellow in the figure). The minimum and

maximum distances from the laser scanner to the various parts of the statue were, for all nine scans, of the order of 1 to 2 m, respectively: this implies that with the angular step adopted, the distances between each point acquired is estimated between 0,7 to 1,4 mm. In total, more than 84 million points were acquired, of which 9.997.224 belonging to the statue and the pedestal. In order to register the nine scans, first step of phase 2 of *Scheme 1.8*, twenty-three targets were placed, including six spherical (diameter 14,5 cm) and eighteen paper "checkerboard" (four home made squares of 10x10 cm) (*Figure 3.13 a)*).

Figure 3.13 – a) Scan station positions b) Instrumental settings on the scanner screen.

No topographical measures of targets have been taken and, in order to proceed to the registration of the nine scans, several steps have been done and also different software have been used.

It will be therefore necessary to process all the data following the pipeline represented in *Scheme 1.8*, being in the second phase, and namely in that one that consist in all the operation related to data registration, data cleaning and data resampling.

Initial calculations were performed by the software Scene© ver.4.8.4 (Faro, 2011), starting from the fundamental phase "*Find Objects*" in order to localize all the targets (*Figure 3.14*), both spherical than checkerboards, nonetheless this operation proved to be insufficient. In order to improve the registration, also the geometric characteristics of the scanned scene were detected with the "*AutoFeatures*" command, and also the plans of the floor, walls and wooden supports (planes), the rectangles of a certain size "Rectangle" and the vertices of the edges between floors "Corner Points" were used as reference (*Figure 3.15*). This procedure, although highly automated, needed to be adequately manually corrected, eliminating

the features mistakenly identified ("*II type statistical error* ") and introducing those wrongly not found ("*I type statistical error*"). After eliminating some false matches identified by the command *"Registration"*, scans were properly recorded, obtaining an average residual of 3.2 mm: this value, which is considered optimal for the processing of large objects or average size is not sufficient for those finely modelled and with small size as a statue.

Figure 3.14 – Processing with Scene: search for "Auto Features"

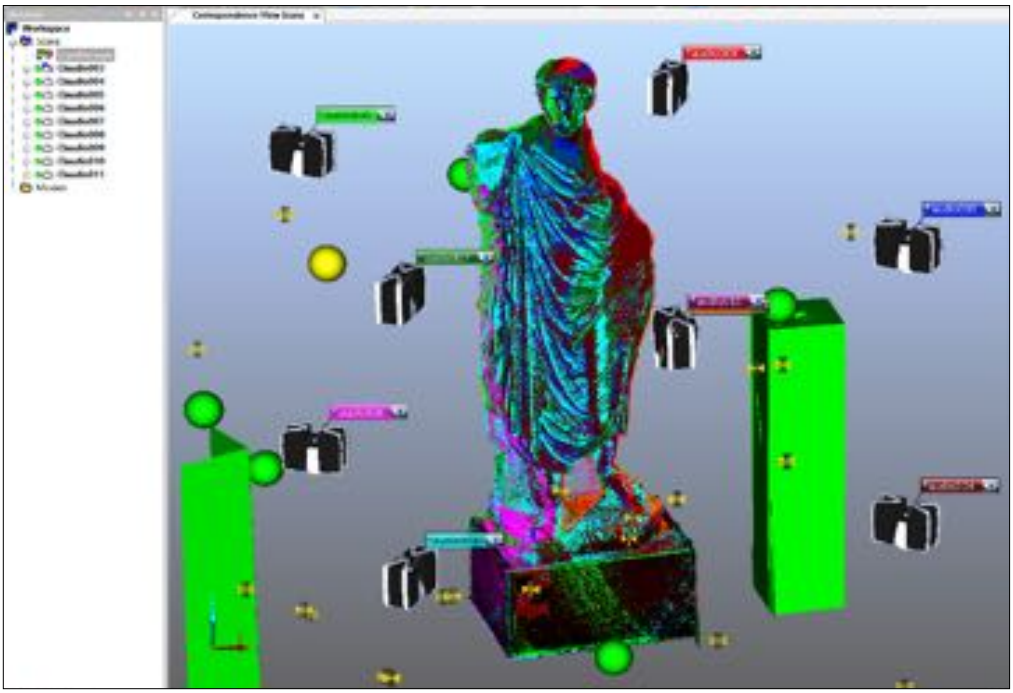

Figure 3.15 - Processing with Scene: and registering.

Once completed the operations in Scene©, the nine points clouds, still separated, related only to the statue and its pedestal, were exported in ASCII format with command "Export Scan Points" and imported in the software MeshLab ver.1.3.3 (Visual Computing Lab - ISTI - CNR, 2014) already mentioned in 1.4.2, which is well known excellent open source software for complex processing of points clouds, also obtained by TLS. In *Figure 3.16* the nine point clouds are displayed with different colours.

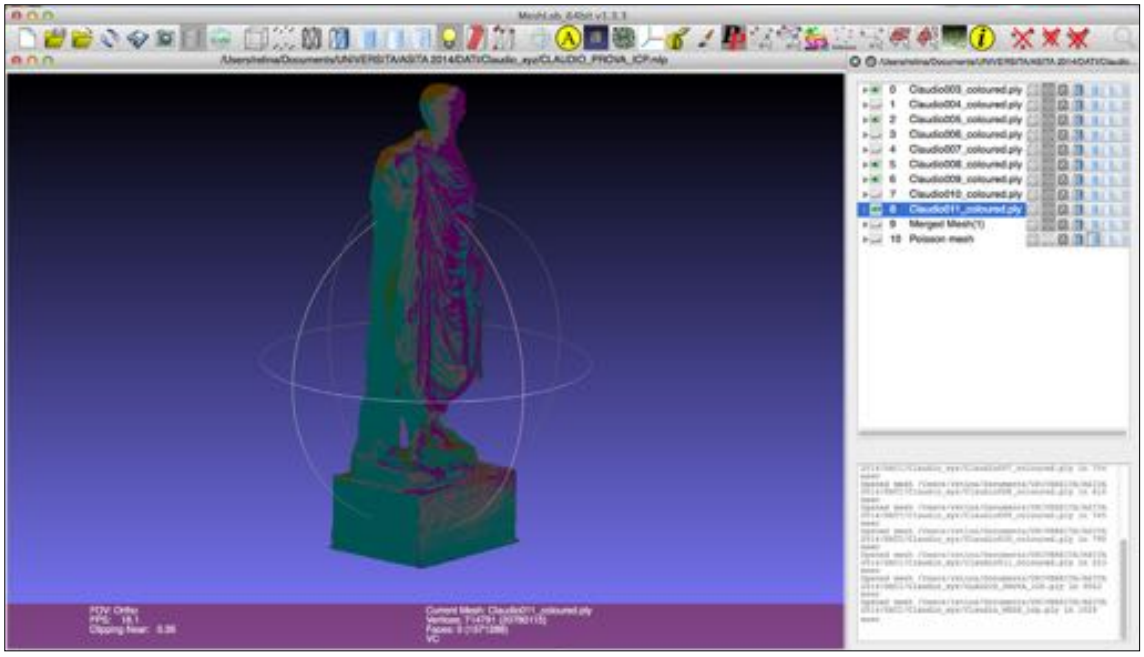

Figure 3.16 – Different scans in MeshLab enviroment

In Meshlab were performed various operations on each cloud, like cleaning (removing outliers points, removing duplicated vertexes, merge close vertexes, noise cleaning) and resampling; otherwise, as operating procedure, it was decided to maintain all existing points before the completion of registration and afterward proceed with various treating on the resulting cloud.

MeshLab was used mainly to improve the alignment between the scans done by Scene: therefore, first of all, the "Align" command (*Figure 3.17 a)*) was exploited. It implements the well-known ICP (Iterative Closest Point) method so minimizing the distance among the surfaces obtainable by the various TLS clouds, roto-translating them and improving the registration.

The command requires the definition of six parameters (*Figure 3.17 b)*):

- Sample Number — represents the number of samples chosen for each ICP iteration;
- Minimal Starting Distance (MSD) — in the sample number of point chosen with the previous parameter only the samples nearer than the value MSD are considered for ICP. This value is changing dynamically through the "MSD Reduce Factor" parameter;

- Target Distance, when 50% of the chosen samples reaches a distance value which is below the Target Distance, the meshes are considered aligned;
- Max Iteration Number maximum number of iteration that ICP is allowed to perform;
- MSD Reduce Factor at each ICP iteration, the MSD is reduced to be 5 times the percentile of the sample distance;
- Sample Cut High at each ICP iteration, all the sample farther than the percentile are discarded.

Due to the high variability, various values to set as parameters have been tested, in order to obtain the best results; at the end the ones reported in *Figure 3.17 b)* are adopted and the average final residual was decreased down to 1,8 mm from the starting one 3,2 mm.

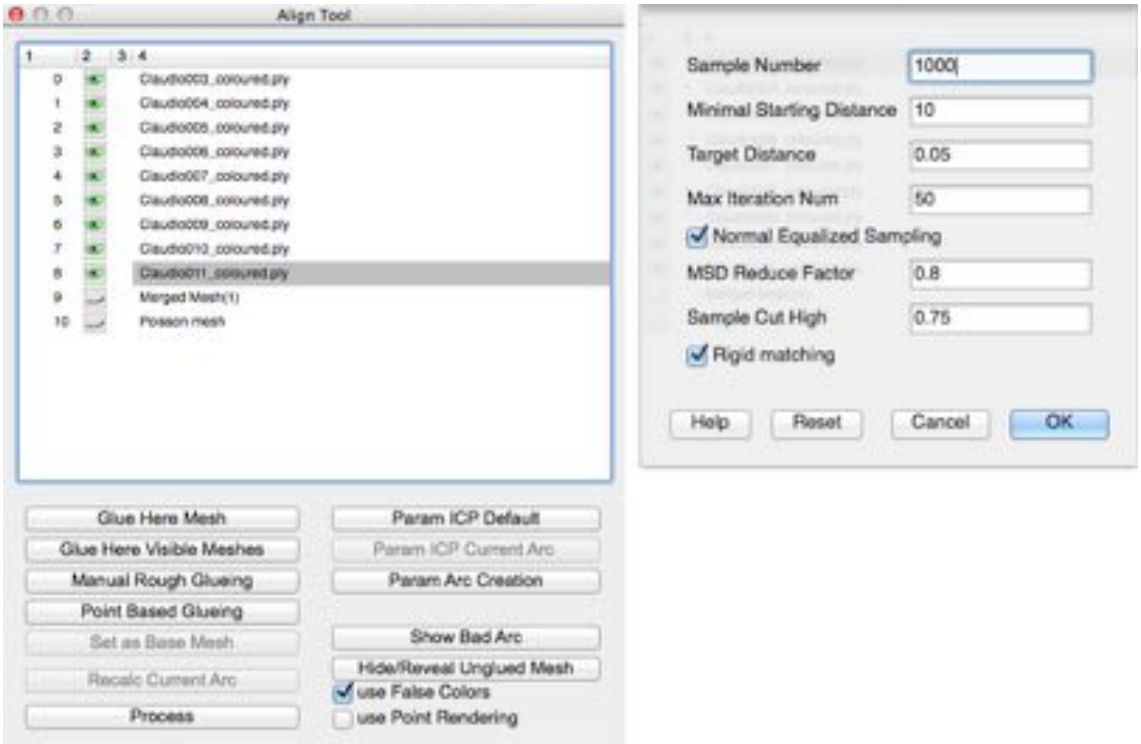

Figure 3.17 – a) Align tool command in MeshLab b) Parameters to fix ICP

After this alignment, clouds were finally unified in a single layer and treated with the appropriately commands of cleaning and repairing, such “Remove duplicated vertex” and “Remove isolated pieces”.

The biggest problem with this surveying was due to the residual noise of the scans, due probably both to the excessive closeness of the TLS to the object (proximal to the minimum distance range of the instrumentation) both to the irregular lighting conditions of the room, because of which the object was overexposed on the right side and in shade on the left side. This problematic has been partially overcome by the application of the filter “Clean - noise

filter" implemented in the software CloudCompare, introduced in sub paragraph 1.4.3. This algorithm locally fits a plane (around each point of the cloud) then removes the point if it is too far away from the fitted plane; this filter can be basically considered as a low pass filter. To estimate the underlying (planar) surface, the user can define a radius or a (constant) number of neighbours. The user has the choice between a relative error (as Statistical Outlier Removal) and an absolute error. Eventually isolated points can be removed in the same process.

3.4.3. Calculations of the model surface

In order to proceed with the structural analysis of the object, as reported in *chapter 2*, it is necessary to obtain a closed surface of the object and, therefore, the originated cloud has to be further processed, in order to obtain a DSM (Phase 3 to 5 of *Scheme 1.8*), as much possible similar to the reality, digital output well known in the geomatic community.

MeshLab, as well as other software dedicated to point clouds processing, offers different algorithms for surface reconstruction starting from 3D point sets: the one used for the definition of the statue's DSM is Poisson Surface Reconstruction, already cited in sub paragraph 1.4.1.

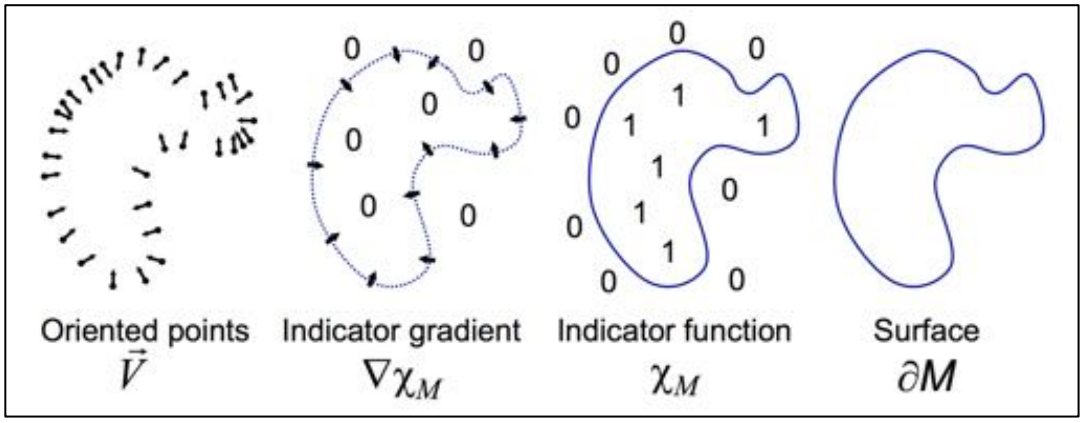

Figure 3.18 – Intuitive illustration of Poisson reconstruction in 2D (Kazhdan, Bolitho, & Hoppe, 2006).

This algorithm takes into account all the cloud points at one time (*Figure 3.18*), without resorting to a partition space, greatly reducing surface noise, maintaining a high level of detail, and it is very adaptable to the case of closed surfaces. The formulation of surface reconstruction as a Poisson problem implies that, considering the scalar function χ, whose gradient best approximates a vector field $\vec{V}$ defined by the samples, and namely $min\chi = \|\nabla\chi - \vec{V}\|$, and applying the divergence operator, it will results the following equation $\Delta\chi \equiv \nabla \cdot \nabla\chi = \nabla \cdot \vec{V}$, as explained in extension form in (Kazhdan, Bolitho, & Hoppe, 2006).

This command implies, therefore, the preliminary calculation of the normal of the surface being constructed, along the command "*Compute normals for point sets*". Though many different normal estimation methods exist, the one that on which MeshLab command is set on is one of the simplest, and is formulated as follows. The problem of determining the normal to a point on the surface is approximated by the problem of estimating the normal of a plane tangent to the surface, which in turn becomes a least-square plane fitting estimation problem. The

solution for estimating the surface normal is therefore reduced to an analysis of the eigenvectors and eigenvalues of a covariance matrix created from the nearest neighbours of the query point. More specifically, for each point p_i the assembled covariance matrix C will results:

$$\begin{cases} \mathrm{C} = \frac{1}{k}\sum_{i=1}^{k}(p_i - \bar{p}) \cdot (p_i - \bar{p})^T \\ \mathrm{C} \cdot \vec{v_j} = \lambda_j \cdot \vec{v_j} \quad j \in \{0,1,2\} \end{cases}$$

Where k is the number of point neighbors considered, in the neighbourhood of p_i, $\bar{p}$ represents the 3D centroid of the nearest neighbours, λ_j is the j-th eigenvalue of the covariance matrix, and $\vec{v_j}$ the j-th eigenvector.

The command requires the definition of two parameters (*Figure 3.19 a)*):

- Neighbour number — which represents the value of k in the previous equations;
- Smooth iteration — which represents the number of smoothing iteration done on the $\bar{p}$ used to estimate and propagate normal.

At the same way, the command "Poisson Surface Reconstruction" requires the definition of four parameters:

- Octree Depth — set the depth of the octree structure used for extracting the final surface. The higher is the number the finest will be the precision of reconstruction, and therefore the processing time needed;
- Solver divide — specifies the depth at which a block Gauss-Seidel solver is used to solve the Laplacian equation.
- Samples per node — minimum number of sample points that should fall within an octree node as the octree construction is adapted to sampling density.
- Surface offsetting — correction value for isosurfaces threshold that is chosen.

Adopting therefore the parameters of *Figure 3.19 a)* it was obtained a computation of normal which result is represented in *Figure 3.20*.

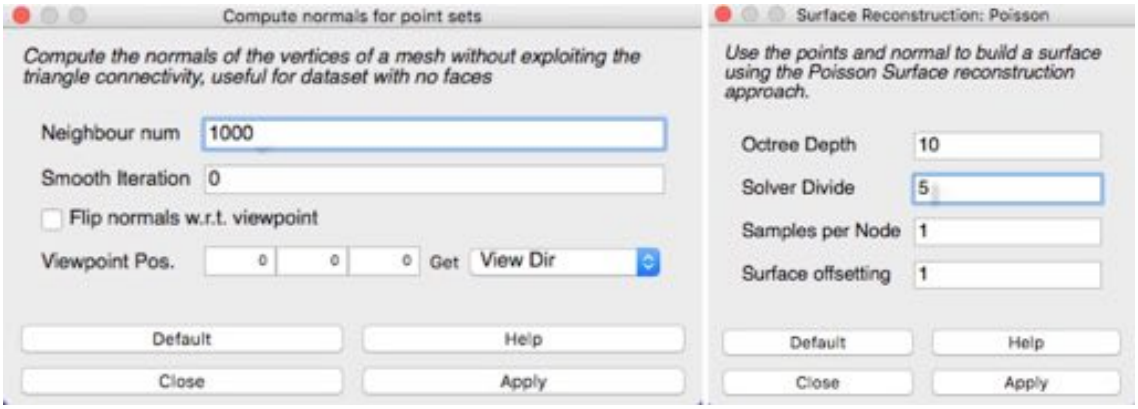

Figure 3.19 – a) Compute normals for point sets parameters
b) Surface Reconstruction: Poisson parameters.

At the same way various values were tested for the four required parameters in the function "*Surface Reconstruction: Poisson*" and in relation to the results obtained and the computing capacity, were adopted the ones of *Figure 3.19 b)*. In particular, it was noted that a number greater than 10 for the parameter "Octree Depth" appeared to be, for the present object, not sustainable for the timing of calculation, while the other parameters, if modified, provided no correct solutions, or even completely unreal.

The result consists in a surface composed of 1.595.466 triangles (*Figure 3.21*), which requires further processing, as in the following explained.

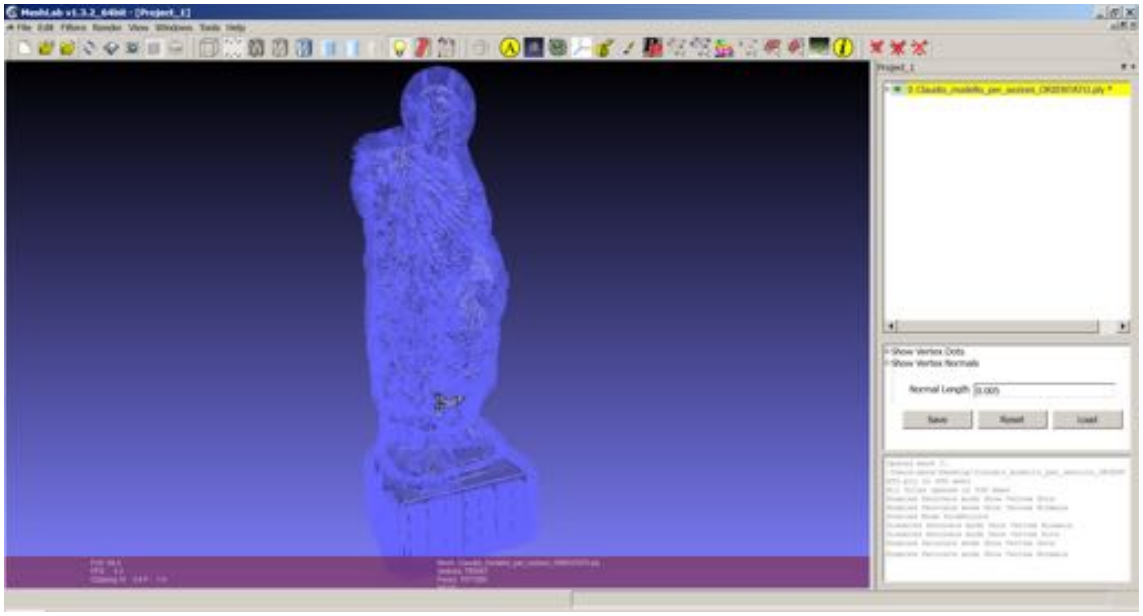

Figure 3.20 – Normals computed on the point cloud

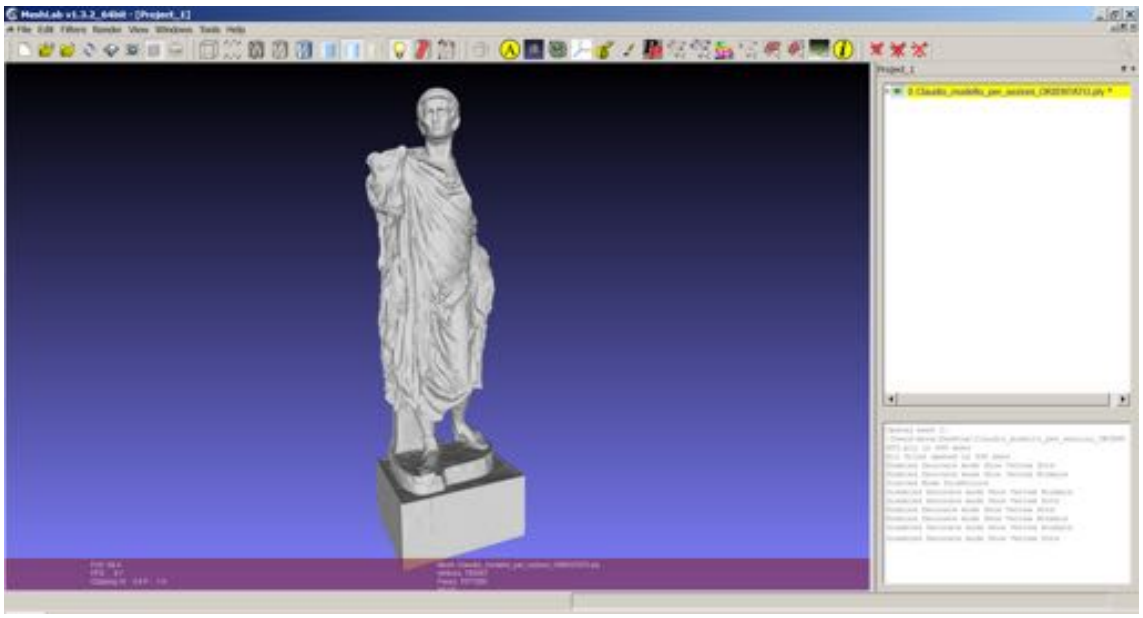

Figure 3.21 – Poisson surface obtained after calculation

The subsequent steps then include the application of various filters, in order to obtain a regular surface, free from the previously reported mesh incongruences that, otherwise, would make the mesh-surface useless for the following analysis.

In order to eliminate the incongruences by now listed, the following operations were iterated several times, through the filters present in MeshLab and, in detail, through the selection filters "*Self Intersecting Faces*", "*Not Manifolds Select Edges*", "*Select Redundant Faces*", all these kind of discrepancies have been detected on the surface and subsequently removed. These steps have been iterated until the complete purging of all the "*not Manifolds surfaces*" had been reached. Applying these commands, the number of holes and gaps clearly increased and therefore it resulted necessary to use other filters, this time belonging to the family "*Remeshing, Simplification and Reconstruction*" in order to fix the problem, and in particular the commands "*Fill Hole"* (automatic) and "*Close Holes*" (parameterized function) have been used to fill the open edges.

In summary, the final surface obtained is a mesh of 1.571.286 triangles, for a total of 5,93 m^2 (4,36 m^2 without the base) and the average size of the triangles is 3,77 mm^2.

3.4.4. Structural analysis

In order to proceed with the structural analysis, the model was imported into Rhinoceros, where the plug-in Scan-and-Solve™ ver.1.6 had been implemented. This software, described previously in chapter 2, works within this modeling environment and allows examining the results of the analysis in a very user-friendly way; an excellent feature of Scan & Solve is that it uses directly the surface model obtained without any re-meshing task. This capability is essential in the flow chart that starts from the TLS surveying and comes to the structural analysis: the end product of Geomatics modeling can be used here as it is, without any changes, in a FEM model.

Before going ahead with the structural analysis, the surface was again verified by means of Rhinoceros command "*Verify geometry*", which detects the presence of any further inconsistencies of the mesh.

Although the surface appeared perfectly congruent for MeshLab, other incongruences were now identified, as degenerated faces, non-manifold edges, naked edges, inconsistent orientation. These problems could be generated as the result of importing the output file from MeshLab within Rhinoceros, because of a loss of data, or simply because of the different way of reading data, according to different conventions of software. Whenever the verification of mesh gives a bad result, by Rhinoceros tools "Mesh Repair" (*Figure 3.22*) fixes all the problems in a process similar to the one done in MeshLab.

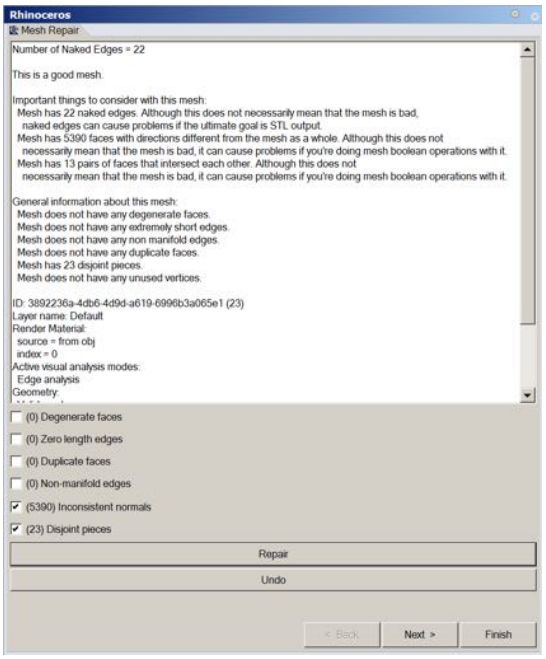

Figure 3.22 – Mesh Repair function in Rhinoceros

Other operations performed in Rhinoceros have been the elimination of the base, not of interest for the structural calculation, and the definition of a new reference system with origin in a corner of the base, X-axis parallel to the side front of the same, Y-axis and Z-axis orthogonal to it vertical (upward), so as to form a right triad. The final model, on which all the analysis has been carried, is featured in *Figure 3.23*.

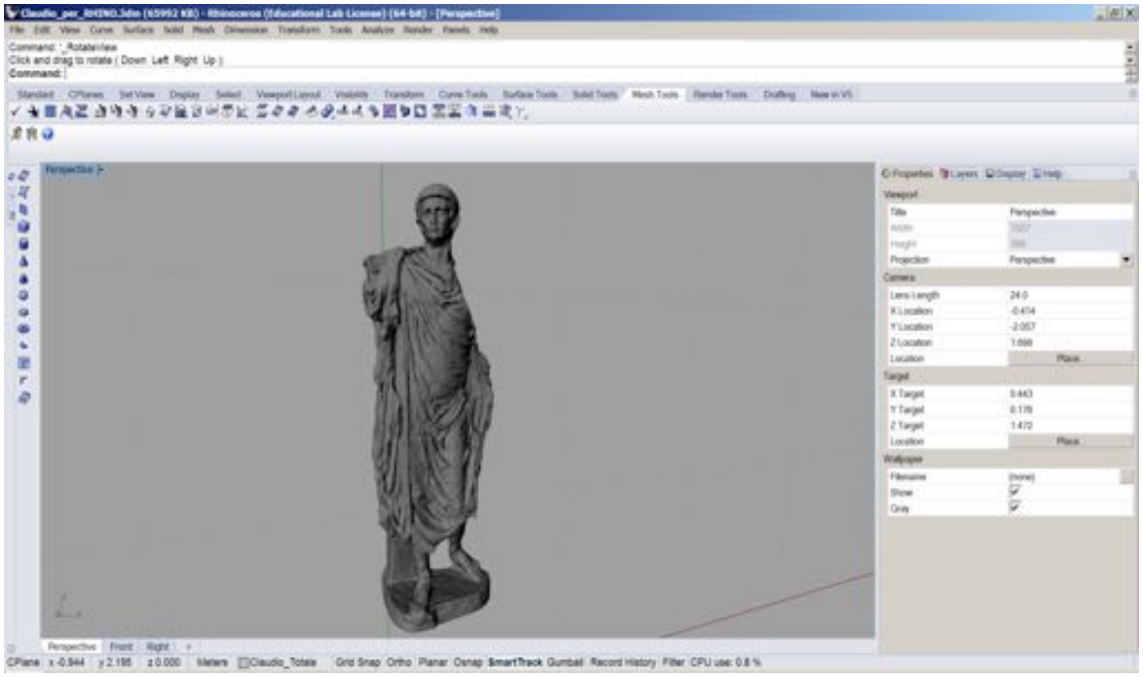

Figure 3.23 – 3D model after processing in Rhinoceros

Preliminary to the structural analysis, with Scan & Solve, it is the definitions of four steps, corresponding to the setting of the following structural data (*Figure 3.24*):

- Material can be chosen from a library or specifically defined through mechanical and physical parameters;
- Restraints are defined by selecting the meshes where the displacements are fixed;
- Loads four types of surface loads are supported: Vector Force, Scalar Force, Pressure, and Torque or, otherwise, only the body load due to gravity can be considered;
- Resolution the number of elements used for the analysis.

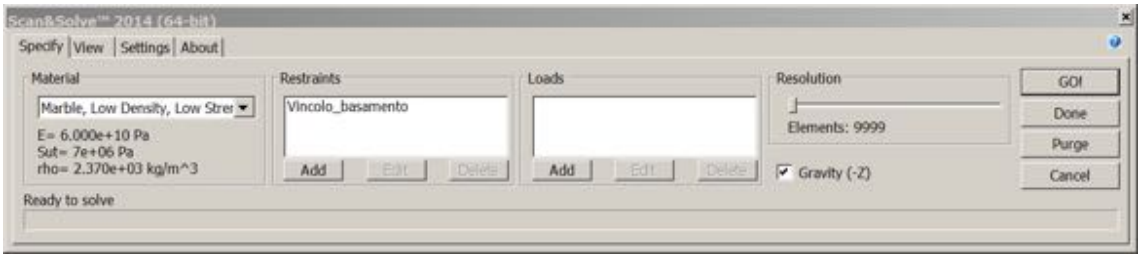

Figure 3.24 – Scan & Solve parameters selection tool

Therefore *step 1* consists in selecting material: "*Marble of low density*" was the adopted material, whereas the white marble statue has similar mechanical characteristics and taking into account also the fact that the statue has been subjected to fire, and therefore lost some of its resistance characteristic. The mechanical values are therefore reported in *Figure 3.25*:

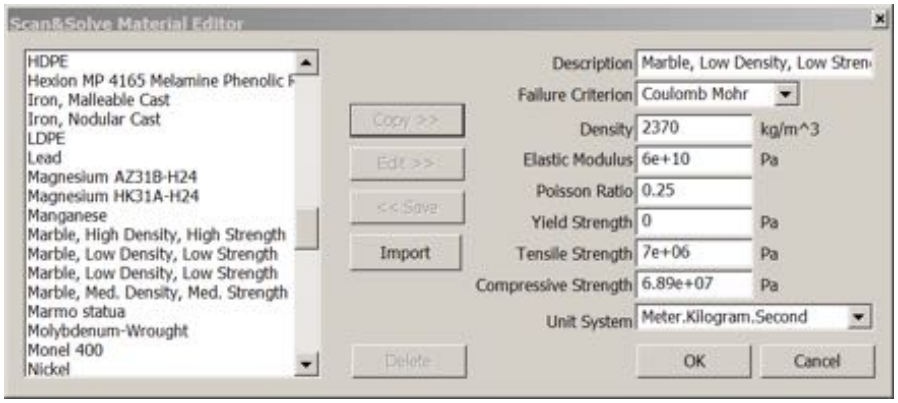

Figure 3.25 – Material editor in Scan-and-Solve:
parameters chosen for the Marble of the statue of Emperor Claudio.

Step 2 consists in defining restraints: in the case of the statue, which is bounded to the pedestal, it was decided to adopt a fixed end, with no translation or rotation admitted. Restraints are graphically reported in *Figure 3.26*, with a different colour for each direction, and namely red for X-axis, green for Y-axis and blue for Z-axis.

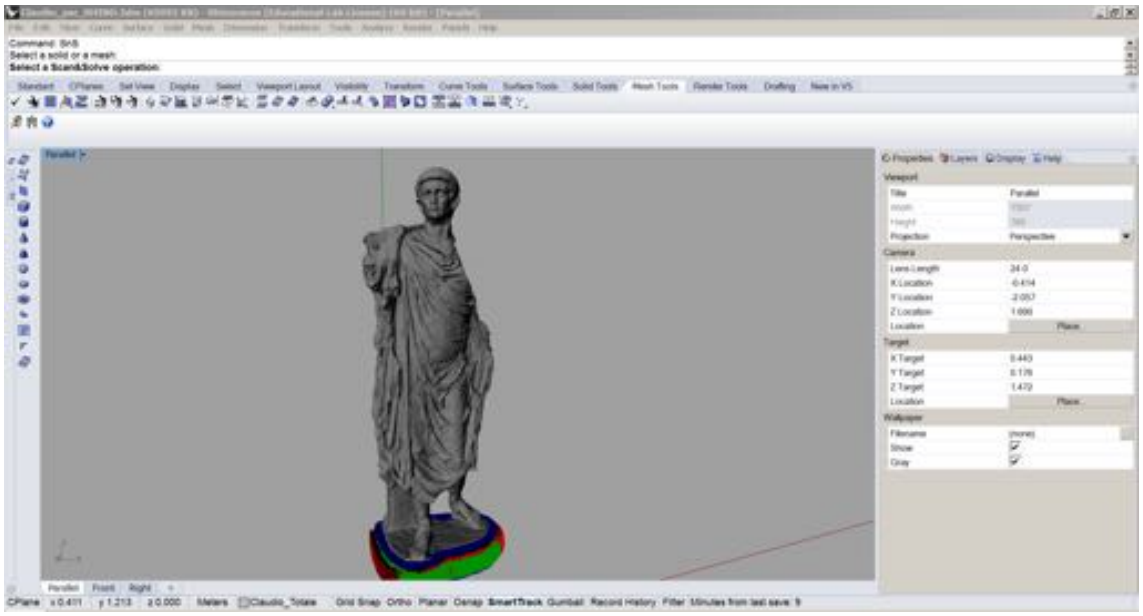

Figure 3.26 – Restraints definition

As it concern with *step 3* – definition of loads – the analysis was performed only with regard to the static aspect and therefore the only load imposed was the gravity load.

The last *step 4* to take in consideration is the definition of the resolution of the FEM analysis: the software allows selection of a number between 10,000 and 500,000 cubes. It is evident that, in contrast, the more dense is the grid, will be more expensive in terms of calculation time. For the purpose of the example, it was considered appropriate to limit the number of cubes to the minimum, to the advantage of the speed of calculation. The subdivision into the cubes are graphically reported in *Figure 3.27*, this argument will be widely treated in sub paragraph 4.2.8.

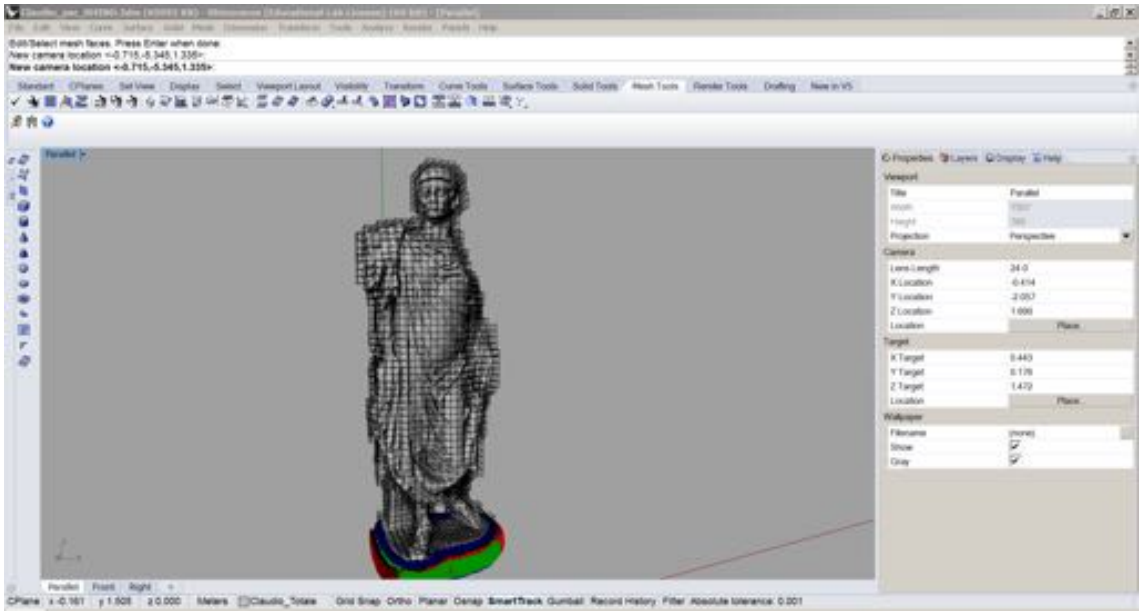

Figure 3.27 – Definition of structural resolution

Once all the settings are completed, it is finally possible to compute the structural analysis. The software takes into account different failure criteria: the one considered the most significant for the type of material used is certainly Mohr-Coulomb failure criteria, which describes the response of brittle materials to shear stress as well as normal stress, and generally applied to materials for which the compressive strength far exceeds the tensile strength. In this case, the critical maximum is given by the lower tensile strength. The criterion in question determinate what is the stress that reaches first to the value of crisis between maximum principal tensile stress, minimum principal compression stress, and a combination of the two, in the case where the minimum compressive stress exceeds in module maximum traction.

The numerical results (minimum and maximum) obtained from the analysis are shown in the following table of *Table 3.28*.

	Minimum	Maximum
X-Displacement	-4.74875e-06 m	1.0146e-05 m
Y-Displacement	-3.34148e-05 m	4.76362e-07 m
Z-Displacement	-9.83628e-06 m	6.28538e-07 m
Total Displacement	1.97794e-13 m	3.53881e-05 m
Von Mises Stress	62.6934 Pa	1.61865e+06 Pa
Max. Principal Stress	-451382 Pa	451937 Pa
Mid. Principal Stress	-477613 Pa	159775 Pa
Min. Principal Stress	-2.08299e+06 Pa	59433.2 Pa
Danger Level (Rankine)	1.96955e-06	0.0645624
Danger Level (Coulomb Mohr)	1.96955e-06	0.0661277
Danger Level (Modified Mohr)	1.96955e-06	0.0645624

Table 3.28 – Minimum and maximum results of the structural analysis

Despite the numerical values of the results, it is interesting to represent them as rendered on the same object model since, in this way, it is possible more intuitively understand what is the trend of displacement, and tensions and danger level along the body. *Figure 3.29* shows, in fact, the total displacement, which represent a magnitude of the displacement vector: X-, Y-, Z- quantities measuring where each point of the body moves after the loads are applied. Clearly, being the statue constrained to the base, and having assumed a fixed end, the displacement will be equal to zero at the base and will tend to become more and more elevated upwards, up to a maximum value of $3{,}53 \cdot 10^{-5}$ m.

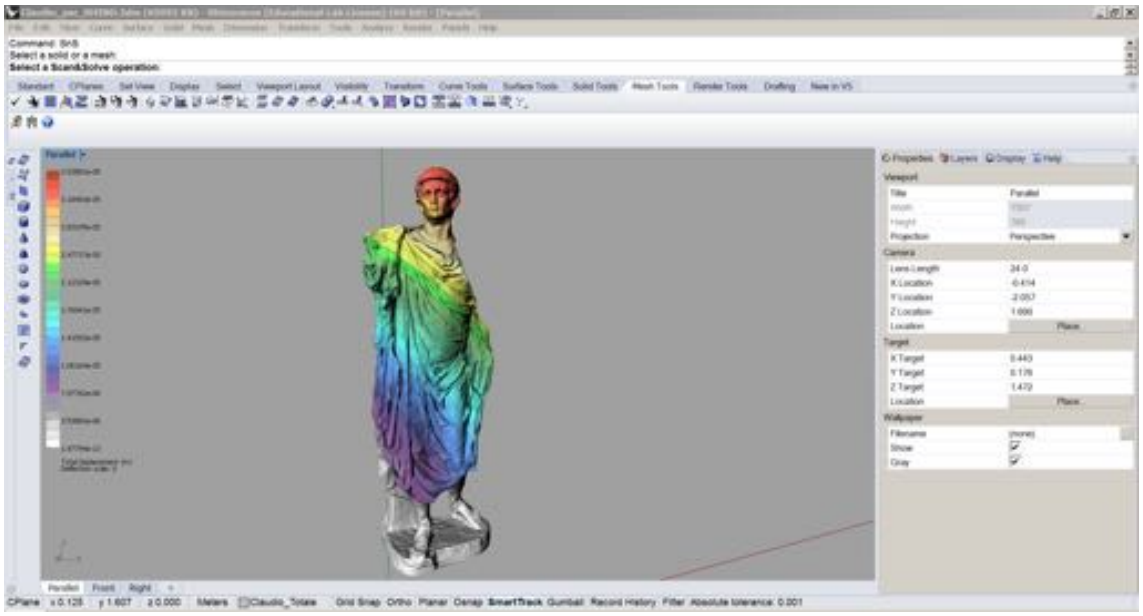

Figure 3.29 – Total displacement

As previously explained in sub paragraph 2.3.4, local total displacement is the most important value to be determined since, starting from it, it is possible to calculate all other values, therefore also minimum values assume a certain importance, since they influence any derived results. It was considered significant also report the values of principal tension/compression, where positive stresses are tensile (red), and negative stresses are compressive (blue) (*Figure 3.30*).

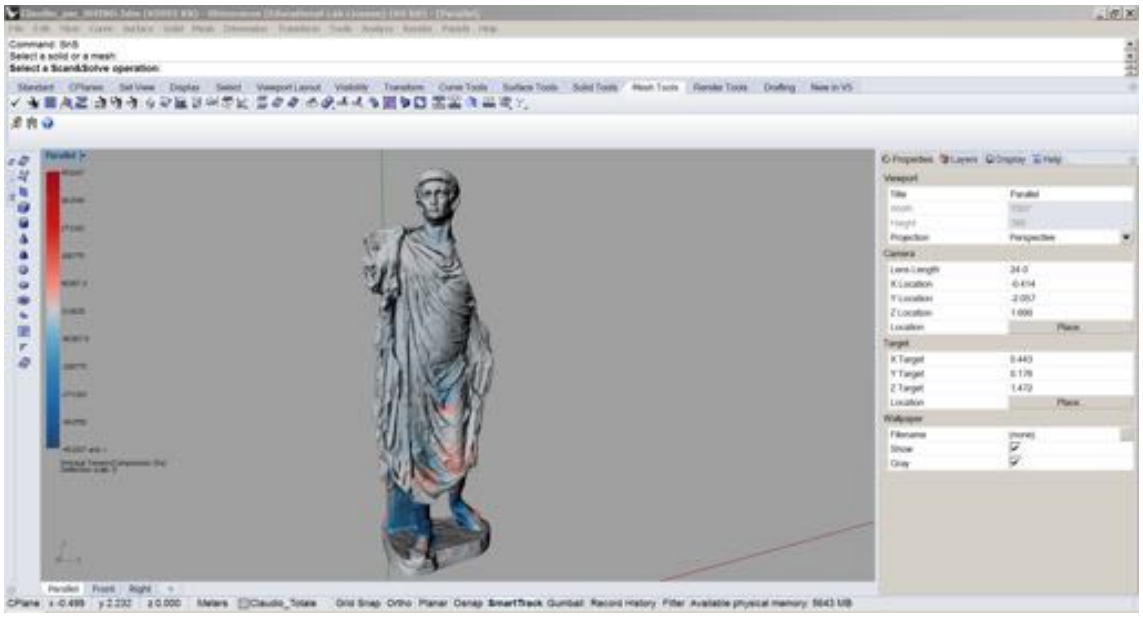

Figure 3.30 – Principal tension/compression

Focusing therefore on the detail of ankles (*Figure 3.31*), it appears soon clear that they are the most stressed zones of statue: this result was doubtless expected, in fact, the centre of

gravity of the statue is obviously placed above the area of the legs, which, in contrast, are very slender. Furthermore, the majority of cracks and lesions are concentrated precisely in that area.

Figure 3.31 – Details of ankles from front side (on the left) and back side (on the right) reporting values of displacement, principal tension/compression and corresponding pictures

Figure 3.31 shows clearly how the area subjected to the main difference between tension and compression, otherwise, the lines which identify the sudden transition from a state of traction to a state of compression, match with the area where are present the cracks and the grouting.

From the carried out analysis, it appears clear that the largest part of the gravity efforts is absorbed by the left ankle of the statue and the right support, used as an artifice in order to give more strength to the whole complex, which otherwise would have collapsed under its own weight.

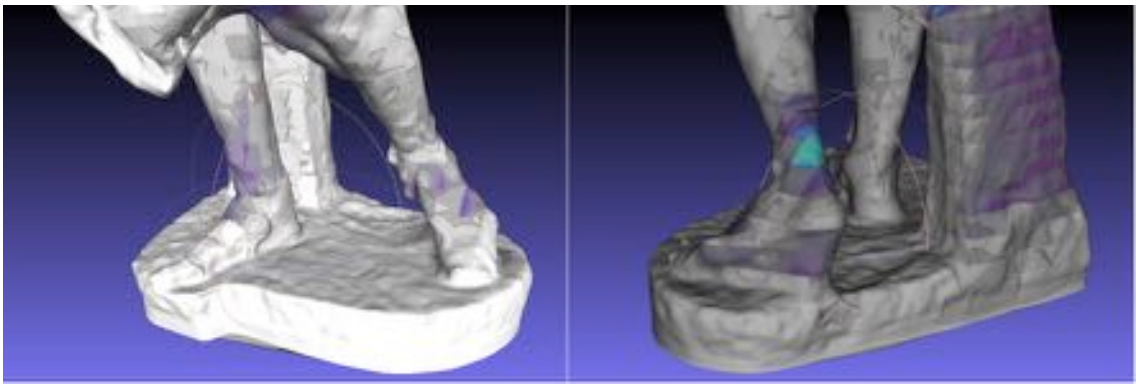

Figure 3.32 – Details of ankles from front side (on the left) and back side (on the right) reporting values of Coulomb-Mohr

Considering also the values obtained from the application of Coulomb-Mohr criterion, (*Figure 3.32*) it resulted that the section most stressed is located at the height of 45 cm. Using therefore the function "*Compute Planar Section*" in MeshLab was extracted the section corresponding to the maximum stress for which, after having obtained the necessary mechanical-geometric values (centre of gravity, moments of inertia, etc.), it is possible to calculate the stress diagram with traditional combined compressive and bending stress Static formulas (*Figure 3.33*).

Figure 3.33 – Details of ankles from front side (on the left) and back side (on the right) reporting the sections computed with MeshLab.

3.4.5. Structural analysis of hypothetical models

Another opportunity offered by the 3D modeling is to proceed with virtual reconstructions, and namely to the relocation in the original position of all those lost elements that were part of the artefact and that may be composed again through the other disconnected fragments or from the simulated modeling of the lacking elements, this last method called "model of reintegration".

According to a statement from Limoncelli (2012), as in painting restoration are present restorable gaps, similarly it can be done in sculpture, as long as it possible to have data useful to complete the lacks. Some gaps anyway cannot be rebuild because lack of information. In this second case, to avoid iconographic reconstruction errors, it is necessary to use any possible information that can be derived from archival sources or literature, photographs, engravings and

prints, paintings, drawings, surveying and plastic, according to the concept of historic restoration. The rebuild operation requires therefore an inter/multidisciplinary approach bringing together the skills of archaeology, art history, architecture and restoration, with those of Geomatics and digital technologies.

The historical path of the statue analysed is not completely known, but it is easy to imagine, even considering similar sculptural complex, that the statue had the typical position of the "*adlocutio*", which is the act by which a speaker addresses his audience starting the speech, and not a real salute. Augustus was copied on this act by all the following emperors, therefore is interpreted not only as a simple *adlocutio* but as an act of divine, indicating to the celestial. This statutory type was then imitate during the following centuries taking as exempla the famous statue of Augusto Iocariato (*Figure 3.34*). The statue of Claudio had probably, as already said, the right arm lifted upwards and the left one flexing to hold the garment or something else. The right arm was probably attached to the body of the statue with a pin, of which remains the footprint, while the right side was an integral part of the sculpture. It is evident that these elements were going to change the static of the statue and then structural analysis would lead to completely different values.

Figure 3.34 – Emperor Augusto in the statue known as "Augusto Iocariato"

For the statue of Claudio, two different virtual models have been realized: the first one, starting from the original model and eliminating only the rear sustenance, close to the right leg, in order to understand which is its contribute to the support of the statue; the second one is instead a reconstruction of what could have been originally the statue, virtually integrating all the lacking elements.

The realization of the first model was really simple, since it implied only the elimination of the model triangles belonging to the support and the remeshing of the created hole. The obtained model was analysed assuming the same conditions as regards to materials, restraints and type of load, obtaining the results explicated in the following.

All the values calculated have been deliberately represented in the same scale of the previous model, in order to make visually evident the increase of the stresses and of the displacement; it appears clear that, in some cases, the values are largely out of scale (*Figure 3.35-3.37*).

Comparing the results, it is clear that the right leg and the rear support stone plays a fundamental role in the static balance of the statue: the displacement without the rear support would be really amplified and, consequently, also all the other values. The height of most stressed section lowered to 30 cm and had a significantly higher level of stresses: the value of the maximum principal stress reached 3,918 MPa compared to the value of 1,619 MPa, of the same section, obtained previously in the case of the rear support, and more than twice as close

to the limit values of rupture. On the *Figures 3.35*, *3.36* and *3.37* are respectively reported the trend of Total Displacement, Principal tension/compression and Mohr/Coulomb stresses analysis.

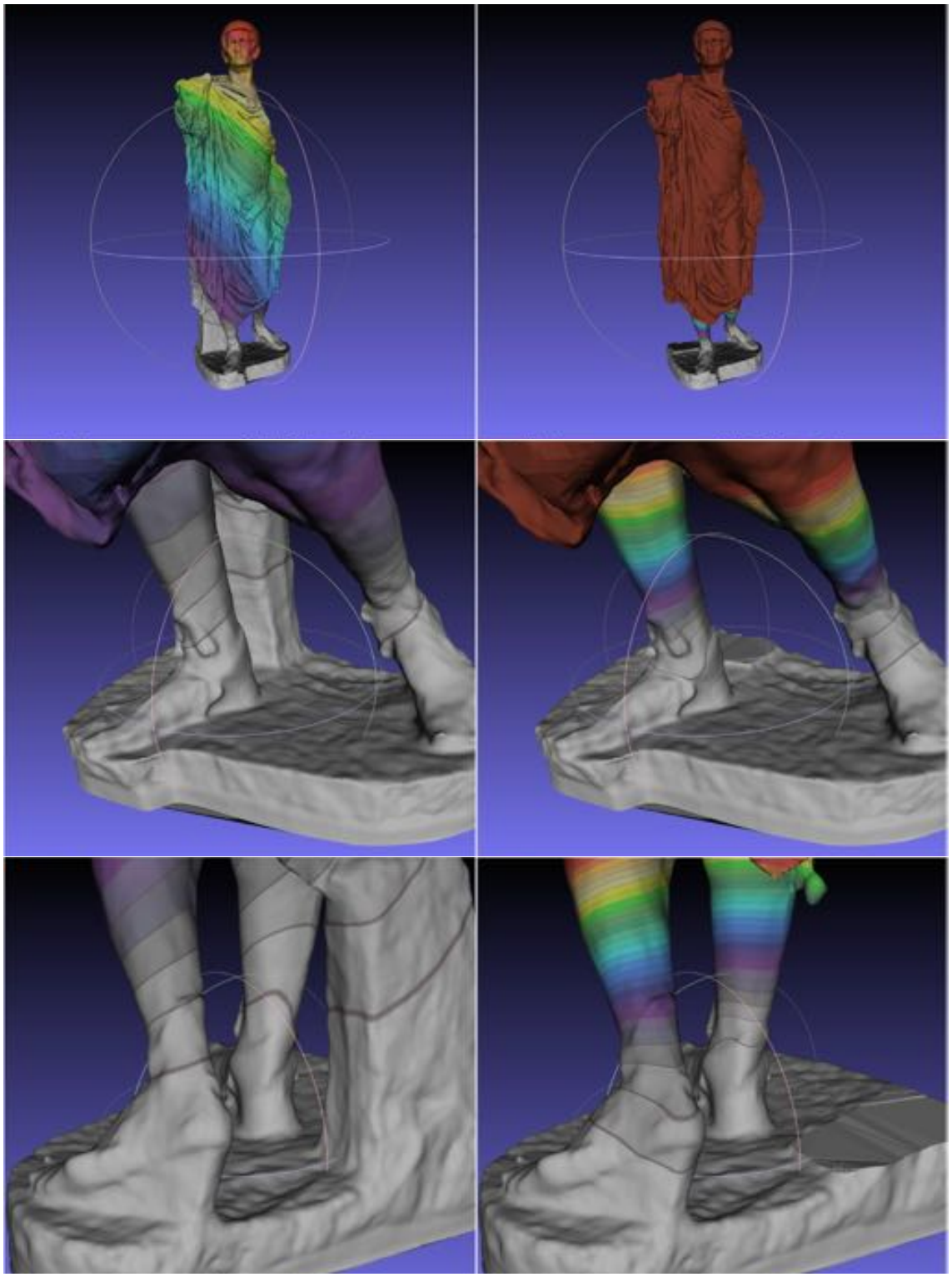

Figure 3.35 – Displacement of the original model (left) and model without support (right)

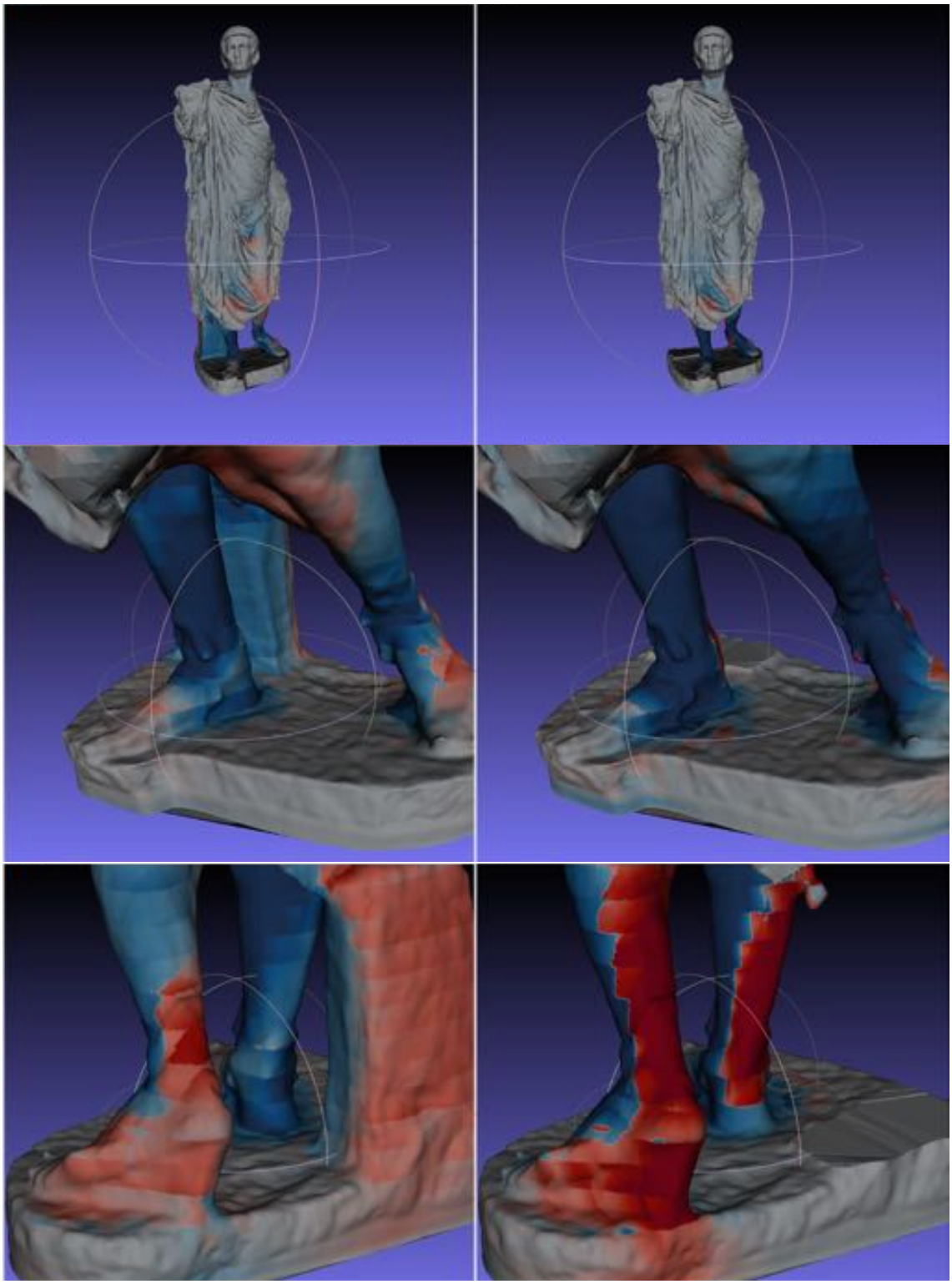

Figure 3.36 – Principal tension/compression of the original model (left) and model w/o support (right)

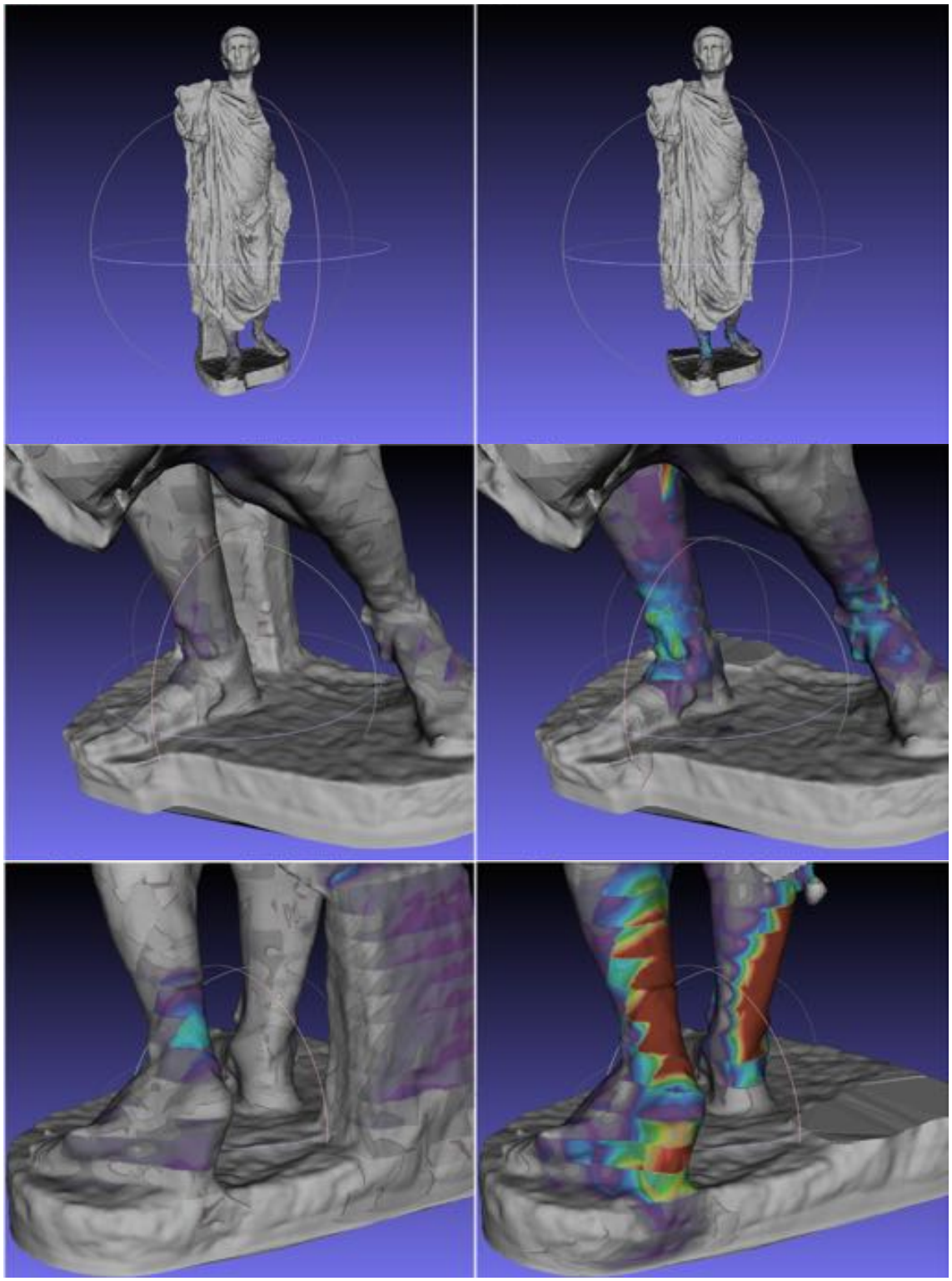

Figure 3.37 – Mohr/Coulomb stress of the original model (left) and model w/o support (right)

The realization of the second model was quite more articulated since it has been necessary to integrate the numerous lacking parts. It was therefore identified a statue, and its 3D surface, of Emperor Trajan (preserved in Rome), depicted in a similar position with regard to

the arms, and then the data were processed in order to merge it with the one of the Claudio surface.

The first operations required the scaling of the statue in order to obtain the same dimensions (the statue of Emperor Trajan is definitely wider) and subsequently were selected only the parts that covered the lacking elements, namely the right standing arm and the limbs and *paludamentum*. It proceeded with the merging of the two different surfaces, but the first result obtained was far from being suitable for further operation since it was fulfilled of incongruences. The reason for the unsatisfactory result is probably due to the fact that the two surfaces did not melt completely but in some parts persisted into an almost osculatory position. For these reasons, it was necessary a further processing in order to eliminate topological noise, surface holes, surface gaps and many self-intersections and near-degenerate elements. All these operations were completed through the software Geomagic Wrap and the final result is reported in *Figure 3.38*.

Figure 3.38 – From the left: the original model of the Claudio statue, the resulting merge of the virtually restored statue of Claudio and the model of the Statue of Trajan.

The model was subsequently analysed, assuming again the same conditions as regards to materials, restraints and type of load, and obtaining the results reported in the following *Table 3.39*, and in Figures *3.40*, *3.41* and *3.42*.

	Minimum	Maximum
X-Displacement	-9.86462e-06 m	1.61919e-05 m
Y-Displacement	-7.60465e-05 m	1.32641e-06 m
Z-Displacement	-2.90323e-05 m	1.93506e-06 m
Total Displacement	2.4113e-13 m	7.86277e-05 m
Von Mises Stress	51.2867 Pa	2.82484e+06 Pa
Max. Principal Stress	-435508 Pa	1.16348e+06 Pa
Mid. Principal Stress	-787960 Pa	272041 Pa
Min. Principal Stress	-3.2378e+06 Pa	193594 Pa
Danger Level (Rankine)	1.24574e-06	0.0861837
Danger Level (Coulomb Mohr)	1.24574e-06	0.0861837
Danger Level (Modified Mohr)	1.24574e-06	0.0861837

Table 3.39 -Minimum and maximum results of the structural analysis.

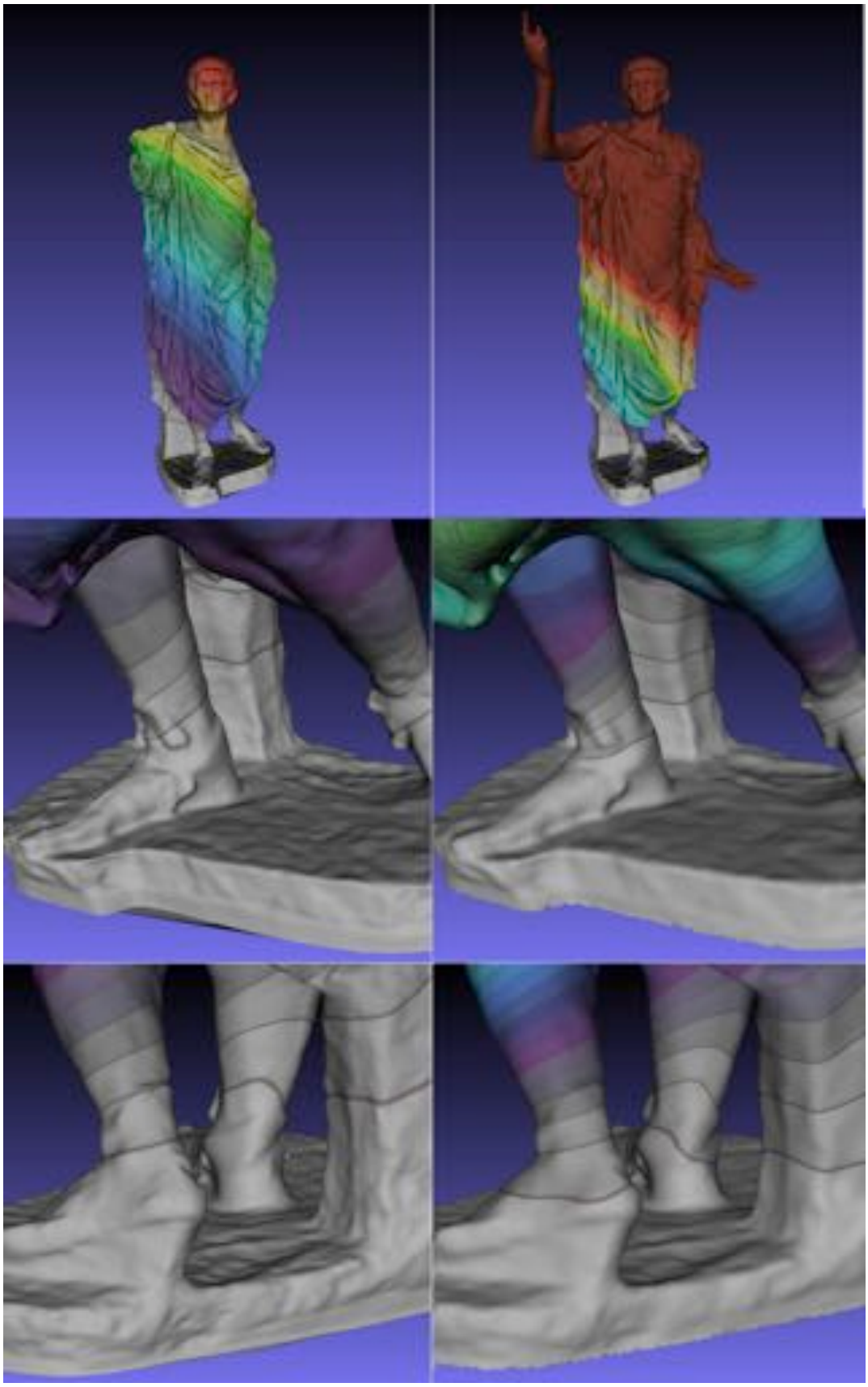

Figure 3.40 – Displacement of the original model (left) and virtually restore model (right).

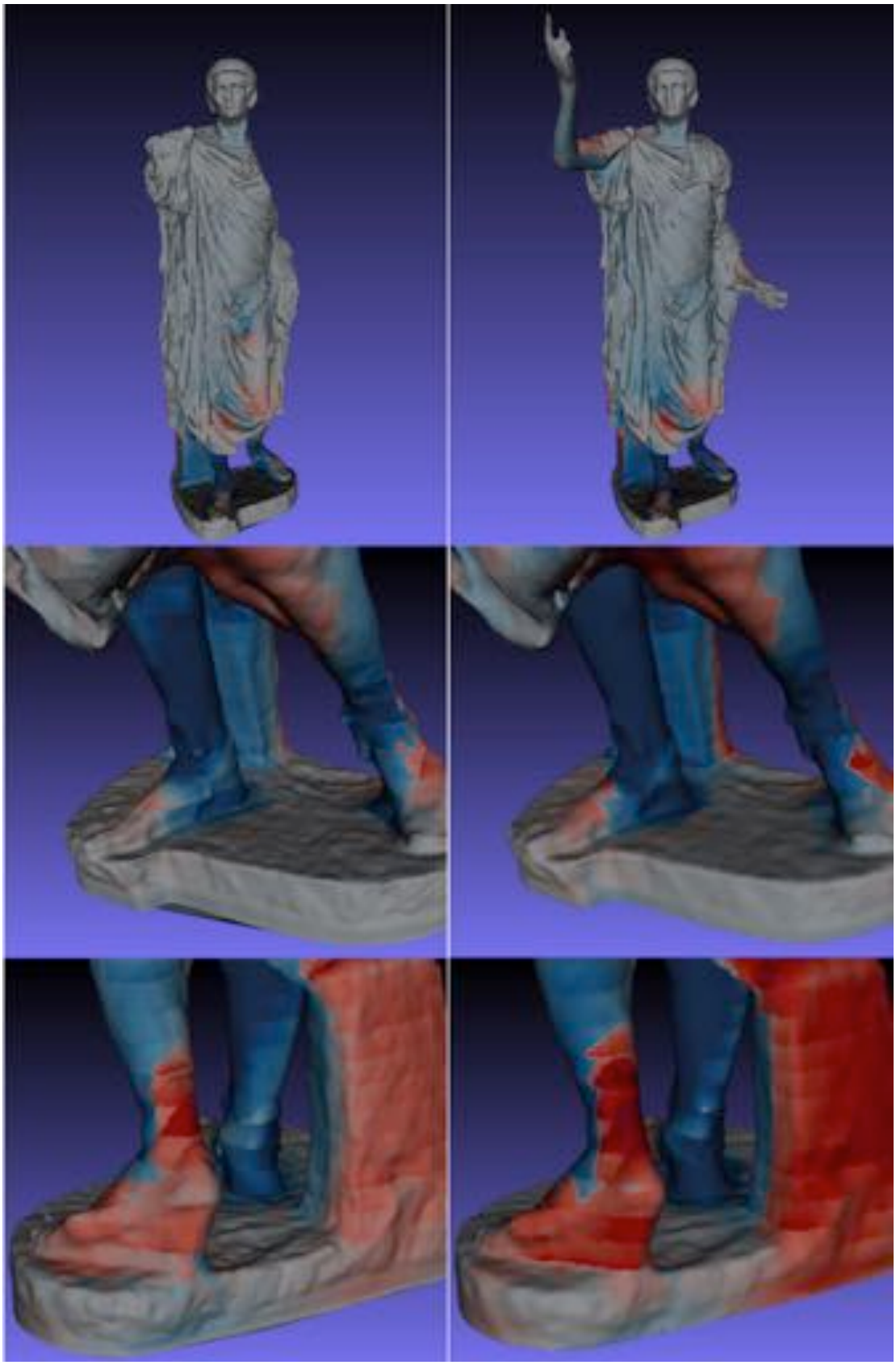

Figure 3.41 – Principal tension/compression of the original model (left) and virtually restore model (right).

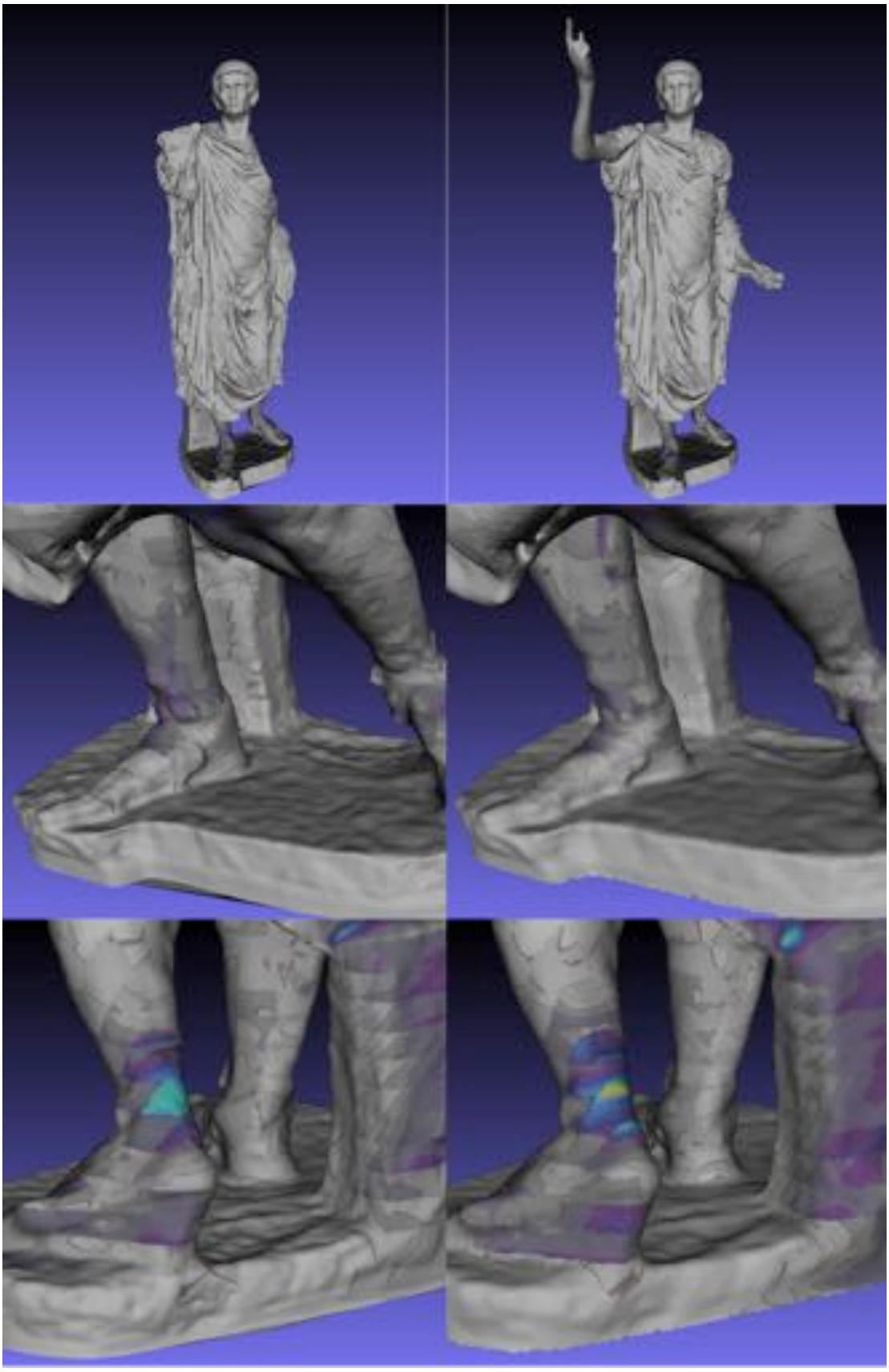

Figure 3.42 – Mohr/Coulomb stress of the original model (left) and virtually restore model (right).

Also in this case, calculated values have been deliberately expressed in the same scale of the original model, in order to make visually evident the increase of stresses and displacements: it appears clear that, in some cases ,values are largely out of scale. Undoubtedly the weight was originally distributed in a different way, and probably was more incisive on the right leg. Anyway both the legs and the support resulted generally more stresses, obviously because of the greater weight.

3.5. Second case of study: the statue of St. John the Baptist

3.5.1. Historical analysis

The second case of study is the statue of St. John the Baptist, also known as St. John the Child Martelli (full-figure statue), whose attribution is uncertain and still much debated among art historians, who are partly inclined to consider Donatello as the sole executor, partly instead prefer the hypothesis that Desiderio da Settignano is the author, as a student of the first, or, at last, was also supposed for a collaborative work between the two artists. The statue is currently conserved in the Bargello Museum of Florence from 1913, since its donation from the Martelli family, which commissioned it for sure to Donatello presumably in between 1455 and 1460 as reported in "The lives of the most excellent painters, sculptors and architects" by Vasari (1568).

Figure 3.43 – The statue of St. John The Baptist in Bargello Museum in Florence.

The young man represented is no more than ten or twelve years old, but it seems too much and badly developed, so high (about m 1,60) and with feet and hands so big. It is set in the act of walking to the left, with the step just opened, with the left leg, on which the body rests, not stuck solidly but a bit tilted in the direction of the path, and his foot sinking the thumb into the ground, while the right leg participates with reluctance to the movement, so that the foot is all still adhering to the ground. The same fatigue is shown in the arms: the right falls down the side, calling support, the hand holding the cross with three fingers and the stone of penance folded with the other two; the left, also close to the body, tightens only with his thumb and index finger, and not even strongly, the folder where the other fingers lie. The mantle of goatskin, which goes down to the knees, fastens with his end on the right side, that is narrow at the waist, with a woven cloth, and the mantle released hanging, as something insignificant, from the left shoulder can not hide the delicacy body, tapered, with sloping shoulders, with skinny chest on which he plunges his neck (De Nicola, 1913).

The statue, realized in marble, even if in full-figure, was probably set on a pedestal against a wall, as it is possible to see in the right part of a painting representing the Martelli family and dated 1777 (*Figure 3.44*). Since it was always conserved in closed places, it has a perfect state of preservation, only the gilding decayed because of the time.

Figure 3.44 – The paint representing the Martelli family where, on the right, it is possible to see the statue of St. John the Baptist in its original position (Ministero dei beni e delle attività culturali e del turismo (MiBACT), 2013).

3.5.2. The geometric survey and the calculations of surface modeling

The surveying of the statue of St. John the Baptist is part of the project "*Digital technologies for the documentation, management and divulgation of cultural heritage in the Museum of Casa Martelli in Florence*", held between the Superintendence for the Historical, Artistic and Ethno-anthropological Heritage of the Museums of City of Florence and the

Geomatics Laboratory for Conservation and Communication of Cultural Heritage of the University of Florence, which has, as its goal, the purpose to use the reprinted model, or otherwise the virtual model, in the Museum of Casa Martelli (GECO, 2013).

The survey of the statue was executed on May 10th, 2014 in the Bargello Museum in Florence, during the course "*Digitalization of archaeological finds and works of plastic art with scanner triangulation*" held at the Geomatics Laboratory for Conservation and Communication of Cultural Heritage of the University of Florence.

The instrument used for the survey is the ModelMaker MMDx/MMC Handheld equipped with MCAx Manual Coordinate Measuring Arm which is a precise, reliable and easy-to-use portable 7-axis measuring arm optimized for the scanning of even the most complex surfaces; it has been used by two operators of Leonardo 3D Metrology, the reseller of Nikon instrumentations, the manufacturer of the used system. The system is shown in *Figure 3.45* and its characteristic in *Table 3.46*.

Figure 3.45 – The ModelMaker MMDx/MMC Handheld equipped with MCAx Manual Coordinate Measuring Arm (Nikon Corporation, 2013).

Measuring range	Point repeatability	Volume length accuracy	Arm weight
2,5 m	0,027 mm	±0,038 mm	8,5 kg

Table 3.46 – Characteristics of ModelMaker MMDx/MMC Handheld equipped with MCAx Manual Coordinate Measuring Arm (Nikon Corporation, 2013).

As anticipated in paragraph 1.3, the instrumentation of this type differs substantially from the principle of operation seen previously. Undoubtedly, having a smaller scanning range and greater accuracy, as well as a much higher flexibility of movement, the obtained model will be extremely close to reality and precise in details and can be considered the instrument that best fit the needs of such a specific kind of surveying.

This family of tools is defined by the term "Articulated Arms of Measurement or Anthropomorphic Measuring Arms" or even by the acronym AACMM, namely "Articulated Arm Coordinate Measuring Machines". AACMM are manually controlled by the operator and work through the collection of 3D points of the volume by a series of rotary axes. They are usually equipped also with measuring probe, which is indispensable for the correct alignment of the point clouds, which is realised within the software of the machine.

They are typically constituted by three rods, connected together at their ends by joints, which allow rotational movements, which give rise to five, six or even seven degrees of freedom (*Figure 3.47*).

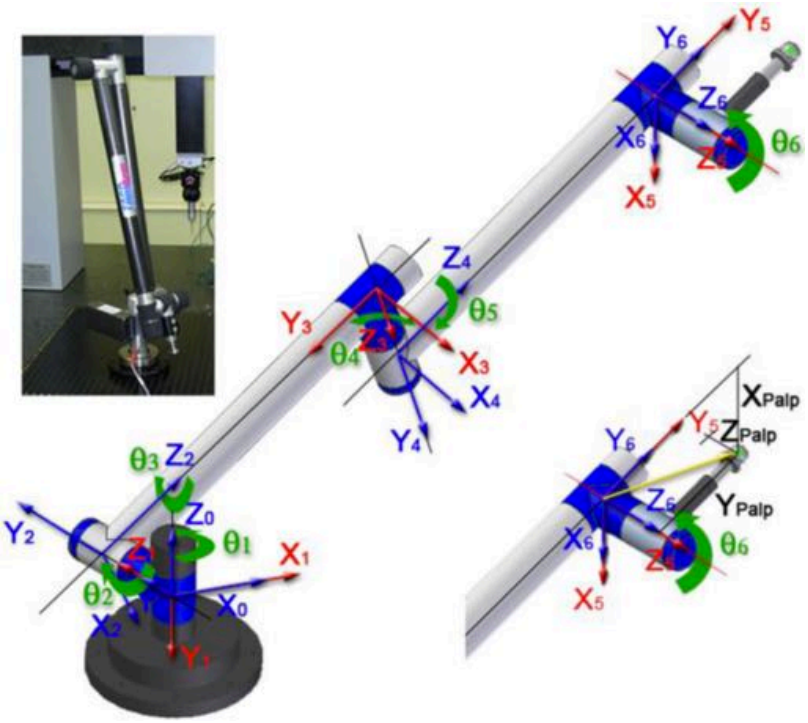

Figure 3.47 – Degrees of freedom in AACMM machine (Santolaria, Guillomia, Cajac, Albajez, & Aguilar, 2009).

A further joint is placed at the lower end of the first segment and connects it to the support base, while the end of the second segment is a third coupling that allows the mounting of the probe system. In the case of use of measuring sensors not in contact, for example in a laser stripe, some manufacturers propose a seventh rotary axis that allows the sensor to rotate around its own axis, ensuring better manoeuvrability of the system in the presence of pieces of morphology complex. Each joint has two angular encoders. The set of angular positions of all the encoders, associated to the relative lengths of the segments, allows the calculation of the position coordinates X, Y and Z of the tip of the contact element, which describes a measuring volume of spherical shape.

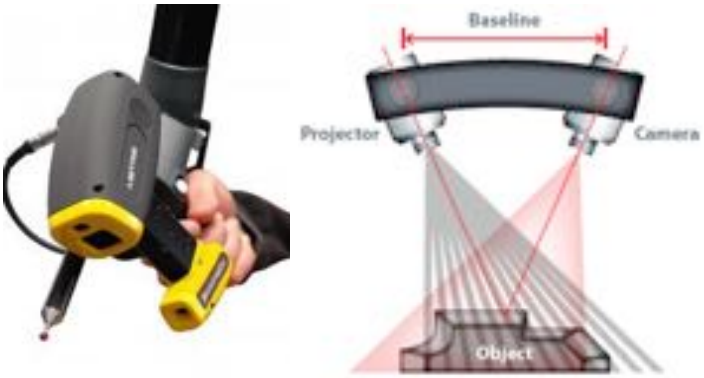

Figure 3.48 – a) The laser scanner applied to the machinery b) Triangulation scanner principles.

The laser device applied to the machinery (*Figure 3.48 a)*) works with the triangulation principles (*Figure 3.48 b)*): the global coordinates of points belonging to the laser stripe image are computed through camera model and laser plane equation. It is possible in this way to obtain the coordinates of all the surveyed points of the object.

As it regards the statue of St. John the Baptist, acquiring operations (phase 1 of *Scheme 1.8*) took about four hours of work (*Figure 3.49*): all the surface was surveyed and the obtained point cloud directly processed into the software Geomagic Wrap, which allows the rapid transformation of point cloud data and probes into 3D polygonal surfaces (phase 2, 3 and 4 of the same *Scheme 1.8*).

Figure 3.49 – Surveying of the statue of St.John Child : the operator acquiring data moving manually the AACMM. The laser stripe is clearly shown on the face of the statue.

Procedures of data alignment and registration are automatically applied within the software: this implies that, if on the one hand the process is very rapid on the other hand is not controllable by the operator. The processed data are returned from the software directly in the form of a three-dimensional surface model consisting in an extremely dense mesh, already checked for consistency and therefore free of errors such non-manifolds, double or self-intersecting surfaces (*Figure 3.50*). The final surface consists in a mesh of 5.178.132 triangles. In this case, therefore, the only operation necessary to obtain a closed surface, and therefore a 3D solid model, consist in closing the only hole, which is given by the opened base of the statue, and namely the surface adherent with the pedestal.

Figure 3.50 – On the left a detail of the statue and on the right the same detail on the surface mesh. As it is possible to see the mesh has a realyy high LoD.

3.5.3. Analysis of possible movements

Referring to paragraph 3.2 the analysed object belongs to typology T3 of *Table 3.1*, and leaning on a flat surface, on a pedestal, possible mechanism of dynamic reaction and related damage mechanism that could afflict it, according to *Table 3.3* and *3.4*, are:

- adherent movement over stressing;
- slipping movement over displacement;
- oscillation movement repeated collision and overturning.

It will be therefore interesting to determinate which one of the above mechanism will intervene on the statue, starting from the geometrical data deducible from the 3D model obtained.

Importing the 3D model into MeshLab it is possible to obtain most general geometric information like dimensions, visualizing them on a "*Quoted box*", in order to foresee the main measures (*Figure 3.51 and 3.52*). Another possibility offered by the software, is the automatic determination of several geometric parameters, by means of the command "*Compute geometric measure*", like (*Figure 3.51*):

- Mesh Volume 0,066 m^3;
- Mesh Surface 2,066 m^2;
- Thin shell barycentre (3,06 cm; 2,01 cm; 66,01 cm);

- Centre of Mass (3,47 cm; 2,14 cm; 72,29 cm);
- Inertia Tensor $\begin{vmatrix} 0{,}012450 & -0.000092 & -0.000281 \\ -0.000092 & 0{,}012671 & 0{,}000016 \\ -0.000281 & 0{,}000016 & 0{,}000808 \end{vmatrix}$
- Principal axes $\begin{vmatrix} 0{,}024128 & 0{,}999708 & 0{,}001130 \\ 0{,}937403 & -0{,}022232 & -0{,}347537 \\ 0{,}347410 & -0{,}009445 & 0{,}937666 \end{vmatrix}$

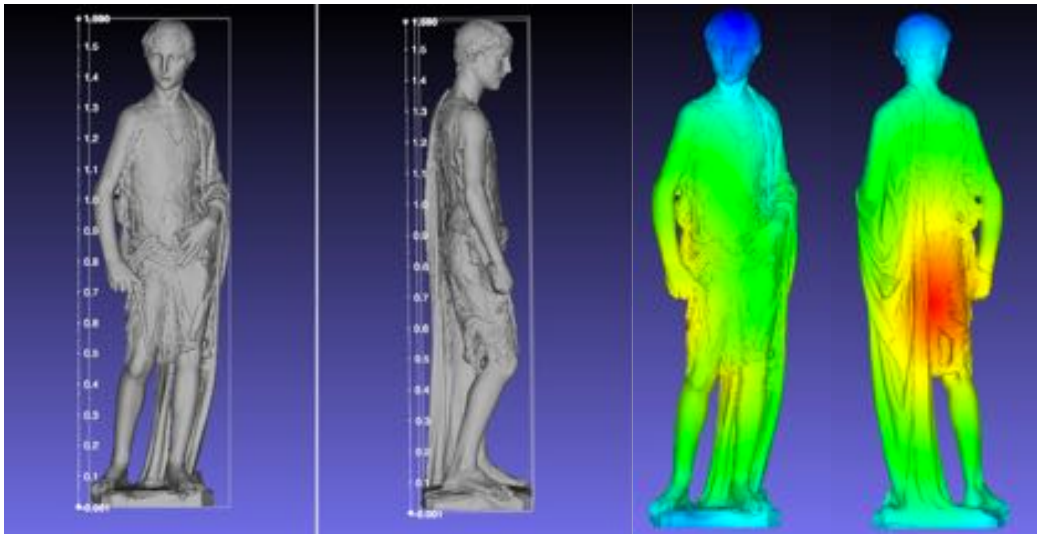

Figure 3.51 – On the left the statue seen from front and side in quoted box in order to visualize quickly the dimensions. On the right the mesh from the front side and the back side colorized by distance from the centre of mass, localized in G (3,47 cm; 2,14 cm; 72,29 cm).

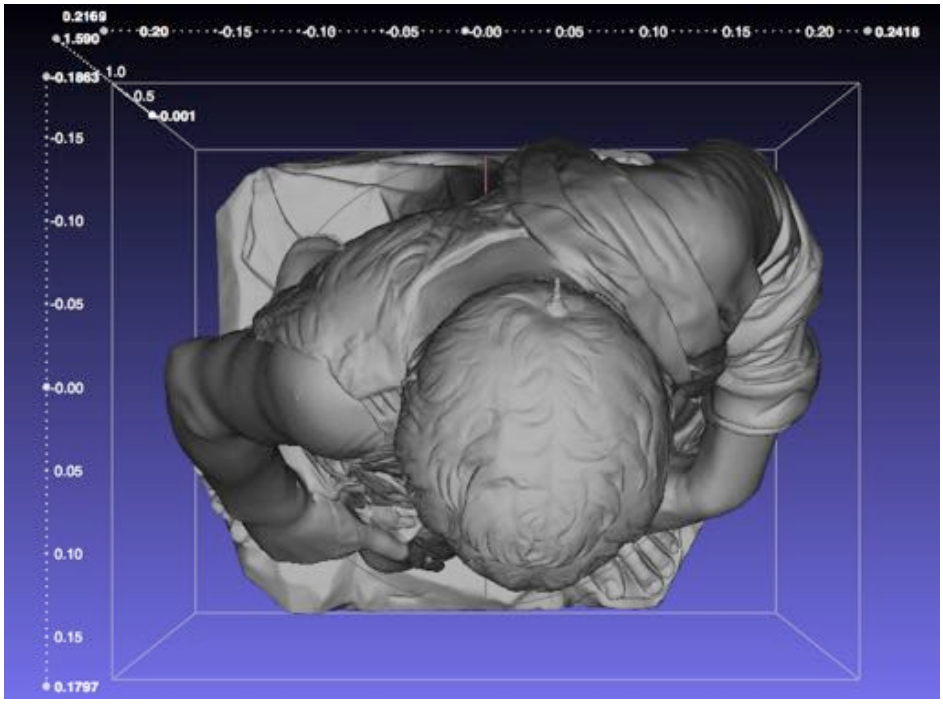

Figure 3.52 – The quoted box seen from the top of the statue in order to visualize quickly the dimensions.

From the dimensions of the quoted box it is possible to calculate the horizontal distances between the projections of centre of mass of the statue G and the axis of rotation:

$$\begin{cases} B_x^1 = 24{,}18 - 3{,}47 = 20{,}71\ cm \\ B_x^2 = 21{,}69 + 3{,}47 = 25{,}16\ cm \end{cases} \quad \begin{cases} B_y^1 = 18{,}63 - 2{,}14 = 16{,}49\ cm \\ B_y^2 = 17{,}97 + 2{,}14 = 20{,}11\ cm \end{cases}$$

Therefore, according to paragraph 3.2, in order to verify which force has to be applied for having adherent, slipping or oscillatory movement, the minimum distance between the projection of centre of mass of the statue G and the axis of rotation has to be considered, and related to the height of the centre of mass G:

$$\frac{B}{H} = \frac{B_y^1}{H} = \frac{16{,}49\ cm}{72{,}29\ cm} = 0{,}228$$

whence derives that the minimum acceleration that must be applied, in order to have an oscillation of the object, will results:

$$a_g = \frac{B_y^1}{H} g = 0{,}228 \cdot 9{,}81 = 2{,}24\ \frac{m}{s^2}$$

Considering that the volume of the statue is equal to 0,066 m^3 and the specific weight of marble can be considered equal to γ = 2.650 kg/m^3, it will result that the mass *M* of the statue will be approximately 175 kg, therefore the force necessary to start an oscillatory movement will be:

$$F = Ma_g = \frac{B_y^1}{H} g = 175kg \cdot 2{,}24\ \frac{m}{s^2} = 392\ N$$

It will be therefore interesting to estimate if the statue, in case of an horizontal force applied, will be collapsing because of over stresses or because of a crash due to over turning, this analysis will be held in sub paragraph 3.5.5.

3.5.4. Simplification of the 3D solid model

As anticipated in sub paragraph 3.5.2 the main purpose of this surveying was the intention to use the 3D model for reprinting or virtual reality, therefore the LoD results at its maximum possible definition. As know, in order to perform a structural analysis such a high resolution is not necessary, on the contrary, it will led to an excessive computation of the FEA software.

In order to make the model more suitable for structural analysis, it is necessary a simplification of the mesh, paying attention to not change some important values like the coordinates of the centre of mass or the total volume of the object. The chosen procedure for simplification was the decimation, further and better described in sub paragraph 4.2.7, which fundamentally consist in decrementing the number of the "useless" triangles composing a mesh. As it is possible to see in *Figure 3*.5,3 the mesh after this operation appears really simplified

and suitable for FEA softwares, being composed of 358.230 triangles, less than the 10% of the initial mesh.

Figure 3.53 – On the left the original model of the statue, on the right the simplified mesh. On the top the full figure and on the bottom a detail. The second model appears much smoother and details are removed.

In order to verify if the geometrical characteristic were maintained also in the simplified model, the command "*Compute geometric measures*" was applied obtaining the values synthetized, and compared to previous one, in *Table 3.54*.

		Original model	Simplified Model	Difference
Mesh Volume		0,066013 m^3	0,065988 m^3	0,000025 m^3
Mesh Surface		2,065576 m^2	2,005458 m^2	0,060118 m^2
Thin shell barycentre	X	0,030579 m	0,030665 m	-0,000086 m
	Y	0,660129 m	0,663272 m	-0,003143 m
	Z	-0,020131 m	-0,020457 m	0,000326 m
Centre of Mass (G)	X	0,034721 m	0,034693 m	0,000028 m
	Y	0,722907 m	0,722269 m	0,000638 m
	Z	-0,021406 m	-0,021405 m	-0,000001 m

Table 3.54 – Main geometric value of original and simplified model compared.

As it is possible to see from the third column of the above Table the difference is almost irrelevant, except for the surface value, which differs for about 6 cm^2. As logical this difference is due to the fact that the surface was simplified, but this factor has no influence on the structural analysis.

3.5.5. Structural analysis

Recalling therefore what have been explained in sub paragraph 3.5.3, the statue will be analysed supposing two conditions:

1. only gravity load acting,
2. gravity load and a horizontal force applied in barycentre with the minimum value necessary to start an oscillatory movement,

in order to verify the static condition and also, as already said, if over stresses will be the cause of collapsing or otherwise if such a force will cause an over turning.

The procedure adopted was the same described in sub paragraph 3.4.4: the model was imported in Rhinoceros, verified, and the through the plug-in Scan-and-Solve structurally analysed. Assuming that there will be no movement on the base of the statue, caused by the forces, a fixed end was there adopted. In the first of the two conditions only the gravity load was considered, while in the second, beside gravity, another body load was applied, considering a vector with components (-2,24, 0, 0) $[m/s^2]$, where the first component represents the critical dragging acceleration, estimated in sub paragraph 3.5.3, which will be multiplied for the body weight by the software. In both conditions the material is supposed to be a stronger marble than the one adopted for the case of Emperor Claudio Statue. The mechanical parameters of *Figure*

3.55, deduced by a similar condition treated by Sorace & Terenzi (2015), were assumed. The chosen resolution was the minimal, and namely 9.999 elements.

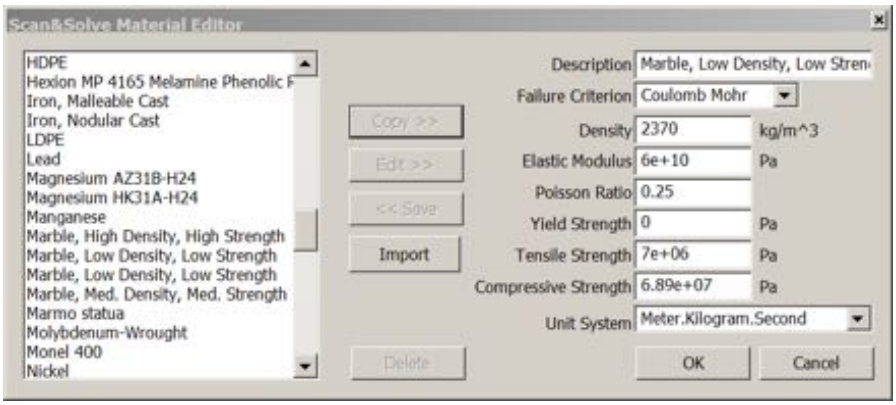

Figure 3.55 – Material editor in Scan-and-Solve: parameters chosen for the Marble of the statue of St. John Child.

Proceeding therefore with the analysis, the numerical results (minimum and maximum) obtained are shown in *Table 3.56*, for first load condition, and in *Table 3.57*, for second load condition.

	Minimum	Maximum
X-Displacement	-3.23979e-07 m	1.65324e-06 m
Y-Displacement	-1.03603e-05 m	5.51093e-08 m
Z-Displacement	-2.50413e-06 m	2.2527e-07 m
Total Displacement	5.37129e-14 m	1.05146e-05 m
Von Mises Stress	59.4832 Pa	348212 Pa
Max. Principal Stress	-69007.8 Pa	100285 Pa
Mid. Principal Stress	-87897.8 Pa	32670.3 Pa
Min. Principal Stress	-395982 Pa	16645.7 Pa
Danger Level (Rankine)	2.48955e-06	0.0364672
Danger Level (Coulomb Mohr)	2.67831e-06	0.0364672
Danger Level (Modified Mohr)	2.67831e-06	0.0364672

Table 3.56 – Minimum and maximum results of the structural analysis in the condition of gravity load

	Minimum	Maximum
X-Displacement	-1.09279e-07 m	0.000229977 m
Y-Displacement	-4.73835e-05 m	1.37987e-05 m
Z-Displacement	-3.5592e-05 m	3.88972e-05 m
Total Displacement	8.24927e-13 m	0.000234425 m
Von Mises Stress	98.6105 Pa	7.87833e+06 Pa
Max. Principal Stress	-2.06326e+06 Pa	8.58484e+06 Pa
Mid. Principal Stress	-2.13354e+06 Pa	1.73215e+06 Pa
Min. Principal Stress	-9.09999e+06 Pa	1.44748e+06 Pa
Danger Level (Rankine)	4.86741e-06	Criterion Limit Exceeded
Danger Level (Coulomb Mohr)	4.86741e-06	Criterion Limit Exceeded
Danger Level (Modified Mohr)	4.86741e-06	Criterion Limit Exceeded

Table 3.57 – Minimum and maximum results of the structural analysis in the condition of gravity load and a horizontal force due to critical dragging acceleration

From the results above reported, it is possible to imagine that in case of application of the horizontal force, determined in 3.5.3, the collapsing of the object will be due to over stress, since the resistance criterion is exceeded for a value of force inferior than the one needed for overturning. Results are therefore reported in the following *Figures 3.58*, *3.59* and *3.60*, where the trends of values are reported in the same scale for both the load conditions, in order to make them easily comparable.

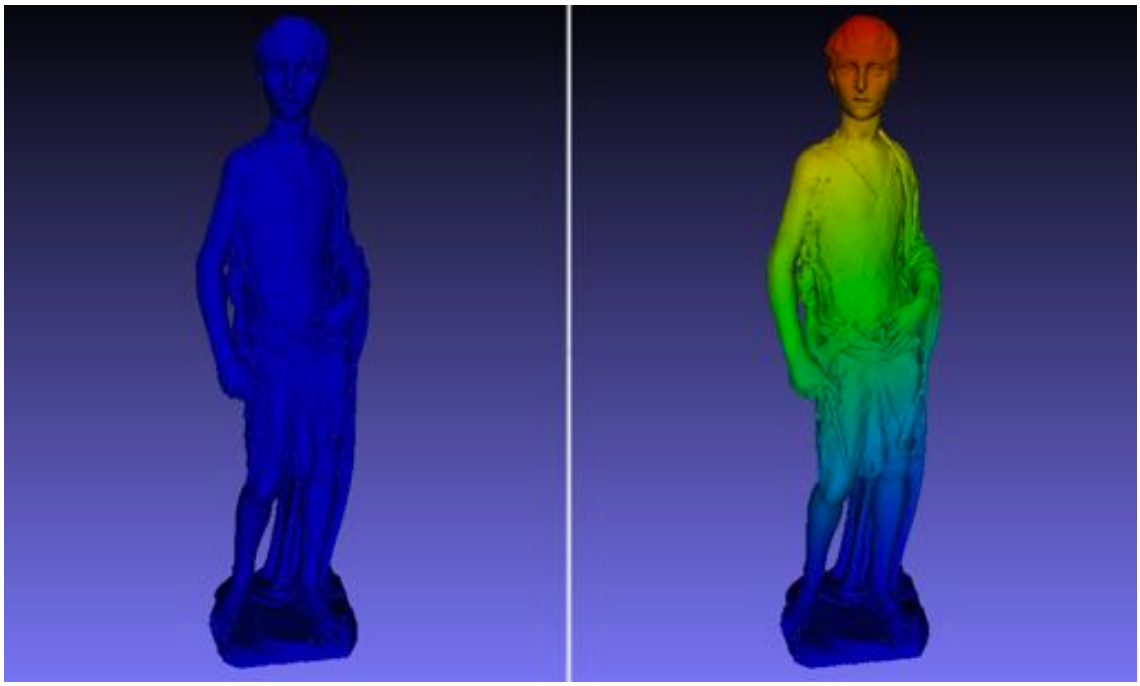

Table 3.58 – Total displacement trend from the value 0 (blue) to 0,005 mm (red) – on the left the first load condition and on the right the second load condition.

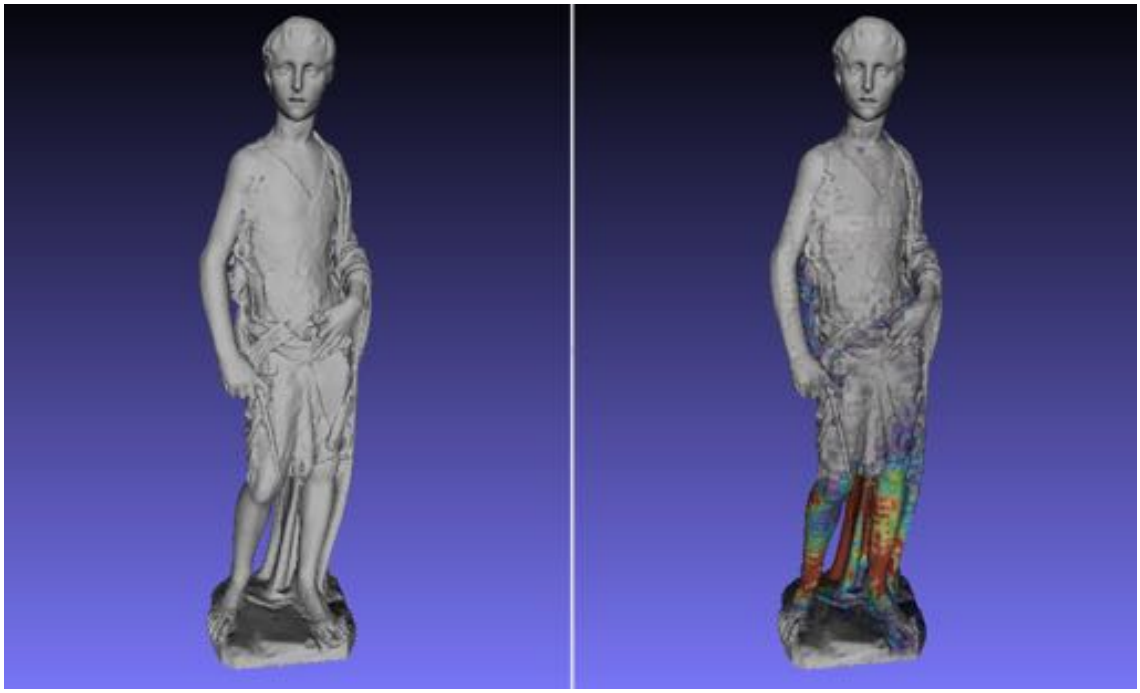

Table 3.59 – Verification fo Coulomb-Mohr Criterion trend from the value 0 (blue) to 1 (red) – on the left the first load condition and on the right the second load condition.

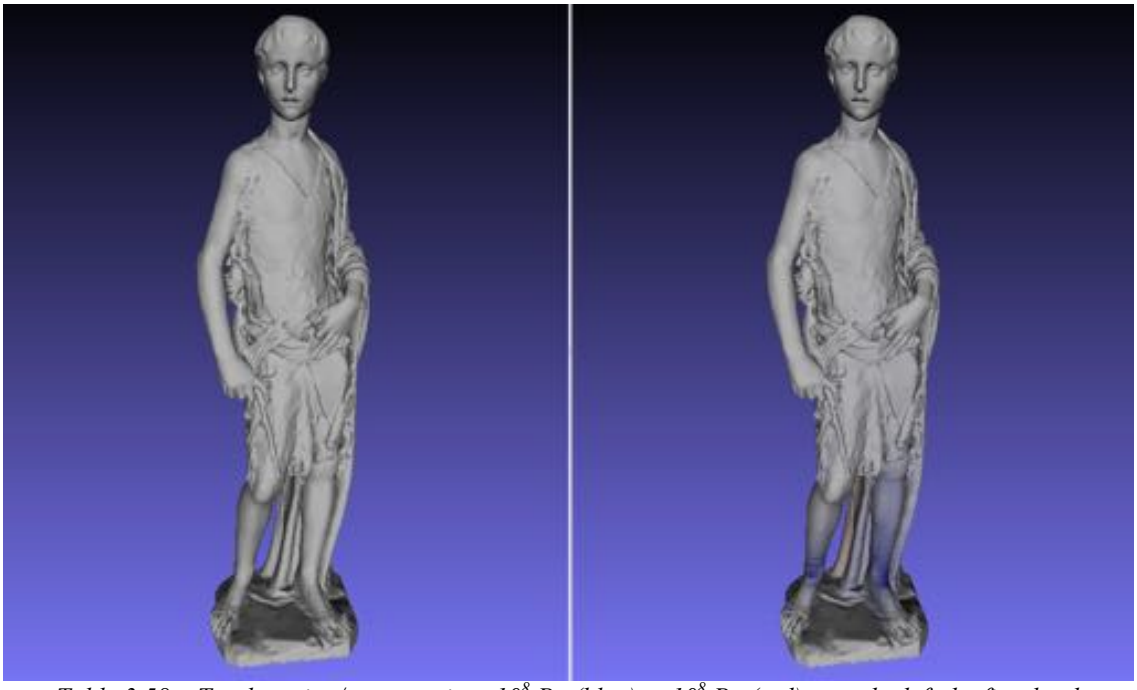

Table 3.58 – Total tension/compression -10^8 Pa (blue) to 10^8 Pa (red) – on the left the first load condition and on the right the second load condition.

3.6. Conclusions

In this chapter the case of small size objects was focused: first and foremost the current Legislation was analysed and then some example of the current trends on surveying of such subjects were reported. Two case of study were faced: both of them are represented by statues, the first one is a sculpture in a poor state, for significant lacks, surveyed with a TLS, the second one is a famous statue in an excellent state of preservation surveyed with a close range sensor system. The models obtained were really dissimilar as regards the LoD and therefore were treated in a very different way: the procedures were described as it refers the surface modeling, the transformation of this model to a solid one, the subsequent structural and geometrical analysis held. The chapter also deals with the hypothesis of virtual restoring of the objects.

3.7. Bibliography

Attene, M., Campen, M., & Kobbelt, L. (2013). Polygon mesh repairing: An application perspective. *Journal ACM Computing Survey , 45* (15).

Augusti, G., & Ciampoli, M. (2000). *Vulnerabilità sismica degli oggetti esibiti nei musei: interventi per la sua riduzione.* (D. Liberatore, A cura di) Roma: Tipografia Esagrafica.

Betti, M., Orlando, M., & Spinelli, P. (2015). La Rocca Strozzi a Campi Bisenzio: Analisi strutturali e proposte di interventi di consolidamento e miglioramento sismico. *Bollettino Ingegneri* (5), 3-24.

Binda, L., Cardani, G., & Saisi, A. (2005). *A classification of structures and masonries for the adequate choice of repair - International RILEM Workshop on Repair Mortars for Historic Masonry*, (p. 20-34). Delft.

Binda, L., Penazzi, D., & Saisi, A. (2003). Historic Masonry Buidings. Necessity of a Classification of Structures and Masonries for the Adequate Chioce of Analytical Models. *VI International Symposium Computer Methods in Structural Masonry* (p. 22-24). Rome: STRUMAS.

Borri, A., Falletti, F., Fastellini, G., Grassi, S., Grazini, A., Marchetti, L., et al. (2005). *La stabilità delle grandi statue: il David di Michelangelo.* (A. Borri, A cura di) Roma: DEI s.r.l. Tipografia del Genio Civile.

Croci, G., D'Ayala, D., & Liburdi, R. (1995, 11/2). History, observation and mathematical models in the seismic analysis of the Valadier abutment area in the Colosseum. *Annali di Geofisica , XXXVIII* (5-6), p. 957-970.

De Canio, G. (2012). Marble devices for the Base isolation of the two Bronzes of Riace: a proposal for the David of Michelangelo. *The 15th World Conference on Earthquake Engineering.* Lisboa, Portugal.

De Nicola, Giacomo. (1913). Il San Giovannino Martelli di Donato. *Bollettino d'Arte , VII*, p. 277.

GECO. (2013). *Geomatica e conservazione*. Tratto il giorno 2015 da http://www.geomaticaeconservazione.it/: http://www.geomaticaeconservazione.it/

Giangreco, E. (2002). *Ingegneria delle strutture - Progettazione strutturale* (Vol. 3). Torino: UTET.

Grün, A., Remondino, F., & Zhang, L. (2004). Photogrammetric Reconstruction of the Great Buddha of Bamiyan, Afghanistan. *The Photogrammetric Record , 19* (107), 177-199.

Intact Solutions, LLC. (2009). Scan&Solve: FEA without meshing - White paper.

Istituto Regionale per il Patrimonio Culturale del Friuli Venezia Giulia. (2008). *http://www.sirpac-fvg.org/.* Tratto il giorno 2013 da Sistema informativo regionale del

patrimonio culturale : http://46.137.91.31/web/catalogazione/search/SchedaDetail.aspx?TSK=RA&ID=15371&g=5

Istruzioni per l'applicazione delle Norme tecniche per le costruzioni di cui al D.M. 14 gennaio 2008 , Circolare n. 617 (Consiglio Superiore dei Lavori Pubblici febbraio 2, 2009).

Kazhdan, M., Bolitho, M., & Hoppe, H. (2006). Poisson Surface Reconstruction. *Eurographics Symposium on Geometry Processing* (p. 61-70). Aire-la-Ville: Dieter W. Fellner, Werner Hansmann, Werner Purgathofer, François Sillion Series Editors.

Levoy, M., Pulli, K., Curless, B., Rusinkiewicz, S., Koller, D., Pereira, L., et al. (2000). The digital Michelangelo project: 3D scanning of large statues. *Proceedings of the SIGGRAPH '00 - 27th annual conference on Computer graphics and interactive techniques* (p. 131-144). New York: CM Press/Addison-Wesley Publishing Co.

Limoncelli, M. (2012). *Il restauro virtuale in archeologia.* Roma: Carrocci editore.

Linee Guida per la valutazione e riduzione del rischio sismico del patrimonio culturale, prot. n. 92 (Consiglio Superiore dei Lavori Pubblici luglio 23, 2010).

Lolli, A. (2010). Monitoraggio per la diagnostica strutturale del David di Michelangelo. University of Bologna, Italy.

Lourenċo, P. B. (2002, 7 17). Computations on historic masonry structures. *Progress in Structural Engineering and Materials , 4* (3), p. 301-319.

Macchi, G., Ruggeri, G., Eusebio, M., & Moncecchi, M. (1993). Structural Assessment of the Leaning Tower of Pisa. *IABSE reports of the working commissions , 70* (351), p. 401-408.

Ministero dei beni e delle attività culturali e del turismo (MiBACT). (2013). *Museo di Casa Martelli - Firenze*. Tratto il giorno 2015 da museiditalia - musei digitali: http://www.culturaitalia.it/opencms/museid/viewItem.jsp?language=it&case=&id=oai%3Acultu raitalia.it%3Amuseiditalia-mus_8175

Nikon Corporation. (2013). *www.nikon.com*. Tratto il giorno 2014 da Nikon metrology.

Norme tecniche per le costruzioni (Decreto Ministeriale gennaio 14, 2008).

Pascale, G., Bastianini, F., & Carli, R. (2011). Monitoring marble cracking in the David by Michelangelo. (11), 21-24.

Pinto, P. E., & Franchin, P. (2008). Assessing existing buildings with Eurocode 8 part 3: a discussion with some proposal. *Eurocodes: background and application Workshop.* Brussels.

Riccardelli, C., Soultanian, J., Morris, M., Becker, L., Wheeler, G., & Street, R. (2014). The Treatment of Tullio Lombardo's Adam: A New Approach to the Conservation of Monumental Marble Sculpture. *Metropolitan Museum Journal* (49).

Roca, P., Cervera, M., Gariup, G., & Pelà, L. (2010, 7 22). Structural Analysis of Masonry Historical Constructions. Classical and Advanced Approaches . *Archives of Computational Methods in Engineering* (17), p. 299-325.

Santolaria, J., Guillomia, D., Cajac, C., Albajez, J. A., & Aguilar, J. J. (2009). Modeling and Calibration Technique of Laser Triangulation Sensors for Integration in Robot Arms and Articulated Arm Coordinate Measuring Machines. *Sensors , 9*, p. 7374-7396.

Smoljanović, H., Živaljić, N., & Nikolić, Ž. (2013, 7 25). Overview of the methods for the modeling of historical masonry structures. *Građevinar , 65*, p. 603-618.

Sorace, S., & Terenzi, G. (2015). Seismic performance assessment and base-isolated floor protection of statues exhibited in museum halls . *Bull Earthquake Eng* , 1873-1892.

Vasari, G. (1568). *Le vite de' più eccellenti pittori, scultori e architettori.* (M. Marini, A cura di) Roma, Italia: Newton Compton editori s.r.l.

Visintini, D., & Spangher, A. (2013). Rilevamento laser scanning, modello della superficie (DSM) e modello per il metodo agli elementi finiti (FEM) di una struttura . *Atti 17a Conferenza Nazionale ASITA* (p. 1287-1294). Riva del Garda: ASITA.

4. MEDIUM SIZE OBJECT

4.1. Introduction

The second class of objects that is going to be investigated, through this thesis, is the "medium" size one that, properly, for its intermediate connotation can collect a wide range of cases. It is intended then, with this definition, to not include all those objects that do not represent a separable portion from the structure and for which it is necessary to achieve a high level of detail, like the statues previously analysed, and, at the same time, to exclude building in its entirety, that will be treated in the following chapter. Thereby, under this class can be included the so-called "constructive elements" that play a key role in the structure and that, for this reason, require specific and localized analysis but, at the same time, need a lower level of detail, with respect to the "small size" objects.

This class of objects could therefore include:

- arches;
- vaults;
- colonnades;
- façades;
- arcades;
- walls;
- other constructive elements;

as long as they could be considered as a part of a more complex structure, connected in their structural behaviour to the rest albeit with their own dynamics.

In particular, most of the geomatic surveying performed in this field involve cases of objects of average size, as before defined. Scientific literature offers, therefore, a wide excursus into this typology of objects, also because they are, all things considered, the easiest to modeling since:

- it is not required such a high level of detail (like in the case of small size objects);
- the surveying can be realized from few station points and it is not difficulty articulated (like for a whole building);
- it can be used only an instrument, since on one side station are pretty close to each other and there is a sufficient overlapping of scans and it is not strictly necessary topographic measures for the registration of scans, on the other side is not necessary to employ close range laser scanners, since performances offered by TLS is more than sufficient;
- modeling has minor occlusion problems and surfaces are generally more regular.

Nevertheless as in previous case, the model obtained must be treated in order to be structurally analysable by means of the existing software. From the legislative point of view, it is sufficient to refers to what have been recalled in the second chapter of this thesis, remembering that the study of "constructive details" requires a specific analysis of the same,

taking in consideration the influence of the boundary condition, like the imposed restraints or forces due to the surrounding buildings or other elements of the considered structure.

The chapter will therefore focus on the example considered as case of study, which is the Bollani Arch in Udine, describing, beside the object itself and its surveying and modeling, the aspects related to the structural analysis and focusing, particularly, on the level of detail concept.

4.2. Analysis of medium-size objects: current trends

Even if the modeling of medium size objects is quite simpler than the one of large size buildings, and also the structural analysis appears easier if related to a single object, there are not so many examples of medium size object structural analysis derived from a geomatic model.

One of the most recent example is represented by the work "*Laser scanning technology for static evaluation of historic structures*" (Chiabrando, Donadio, Spanò, & Sammartano, 2015). In this paper are presented some models obtained from dense TLS clouds, the orthophotos produced and the following extraction of features and subsequent realization of the structural model (*Figure 4.1*).

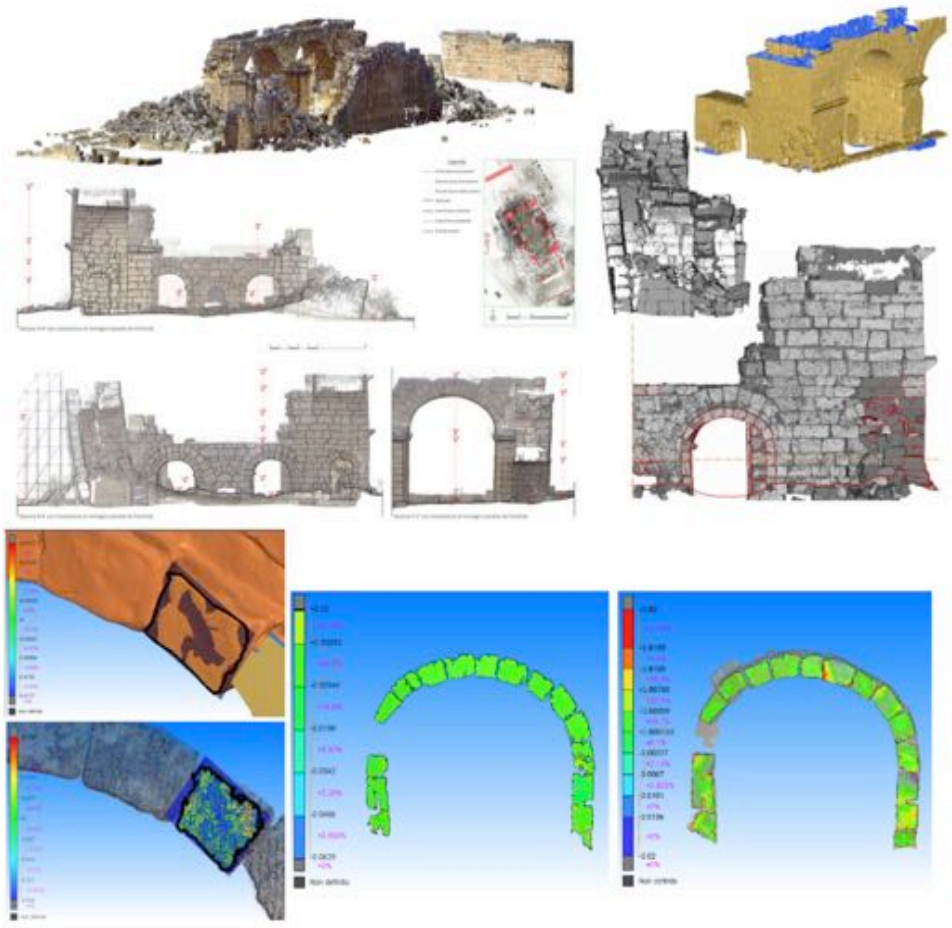

Figure 4.1 – Textured point cloud model, surface model of a portion of the buildings' rests. Different algorithms for the definition of the ashlars composing the arch (Chiabrando, Donadio, Spanò, & Sammartano, 2015).

Another interesting work is "*Digital Unwrapping and visualization of complex architectural surfaces for the documentation and the restoration*" (Cannella, 2015), where is not carried out a specific structural analysis, but is shown an interesting extraction of geometrical data, useful for engineering purposes (*Figure 4.2*), from the mesh obtained with a TLS surveying. In this work, only simplified geometries are obtained, hence it should be implemented in order to obtain more detailed features, but the approach is quite interesting, since the single elements were considered separately.

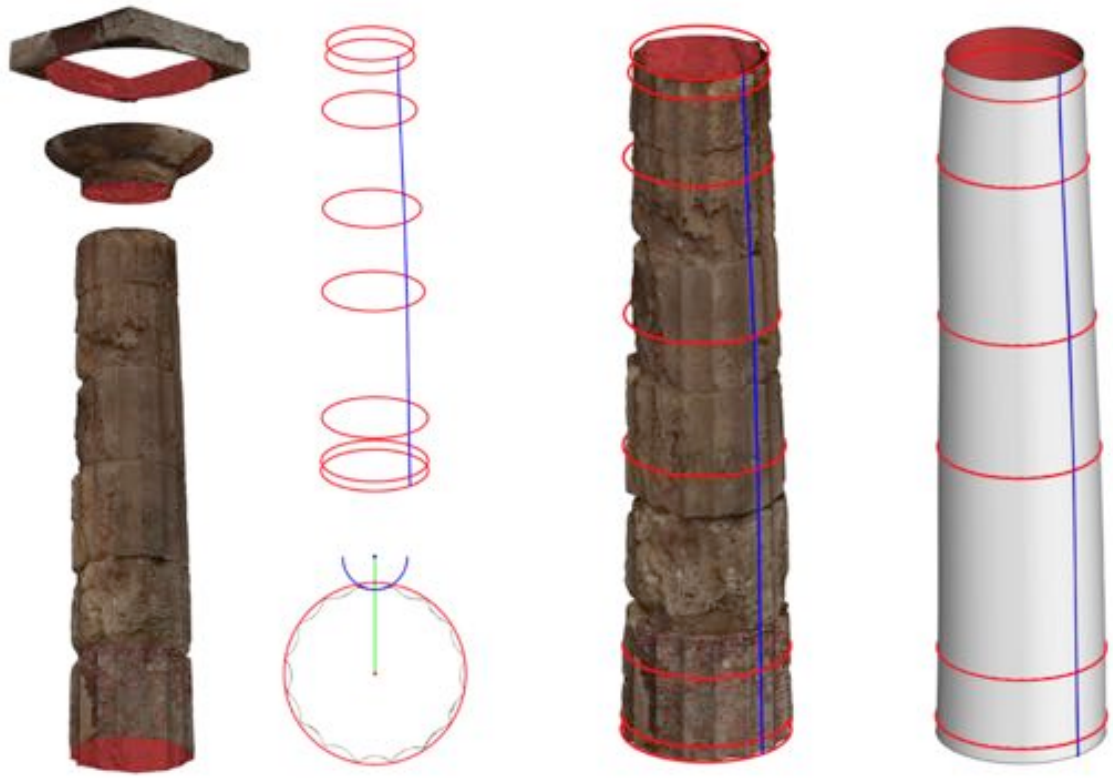

Figure 4.2 – Textured point cloud model, surface model of a portion of the buildings' rests. Different algorithms for the definition of the ashlars composing the arch (Cannella, 2015).

In "Terrestrial Laser Scanning and settled techniques: a support to detect pathologies and safety conditions of timber structures" (Bertolini Cestari, Chiabrando, Invernizzi, Marzi, & Spanò, 2013) is illustrated the surveying executed on the vault of the Hall of Honour of the Valentino's Castle in Torino that revealed the deformations and the damages suffered by the abutments. The paper illustrates the generation of the 3D high-resolution model and its relations with the results of the structural survey; both of the models obtained support the Finite Element numerical simulation of the dome (*Figure 4.3*).

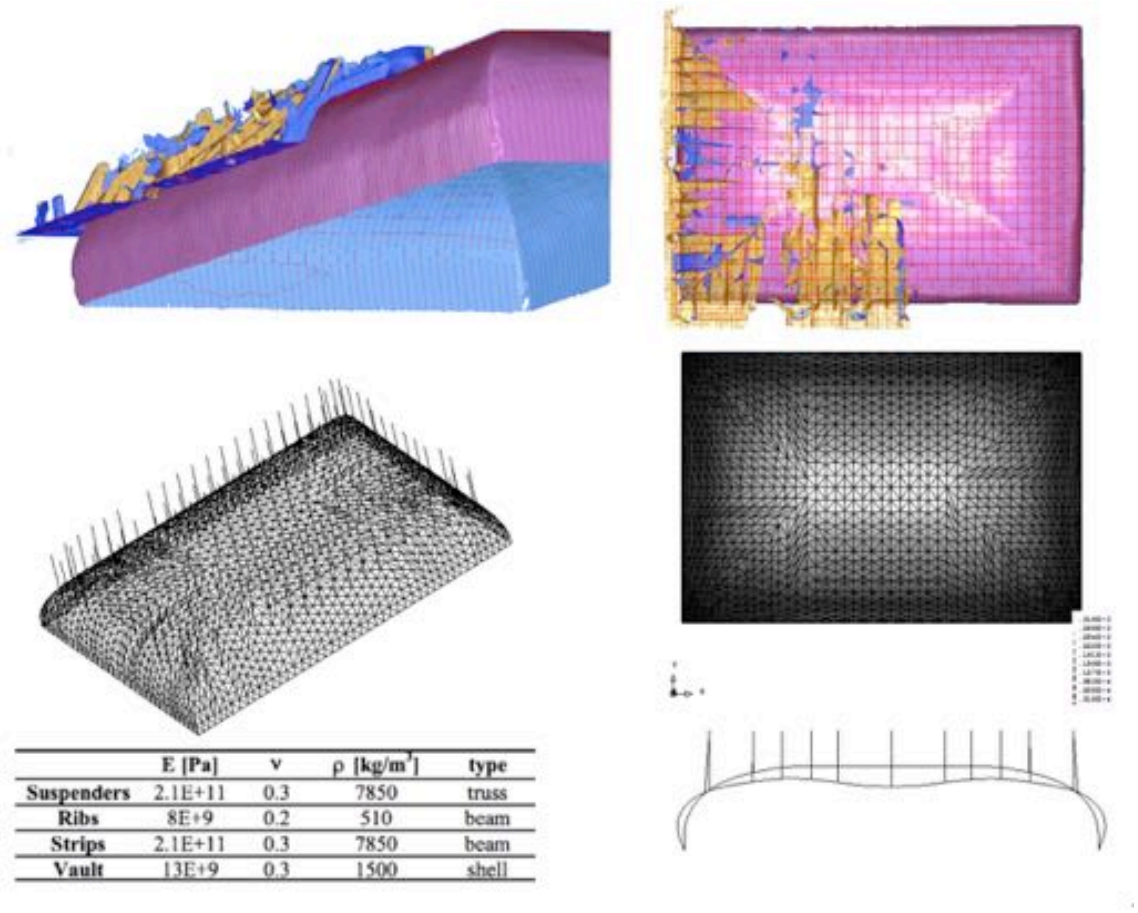

	E [Pa]	ν	ρ [kg/m³]	type
Suspenders	2.1E+11	0.3	7850	truss
Ribs	8E+9	0.2	510	beam
Strips	2.1E+11	0.3	7850	beam
Vault	13E+9	0.3	1500	shell

Figure 4.3 – The surfaces of the vault from the interior (blue) and the exterior (pink) in order to obtain the correct thickness. The subsequent FEM analysis (Bertolini Cestari, Chiabrando, Invernizzi, Marzi, & Spanò, 2013).

In "Automatic 3D modeling of metal frame connections from LiDAR data for structural engineering purposes" (Cabaleiro, Riveiro, Arias, Caamano, & Vilan, 2014) a new method for the detection, from TLS data and automatic 3D modeling, of frame connections and the formation of profiles comprising a metal frame, is described. In this case, structure connections are identified selecting areas in the point cloud. As a result, the coordinates of the connection centre, composition (profiles, size and shape of the haunch) and direction of their profiles are extracted. The 3D model of connections and metal frames, which are suitable for processing software for structural engineering applications, are finally defined and structural calculations so performed. The procedure is described in *Figure 4.4*.

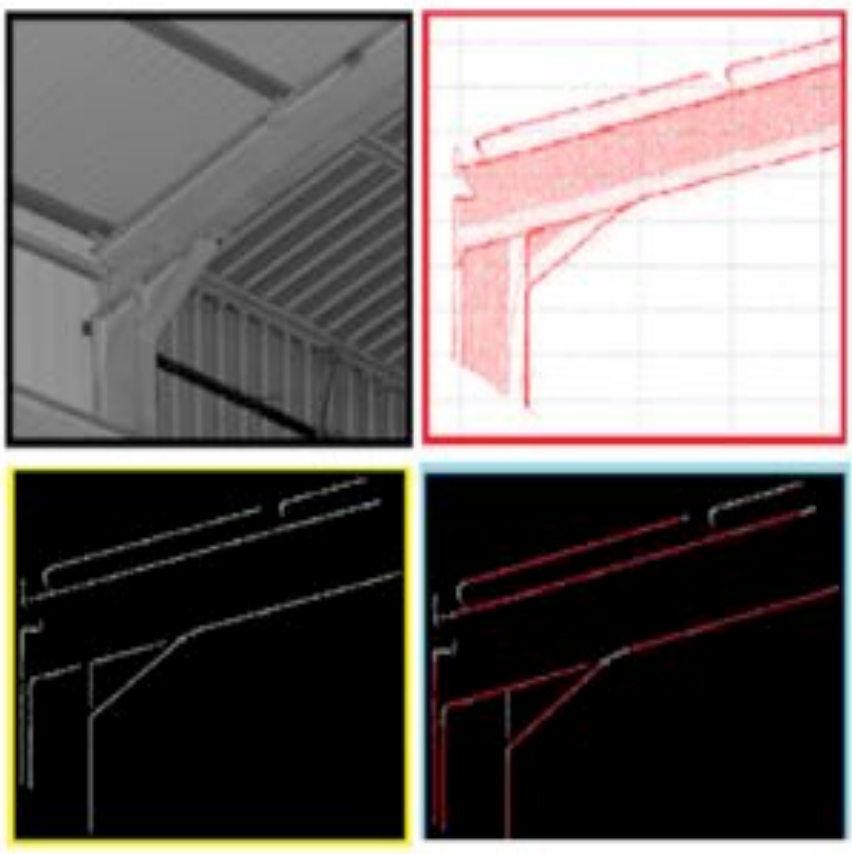

Figure 4.4 – Point cloud of apex connection - Projection of the point cloud - Binary image - Lines found by applying the Hough transform (Cabaleiro, Riveiro, Arias, Caamano, & Vilan, 2014).

4.3. Case of study: the Bollani Arch in Udine

4.3.1. Historical description

The "medium" size case thesis example is represented by the Bollani Arch, erected in 1556 and located at the foot of the monumental uphill leading to the Castle of Udine, on the left side of the Venetian Lodge of St. John, in the central Liberty Square (*Figure 4.5*).

The celebratory arch was erected in honour of the Venetian lieutenant Domenico Bollani, as reported by the epigraph, even if it is unknown whether the epigraph was placed as an award from community, as gratitude, or, more likely, by the Bollani with self-celebratory intent. The designer is supposed to be Palladio, as results from contemporary sources, as well as documented in an involvement of the same, seven years later, for the realization of the expansion of the road ascent to the Castle and the enhancement of the visibility of the arc. The authorship of Palladio is also supported by the similarities on construction methods and materials used in the arch, as well as in his other works, like the nearby Antonini Palace and the arch of Gemona Portal in San Daniele del Friuli, which was built about twenty years later and it is almost a reproduction of the arch object of study.

Figure 4.5 – Liberty square in Udine with the Bollani arch on the left at the bottom of the monumental uphill to the castle.

The single "fornice" semi-circular arch structure is made, on the front side (*Figure 4.6 a)*), of *piasentina* stone, from Torreano of Cividale, with piers realized with rustic ashlars blocks, with frieze and architrave in Doric style, topped by the winged lion of St. Marc, as symbol of the Venetian domain. The arch (*Figure 4.6 b)*) is connected to other structures on its sides. The backside is all realized with the same material, namely masonry pretty regular in the arch, characterized by a particular curvature, very difficult to survey with direct methods.

Figure 4.6 – a) The Bollani Arch from the front side b) The Bollani arch from the rear

The structure is 8,24 m high and 7,74 m wide and, for the conformation of the segments, it is presumed that had been realized according to the measurements of the foot of Udine, corresponding to about 34,05 cm, and its multiple (Frangipane, 2007).

During 2012 the arch has undergone a restoration supported by the FAI, thanks to which it was cleaned as well as the higher structure made of Vicenza stone statue, which is porous and therefore more prone to micro flora formation. The intervention did not affect anyway the structural part, which result, so far in a good state of conservation.

4.3.2. The geometric surveying

Referring to *Scheme 1.8*, Phase 1 consisted in the laser scanning surveying of the arch, carried out with the TLS system Riegl Z390i, integrated with a Nikon D200 metric camera, owned by CIRMONT Amaro (UD, www.cirmont.it). Three scans were acquired (*Figure 4.7*), two in front of the arc and one from the back of the same, a bit foreshortened because the arch is located on a road open to traffic. The two higher-resolution scans performed on the primary side have a total of about 3 million points (average density of 120 points/dm^2).

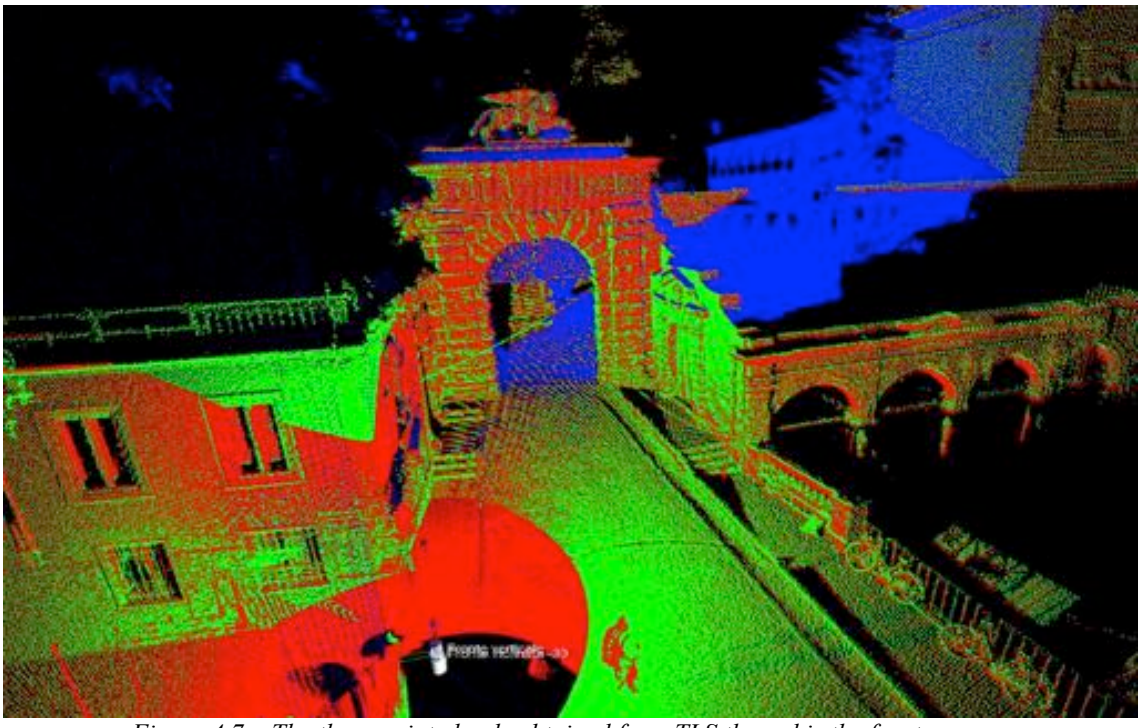

Figure 4.7 – The three point clouds obtained from TLS the red is the front one, the green is also frontal, but inclined, and the blue is the rear one.

In order to proceed with the registration of the three scans, second Phase of Scheme 1.8, 14 cylindrical Ø10 cm reflecting targets have been used, placing them on the threshold of the arch. Beside the targets, it had been necessary in any case to use also 10 additional natural points, chosen mostly in areas not accessible at the top. All the operation of registration have been managed inside the software RiSCAN, proper of the instrument: the alignment residual error have a medium value of 0,8 cm, that, for the scope of the present research can be considered appropriated (*Figure 4.8*) but is not for other uses, like 3D reprinting.

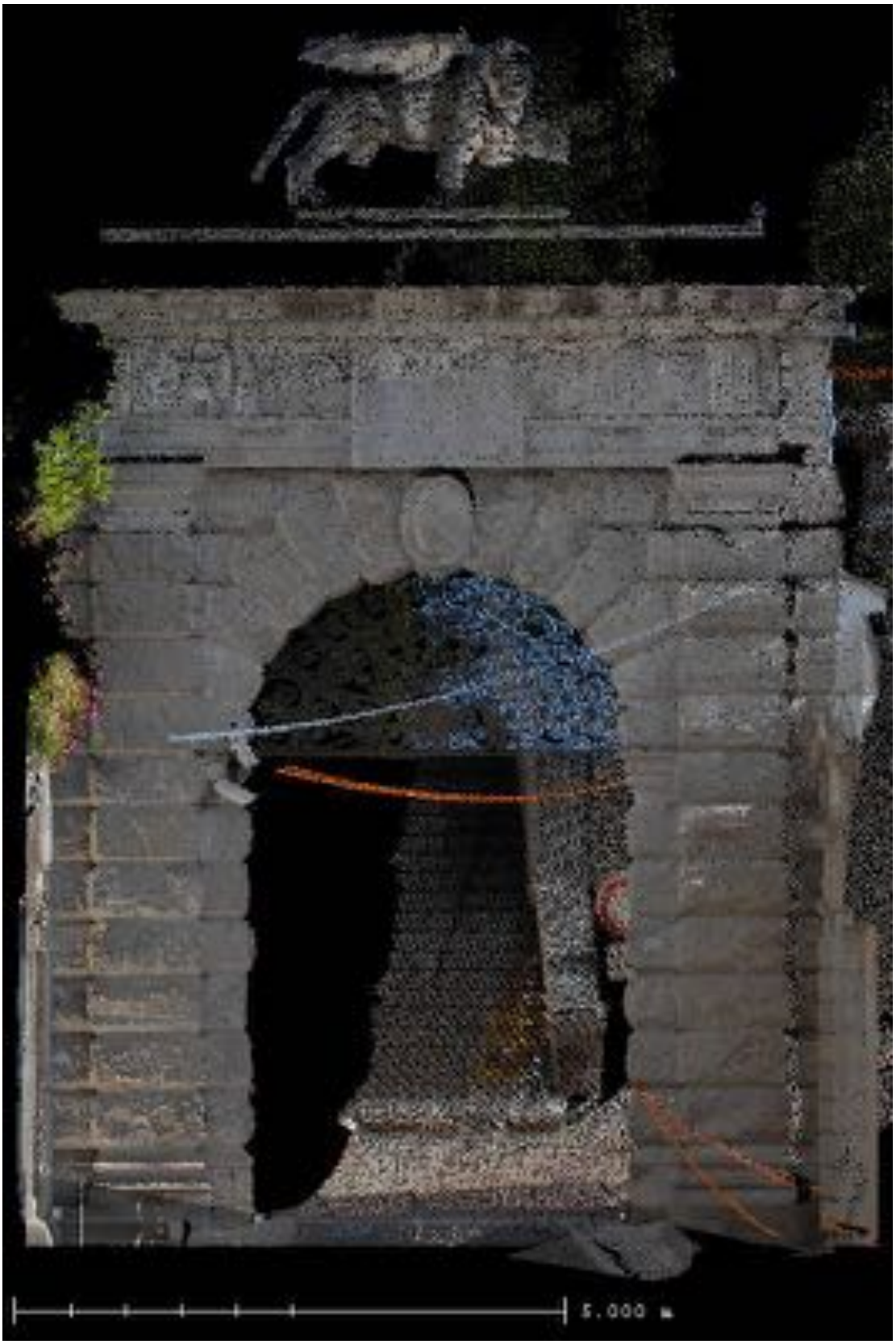

Figure 4.8 – The point cloud of the arch coloured with the RGB values from the images taken with the metric camera.

4.3.3. Modeling of the arch surface

The phase of the modeling of the arch has been performed with different software, choosing, from each one, the most performing algorithm, off course starting from the three point clouds exported from RiSCAN. Even if the registration, and the residue obtained, were good enough for the set purposes, it was considered appropriate to provide it, in order to make the model useful also for any more accurate scope.

The software used for this purpose was CloudCompare, already cited in 1.4.3, through the command "Cloud-registration" (*Figure 4.9*) implementing the ICP method, already described in sub paragraph 3.4.2.

This command allows aligning the scans by couple and, once it is decided which one to set as reference ("model"), the number of iteration to perform or the minimum error difference have to be fixed. It is even possible to adjust the scale of the scan that is going to move ("data"), but it was obviously set a rigid transformation. It is optionally possible to set additional parameters as:

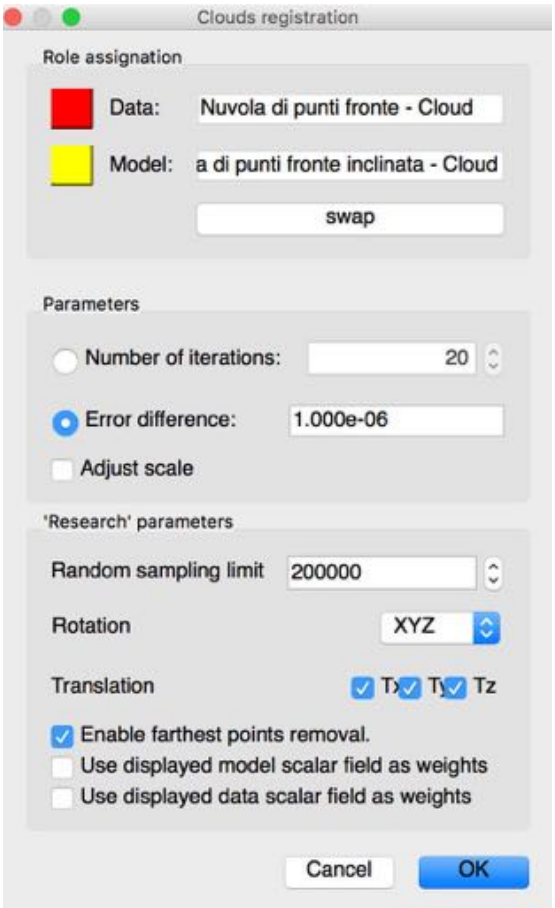

Figure 4.9 – Cloud Registration Command in Cloud Compare.

random sampling limit: to drastically increase computation speed on big clouds, by randomly sub-sampling the data cloud at each iteration. This parameter is the maximum number of sub-sampled points: default value (50.000) is generally a good guess and its incidence on the result is not perceivable.

rotation: it is possible to constrain the rotation around a given axis (X, Y or Z).

translation: it is possible to constraint the translation along none, one or several dimensions (among X, Y and Z).

enable farthest point removal: this option is very interesting if the shapes of the two clouds are quite different, since implicates the removal, at each iteration, of the points of the "data" cloud that are too far from the "model" cloud.

use displayed model/data scalar field as weights: this option could enable the user to use scalar values as weights (either on the data or the model cloud); - it is not advised to use weights on both clouds at the same time.

This operation was reiterated several times, raising each time the random sample limit, since the residual error was inferior to 0,33 cm, and therefore the joined point clouds resulted optimal for every kind of subsequent application.

The operation of the cleaning from noise, also belonging to Phase 2 of *Scheme 1.8*, was performed through the command “Clean - Filter Noise”, in CloudCompare software.

Figure 4.10 – The point cloud of the arch – resampling in Geomagic WRAP.

The following operations were processed within the software Geomagic WRAP, already mentioned in sub paragraph 1.4.4:

- regularization of the density of the points through resampling (*Figure 4.10*);
- integration of the points by manual reconstruction of geometry.

Figure 4.11 – The function parameters of wrapping in Geomagic WRAP.

Finally, applying the function of wrapping in Geomagic WRAP, it was obtained a the DSM arch with a total of 1.197.598 triangles, optimal as regards the LoD from the geometric point of view. It was subjected to further processing (elimination of incongruent surfaces, non-manifold, smoothing and holes) to make it usable by FEM analysis software.

The command has different parameters to set (*Figure 4.11*) in order to:

- fixing the kind of noise reduction (low, mean, high);
- keeping or not the original data;
- erasing or not small components;
- fixing distance in the point cloud resampling;
- defining the maximum number of triangles.

In the specific case, no further noise reduction and no resampling have been applied since those processes had been treated separately. The improvement of the surface quality, Phase 3 of *Scheme 1.8*, was therefore implemented through the command "Mesh Doctor", which allowed eliminating all the incongruences listed in sub paragraph 3.4.2. The final surface obtained was therefore composed by 998.000 triangles and it appears as in *Figure 4.12*.

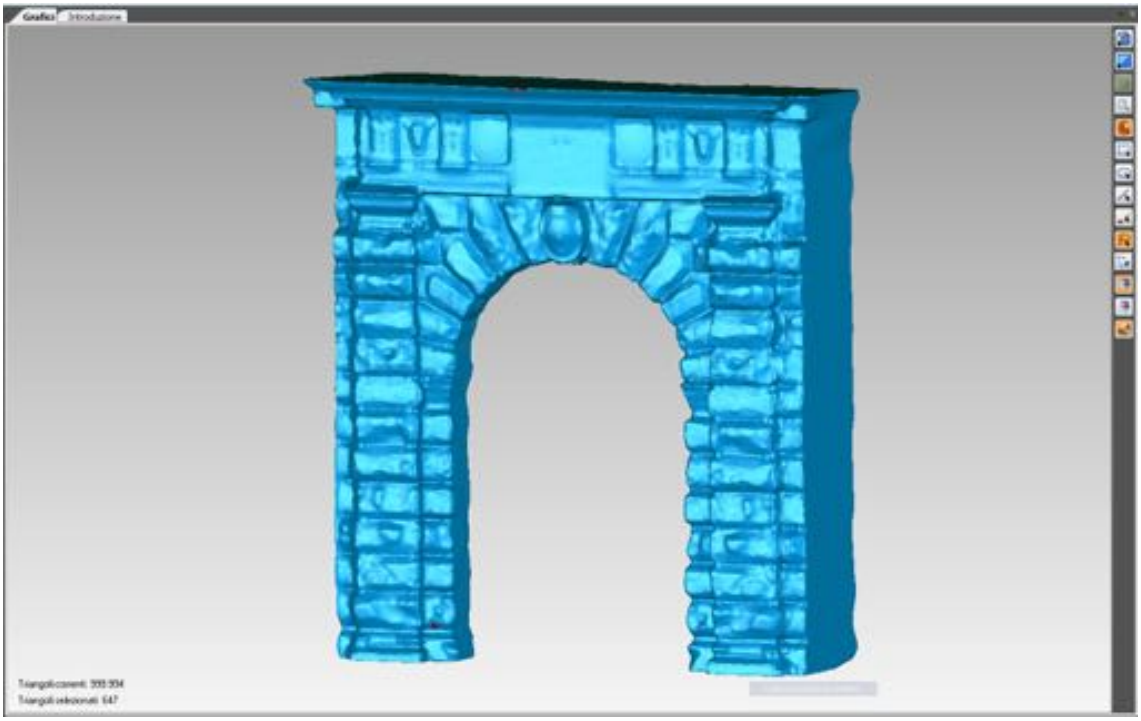

Figure 4.12 – The final model obtained in Geomagic WRAP.

4.3.4. Solid model and the results FEM analysis

Once obtained the DSM, it is mandatory to transform it into a solid model, as expected by Phase 5 of *Scheme 1.8*. Only for solid modes, in fact, it is possible to perform the structural analysis, as done for the small size objects of the third chapter with the software Scan-and-Solve.

In order to simulate the composite behaviour of the masonry, partially realized with stone ashlars and partially with clay bricks, were chosen the parameters reported in *Table 4.13*, adopting average values with respect to those reported in the literature (Di Sivo, 2004):

Property	Value
Description	Bricks_Stone_Composite
Density	2000 kg/m^3
Elastic Modulus	2.7e+09 Pa
Poisson Ratio	0.25
Default Failure Criterion	Coulomb Mohr
Ultimate Tensile Srength	1.725e+06 Pa
Ultimate Compressive Srength	7e+06 Pa

Table 4.13 – Materials properties

At the same time, were set the restraints, as reported in *Figure 4.15 a)*, imposing a fixed end constraint to the base of the arch and links on the sides, in order to simulate the thrust or the support of the two buildings bounding the arch.

The only load imposed on the structure was the gravity one. From the structural analysis were obtained the results reported in *Table 4.14*.

	Minimum	Maximum
X-Displacement	-1.31037e-05 m	0.000566259 m
Y-Displacement	-2.98295e-05 m	3.35791e-05 m
Z-Displacement	-0.000587959 m	2.1239e-06 m
Total Displacement	2.17121e-09 m	0.000809934 m
Von Mises Stress	233.152 Pa	677554 Pa
Max. Principal Stress	-228099 Pa	359509 Pa
Mid. Principal Stress	-244607 Pa	147342 Pa
Min. Principal Stress	-872521 Pa	92198.7 Pa
Danger Level (Rankine)	4.4384e-05	0.208411
Danger Level (Coulomb Mohr)	6.73385e-05	0.208411
Danger Level (Modified Mohr)	6.05347e-05	0.208411

Table 4.14 – Minimum and Maximum results obtained from the analysis

Figure 4.15 b) shows the trend of the total displacement over the arch: of course, it results null at the base of the arch and grows little by little until reaching the maximum value in correspondence with the rear keystone of the arch, for the value of 0,809 mm.

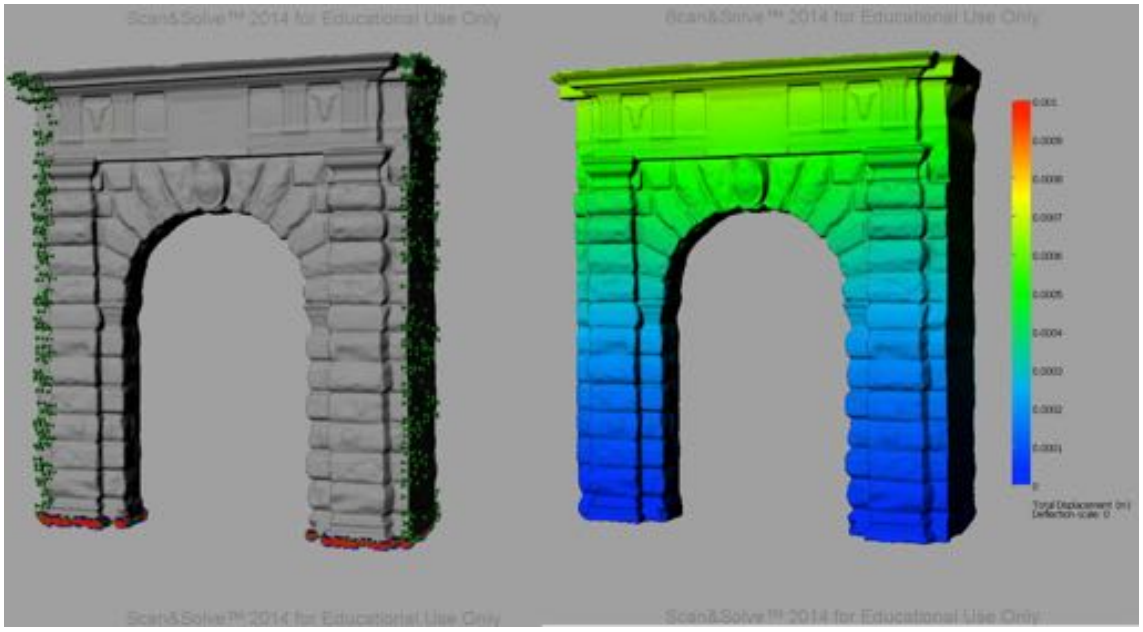

Figure 4.15 –a) Restraints imposed – b) Displacement obtained from the analysis

4.3.5. Ashlars three-dimensional model and the results FEM analysis

The adaptation from the DSM surface to the "vector model" used for a second FEM analysis was done manually, redrawing the 3D profiles of the ashlars from the texturing of DSM with the photogrammetric images, as reported in *Figure 4.16*.

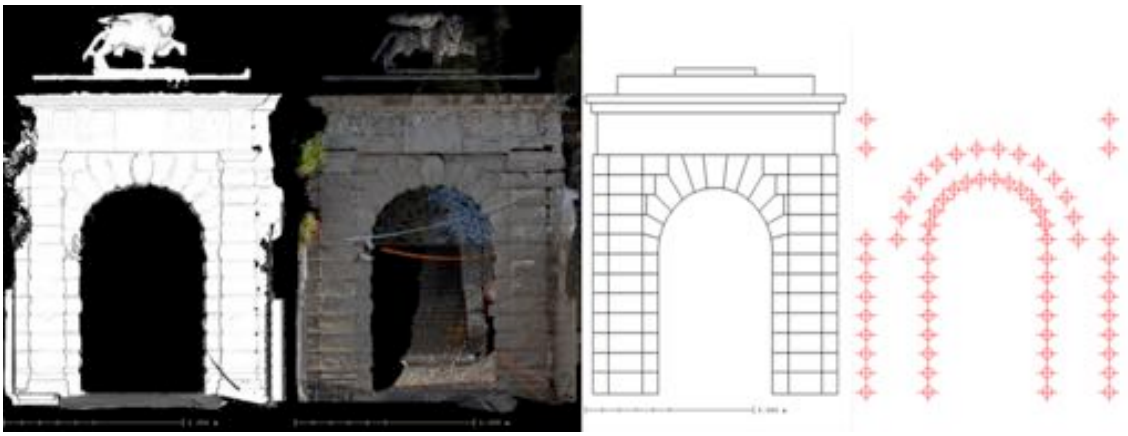

Figure 4.16 – From the left: 3D model, the colorized point cloud, the vectorized image and the vertices of the identified ashlars

The 3D vertexes where subsequently imported in the open-source software Lisa FEA, mentioned in 2.3.4, where they assumed the role of nodes, from which the ashlars have been modelled. The structure was modelled with solid elements defined as "wedge6" (6 vertices - wedge) and "hex8" (8 summits - rectangular), depicted in *Figure 4.17*.

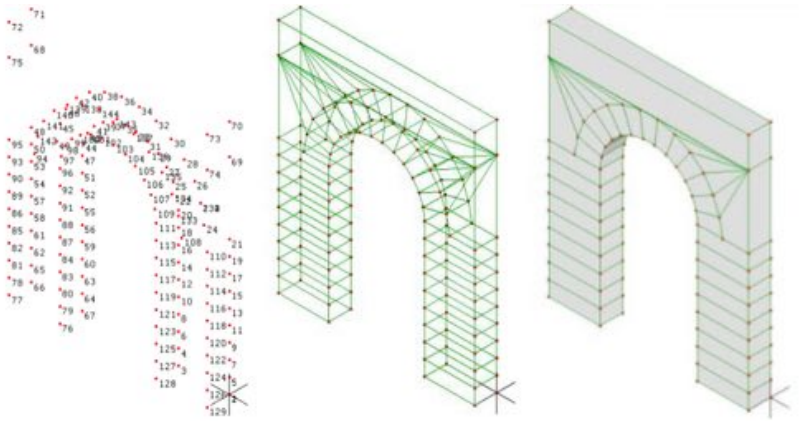

Figure 4.17 – From the left: the node of the ashlars, the ashlars in wireframe and in solid form.

To the 3D solid model obtained were assigned mean values to the constitutive feature of the material, congruent with those used in the structural analysis of the DSM model, described in the previous sub paragraph. Usually it is assumed that masonry has an orthotropic behaviour, but for the purposes of the experiment - that concerns the mere geometric aspect of a structural analysis - and in order to simplify the matrix calculation, it was assumed an isotropic behaviour, with average values of the coefficients of elasticity, Poisson and density. Besides this, through the command "constrains", the structure was bound more rigidly along the vertical axis (Y in the case of Lisa FEA), for simulating the higher resistance to compression offered by the stone material. Similarly were considered the same constraints and loads of the previous solution of Scan-and-Solve.

In *Figure 4.18* are reported the results related to the trend of the principal stress in vertical direction on the front side and on the rear one. Clearly, the most stressed part is the keystone, specifically the rear one, where resistant section has minimum height.

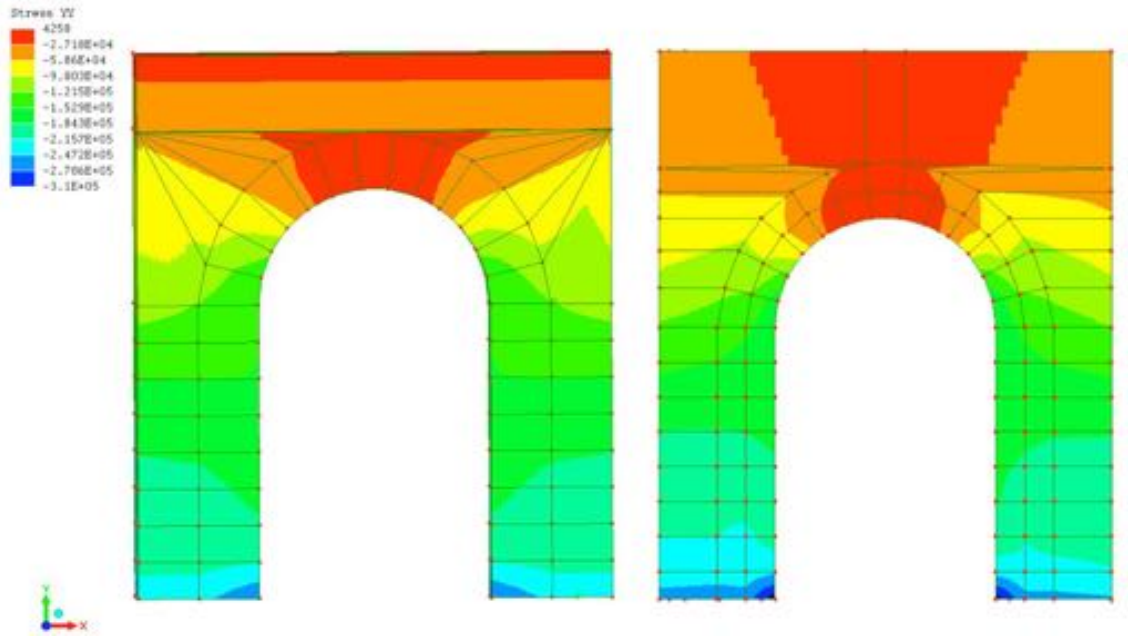

Figure 4.18 – Trend of principal stress in vertical direction on the front side (in the left) and distribution on the rear side (in the right)

4.3.6. Comparison between the ashlars model and the DSM model

The main purpose of the structural analysis, in the broadest sense of the term, is to define, through mathematical procedures, the characteristics of stress and deformation over a body subject to certain loads, wherever these are gravitational or other. As explained in 2.3.4, analyses of this kind involve the use of differential equations (balance, congruence and of constraints, known from the science of construction) that describe the behaviour of a continuous body subjected to external actions (loads) and reaction forces. These equations involve such a high number of variables as to make impossible their solution without the aid of appropriate calculation software, which operation must be based on discrete models formed by a finite number of nodes and elements (FEM). Structural modeling entails the creation of a discrete mathematical model that could interpret the real physical behaviour of the continuous structure. In this way, mathematical model not only implies a geometric discretization of the building, but also the simplification of the applied loads and the imposed constraints, as well as of the materials constituting the structure itself.

The FEM analysis, precisely because of this process of schematization, is not an exact method, but approximated, and therefore, it is always appropriate to proceed to the verification of results obtained using a series of tests which should include at least (Cesari, 1982):

- manually monitoring the results, by simplified schematizations;
- controlling the magnitude of the expected results;
- comparison of different software with each other and with exact theoretical solutions.

In order to verify if the assumption taken in the analysis were correct, the same "ashlar" model, as obtained in 4.3.5, was suitably imported into Rhinoceros, where it was analysed,

using again Scan-and-Solve, adopting the same static conditions, the same materials and, of course, the same restrains.

The obtained results, related to the trend of principal stress in vertical direction, are reported in *Figure 4.19* and *Figure 4.20*, where on the left there is the Scan-and-Solve values and on the right the Lisa ones, with the front in the first figure and the rear on the second.

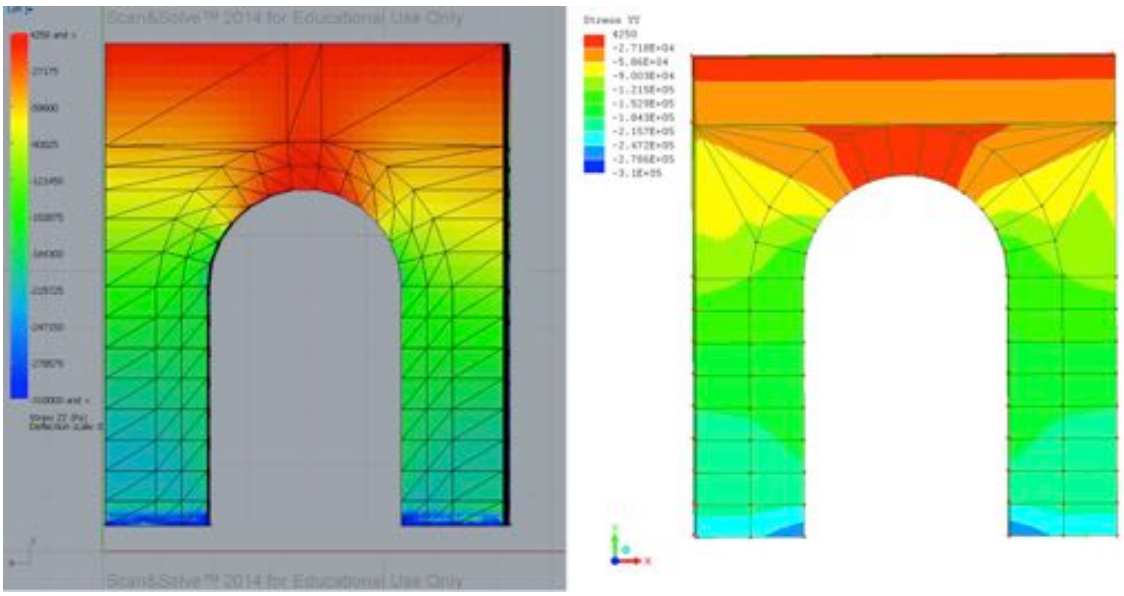

Figure 4.19 – Trend of principal stress in vertical direction on the front side in Scan-and-Solve (in the left) and in Lisa (in the right).

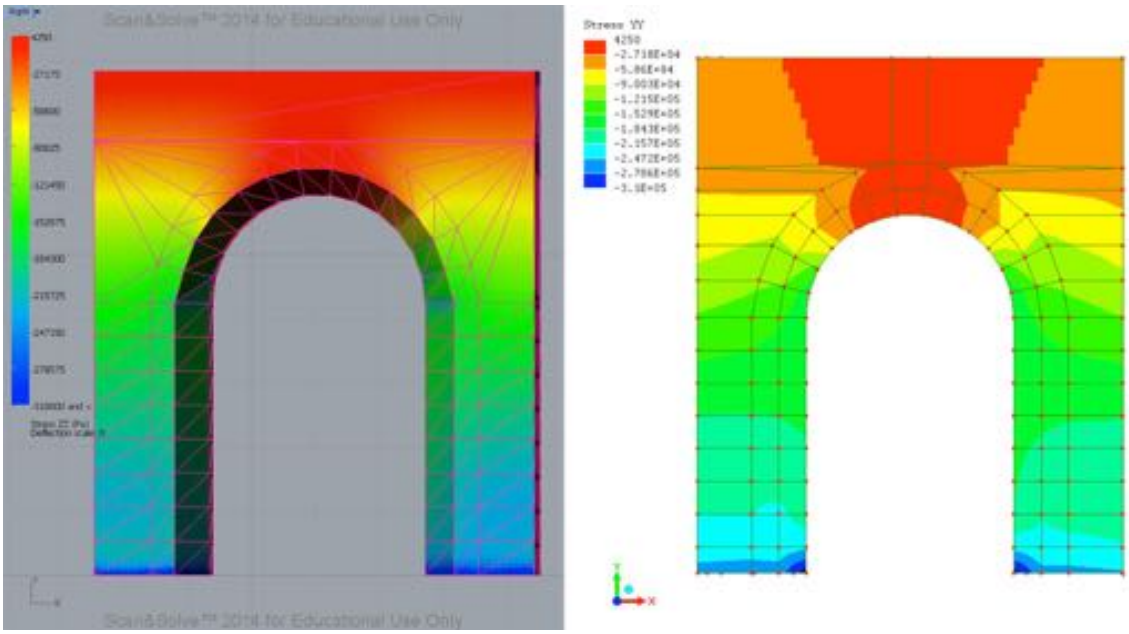

Figure 4.20 – Trend of principal stress in vertical direction on the rear side in Scan-and-Solve (in the left) and in Lisa (in the right).

It is clear that, unless of the different graphics features, the geometric distribution of results and maximum and minimum values obtained are equivalent: this correspondence is of considerable interest, primarily to validate the correctness of the methodology adopted. Even

more significant is the fact that, in reality, Scan-and-Solve can directly process a Geomatics DSM and provides the same results as LISA FEA, without having to manually design the ashlars (Visintini & Spangher, 2013).

4.3.7. Models with different geometrical level of detail

The Level of Detail (LoD) of the obtained model can be considered the maximum possible with the used equipment and the current know-how. This LoD resulted optimal for an architectural surveying and other application like 3D printing, but first and foremost, is rather excessive for a structural analysis. Therefore it is possible to affirm that the "necessary and sufficient" geometrical LoD depends by the use of the model: a high LoD for producing a high correspondence with reality, a lower LoD for structural analysis.

In order to define which geometrical LoD is sufficient for the structural analysis, different models were created, starting from the one with maximum LoD and gradually increasing the simplification of the surface, namely reducing the LoD, and then comparing the obtained results, of course imposing the same conditions of load and constraint.

There are several algorithms that lead to the simplification of the mesh, but all of the techniques proposed in literature are based on some variation or combination of two primitive basic mechanisms: the union of vertices and the decimation of the meshes. The first method relies on the use of clustering algorithms where, by setting up a voxel grid, it is possible to combine the vertices lying in the same voxel. These algorithms provide only limited control over the complexity, topology or the quality of the resulting mesh and, therefore, are not suitable for this purpose case (Bischoff and Kobbelt, 2004). The decimation instead describes that class of algorithms that allows to obtain, a mesh, with fewer faces, edges and vertices, by iterative processes which are based on the removal of the vertices "less important" and faces relating to them and on re-triangulation of the resulting hole. Such algorithms allow keeping the main edges of the model (*Figure 4.21*) and therefore are the most suitable for the purposes that we are prefixing.

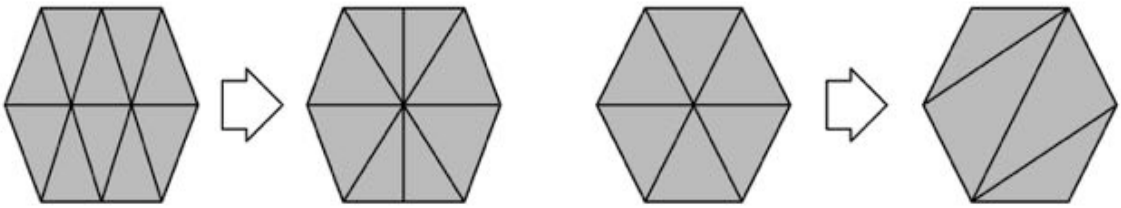

Figure 4.21 – Simplification of the mesh through decimation

Within Geomagic WRAP software, this algorithm has been implement in the function "Decimation". Therefore, starting from the original DSM of the arch made of 998,000 triangles and applying the decimation filter, by setting the maintenance of edges and curvature, and fixing the percentage of decreasing of the triangles, different models were obtained, built respectively by 500.000, 200.000, 100.000, 50.000, 20.000 and 10.000 triangles, which are shown in the following figures (*Figure 4.22* to *Figure 4.27*).

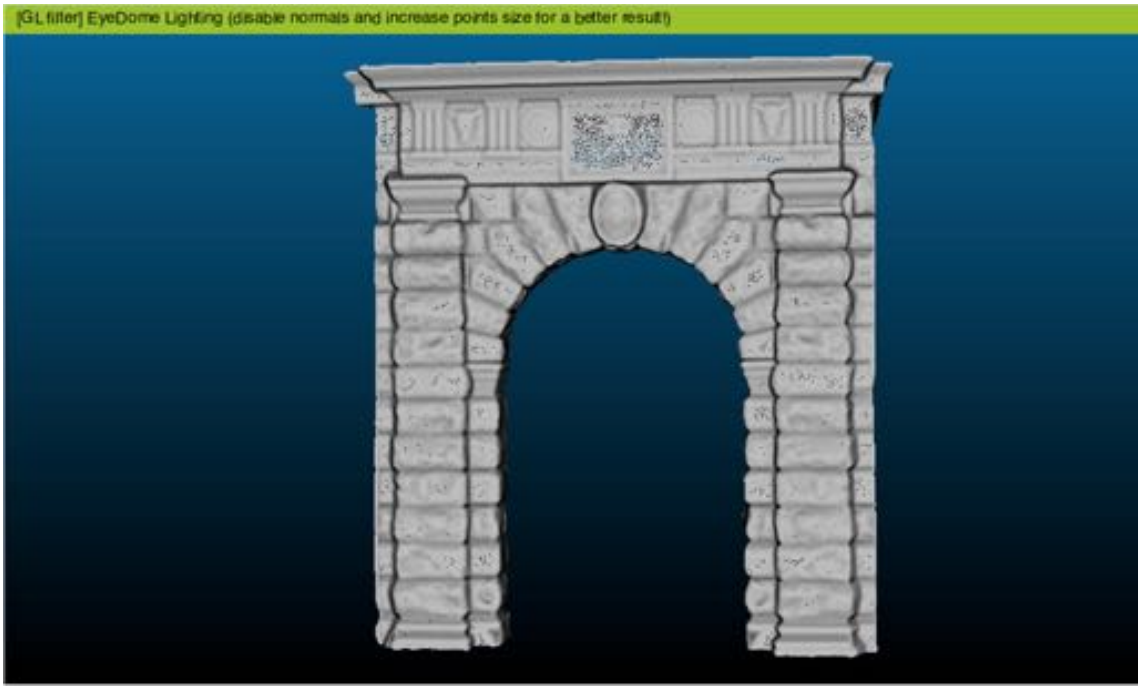

Figure 4.22 – Wireframe representation of the DSM obtained reducing triangles to 500.000

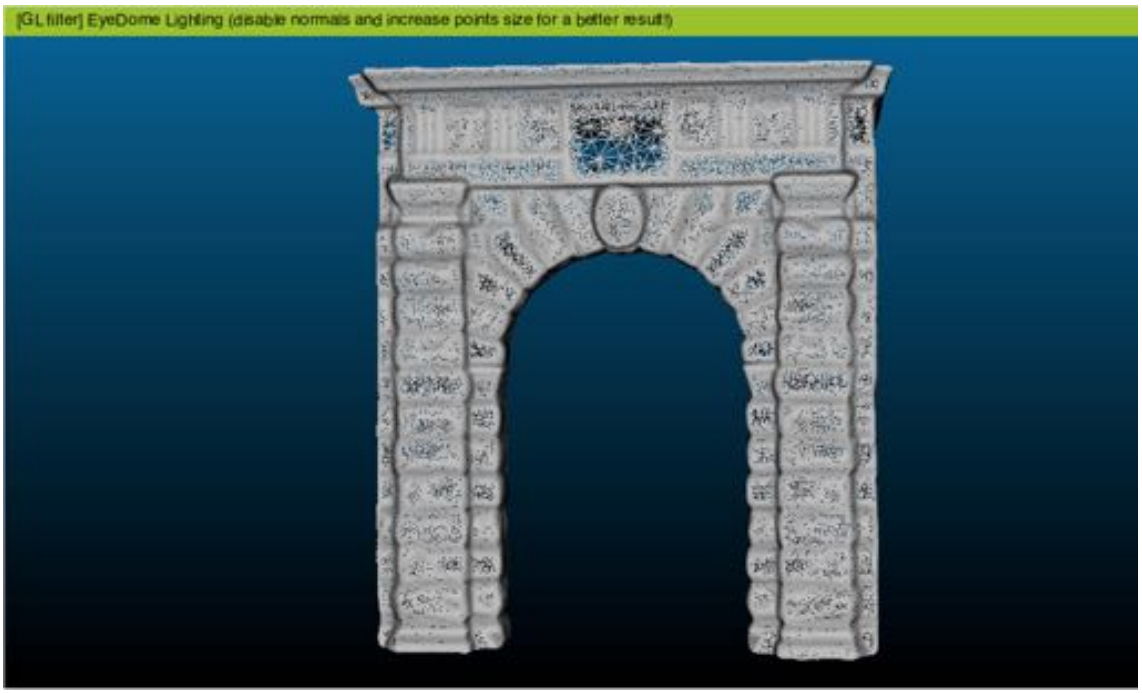

Figure 4.23 – Wireframe representation of the DSM obtained reducing triangles to 200.000

Figure 4.24 – Wireframe representation of the DSM obtained reducing triangles to 100.000

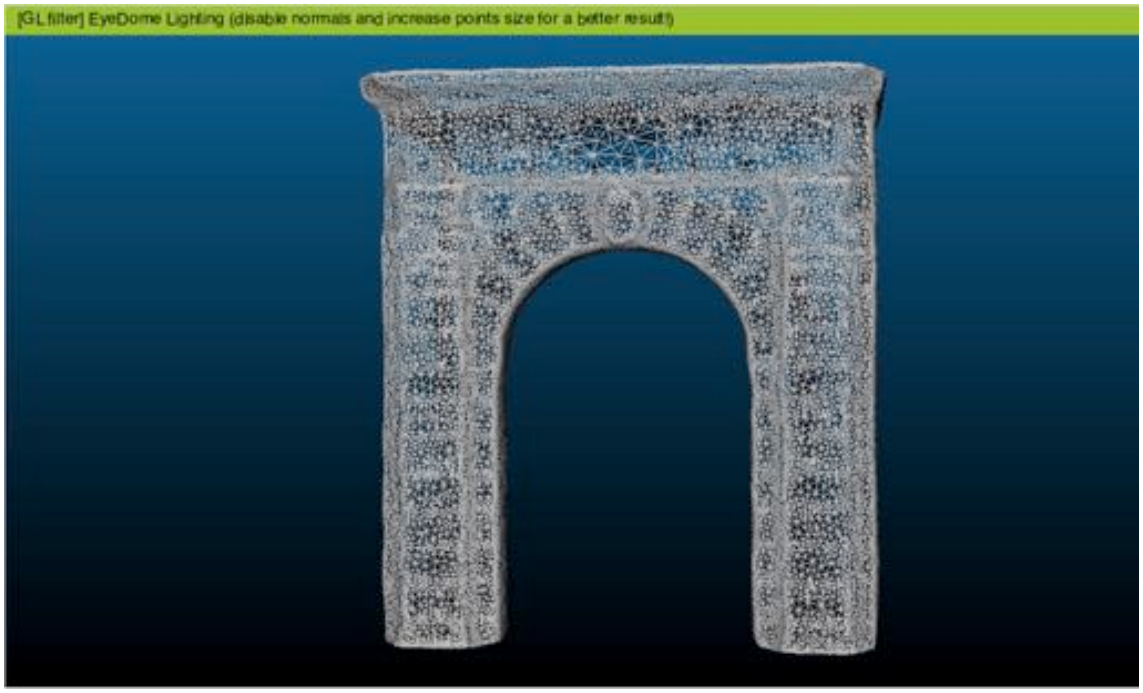

Figure 4.25 – Wireframe representation of the DSM obtained reducing triangles to 50.000

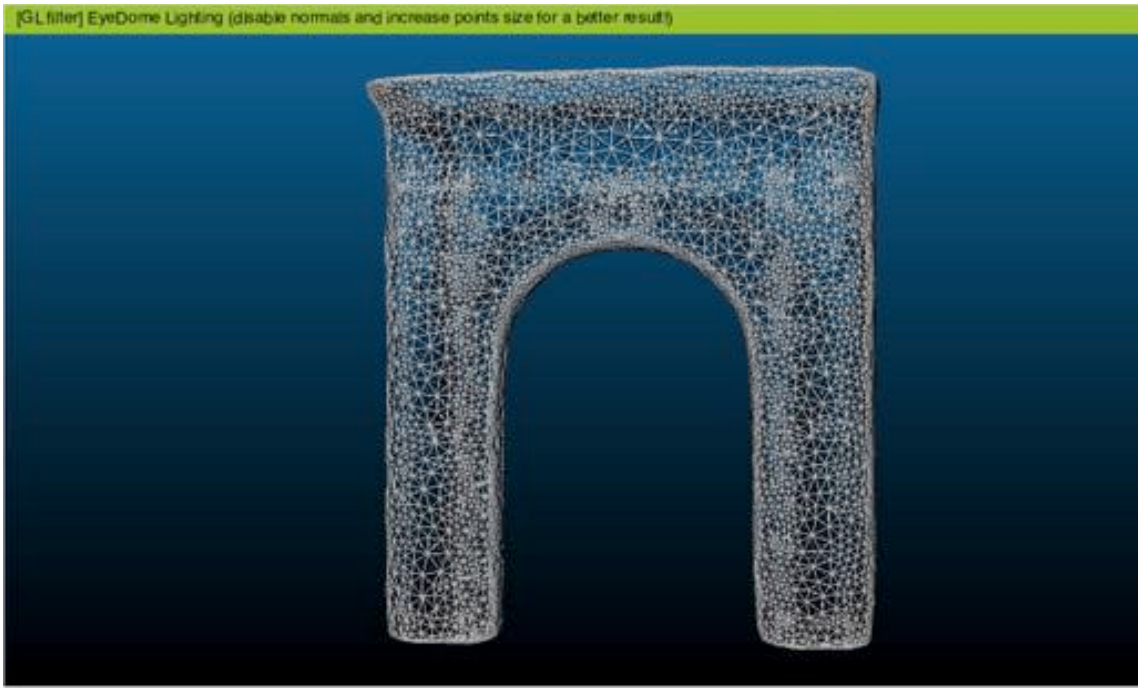

Figure 4.26 – Wireframe representation of the DSM obtained reducing triangles to 20.000

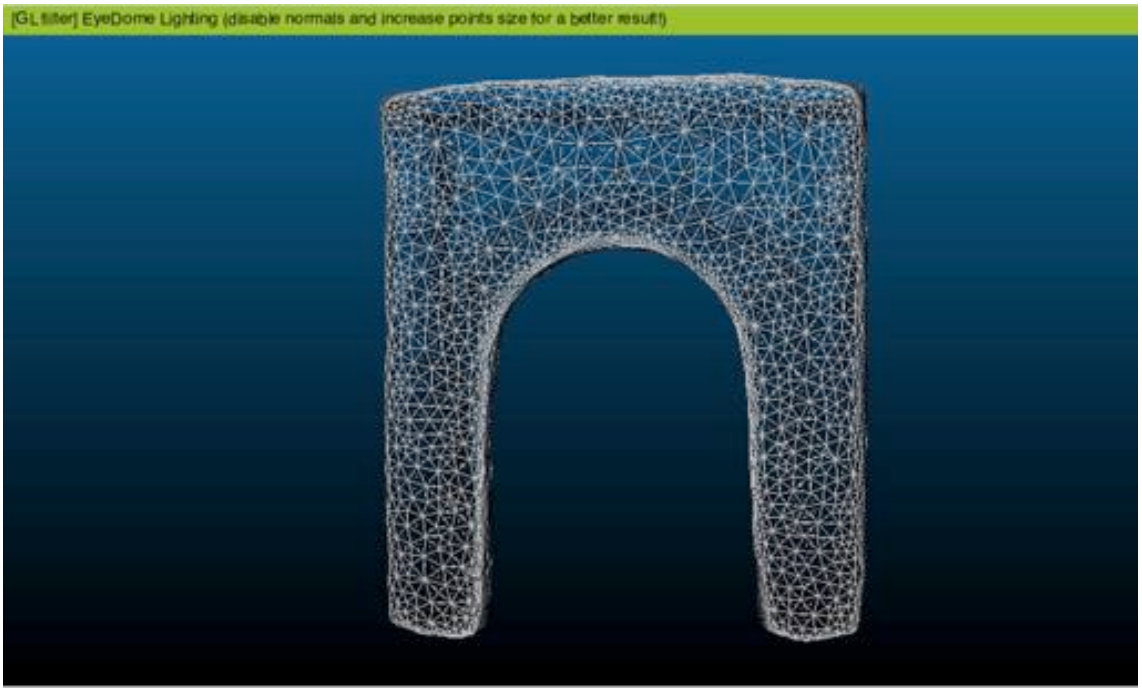

Figure 4.27 – Wireframe representation of the DSM obtained reducing triangles to 10.000

Obviously, the greater is the number of triangles shaping the mesh, the higher will be the correspondence to reality. In order to analyse the difference of each single model to the original one, all of them were matched in CloudCompare by means of the function "Compare", which allows choosing a *Reference model* (the original 998.000 triangles mesh) and a *Compared model* (hence all the models obtained from the decimation).

The last 10.000 triangles model obtained, for its smoothness and absence of detail, could be considered as a model resulting with simplest 3D drawing software (for example SkethUp) and is geometrically similar to the one analysed in 4.3.6.

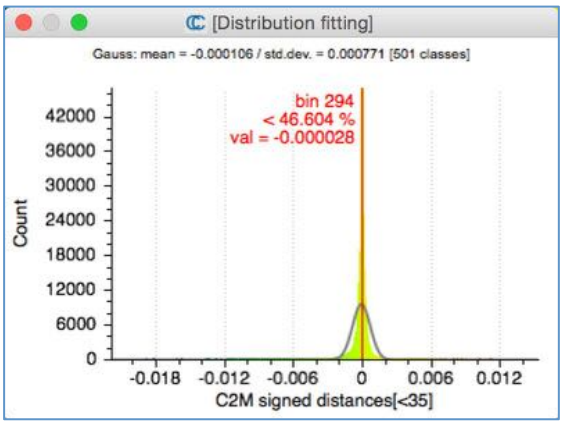

Figure 4.28 – Distribution of values of distances measured between the original model and the 500.000 triangles model

From the comparison of the original model versus the 500.000 triangles one, it resulted that the geometrical difference is minimal: in fact, even if the distance varies in the interval $[-0{,}065\ m \div 0{,}083\ m]$ the medium absolute distance value of $0{,}028$ mm which correspond to about the 46% of the measured distance among triangles, and the 99% of triangles have a difference inferior to the absolute value of 2 mm (*Figure 4.28*). It can be state that an already strong 50% decimation of the triangles returns a model that is approximately the same of the original, as it is possible to view in *Figure 4.29*, where the green colour indicate an almost zero difference.

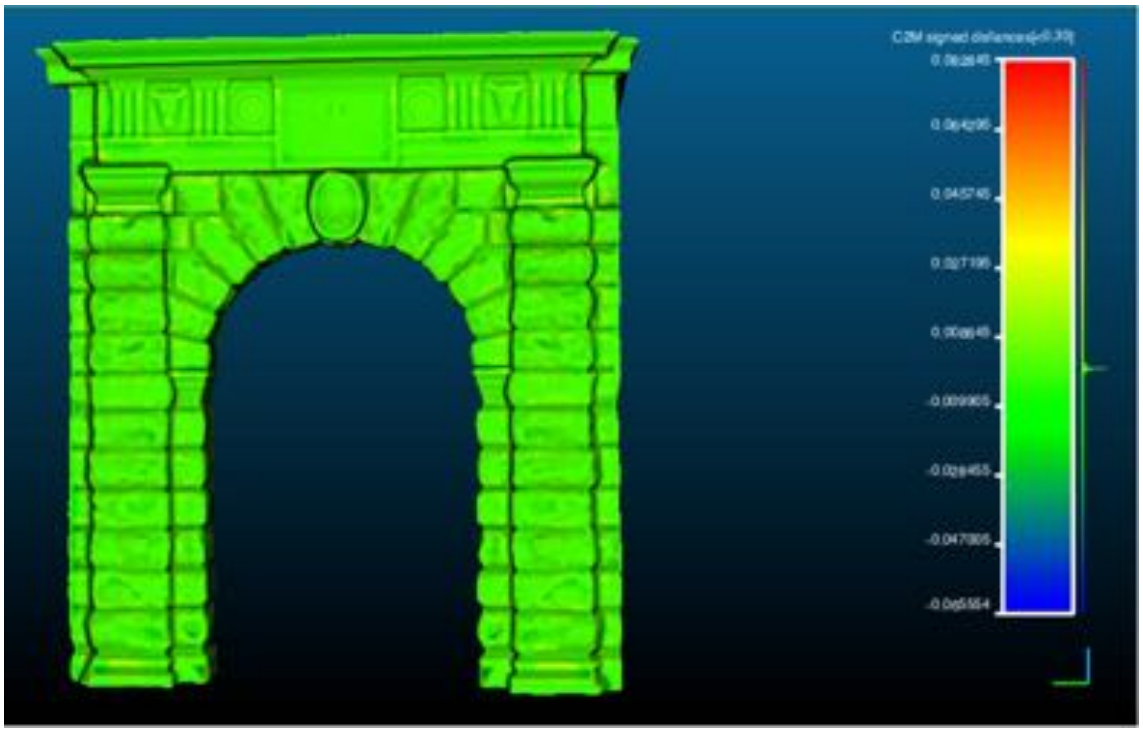

Figure 4.29 – Comparison between the 500.000 triangles model and the original. Trend of distances between the two models.

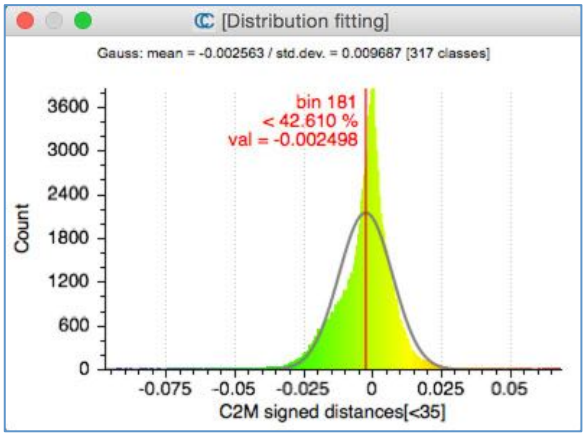

Figure 4.30 – Distribution of values of distances between the original model and the 200.000 triangles model

The distance between the original model and the 200.000 triangles model varies in the larger interval $[-0{,}097\ m \div 0{,}068\ m]$ with a medium absolute distance value of 2,498 mm, corresponding to about 43% of the measured distance of triangles. 99% of triangles have anyway a difference inferior to the absolute value of 2,00 cm (*Figure 4.30*), which means that an 80% decimation of the triangles returns still a model that is a good approximation of the original, as it is possible to view in *Figure 4.31* surface. Details are still well recognizable, as well as the rustication of the stone.

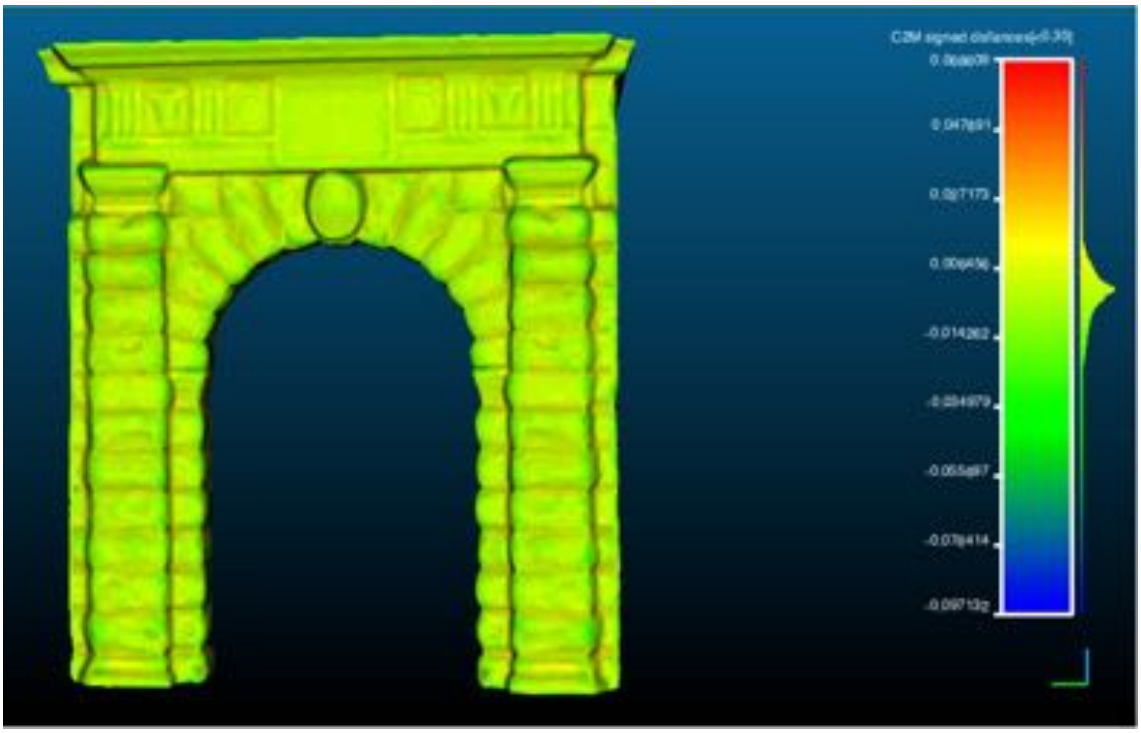

Figure 4.31 – Comparison between the 200.000 triangles model and the original. Trend of distances between the two models.

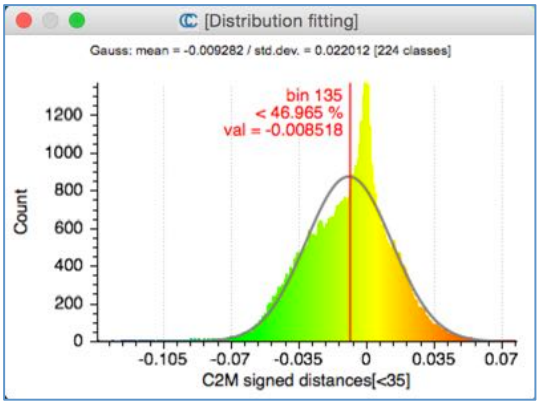

Figure 4.32 – Distribution of values of distances between the original model and the 100.000 triangles model

The 100.000 triangles compared to the original one has a wider interval of values of distances, equal to $[-0{,}139\ m \div 0{,}075\ m]$ with a medium absolute distance value of 8,581 mm , including about the 47% of the distances. By the way, 99% of triangles have in a difference inferior to the absolute value of 4,00 cm (*Figure 4.32*), which can be still considered acceptable, if compared to the dimension of the structure. A 90% decimation of the triangles returns therefore a model that is still an acceptable approximation of the original, as it is possible to view in *Figure 4.33*, since the form of the object is still correctly maintained, while the details start to decade and the rustication of the stone is completely decayed.

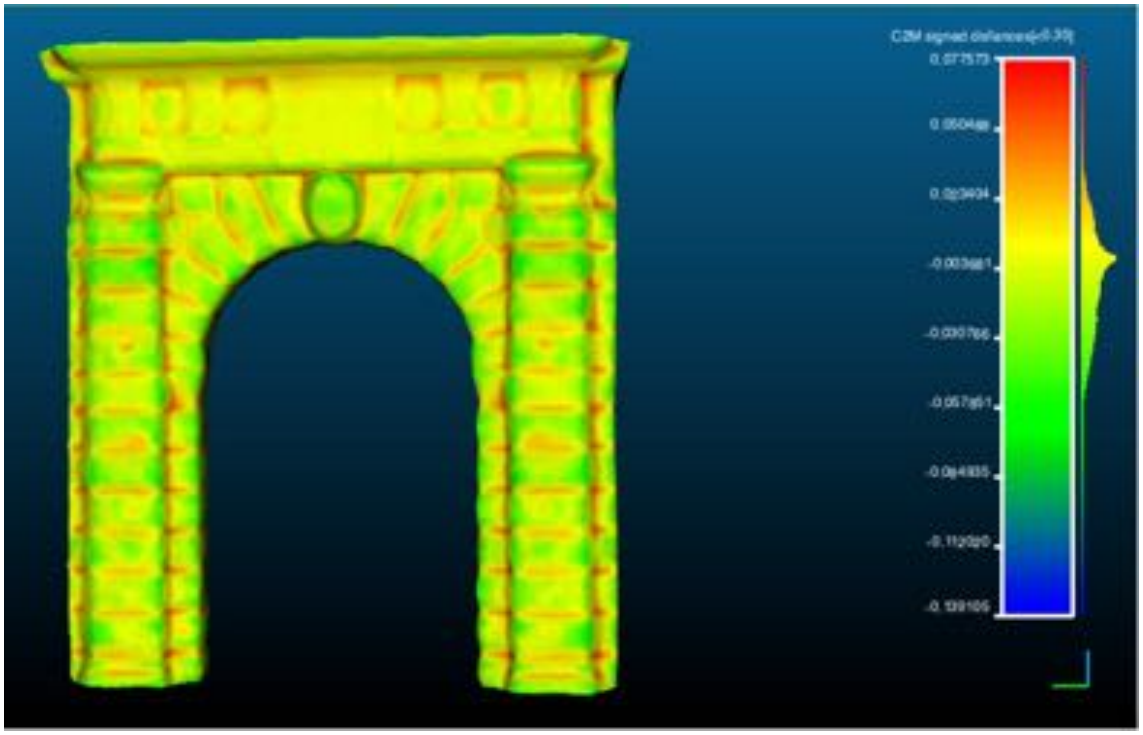

Figure 4.33 – Comparison between the 100.000 triangles model and the original. Trend of distances between the two models.

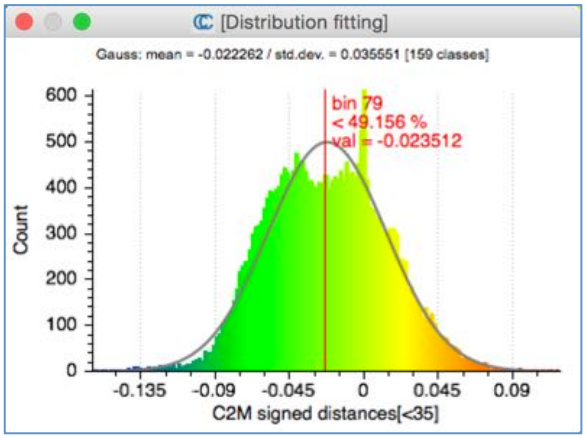

Figure 4.34 – Distribution of values of distances between the original model and the 50.000 triangles model

Considering the 50.000 triangles model, it resulted that the distance varies in the interval$[-0{,}164\ m \div 0{,}119\ m]$, but in this case values are not so concentrated around the medium absolute distance value of 23,512 mm, which correspond to about the 50% of triangles.

99% of triangles have a difference inferior to the absolute value of 5,8 cm (*Figure 4.34*). It can be easily assumed that a 95% decimation of the triangles returns a model that is still a sufficient approximation of the original, as it regards the form, while the details are almost lost and the model appears completely smoothed, as it is possible to view in *Figure 4.35*.

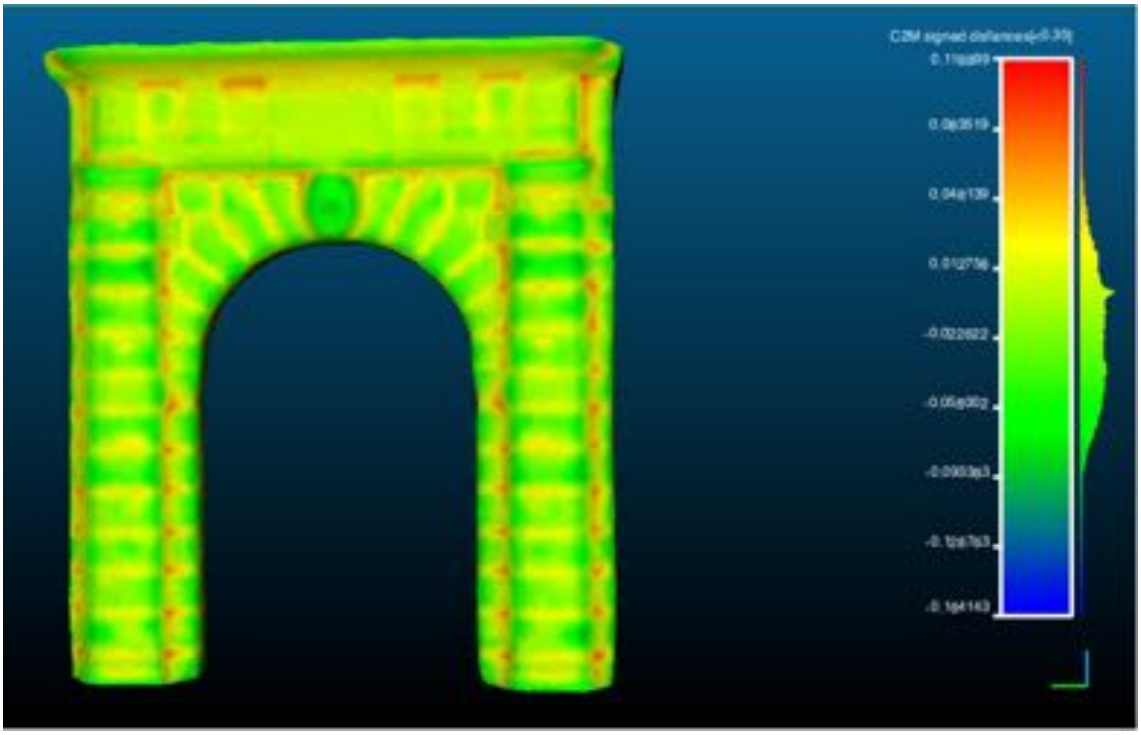

Figure 4.35 – Comparison between the 50.000 triangles model and the original. Trend of distances between the two models.

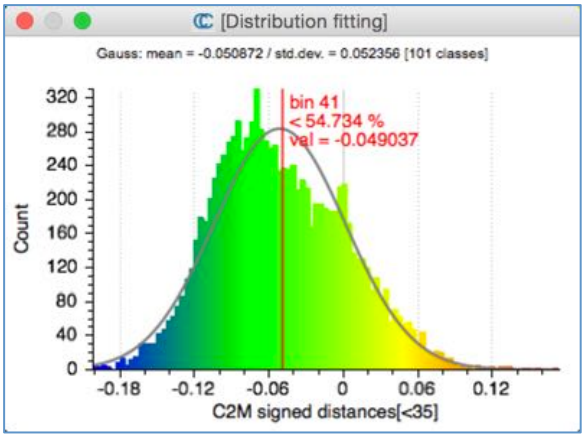

Figure 4.36 – Distribution of values of distances between the original model and the 20.000 triangles model

The compared results between original model and 20.000 triangles have obviously a much wider interval of distance of $[-0{,}202\ m \div 0{,}174\ m]$ with a medium absolute distance value of 49,037 mm corresponding to the 55% of the measured distance of triangles. 99% of triangles have a difference inferior to the absolute value of 7,5 cm (*Figure 4.36*). A 98% decimation of the triangles returns a model, which is not anymore a good representation of the original model. All the details are lost: surface results completely smoothed, as it is possible to view in *Figure 4.37*.

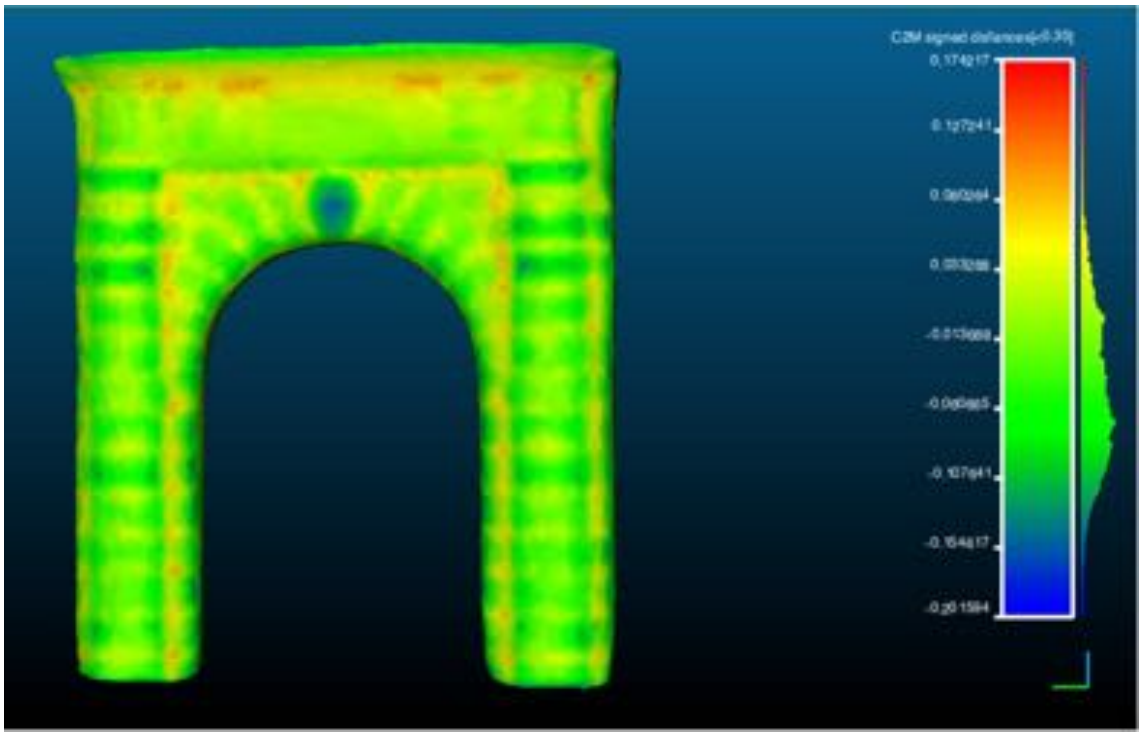

Figure 4.37 – Comparison between the 20.000 triangles model and the original. Trend of distances between the two models.

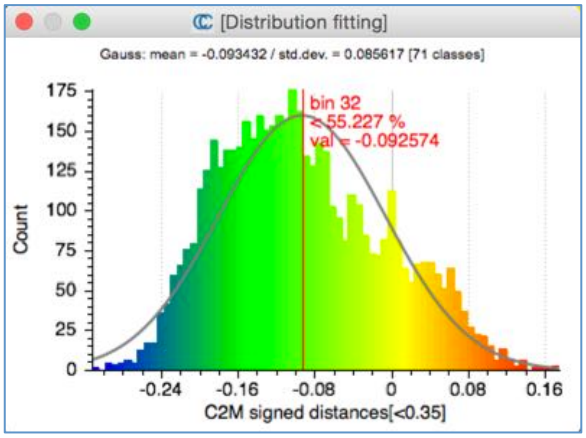

Figure 4.38 – Distribution of values of distances between the original model and the 10.000 triangles model

Comparing at the end the 10.000 triangles model to the original one the distance varies in the enlarged interval $[-0{,}312\ m \div 0{,}175\ m]$ where the 55% of triangles have a distance inferior to 92,574 mm. The 99% of triangles have a difference inferior to the absolute value of 10,10 cm (*Figure 4.38*). A 99% decimation of the triangles returns a model that is geometrically really different from the original, as it is possible to view in *Figure 4.39*. All details are lost and even the form appears really different and simplified. It could represent any other simple arch, not the arch of this thesis.

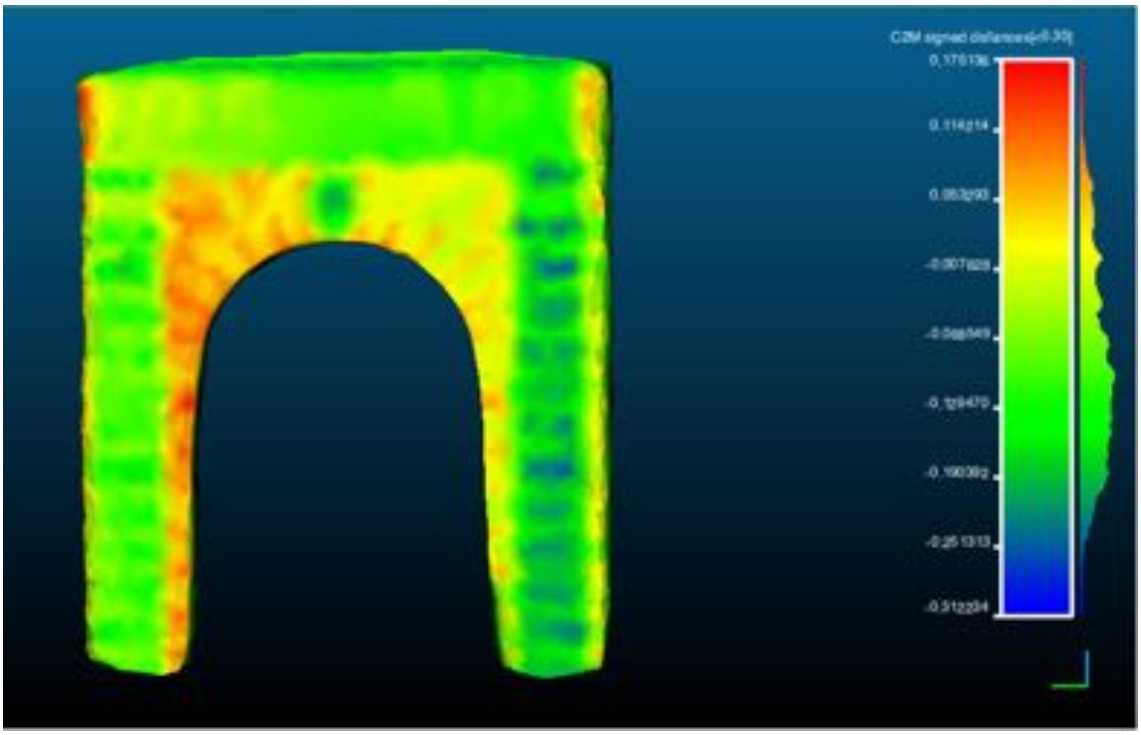

Figure 4.39 – Comparison between the 10.000 triangles model and the original. Trend of distances between the two models.

Summarizing, numerical results confirm that it is possible to proceed with a decimation up to 80%, without losing the LoD of the object. In spite of this, it will however necessary to define which is the acceptable "percentage limit" of decimation in order to obtain structural analysis results not significantly different to those achieved with the original mesh surface.

4.3.8. Models with different structural levels of detail

Besides the different geometric LoD of the model, just not described, it is possible to consider also the "structural LoD", which is determined by the number of finite elements used in the discretization for the analysis. In particular, as seen in 3.4.4, for Scan-and-Solve, the level of detail necessary depends upon the number of cubes used, which can vary from 10.000 to 500.000.

The division of the analysed object in a fixed number of cubes will determine, of course, different size of the same cubes, in function of the dimensions of the structure itself, and therefore the possibility to include (or not) small elements of the structure. Clearly, the different level of detail will give also different evaluation of the variations of the tensions and of the efforts in presence of strong curvatures or singular points. At the same time, the main drawback of using a large amount of cubes, and therefore a high level of detail, is the computational time required, which grows proportionally with the structural level of detail.

From the analytical point of view, for each cube belonging to the structure, will be applied the fundamental equilibrium equations reported in 2.3.4 and, therefore, for the cube completely contained in the body the surface integrals will results nulls, while the cubes on the boundary will keep in account the conditions of loads and constraints imposed.

Considering the original model of the arch, and the possibility to divide it into as many cubes as the structural LoD, were therefore obtained the models later described.

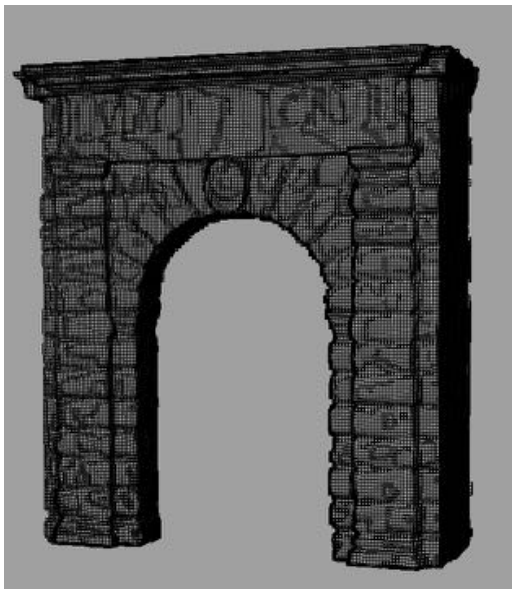

Figure 4.40 – 500.000 cubes model

The 500.000 cubes model with the dimension of cubes equal to 53 mm (*Figure 4.40*). This is the maximum structural LoD obtainable with the used software. The approximate numbers of cubes used for each principal direction are 62x150x158. Of course the multiplication of these numbers give a higher value (2,93 times the fixed value) but it has to be taken into consideration the space of emptiness given, not only by the intrados of the arch, but also by the existing protrusions and the joints between the blocks. Dimension of the cubes allows considering the variation of the values also in the smallest detail which measures are inferior to the fixed value of 53 mm.

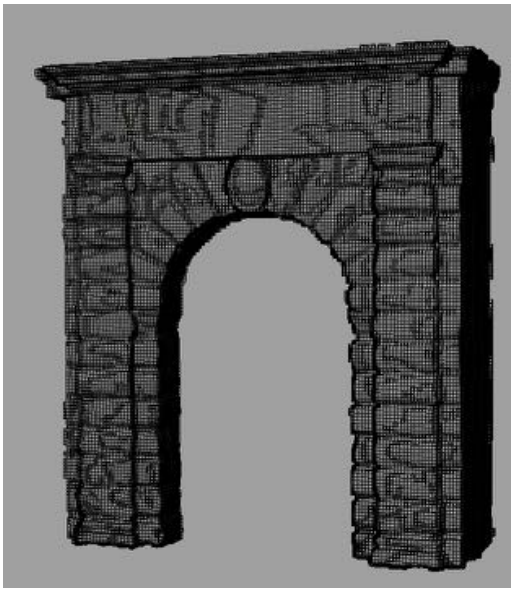

Figure 4.41 – 402.000 cubes model

In case of 402.000 cubes, the dimension will grow to 57 mm (*Figure 4.41*). For each principal direction will be used 57x140x145 cubes. Also in this case the multiplication of these numbers give a higher value (2,88 times the fixed value) since it has to be taken into consideration the space occupied by the emptiness like in previous case, while joints start to assume less importance. As before details are considered in the analysis if inferior to 57 mm.

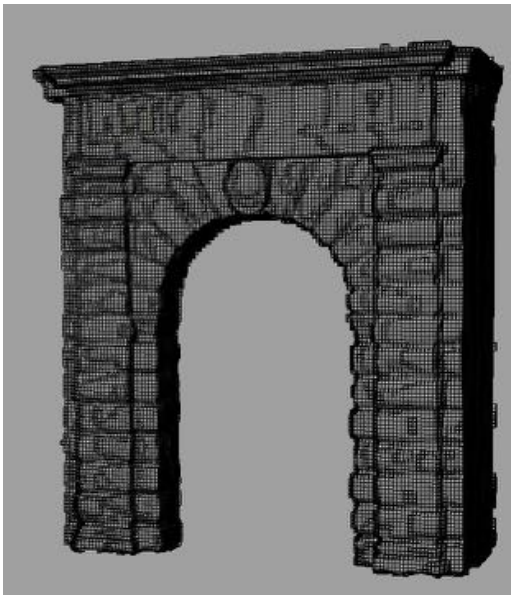

Figure 4.42 – 304.000 cubes model

In case of 304.000 cubes, model cubes are equal to 63 mm (*Figure 4.42*) and 54x126x135 cubes are used for each principal direction. Similarly to the previous case the, multiplication of these numbers give a higher value (3,02 times the fixed value) because of the emptiness. Similarly, if details are inferior to 63 mm are considered in analysis.

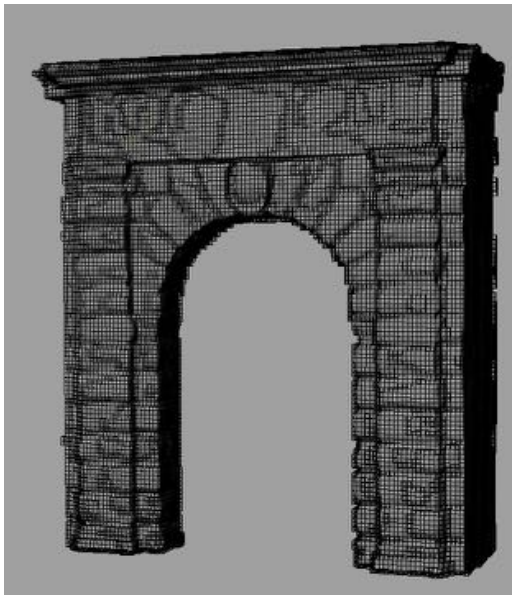

Figure 4.43 – 206.000 cubes model

The dimension of the cube grows till 72 mm for 206.000 cubes model (*Figure 4.43*). Approximate numbers of cubes used in this case for each principal direction are 46x110x115. Multiplication of these numbers give a even higher value (2,82 times the fixed value) since it has to be taken into consideration, not only emptiness but also the existing protrusions, even if they start to assume less and less importance, while the joints are unconsidered unless they are superior to 72 mm.

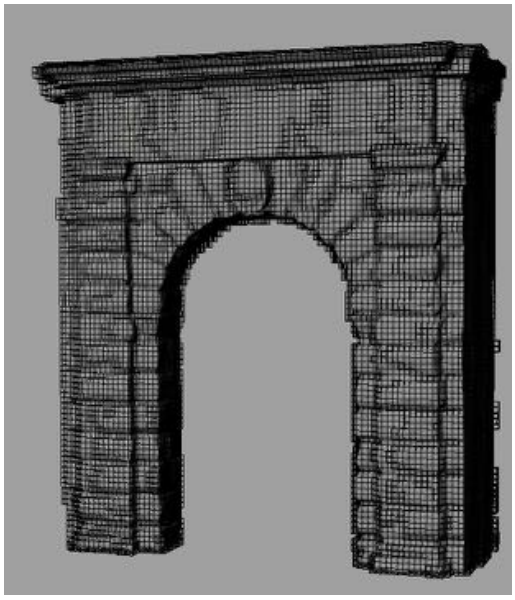

Figure 4.44 – 108.000 cubes model

The 108.000 cubes model has cubes equal to 91 mm (*Figure 4.44*). For each principal direction there are 36x89x92 cubes approximately, which correspond to 2,72 times the fixed value, since, again, it has to be taken into consideration the space occupied by the emptiness. Variations of the values in detail are considered only if the measures of the detail itself are inferior to the fixed value of 91 mm.

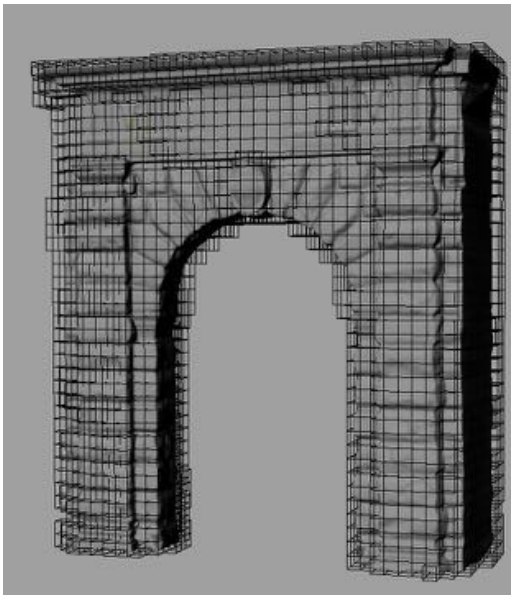

Figure 4.45 – 10.000 cubes model

Last model of 10.000 cubes has cubes equal to 217 mm (*Figure 4.45*). This is the lowest structural LoD obtainable with the used software. The approximate numbers of cubes used for each principal direction are 16x38x40. Still the multiplication of these numbers is higher to the fixed value (2,43 times). Variations are considered only if details are smaller than 217 mm.

4.3.9. FEM analysis of the different LoD models

Each of the previous six models obtained with different geometrical LoD were analysed varying the structural LoD, with the ultimate goal of determining the most appropriate combination of the two LoD to apply to this specific model.

As well as all the structural calculation program, Scan-and-Solve provides several (punctual) values of stresses and deformations as output: it was decided to focus on the results of the total displacement of the structure, which is the linear combination of the displacement in the three main directions X, Y and Z. This choice depends by the fact, as said many times, that from the values of the displacements are later numerically obtained all the other values of deformations and stresses.

The data obtained are reported in the following *Table 4.46*, where geometric LoD increases with the rows, while structural LoD increases with the columns. As can be seen, the six geometrical models differ in volume and surface and therefore also the mass increase: since it is necessary to analyse models with the same characteristic, the mass of the structure was kept constant, by means of multiplication coefficient applied to the specific weight. In the first line of the Table 4.46 are also reported the values obtained from the analysis of the simple model of sub paragraph 4.3.6. In this way, while simplifying the model, the load that affects the analysis remains the same.

GEOMETRICAL LEVEL OF DETAIL.			STRUCTURAL LEVEL OF DETAIL					
			10.000	108.000	206.000	304.000	402.000	500.000
Ashlar model	cube dimension [mm]		208	88	70	61	55	51
	n° of cubes		12x35x42	27x81x97	33x102x121	38x116x138	42x128x152	45x138x164
	max displacement [mm]		0,77888	0,78314	0,78319	0,78330	0,78353	0,78356
	Volume	60,0266 m³						
	Surface	142,792 m²						
	Not corrected Weight	120.053 kg						
10.000 Model	cube dimension [mm]		198	84	67	59	53	49
	n° of cubes		13x38x42	29X87X97	37x108x121	42x124x138	46x136x152	49x147x164
	max displacement [mm]		1,38372	1,40311	1,40695	1,40831	1,40974	1,41028
	Volume	53,919 m³						
	Surface	120,615 m²						
	Not corrected Weight	107.838 kg						
20.000 Model	cube dimension [mm]		207	88	70	61	55	51
	n° of cubes		15x37x41	33x86x94	41x108x118	46x123x135	51x135x148	55x146x160
	max displacement [mm]		1,03784	1,04638	1,04813	1,04887	1,04932	1,04931
	Volume	61,2713 m³						
	Surface	131,15 m²						
	Not corrected Weight	122.543 kg						
50.000 Model	cube dimension [mm]		210	89	71	62	56	52
	n° of cubes		15x37x40	34x87x94	43x108x117	49x124x134	53x136x147	58x147x159
	max displacement [mm]		0,945622	0,95540	0,95686	0,95752	0,95798	0,95832
	Volume	63,7928 m³						
	Surface	138,885 m²						
	Not corrected Weight	127.586 kg						
100.000 Model	cube dimension [mm]		212	90	71	62	57	53
	n° of cubes		16x38x40	35x87x93	44x109x116	50x124x133	55x137x146	59x147x158
	max displacement [mm]		0,90229	0,90627	0,90666	0,90748	0,90755	0,90748
	Volume	64,8658 m³						
	Surface	144,299 m²						
	Not corrected Weight	129.732 kg						
200.000 Model	cube dimension [mm]		214	90	72	63	57	53
	n° of cubes		16x38x40	36x87x93	44x109x116	51x125x132	56x137x146	60x148x157
	max displacement [mm]		0,925607	0,92112	0,91924	0,91953	0,91904	0,91921
	Volume	65,7164 m³						
	Surface	151,425 m²						
	Not corrected Weight	131.433 kg						
500.000 Model	cube dimension [mm]		216	91	72	63	57	53
	n° of cubes		16x38x40	36x88x92	45x110x115	52x126x132	57x139x145	61x149x157
	max displacement [mm]		0,83082	0,81947	0,814565	0,812238	0,81070	0,80993
	Volume	66,0589 m³						
	Surface	157,98 m²						
	Not corrected Weight	132.118 kg						

Table 4.46 – Models at different geometric and structural level of detail

It can be seen that, increasing the geometric LoD, the dimension of the cubes slightly enlarge: for each of the 42 models, are indicated the side of the cubes (mm), the number of cubes respectively along the depth, width and height direction. Most important values are the

maximum displacement (mm), always localized in the highest point (8,41 m), at the middle and at the rear, where the arch has a smaller resistant section.

The trend of the displacement is represented on the DSM with a colour scale that varies from the minimum value of 0 mm (in blue) to the indicative maximum value of 1 mm (in red): obviously, the displacement is zero at the base, bound to fixed end, and increases as ascending up to reach even 1,40 mm for the structure with the lower geometrical LoD.

From the analysis made on the models in 4.2.7, it appears that for a decimation of the surface up to 90% in number of triangles (model 100.000), the geometry of the model is still maintained in its form and the various architectural features are rather well defined. A lower definition involves a fast decay towards geometries that hardly are representative of the object: in particular, if in the models 50.000 and 20.000 are still identified the main components of the structure, like the key of the arc and the upper moulding, while is lost the definition of the segments. In the simplest model these differences are totally absorbed and the surface is completely smooth. In contrast, as regards the different LoD for structural modeling, having to do with an object that presents almost regular geometric peculiarity that is contained in the 10 cm approximately, the results are really similar once exceeded 108.000 the cubes for analysis.

Clearly the greater is the geometric LoD, the smaller will be the size of the cube that is needed to hold the geometrical differences and, therefore, it will be necessary a greater structural LoD. The global analysis of the results obtained, however, leads to the assessment that the general trend of the results becomes more or less constant on a decimated model with no more than 10% and comparable to the size of the cube geometric characteristics of the object surveyed.

4.4. Conclusions

Medium size objects were studied in this chapter: referring to the common standards described in chapter 2, after a quick view on the current trends of geomatic models used for structural analysis, the chapter deals with a practical case represented by the Arch Bollani in Udine.

Considering the LoD needed for medium size objects, which is much lower than the small objects case, and considering also the fact that computation is still rather easy, if compared to the structural analysis of a complex building, this typology can be defined as the most simple. On this particular case was held a study on the level of detail needed both for geometry both for structural analysis, defining which parameters have main influence on the obtained results.

4.5. Bibliography

Bertolini Cestari, C., Chiabrando, F., Invernizzi, S., Marzi, T., & Spanò, A. (2013). Terrestrial Laser Scanning and settled techniques: a support to detect pathologies and safety conditions of timber structures . *Advanced Materials Research , 778*, p. 350-357.

Cabaleiro, M., Riveiro, B., Arias, P., Caamano, J. C., & Vilan, J. A. (2014). Automatic 3D modeling of metal frame connections from LiDAR data for structural engineering purposes. *ISPRS Journal of Photogrammetry and Remote Sensing* (96), p. 47-56.

Cannella, M. (2015, 1 8-14). Digital Unwrapping and visualization of complex architectural surfaces for the documentation and the restoration. *DisegnareCon* (8).

Chiabrando, F., Donadio, E., Spanò, A., & Sammartano, G. (2015). La tecnologia laser scanning per la valutazione statica delle strutture storiche . *XIX Conferenza Nazionale ASITA* , (p. 253-261).

Di Sivo, M. (2004). *Atlante della pietra.* Torino, Italy: UTET.

Frangipane, A. (2007, 1). Natural stone portals of the town of Udine (Italy): their design, construction and materials between the 15th and 20th centuries. *Geological Society London Special Publication* (27), p. 33-42.

Visintini, D., & Spangher, A. (2013). Rilevamento laser scanning, modello della superficie (DSM) e modello per il metodo agli elementi finiti (FEM) di una struttura . *Atti 17a Conferenza Nazionale ASITA* (p. 1287-1294). Riva del Garda: ASITA.

5. LARGE SIZE OBJECT

5.1. Introduction

In this last chapter, dedicated to the examination and application of real cases, it will be considered the class of large size objects, where, despite the general low level of detail needed, other kind of problems have to be faced, related, for example, to the complexity and size of the building, to the dealing with geometrical concavities due to internal spaces among the walls, to the inaccessibility of some areas.

The pointed out problems, how it will be further illustrated, deal more with the spatial modelling of the objects, than with the structural analysis by itself, since the achievement of a "solid model", and not only a "surface model", still represents a real challenge for large objects.

As widely illustrated in paragraph 2.2, standards that govern the structural analysis of the building are fully defined and, from their reading, as already widely highlighted, the accuracy of definition of the geometry of the objects concerns with the delineation of the so-called "confidence factor" F_C, and consequently, with the "level of knowledge" L_C of the structure itself. It is important to notice that the realization of 3D models, within FEA software, as introduced in chapter 2, implies a massive work of simplification of structures, because of the strictness imposed by the modelling tools there developed. These simplifications, of course, entail the overlooking of important geometrical details and, as remedy to this, the adoption of penalization factors. The definition of a correct geometry is often so demanding for the operator that could result more convenient to manage simplified models, as it regards geometry, preferring to focus efforts on the correctness of the other parameters (mechanical and costitutive).

In this chapter, it is therefore intended to highlight how the models, obtained from a TLS surveying, of large size objects, like buildings and constructions, can be directly used instead also for structural analysis purposes, thus overcoming, the noticed difficulties.

The problems so far listed are of course not new, and many other authors have treated this subject; therefore, before the description of the case of study, in paragraph 5.2, some of the most important and representative studies on this field will be examined, in order to focus on the problems and the results obtained.

It will be later described, in paragraph 5.3, the case of study, represented by the Baptistery of Aquileia, examining all the aspects that leaded to the definition of a geometric model. This model will be therefore compared to a simple geometric model, obtained from measures of a direct survey, and therefore not so accurate but, just for this, representative of which could have been the usually adopted model in structural analysis.

5.2. Analysis of large-size objects: current trends

The geometric information about buildings, or, more commonly, about constructions, that result more interesting for structural purposes, besides the ones described by the classical

plans and sections, are generally: the variation of thickness and slope of the walls, the profiles of façades, the tower building inclination and the displacement of barycentre position in function of its height, the position of fractures and cracks, as well as other many data that contribute to a complete knowledge of the structural geometry. All of these data, of course, have to be somehow acquired and it obviously the use of TLS, since its introduction, has been strengthening, also in this field.

Among the existing studies on this field, the most interesting, in relation to the work of this thesis, are the ones shortly described in the following.

In the "3D Surveying for structural analysis applications" (Guarnieri, Pirotti, Pontin, & Vettore, 2006) the authors analyse the results obtained from a FEM structural analysis carried out on some cross sections extracted from a building's wall, presenting a few visible crackings. The model of this wall, belonging to the Venetian Villa Giovanelli near Padova (*Figure 5.1 a)*), was obtained from the data acquired with a TLS surveying. Even if in this article, the dimension of the analysed object is limited to a single section of a wall, this is one of the first applications of FEM to a TLS model (*Figure 5.1 b)*).

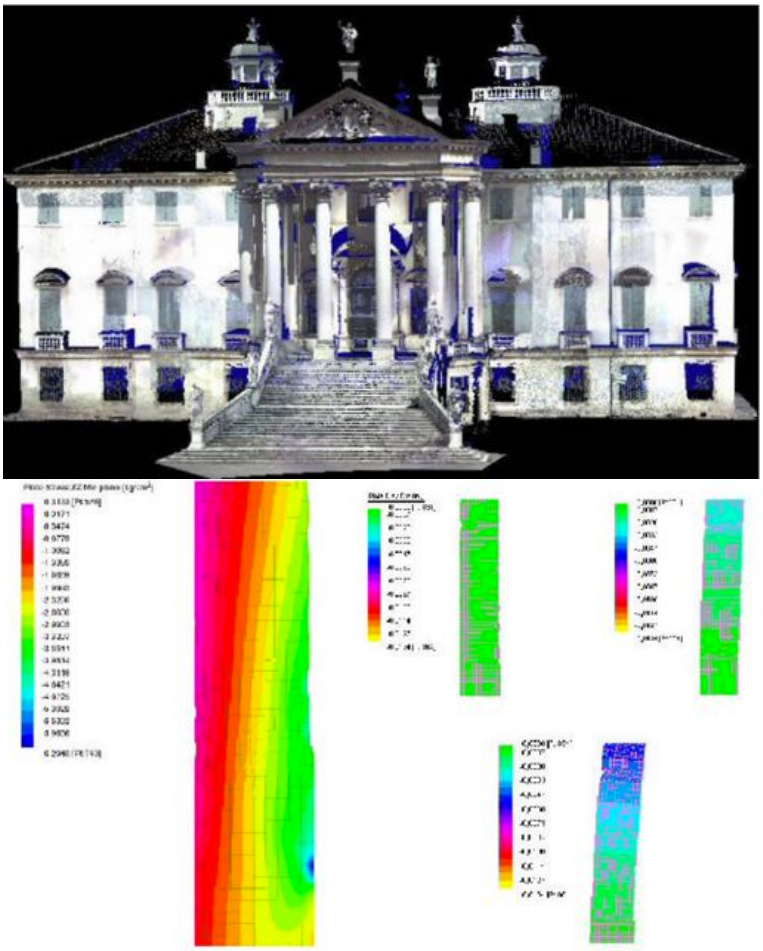

Figure 5.1 – a) The TLS surveying of Villa Giovanelli – b) Sections of the walls analysed, on the left the effects of the proper weight and on the right the effects of the off-plum line.

Another work, which results are really interesting is "Deformation measurements at historical buildings with the help of three-dimensional recording methods and two-dimensional surface evaluations" (Sternberg, 2006), where the vaults of the Meldorf Cathedral (Germany) were repeatedly measured for one day with TLS (*Figure 5.2 a)*), in order to evaluate the possible movement, acting on the building, and therefore for measuring displacement (*Figure 5.2 c)*). The author proposes an interesting evaluation of the structure, starting from a 3D model of the vaults (*Figure 5.2 b)*), but there is not still any solid volume of the building, since operations are carried out on mesh surfaces.

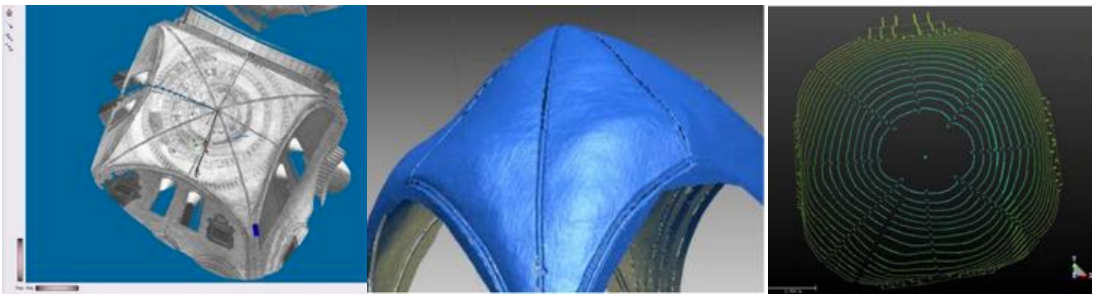

Figure 5.2 – a) The TLS surveying of a vault of Meldorf Cathedral (Germany)
b) The surface obtained from the TLS surveying
c) The contour lines representing displacement measured on the surface of the vaults.

In the paper "Evaluation of structural damages from 3D Laser Scans" (San José, Fernàndez MartIn, Pérez Moneo, Finat, & Martinez Rubio, 2007) the proposed method is the combination among the TLS surveying (*Figure 5.3 a)*) and the acquired images in order to create a surface of the object of interest, the Church of Villamoron (Spain), textured with the images representing damages. The proposed idea is interesting, but the results represented in the work refer only to a coloured point clouds (*Figure 5.3 b)*), and this prove that the obtaining of such a complex structure as a complete surface model is still not an easy operation.

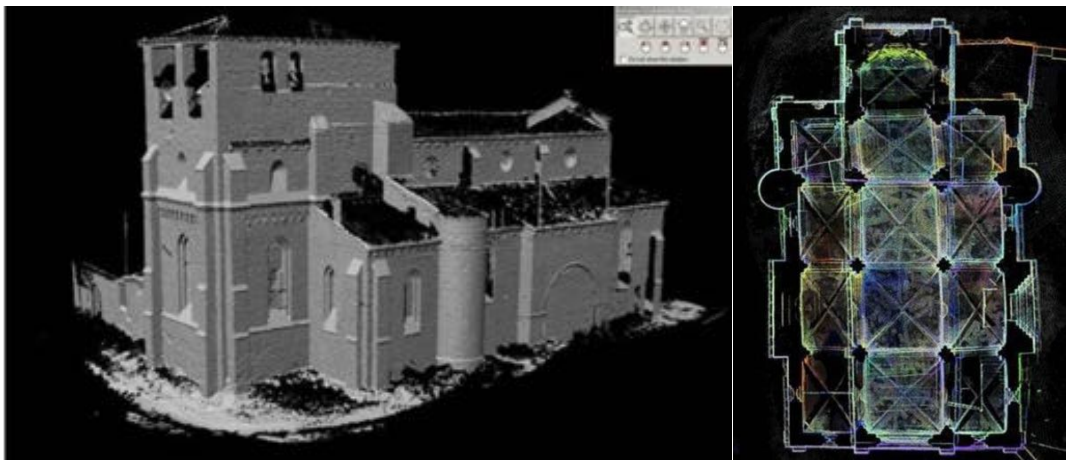

Figure 5.3 – a) The TLS surveying of the church of Villamoron (Spain)
b) The coloured point cloud of the vaults.

"Terrestrial Laser Scanning for Preserving Cultural Heritage: Analysis of Geometric Anomalies for Ancient Structures" (Castagnetti, Bertacchini, Capra, & Dubbini, 2012) presents the analysis held on the Cathedral of Modena and describes the operation of surveying held with

the purpose of obtaining "structural data", with particular regard to the displacement acting on the structure because of the subsidence of the ground (*Figure 5.4)*). The investigations about the identified anomalies are presented together with the differential movements obtained by high precision levelling exploiting on a network of benchmarks installed along the outside perimeter. The integration of the two different techniques allowed the check to correctness of the results.

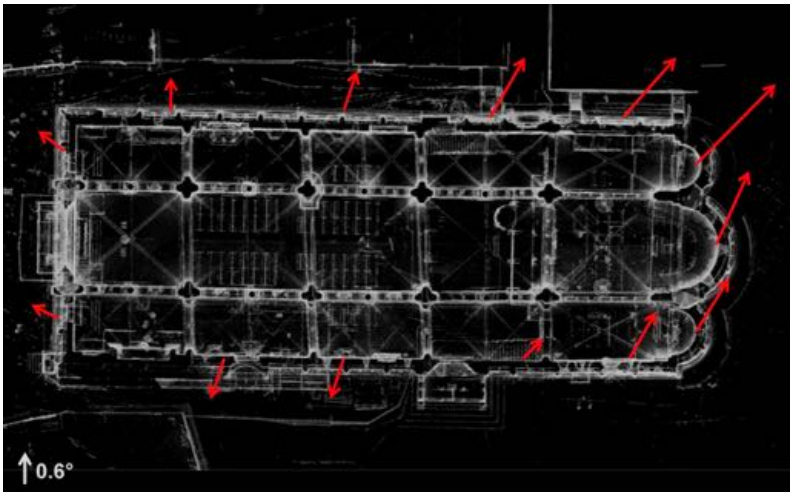

Figure 5.4 – Summary of overhanging directions (red vectors) identified on external columns. Lenght of vectors is proportional to deflection angle value.

In "Dynamic identification of historic masonry towers through an expeditious and no-contact approach: Application to the "Torre del Mangia in Siena (Italy)" (Pieraccini, Dei, Betti, Bartoli, Tucci, & Guardini, 2014), the authors deal with the theme of the tower constructions. Beside the proposed method for the computation of sections (*Figure 5.5*), the 3D FEM model, designed considering the measures of TLS, represents the real innovation. In the paper, in fact, the model keeps in consideration the variation of the sections and the displacement of the barycentre of the structure, comparing the results with a hypothetical symmetric tower.

Many other studies on towers were as well carried out over times, especially at the University of Bologna, Modena and Reggio Emilia, and Florence, because of this frequent typology of structure in those cities. Among all, deserve a citation the works realized on the most important towers of Bologna and Modena by Bertacchini, Boni, Capra, Castagnetti, & Dubbini (2009) and Pesci, Teza, & Boschi (2015)

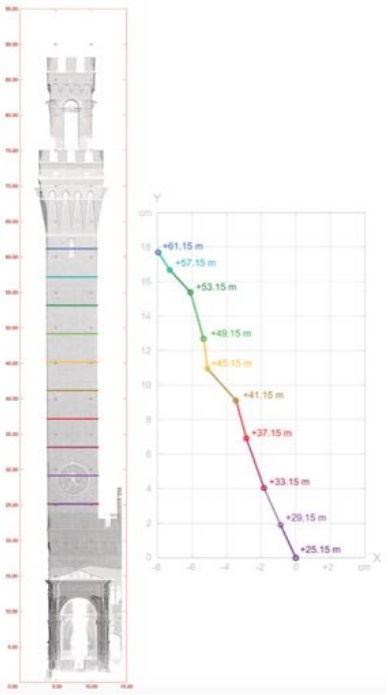

Figure 5.5 - On the left: scheme of the 10 horizontal sections. On the right the graph of displacements of the geometric center and height of the sections at different levels.

In the study "3D geometric analysis of the façades of gothic buildings in Venice: examples of 3D modelling" (Guerra, Balletti, Stevanin, & Vernier) are described the different surveying methodologies used in the research (topographic measures, laser scanning, photo-planes and ortho-photos) and the representations, modeling the building surface (models of warping). The results are representations of the surfaces with the clear definition of the gaps existing between the façades and the vertical plan (*Figure 5.6*).

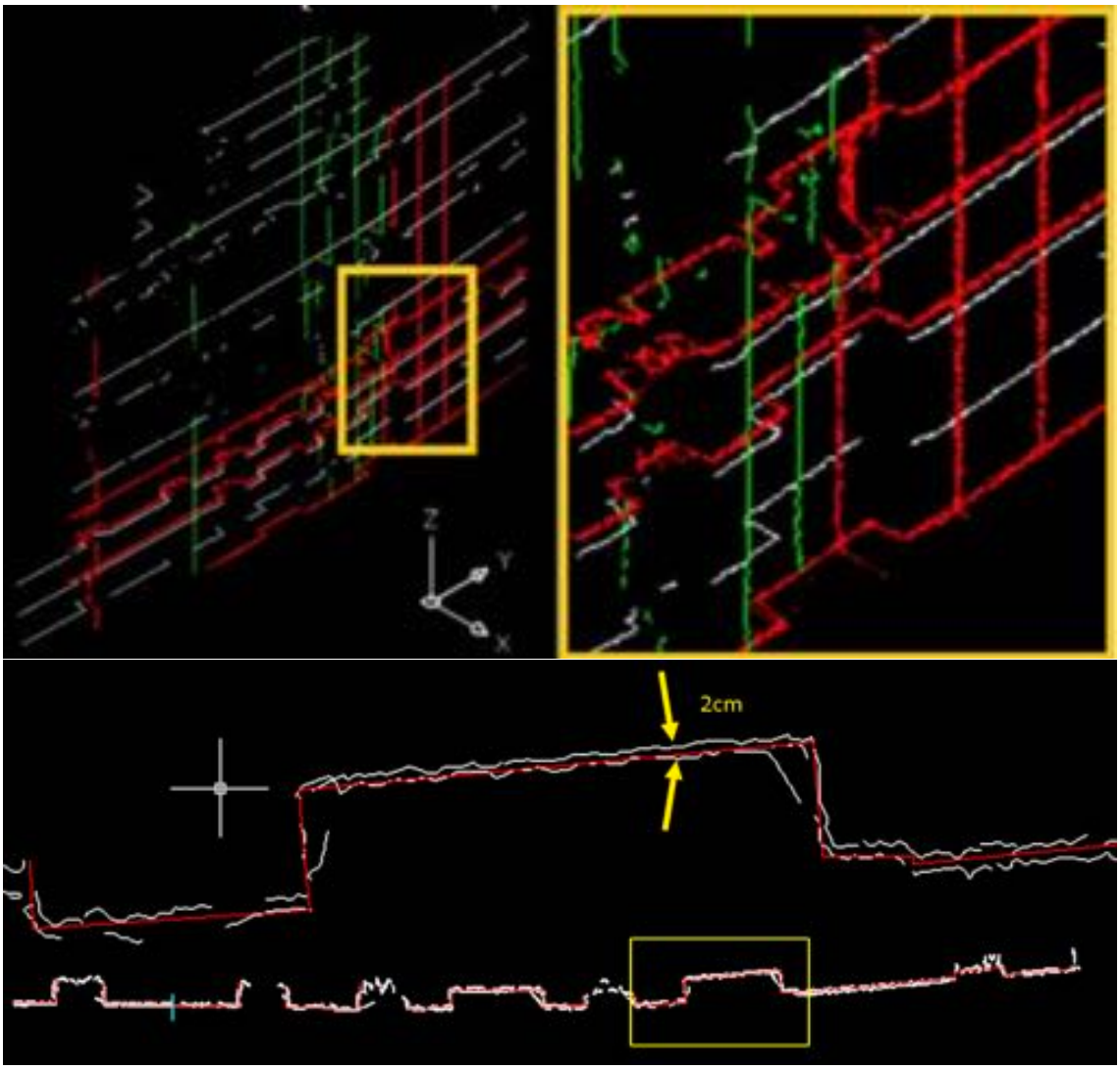

Figure 5.6 – Rough profiles obtained from scanning and interpolation of automatic profiles (Guerra, Balletti, Stevanin, & Vernier).

The last work, that deserve a citation, for the strict similarity of the theme proposed with this thesis approach and also for the alternative process performed, is the article "From laser scanning to finite element analysis of complex buildings by using a semi-automatic procedure" (Castellazzi, D'Altri, Bitelli, Selvaggi, & Lambertini, 2015). Starting from a TLS surveying (*Figure 5.7 a)*), a surface model is obtained (*Figure 5.7 b)*) and sliced, along the vertical axe of the building; each slice is later divided in many voxel of the same dimensions (*Figure 5.7 c)*), for which are applied the mechanical characteristic and the costitutive equations.

In this way, it is obtained a Finite Element Analysis starting directly from the TLS surveying (*Figure 5.7 d)*). The method is still object of study by the same authors.

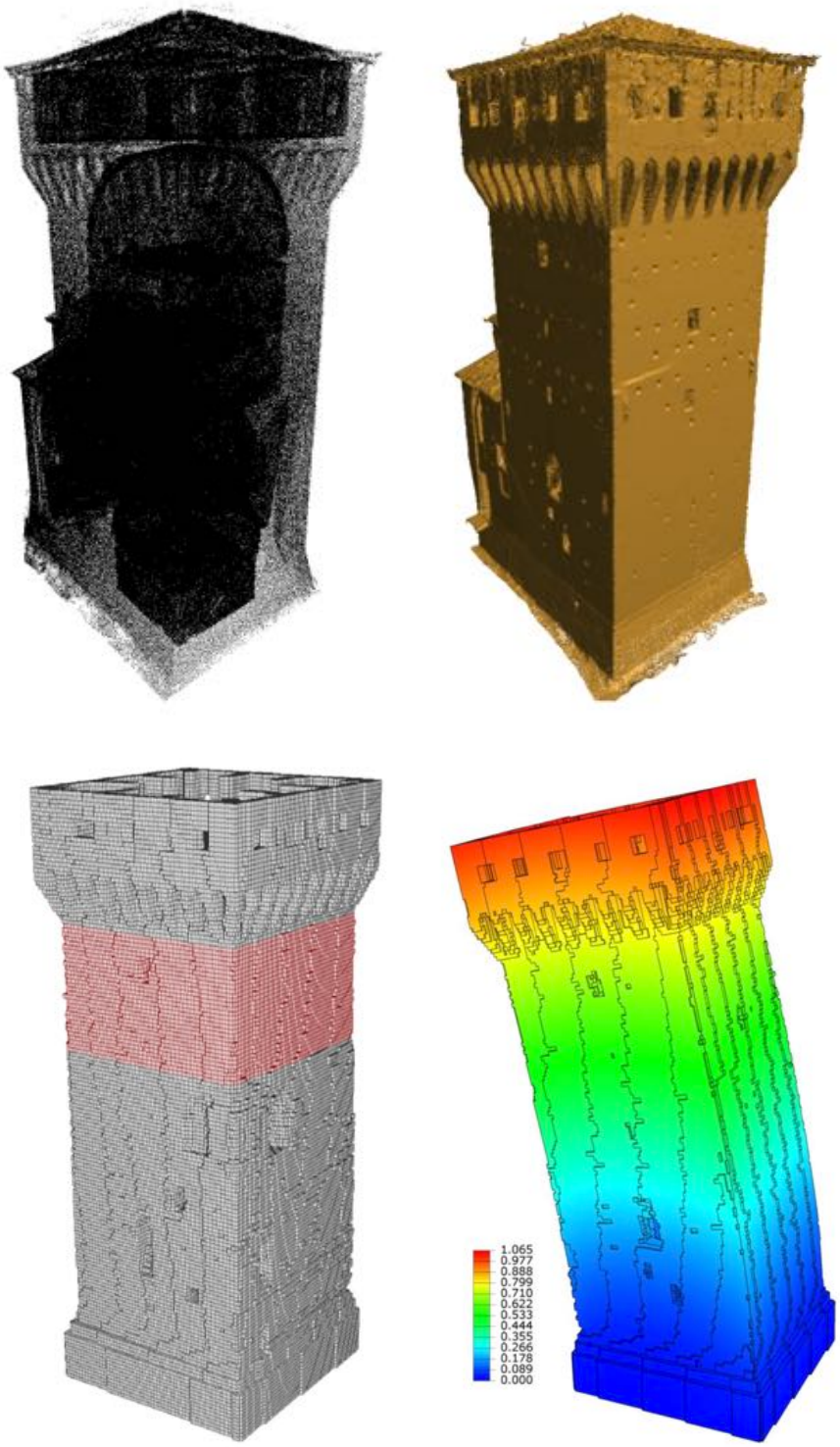

Figure 5.7 – a) Point cloud of the Mastio tower of the Fortress in San Felice sul Panaro (Modena) b) Modellized surface - c) Voxelization of the model – d) FEM analysis.

5.3. Case of study: the Baptistery of Aquileia

5.3.1. Historical description

The structures composing the Basilica of Aquileia (*Figure 5.8 – a)*) were first built in the fourth century and are the result of several extensions and reconstructions implemented over the centuries. The present structure is basically the same of the one consecrated in 1031 by Patriarch Popone after the changes he promoted, including the construction of the majestic bell tower, 73 m high. Close and directly connected to the Basilica are the so-called "Church of Pagans" and the Baptistery, our object of study (*Figure 5.8 – b)*).

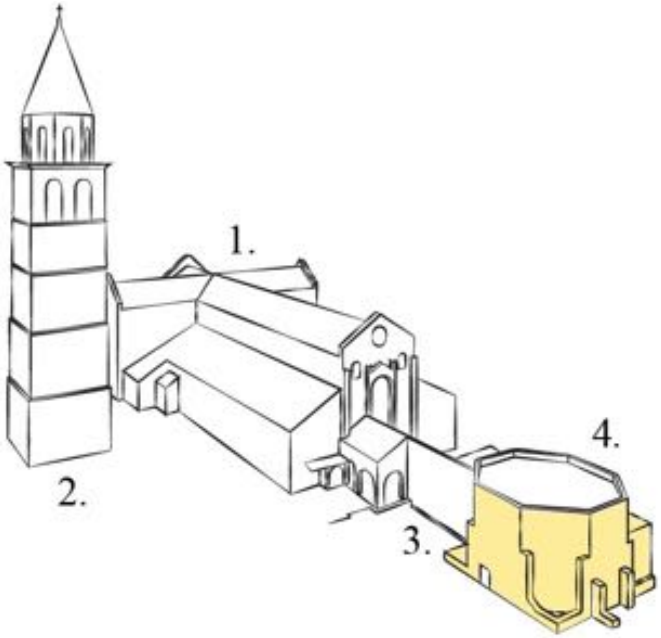

Figure 5.8 – a) Buildings composing the Basilica structures – 1. Church – 2. Bell Tower – 3. Church of Pagans – 4. Baptistery - b) Baptistery seen from the North-East side.

The Baptistery is the result of various modifications and revisions: it has an octagonal shape inscribed, originally, in a square and it is attached, beside to the Basilica, as already said, through the "Church of Pagans", a medieval hall, ending with an open porch, also to the more recent "Mosaic Hall", through an opening on its South part.

The structure is also called "Cromatian Baptistery", since its construction is attributed at the time when Cromazio was Bishop of the diocese (from 387/388 to 407/408), even if the exact date remains doubtful. Certainly the Baptistery is the result of a succession of phases (Tavano, 1972): the latest documents available on this argument are the results of the archaeological excavation of Paola Lopreato and an analysis on the structure of the walls held by Olof Brandt (Brandt, 2009).

From the excavations lead by Lopreato (*Figure 5.9*), it emerges an initially squared foundation with an offset brick all around the niches, on which rested both the first floor both the bases for the columns set at the corners, which had no static function.

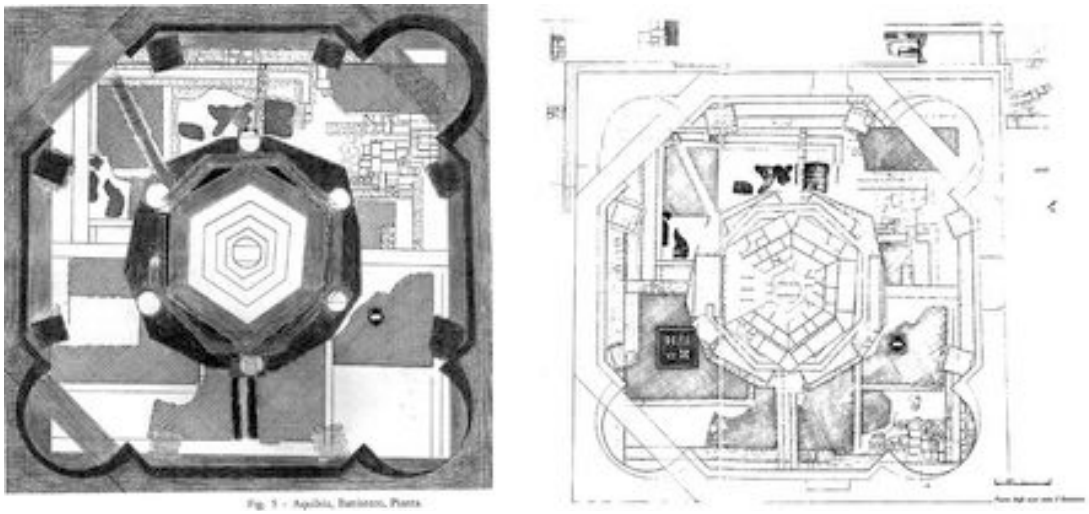

Figura 5.9 – Plants of the excavation in the Baptistery lead by Lopreato in 1989 and in 1991.

On the other side, the analysis of masonry carried out by Olof Brandt, in a more recent formulation, takes advantage of earlier studies and analysis in situ; his study shows three different phases of construction of the Baptistery. The stratigraphic analysis, performed according to the method formulated by Harris, which defines the age of an archaeological excavation according to the order of overlapping of the pattern and according to the continuity of phases, is unfortunately not so accurate, because of the impossibility to dismantle the wall, but defines in a concise way the three different phases of construction.

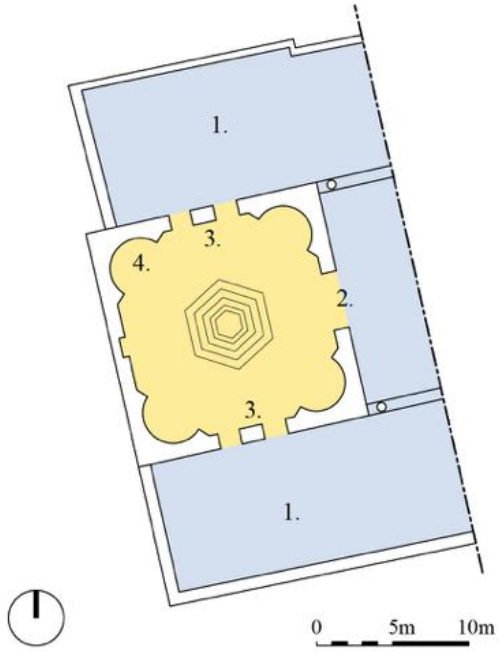

Figure 5.10 – The first phase of the construction of the Baptistery.

Originally, in the IV century, the Baptistery had a squared plan and was placed in a very different context from the current state: it was in fact enclosed between two arcades, indicated with *1.* in *Figure 5.10,* that encompassed the Baptistery in a larger building, likewise squared. These two wings are historically called "Nordhalle" and "Sudhalle", from the excavation realized at the end of the 19th century by George Nienmann and Heinrich Swoboda, and were connected to the Baptistery with two pairs of doors on the North and the South side (*3.*). The remains of the mosaic floor of one of these two lateral halls are still visible, in the new construction called "Mosaic Hall", hosting the former Sudhalle. To the East, where the Baptistery is currently connected to the Church of Pagans, a further door (*2.*), probably larger than the actual opening, leaded to the courtyard outside the building. The interior part of the Baptistery had an octagonal shape, with semi-circular apses in the four diagonal corners (*4.*). With respect to the square foundation, the octagonal shape was maintained even at the top of the building, which towered over the rest of the same. The original parts of this first phase are recognizable by the use of a rather regular masonry clay bricks, with the insertion of few sandstone blocks.

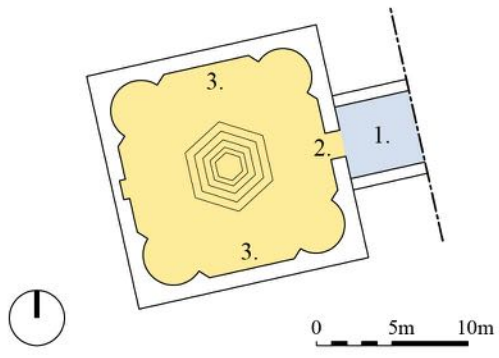

Figure 5.11 – The second phase of the construction of the Baptistery.

In the second constructive phase (*Figure 5.11*), dated to the end of VIII century or the beginning of the IX, the North and South opening had been closed since (*3.*), probably, the two lateral buildings were dismantled. In this period also arose a first building as ancestry of the Church of Pagans (*1.*), while all the apses are still accessible. The masonry of this period was realized with irregular stone blocks, as it is possible to view nowadays in curtain walls used for closing the doors, as well to the side addiction to the East opening (*2.*).

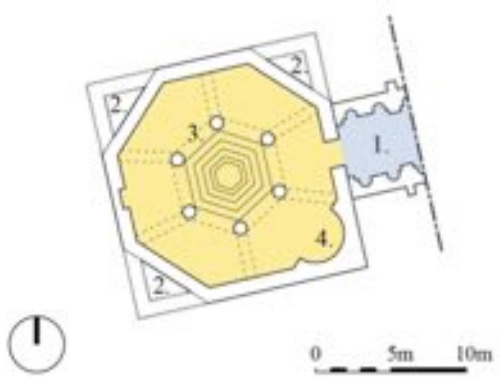

Figure 5.12 – The third phase of the construction of the Baptistery.

The third and last period, dated to XI century, see the transformation of the Baptistery to the construction as it is nowadays (*Figure 5.12)*. Three of the four apses were closed (*2.*) and six arches were realized from the boundary of the hexagonal baptismal font to the exterior wall (*3.*), in order to support a second floor. The forth apse remained open for ritual occasions (*4.*). New arches were inserted in the masonry, in order to unload the weight, since the closing walls of apses had no foundations. The masonry of this last intervention is more ordered and varies between regular clay bricks and some stone blocks.

5.3.2. The geometric surveying

The surveying of the Baptistery has been realized in a campaign organized along with the staff of the Department of Civil, Chemical, Environmental and Materials Engineering of the University of Bologna, since a research on analogous arguments is currently held there, and it would be interesting in a close future, to compare the obtained results.

In order to acquire a complete description of the object, and therefore non only of its surface, but also of those geometries that assume a high importance in the structural definition, among all walls thickness and inclinations, the surveying involved both the interior and the exterior parts of the building.

The laser scanning surveying of the exterior part has been realized by the staff of University of Udine with the TLS system Riegl Z390i (*Figure 5.13 a) and b)*), formerly used for the surveying of Bollani Arch (chapter 4). In the present case, nine scans were acquired from nine different stations, exactly over the vertices of the topographic network, previously defined through a preparatory design (*Figure 5.13*), in order to have a complete covering of all the surfaces of the building.

Figure 5.13 – a) TLS in station E – b) TLS in station I.

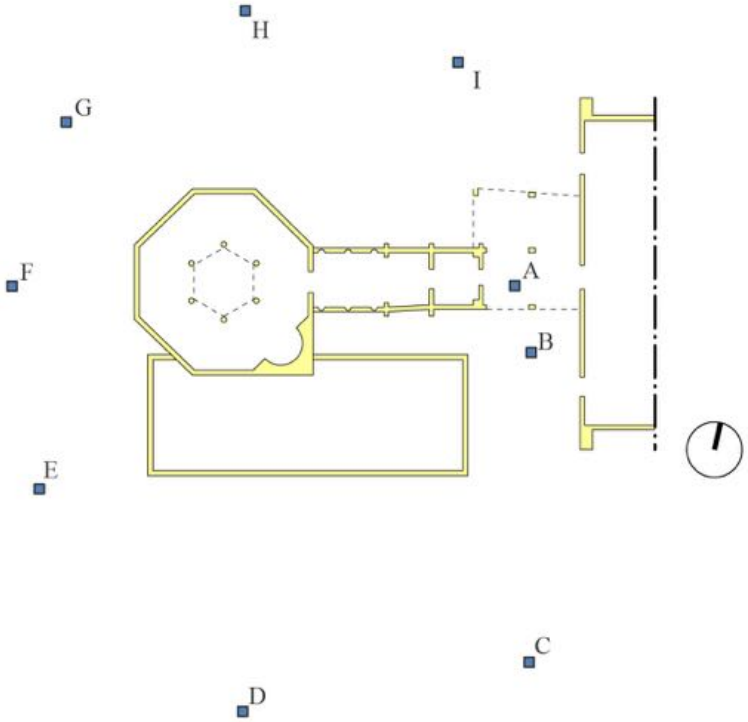

Figure 5.14 – Scans position in the exterior of the structure.

As already pointed on sub paragraph 5.3.1, the building is strictly connected to the Church of Pagans and to the Mosaic Hall and, therefore, also these building have been surveyed as well. The total number of TLS points so acquired amount to 3.219.815 (*Figure 5.14*).

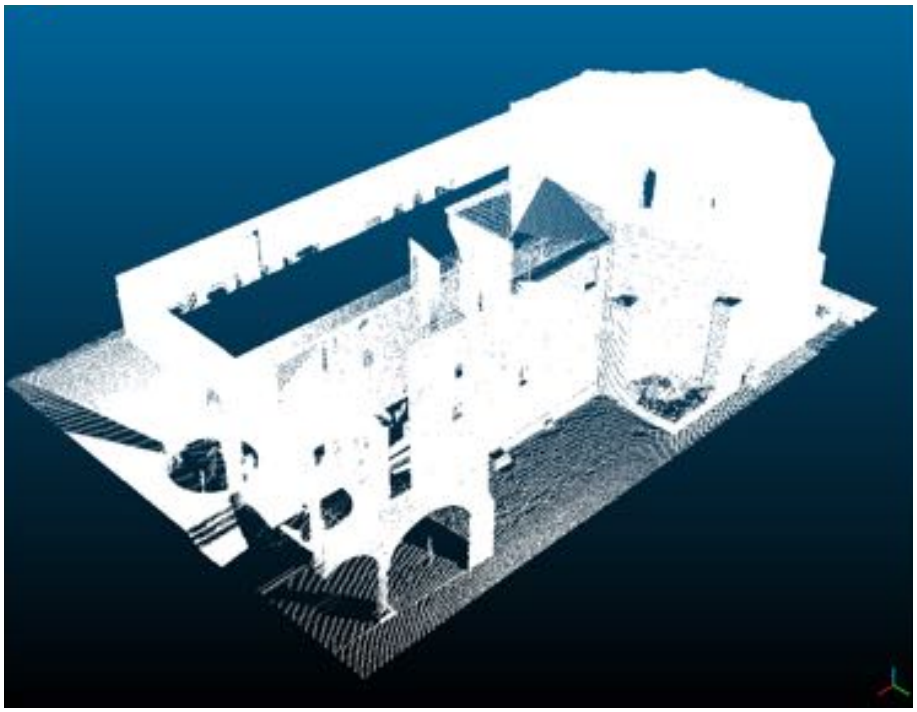

Figure 5.14 – Point clouds of the exterior part of the entire structure after scans registration.

The staff of the University of Bologna surveyed instead the interior part of the building. The surveying was realized with the TLS system Riegl Z400 from 16 different scan positions (*Figure 5.15*), acquiring the same number of scans, in detail: 5 of the Church of Pagans, 1 of the Mosaic Hall and 11 of the Baptistery. Totally, 23.751.491 points were acquired and 17.992.631 of them belonged to the Baptistery (*Figure 5.16*).

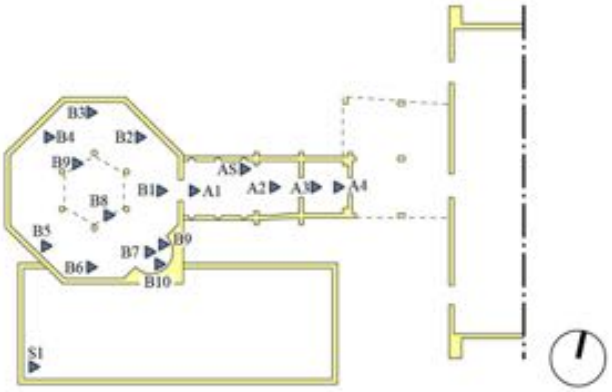

Figure 5.15 – Design of the scan stations in the interior of the structure.

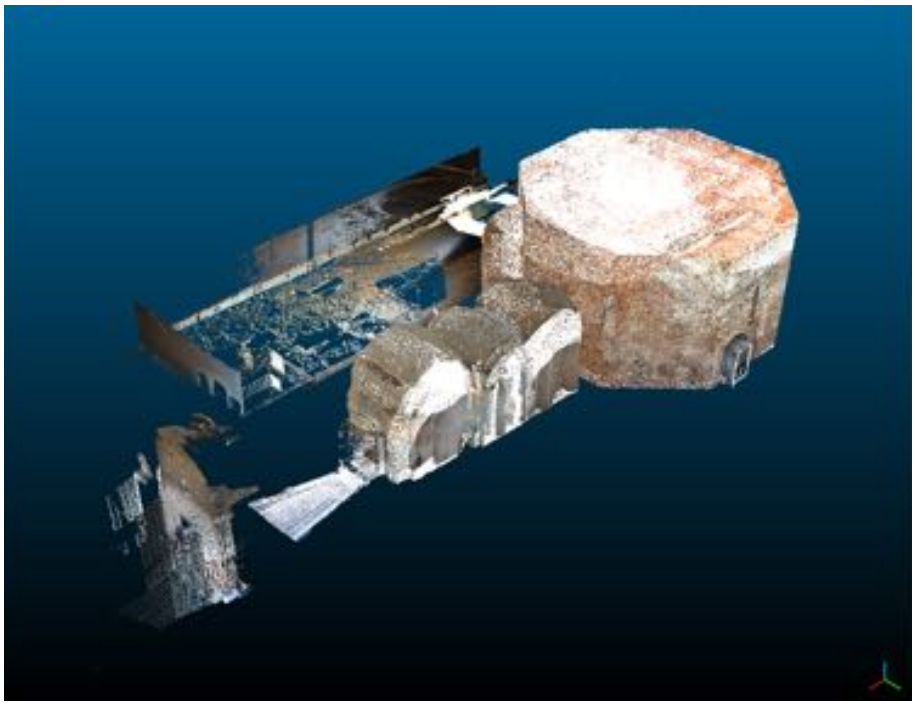

Figure 5.16 – Point clouds of the of the interior of entire structure represented already registered.

After scans registration for the surveying of the roof of the building, the staff of Bologna proceeded with a photogrammetric surveying, adopting an extensible tripod and opportune devices to control the surveying camera commands (*Figure 5.17 – a)*). This operation required 4 different positions of the instrument and a total amount of 77 pictures with a Canon EOS 6D 5.472x3.648 pixel. After processing these images with Agisoft Photoscan a total of further 7.937.044 points were so available and all the exterior surfaces of the buildings resulted therefore surveyed. The University of Bologna managed all the photogrammetric data and operation necessary to obtain the point cloud, which, in this thesis, was used without any participation to the obtaining steps (*Figure 5.17 – b)*).

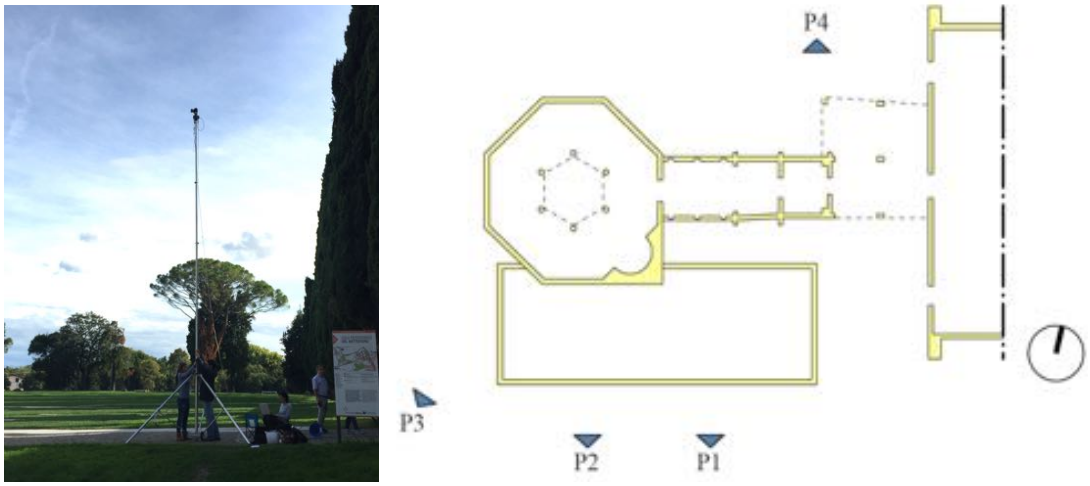

Figure 5.17 – a) Device used for the photogrammetric survey – b) Image acquisition positions.

Figure 5.18 – Point clouds of the of the top part of entire structure represented already registered.

In order to proceed with the registration of the scans, 15 cylindrical (Ø 10 cm) (*Figure 5.19 a)*) and 55 disk reflective targets (Ø 5 cm) have been placed and spread over the external parts of the structure (*Figure 5.19 b)*). For the interior scans, 17(2x2 cm) targets were placed. Furthermore, other 55 natural points have been considered, moreover chosen in high (inaccessible) parts of the walls and topographically surveyed. Two of the exterior scans acquired, namely those located in the stations A and G, allowed the surveying of little portion of the interior of the building, through the opened doors. These acquired points were anyway not sufficient for the registration of the internal scans; as a priori known, was necessary to proceed with the topographical surveying of all internal and external the targets.

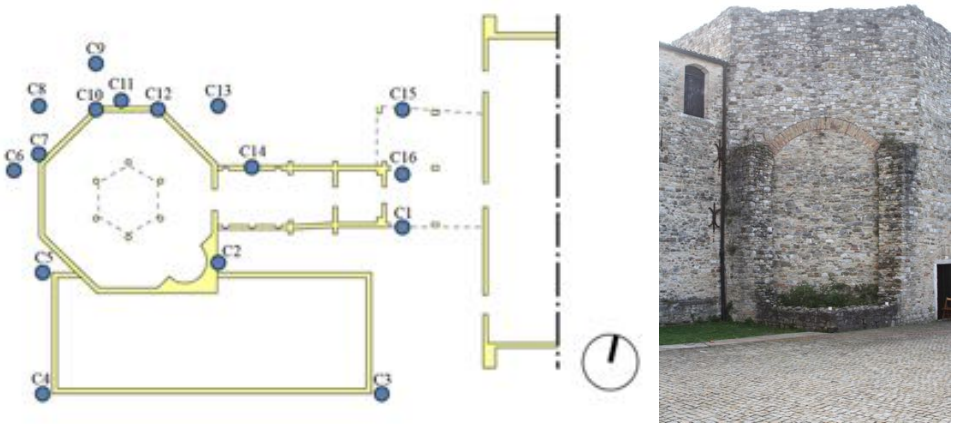

Figure 5.19 – a) Position of the cylindrical reflecting targets – b) Disk reflecting targets on the walls.

Once processed all the topographical surveying acquired measurements, through the software STAR*NET (MicroSurvey), it was possible to obtain a net, as represented in *Figure 5.20*, which data are reported in *Tables 5.21-5.23*. Fixed the vertices positions, the coordinates of all the "control points" have been computed and their values were therefore assigned to the

targets recognized in RiSCAN in order to proceed with the scans registration. The residual medium value obtained, 1,54 cm, can be considered more than satisfactory for the purposes of the thesis and in relation with the dimension of the building.

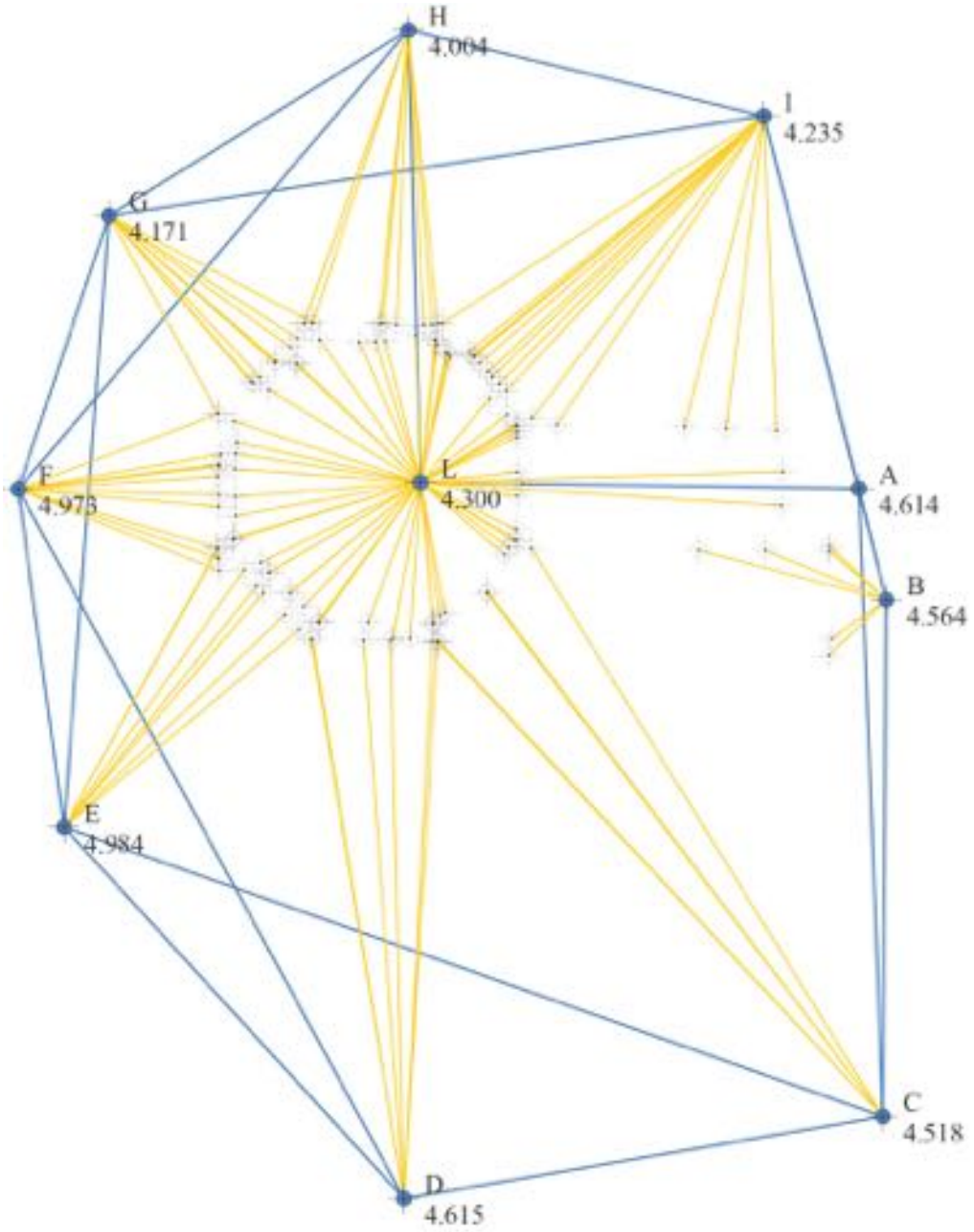

Figure 5.20 – Topographic surveying of network and control points.

In total 34.908.350 points, covering the entire interior and exterior surface of the structure, compose the final point cloud, which represent the union of all the point clouds obtained from each surveying (*Figure 5.24*). Of this huge amount of points, 26.686.648 of them refer to the Baptistery, which is the object of interest.

Adjusted Coordinates			
Station	X	Y	Z
L	0,0000	1,0000	2,0000
A	21,7366	0,0000	4,6140
C	23,2166	-31,2936	4,5180
B	23,1522	-5,6242	4,5638
D	-0,4846	-35,5907	4,6149
E	-17,5112	-17,2995	4,9836
F	-19,9280	-0,0001	4,9730
G	-15,5617	13,1205	4,1707
H	-0,8027	22,4699	4,0041
I	16,8630	18,3600	4,2355

Table 5.21 – Adjusted coordinates of the network vertices [m].

Station Coordinate Standard Deviations			
Station	X	Y	Z
L	0,000000	0,000000	0,000000
A	0,000707	0,000000	0,001078
C	0,002105	0,000681	0,001618
B	0,000781	0,000544	0,001120
D	0,002361	0,001439	0,001742
E	0,001732	0,001971	0,001672
F	0,001374	0,002078	0,001622
G	0,001446	0,001832	0,001562
H	0,001839	0,000953	0,001331
I	0,001461	0,000598	0,001426

Table 5.22 – Verteces Station s Coordinates Standard Deviations[m].

Station Coordinate Error Ellipses (Meters) Confidence Region = 95%				
Station	Semi-Major Axis	Semi-Minor Axis	Azimuth of Major Axis	Elev.
L	0,000000	0,000000	0,00	0,000000
A	0,001731	0,000000	100,00	0,002114
C	0,005172	0,001607	94,30	0,003171
B	0,001915	0,001327	105,22	0,002195
D	0,006150	0,002825	125,17	0,003414
E	0,005639	0,003075	157,61	0,003278
F	0,005102	0,003340	193,34	0,003179
G	0,004883	0,002963	33,22	0,003061
H	0,004684	0,001940	80,37	0,002608
I	0,003576	0,001465	99,84	0,002794

Table 5.23 – Verteces Station Coordinate Error Ellipses "values".

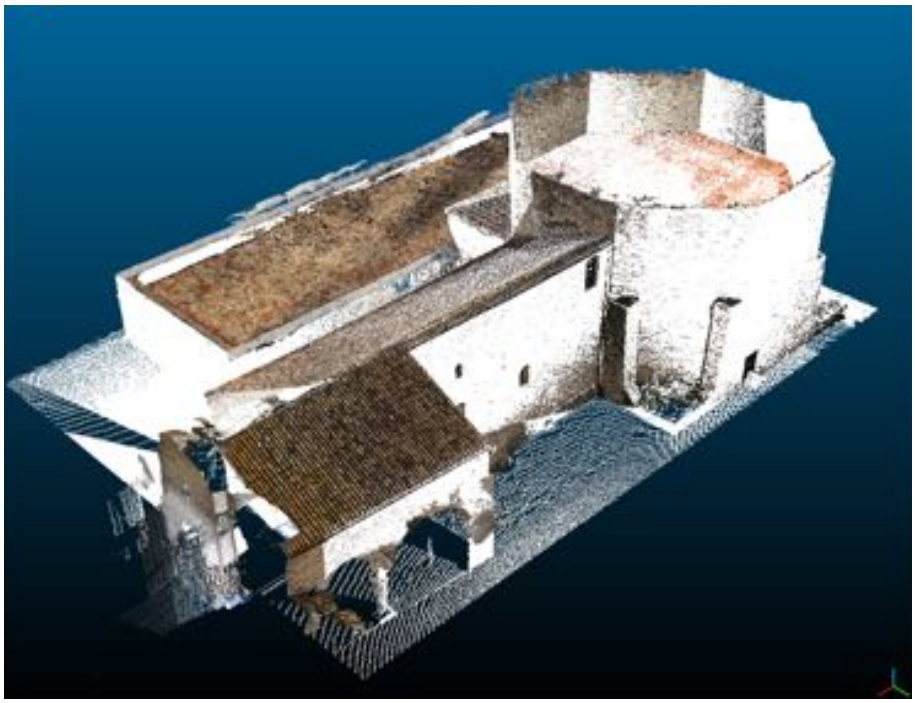

Figure 5.24 – Point cloud of the entire structure.

5.3.3. Calculation of surface modelling

The modelling of the structure was processed through all the software described in paragraph 1.4, using most suitable algorithms and commands for each case. Even if the procedure was apparently the same of the cases previously studied in chapter 3 and 4, since it always included the "transformation" of a point cloud, into a surface the processing was this time much more complicated.

The difficulties were mainly due to:

- the huge number of data to process (35 millions of points), which led to an excessive slowdown, or even to the failure, of the computing processes;
- the mismatching of the interpretation of coordinates, between the two surfaces, in the computing operations;
- the occlusion of some parts of the structure, due to the conformity of the structure, which caused the presence of a consistent lacking of data, especially in proximity of the attachment between the buildings.

In order to solve the listed problems, it was necessary to set an operative strategy that included the following steps:

1. cleaning of each of the 3 data set, both from the outliers and isolated points both from noises;
2. resampling of the point clouds on an uniform grid, also because each instrument used was set on different settings;
3. modelling of the interior and exterior surfaces separately and later merge of the two surfaces;
4. automatic adjustments of the surfaces;
5. manual reconstruction of the occluded parts, taking dimensions from existing documents, and available drawing and images of the building.

The first step of cleaning data was obtained partially manually, operating in the Meshlab environment, where all the points considered useless (like the outliers) or even "damaging" for the future elaborations have been eliminated, partially in an automatic way, through the proper command of the software CloudCompare.

These operations leaded to a strong reduction of the number of points for each point cloud, as it is possible to note in *Table 5.25* and *Figure 5.26*.

Point Cloud	Original data (no. points)	Automatic Cleaned data (no. points)	Manually Cleaned data (no. points)
Exterior TLS	3.219.815	2.000.832	1.684.137
Interior TLS	23.751.481	13.658.958	13.627.377
Exterior Photogrammetric	7.937.044	4.809.333	4.459.029
TOTAL	34.908.350	20.469.123	19.770.543

Table 5.25 – Reduction of the number of points after each operation of cleaning.

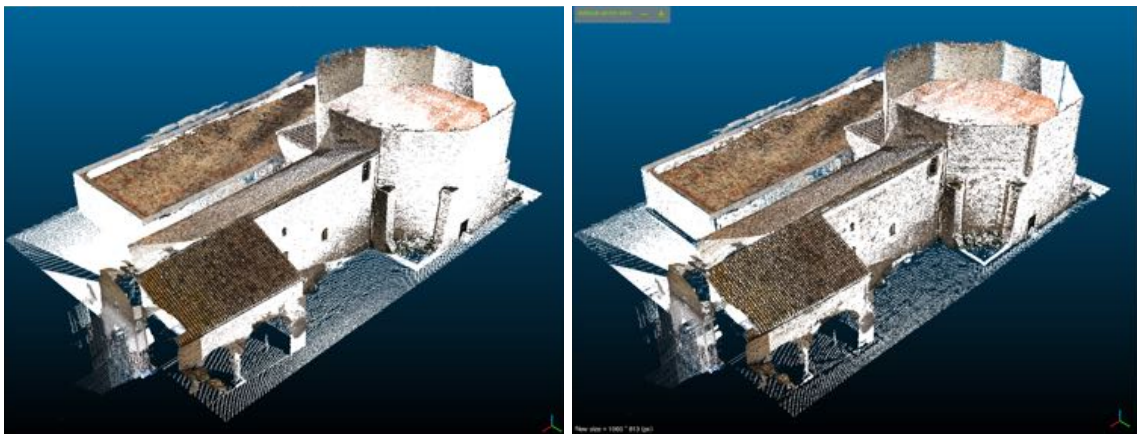

Figure 5.26 – The point cloud before and after the cleaning.

Afterwards, second step implied the resampling of the point clouds over a "constant" distance between each point, for all the point clouds. This operation was processed through the command "Uniform Data" in Geomagic Wrap, adopting a grid value of 3 cm, considered sufficient for the geometrical definition of the structure (*Figure 5.27*).

This operation, besides having regularized the density of the points, allowed a further reduction of their quantity, as it reported in *Table 5.28*, and to obtain the point cloud represented in *Figure 5.29* in the right side.

Figure 5.27 – Resampling command in Geomagic Wrap.

Point Cloud	Original data (no. points)	Cleaned data (no. points)	Resampled data (no. points)
Exterior TLS	3.219.815	1.684.137	998.207
Interior TLS	23.751.481	13.627.377	3.237.531
Exterior Photogrammetric	7.937.044	4.459.029	1.547.648
TOTAL	34.908.350	19.770.543	5.783.386

Table 5.28 – Reduction of the number of points after the operation of resampling.

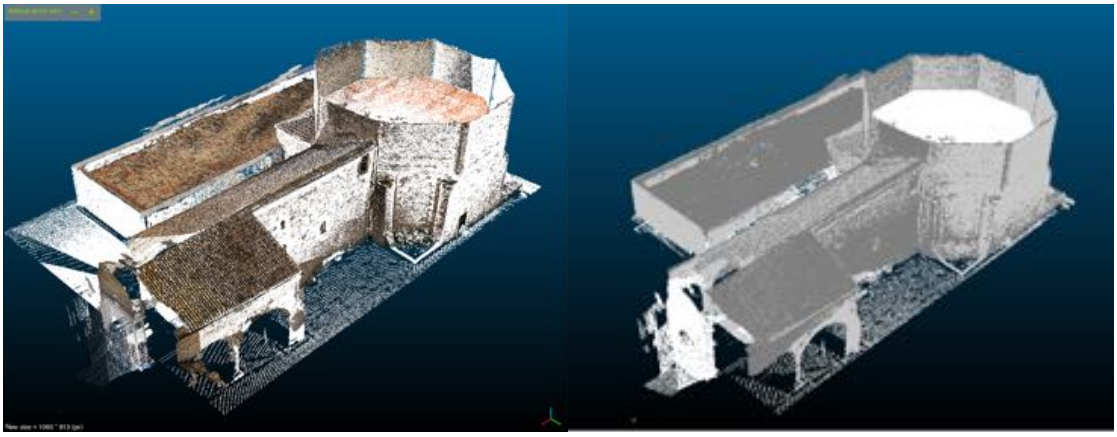

Figure 5.29 – The point cloud before and after the resampling.

The third phase is finally relating to the realization of the model: as introduced formerly, this operation have been carried out considering separately the exterior part, and the interior. The exterior TLS point cloud was therefore merged with the photogrammetric point cloud and, through the command Wrap in Geomagic, it was obtained a mesh of 3.865.602 triangles. For the interior point cloud was instead obtained a mesh of 9.836.892 triangles. The merging of the two meshes gave the result reported in *Figures 5.30* and *5.31*: in the first, the model is seen from the South and is set in transparent mode in correspondence with the Church of Pagans: it is so possible viewing the exterior surface and the interior ones, with the vaults of the hall. In the second, the model is seen from the North side and the transparent mode is set on the Baptistery. This is a first model, still in a raw form, and has to be processed in order to obtain a clean surface with no incongruences, holes or errors.

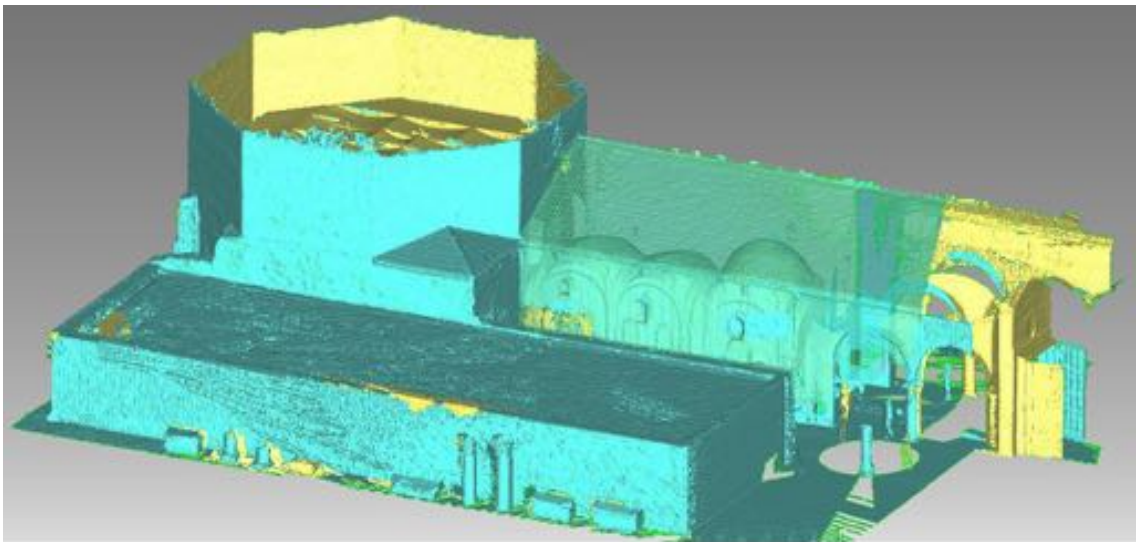

Figure 5.30 – The model seen from the South side.

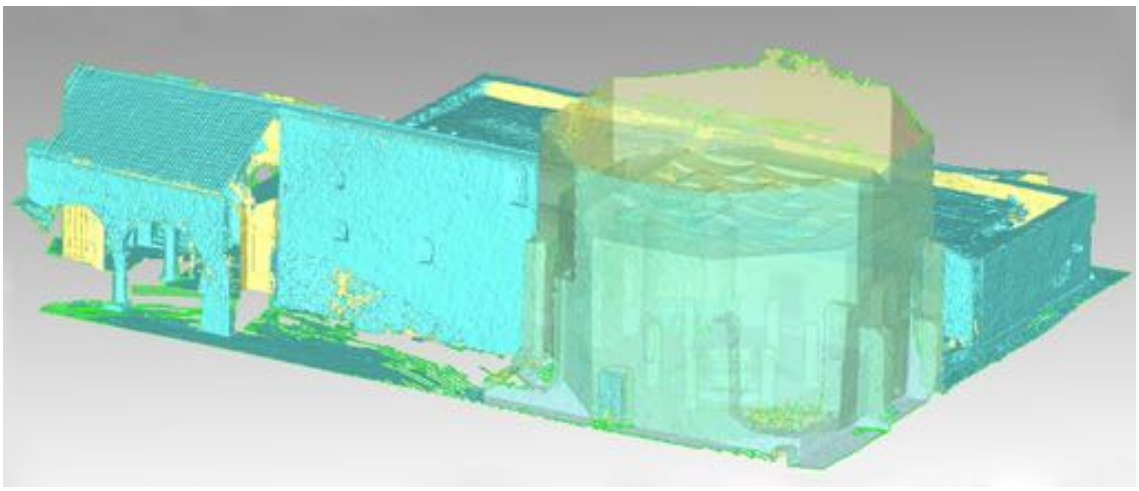

Figure 5.31 – The model seen from the North side.

The forth step refers to the processing of so obtained raw mesh through various automatic operation, as the elimination of non-manifolds surfaces, self-intersections, small tunnels, small holes and all those kind of incongruences, that can be adjusted with the "Mesh Doctor" command of Geomagic Wrap, as done also in sub paragraph 4.3.3.

Anyway, the model obtained was still not a closed surface and was still lacking of those data referred to the occluded surfaces: this problem had to be solved with a fifth step of manual operation which require time and practice of the operator. Since the deal was to obtain a 3D model only of the Baptistery, only this part was considered and processed manually. The operations related to this process are described in the following sub paragraph.

5.3.4. The Baptistery 3D Solid Model

In order to define the 3D Model of the Baptistery it was necessary, once separated the surface of the Baptistery, erasing the parts of the other buildings, to manually reconstruct those parts occluded to the scanning, but also to "close" those holes formed by the missing parts of the surface model that was eliminated. Furthermore, since the goal of the research, was the achievement of a 3D model useful for structural analysis, it resulted necessary to eliminate all those not structural parts, as the decorations, the modern glass and curtains covering, the baptismal font, the internal columns and all the furnishings (*Figure 5.32*): the target model to reach had in fact to represent only the masonry belonging to the Baptistery.

Figure 5.32 – The internal model of the Baptistery complete, before the elimination of the parts of model not related to the masonry structure.

This operation was done manually, in the internal surface through the commands of selection of Geomagic Wrap, and leaded to the transformation from model of *Figure 5.33 a)* to model of *Figure 5.33 b)*.

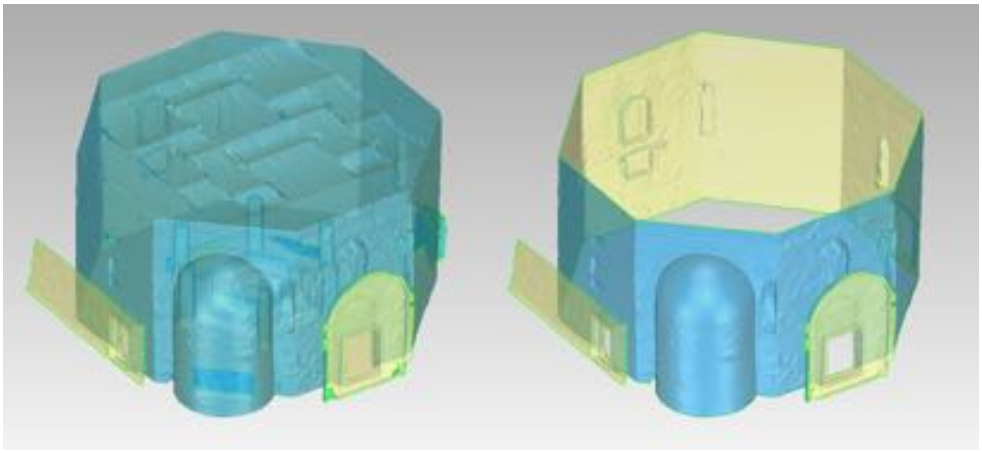

Figure 5.33 – a) The internal model complete – b) The interior model without not structural parts.

The following step was related to the reconstruction of the lacking parts and, in particular as regards to the interior model, of the surface of the wall over the curtains, as reported in *Figure 5.34*, considering as reference the height of the exterior model and extruding the upper border of the model.

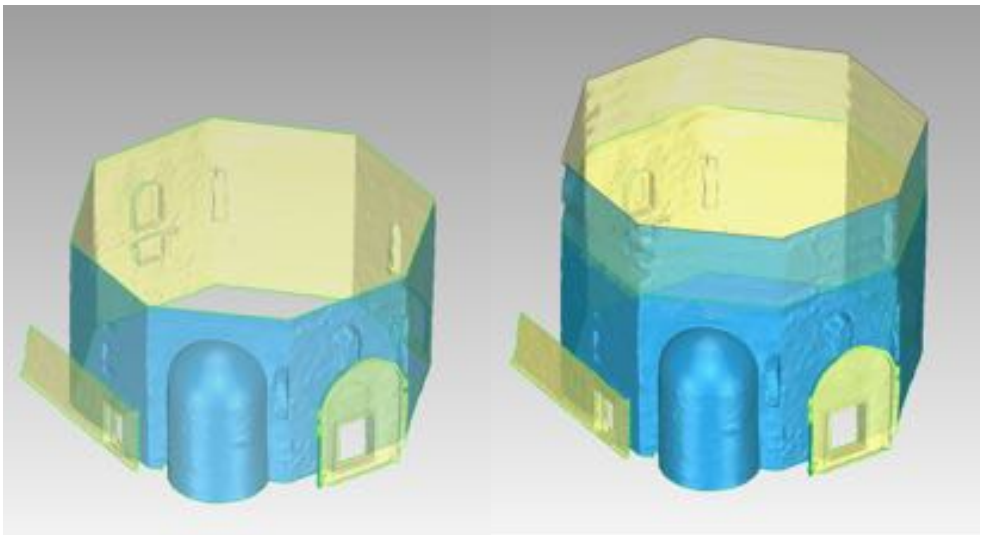

Figure 5.34 – Adding of the lacking surface of the interior wall.

Subsequently the two models, interior and exterior (*Figure 5.35 – a)*), were merged, obtaining an open surface (*Figure 5.35 – b)*). Further operations were carried out in order to close those holes existing between the two surfaces and achieving a 3D solid model composed by 779.006 triangles (*Figure 5.36*).

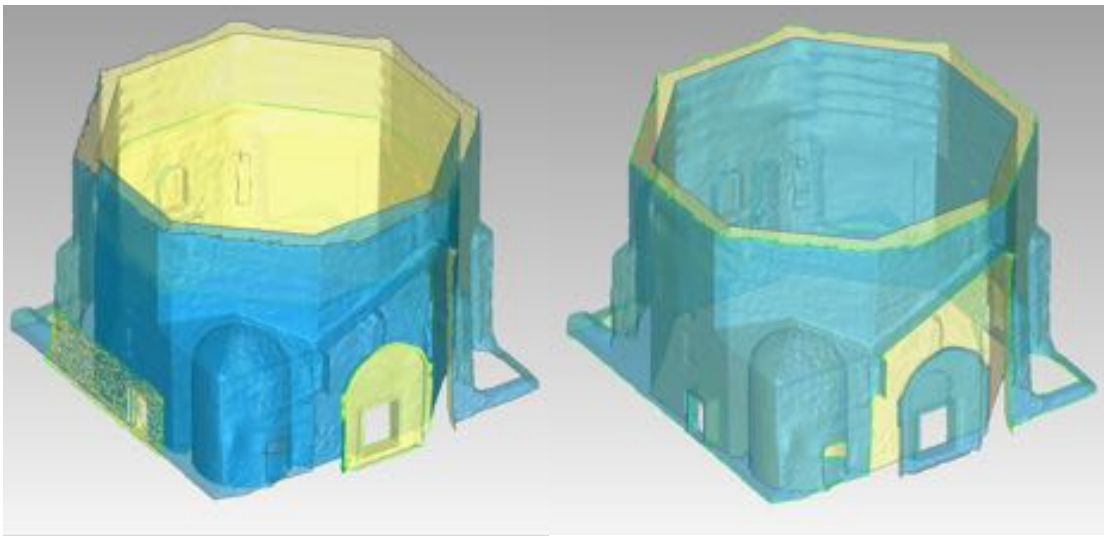

Figure 5.35 – a) Still separeted interior and exterior surfaces–b) Merged interior and exterior surfaces.

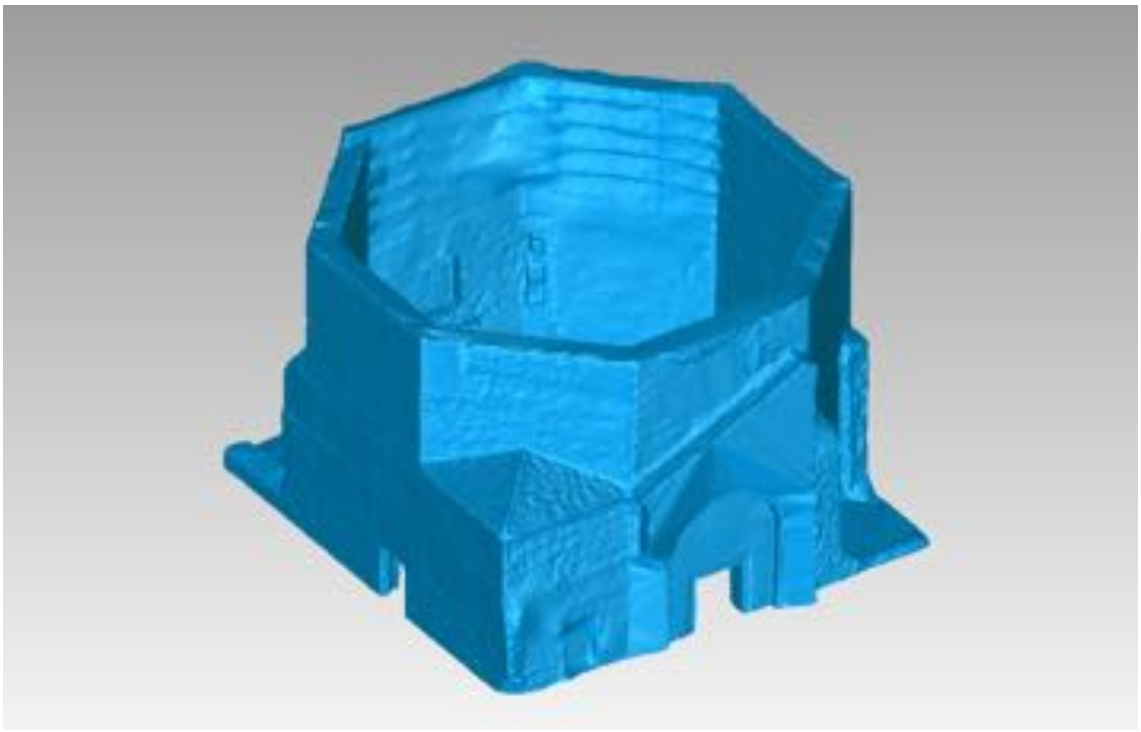

Figure 5.36 – The final 3D Solid Model obtained, composed by 779.006 triangles.

5.3.5. Realization of a simplified model and geometrical comparison

Also simple 3D model was realized, starting from the existing plans and sections of the Baptistery, of course these last coming out from previous direct surveying. This 3D model well represents the typical level of detail usually adopted for the models used in structural analysis (*Figure 5.37*) and was realized with SketchUp (Trimble Navigation, 1999), a well-known software for simplified 3D modelling, for a total of 672 triangular surfaces.

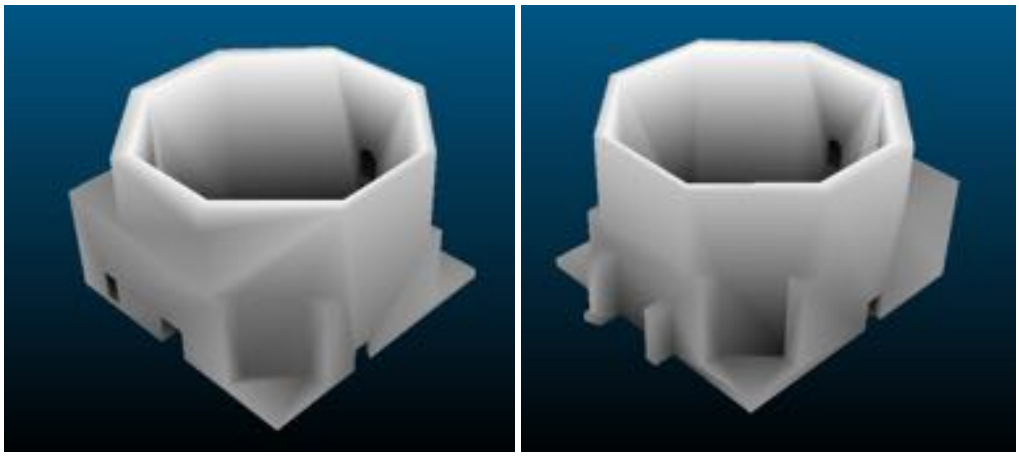

Figure 5.37 – The 3D Simple Model.

In order to highlight which are the differences between this 3D model and the one obtained from the TLS surveying, the two were compared with the apposite "Compare" function of CloudCompare.

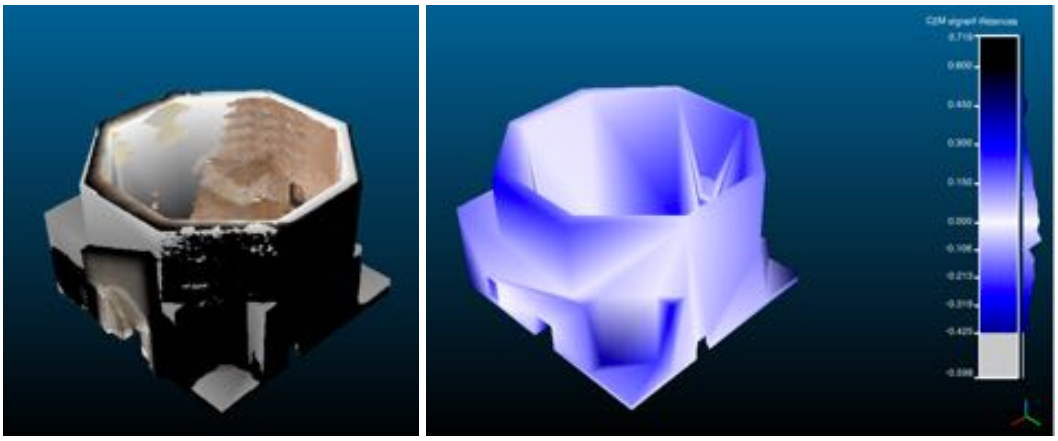

Figure 5.38 – The 3D Simple Model compared with TLS model, viewed from the North-East side.

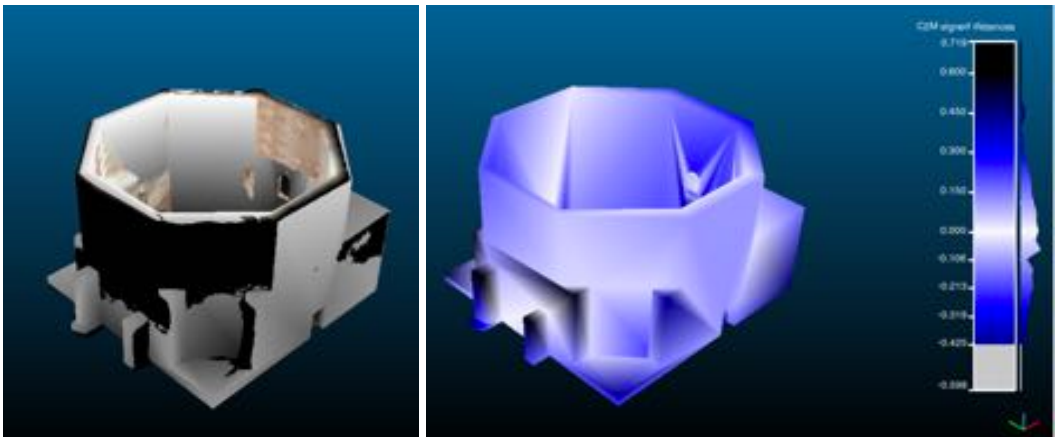

Figure 5.39 – The 3D Simple Model compared with TLS model, viewed from the South-west side.

From the analysis of the two models it resulted that the geometric differences are really relevant (*Figures 5.38* and *5.39* on the left) reaching, in some point, the value of 0,719 m, signed with the darker colour in the right side of *Figures 5.38* and *5.39*, and with an average difference of 0,149 m. Beside these macro-differences, the most significant variances are given by the fact that the simple 3D model does not take into account the slope and the irregularities of the surfaces, but is realized with a central symmetry and a perfectly regular shape.

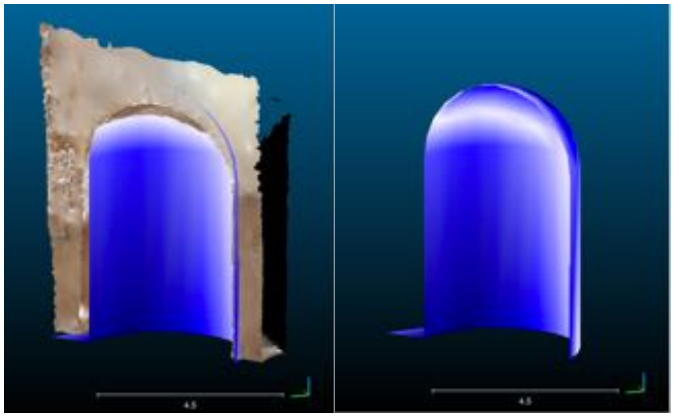

Figure 5.40 – Differences measured in the aps.

An evidence of this fact is particularly visible in the apse and in its vaults, where the difference between the two surfaces is quite constantly over 0,25 m (*Figure 5.40*). On the other hand, this result could be more than expectable, since it is quite hard to proceed with a surveying of such a surface with direct methods, and usually it is simplified with a circular shaped surface (*Figure 5.41*).

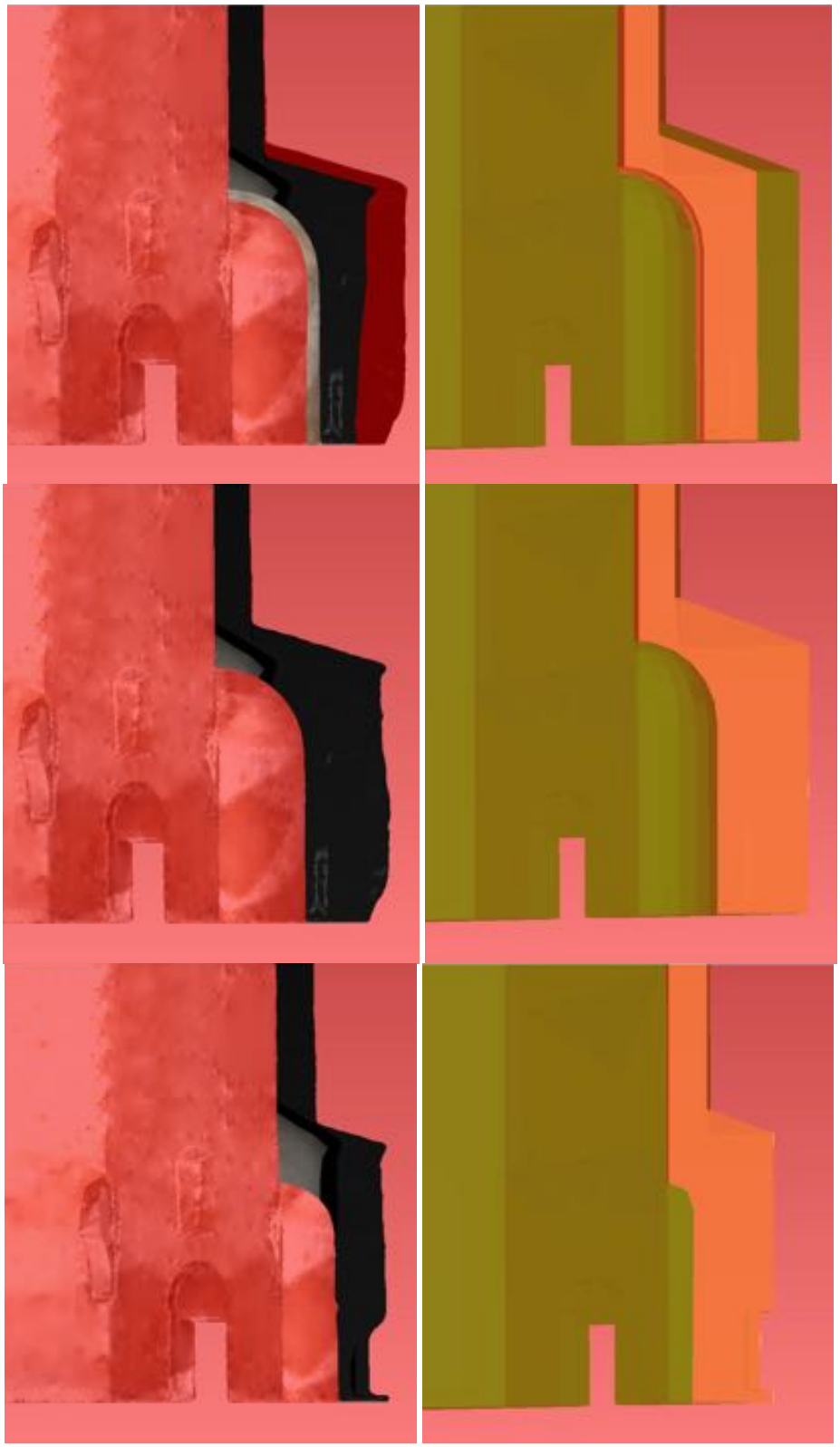

Figure 5.41 – Sections of the two models in corrispondence with the apse. On the left the TLS 3D model and on the right the simple model, where the aps is simplified with a circular shape.

The main differences between the two models are more evident as the height of the building grows, since the drawing of the plans, from which the simple 3D model was realized, derived by measures assessed at the base of the building. Therefore if the plans at the base look sufficiently similar (*Figure 5.42*), it is not the same for the section realized at the middle height of the building, corresponding to 5,5 m (*Figure 5.43*), where the thickness of walls varies, as well as the opening and of course the aps and its vault already examined.

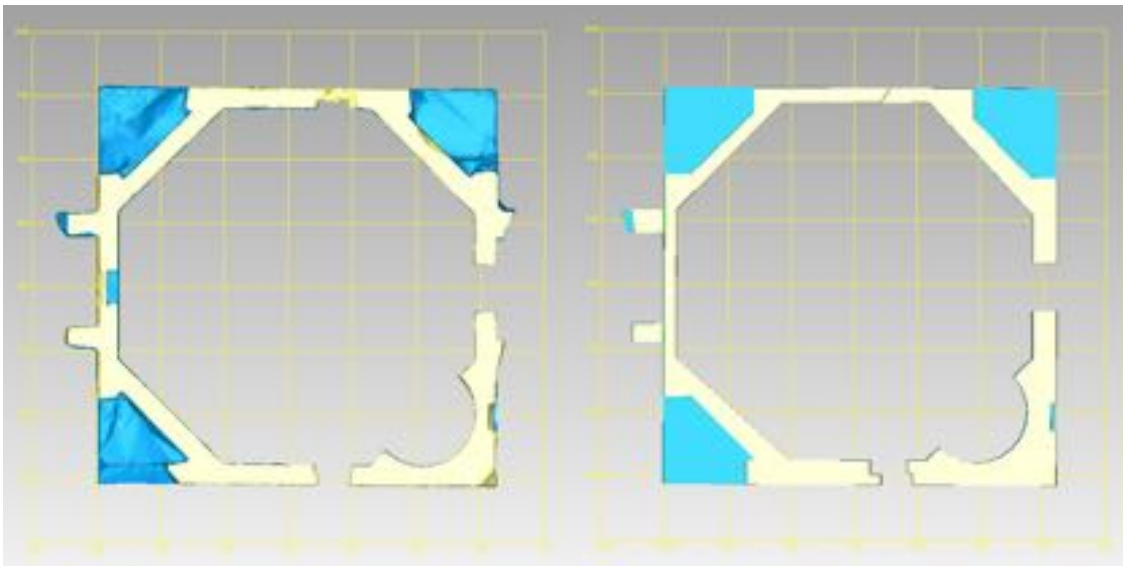

Figure 5.42 – Planar section of the building at the base.
On the left the 3D TLS, model on the right the 3D simple model.

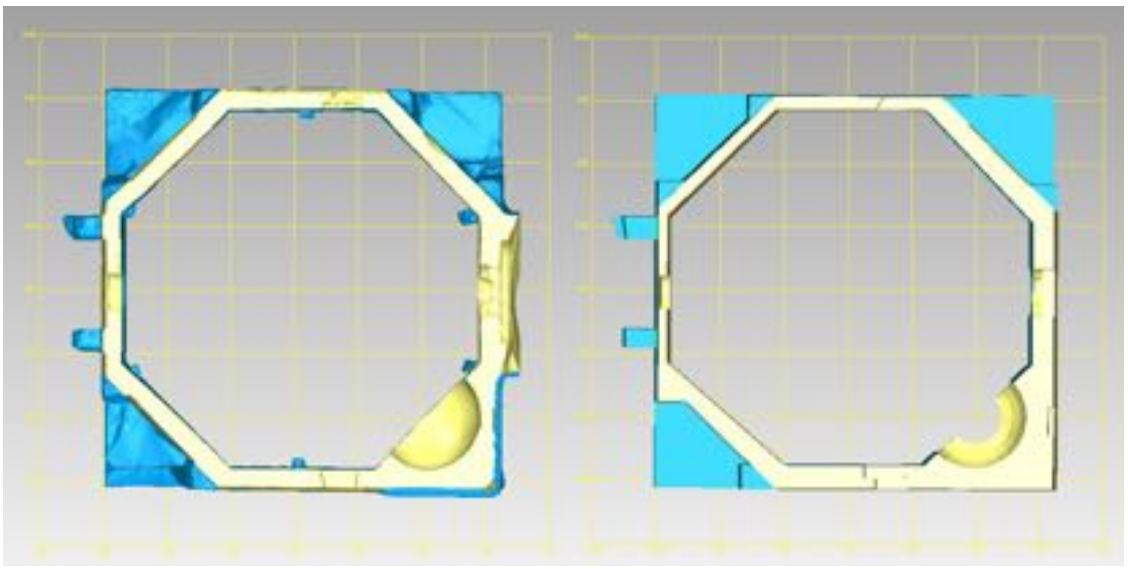

Figure 5.43 – Planar section of the building at 5,5 m height.
On the left the 3D TLS, model on the right the 3D simple model.

5.3.6. Mechanical and costitutive parameters

Whichever method it is going to be applied for structural analysis, there are three common structural aspects to be defined: the composing materials, the boundary conditions to apply and the forces acting on the object to analyse.

In the case of the Baptistery, currently, there are not any known and available core samplings data to identify correctly the interior part of the masonry. In order to define the mechanical characteristic to adopt, it was necessary to know which kind of masonry was used, starting with the available data, like the external materials and the framework of the masonry, and referring to table of listed typologies existing on literature. It easy to suppose, according to the known data, to the various and hypothetical periods of construction, to the similarity with other buildings, that the wall is a two-leaves filled masonry constituted mainly of disordered bricks and stones (*Figure 5.44*) (Roca & Lourenċo, 1998).

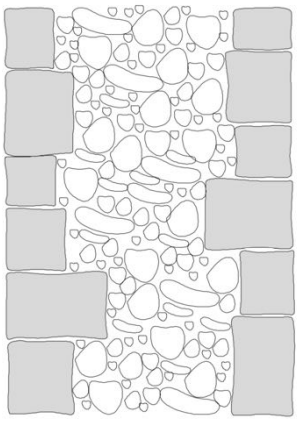

Figure 5.44 – Section of a two-leaves filled masonry.

This kind of masonry is definitely one of the less resistant and, therefore, its mechanical characteristic parameters can be assimilated to the "disordered stones masonry (pebbles, erratic and irregular stones)" of table C8A.2.1, and listed in *Table 5.45*, of the Circular 617 (Istruzioni per l'applicazione delle Norme tecniche per le costruzioni di cui al D.M. 14 gennaio 2008, 2009) described in sub paragraph 2.2.2.

Wall typology	f_m (N/cm^2)	τ_0 (N/cm^2)	E (N/mm^2)	G (N/mm^2)	w (KN/m^3)
Disordered stones masonry (pebbles, erratic and irregular stones)	100	2,0	690	1230	19
	180	3,2	1050	350	

Table 5.45 – Characteristic values for disordered stone masonry
Minumum value on the first line and maximum value on the second one.

It was decided to assume an average value for each parameter and, therefore converting the measure units to the ones applied in the used software, it was defined a new material called "two-leaves filled masonry". The chosen failure criterion was the one defined by Coulomb-Mohr, for the same reason reported in sub paragraph 3.3.4, and namely because it is the most appropriate to describe this kind of material behaviour (*Figure 5.46*).

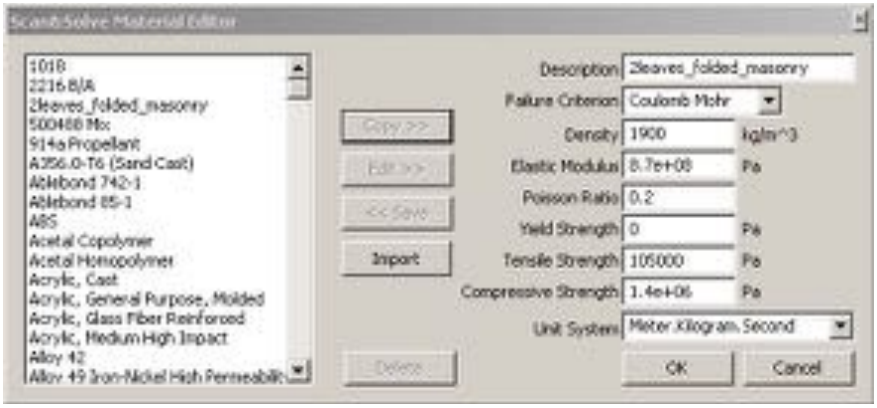

Figure 5.46 – Material editor in Scan&Solve – definition of the parameters for Baptistery.

Once defined the material, it necessary to define the boundary conditions (constraints) and the exterior forces applied.

As it regards to the first problem, the following conventions were assumed (*Figure 5.47*):

- the foundations condition is not well defined but, from the excavations made by Lopreato, it is known that the walls continue for little less than a meter under ground. Of course this is not even similar to the condition of an elastic continue foundation, but assuming that the structure will not move at its basis, it was decided to adopt a fixed end in correspondence of the footing,
- the connection with the "Church of Pagans" was simulated through the introduction of links, in order to simulate the function of direct connection between the two building,
- the connection with the "Mosaic Hall" was not considered since this building was later built and, even if physically connected to the Baptistery, has its own supports and does not contribute anyway with the structural behaviour of the Baptistery itself.

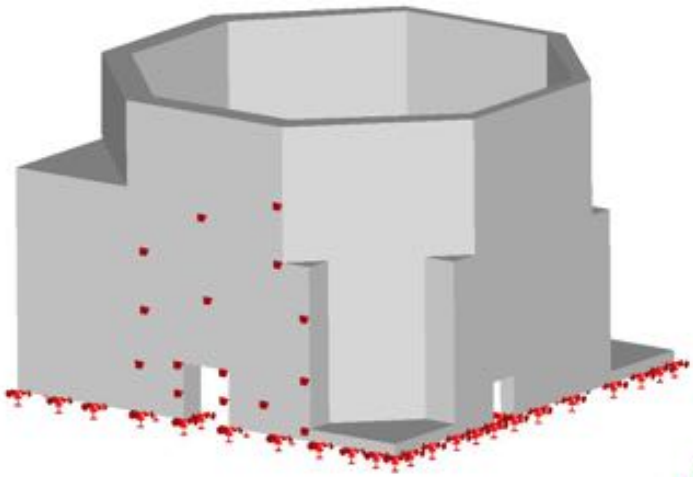

Figure 5.47 – Constraints adopted for the Baptistery.

Concerning to the forces acting on the building, as in the previous cases, the only load imposed for the analysis was the gravity one, since the thesis' purpose was only to verify if the obtained models work within this process, and which are the difference among the results

achieved on the different models considered and in relation, also, with a standard modelling for static FEM analysis.

5.3.7. Structural analysis of the simple 3D model

Therefore, once completed the phase of modelling, and once defined the mechanical and costitutive parameters, the subsequent step consisted in verifying if it was possible to follow the same process used for small and medium object, as previous described respectively in chapter 3 and 4, also for a large size objects, like the one here considered.

As a first and preliminary evaluation, just to test the results and to verify the method, it was decided to proceed with an analysis of the simple 3D model, described in sub paragraph 5.2.5, within Lisa FEA, the same software used for the analysis carried out on the Bollani Arch (sub paragraph 4.1.6).

The simplified solid was imported in the software and automatically *3D remeshed* with the highest structural LoD possible and with elements of approximately the same dimensions (*Figure 5.48*). It is important to notice that, in this case, the concept of Structural Engineering "remeshing" does not refers to a surface, like it is actually meant in Geomatics, but to a 3D solid element.

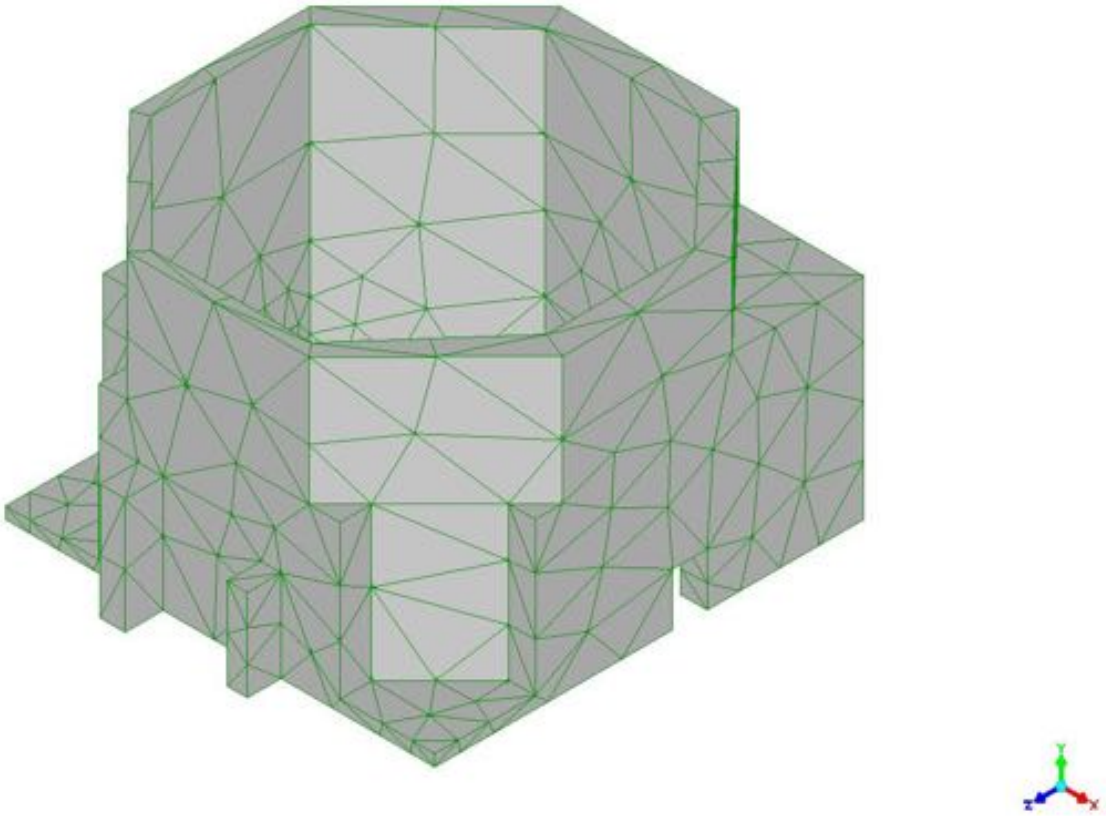

Figure 5.48 – The simple 3D model of the Baptistery imported in Lisa FEA and remeshed with solid elements.

Focusing on the results related to the total displacement, since, as already explained in sub paragraph 2.3.4, from these values it is possible to estimate all the other stresses and strains quantity, it was obtained that the maximum value is 1,22 mm and is located over the top of the vault of the apse. The total displacement is the absolute value of the linear combination of the displacement that the structure withstands in the three principal directions, namely the two horizontal displacements and the vertical one. This last quantity has the major influence on the resulting value of total displacement, and in detail the maximum vertical displacement, that take place again in correspondence of the vault of the aps, is a negative value of -1,25 mm. The negative value is representing a dropping of the structure. The trend of total displacements is shown in *Figure 5.49*. As logical, the movement of the basis of the building is null, since a fixed end have been placed there, an the displacements results anyway close to 0.

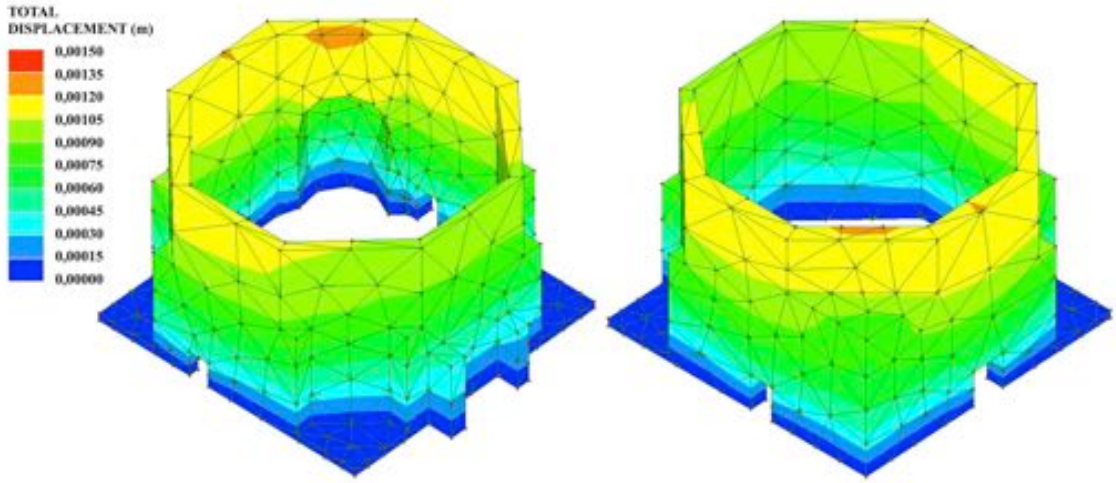

Figure 5.49 – Trend of the total displacement computed from the analysis held with Lisa FEA.

5.3.8. Structural analysis of the TLS 3D model

Following the same procedure so far adopted for all the cases of study, and widely explained in the previous chapters, also the obtained TLS 3D model of the Baptistery was analysed within the software Scan-and-Solve.

In order to perform the analysis with the cited plug-in, the model was imported in Rhinoceros, and the mesh was again verified through the existing commands of this environment, with the same procedure described in sub paragraph 3.3.4. Although the object is larger in dimensions, respect the cases of chapter 3 and 4, it resulted more simple and regular, and therefore with a limited number of incongruences. At the same time, and precisely because of its regularity, it was inappropriate to adopt the highest level of structural detail (*structural LoD*) (*Figure 5.50 – c)*), as defined in sub paragraph 4.3.8, since the architectonic details, that contributes to the structure, have always a larger dimension than the smallest cube. Changing Scan-and-Solve resolution the largest cube (*Figure 5.50 – a)*) has a dimension of 476 mm and, in the highest structural LoD, the dimension of the cube is equal to 108 mm: therefore it was decided to adopt a "Scan-and-Solve" resolution medium structural LoD where the dimension of

the cube is equal to 242 mm, which corresponds, more or less, to the dimension of a clay brick (*Figure 5.50 – b)*).

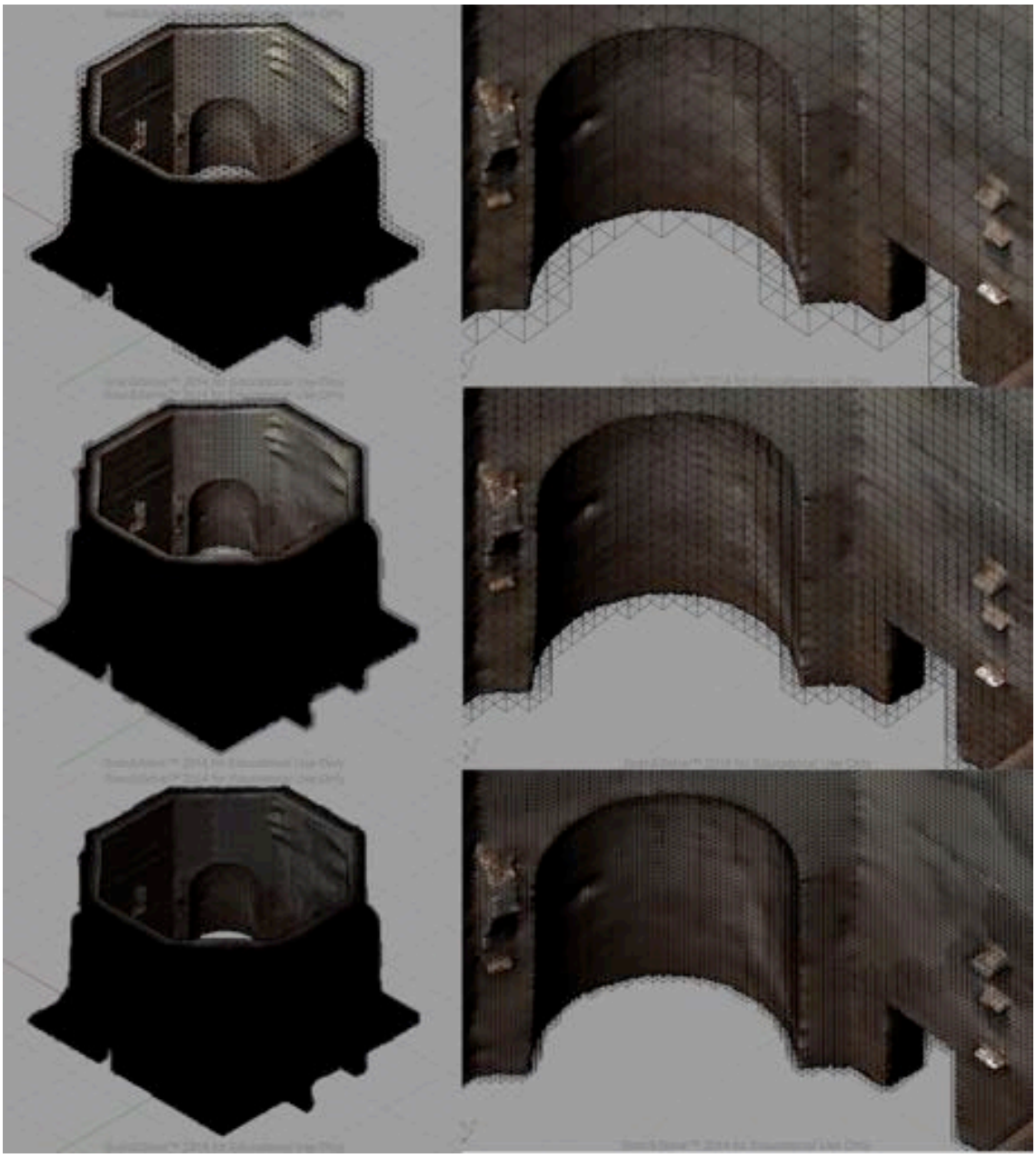

Figure 5.50 – a) The structure divided with the lowest structural LoD (10.000 cubes of 476 mm);
b) The structure divided with the chosen structural LoD (59.000 cubes of 242 mm);
c) The structure divided with the highest structural LoD (500.000 cubes of 108 mm).

Once set the structural LoD, the analysis was carried out with the same procedure already described in the previous chapters, obtaining the results reported in the following *Table 5.51*.

	Minimum	Maximum
X-Displacement	-0.000495638 m	0.000370143 m
Y-Displacement	-0.000593427 m	0.000459871 m
Z-Displacement	-0.00149708 m	7.13093e-06 m
Total Displacement	1.78886e-10 m	0.00156129 m
Von Mises Stress	61.4811 Pa	2.15092e+06 Pa
Max. Principal Stress	-296477 Pa	2.93585e+06 Pa
Mid. Principal Stress	-323059 Pa	788845 Pa
Min. Principal Stress	-1.28754e+06 Pa	781040 Pa
Danger Level (Rankine)	5.4159e-05	Criterion Limit Exceeded
Danger Level (Coulomb Mohr)	5.4159e-05	Criterion Limit Exceeded
Danger Level (Modified Mohr)	5.4159e-05	Criterion Limit Exceeded

Table 5.51 – Minimum and Maximum results obtained from the analysis.

As it is possible to observe, the Maximum value of *Danger Level* exceeds the limit value for all the three different resistance criteria: this "failure" value is reached in correspondence with the attachment of the roof of the Church of Pagans to the Baptistery, signed with the red colour in *Figure 5.52*. Since no cracking or yielding signs are present on the structure, it is reasonable to think that a drift of the values, only in that small area, is due to the existence of some sharpen edge or some kind of singularity, which results is a bad refinement of the calculation and consequently an uncorrected result. Therefore, except this single area of the structure, the all construction is verified and never exceed the failure values, as it is possible to see in *Figure 5.53*.

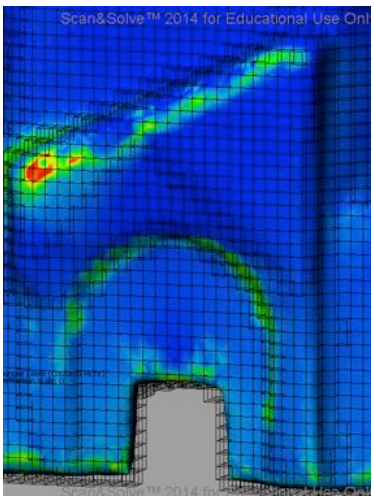

Table 5.52 – The attachment of the Church of Pagans to the Baptistery, values excedeeing the resistence criteria.

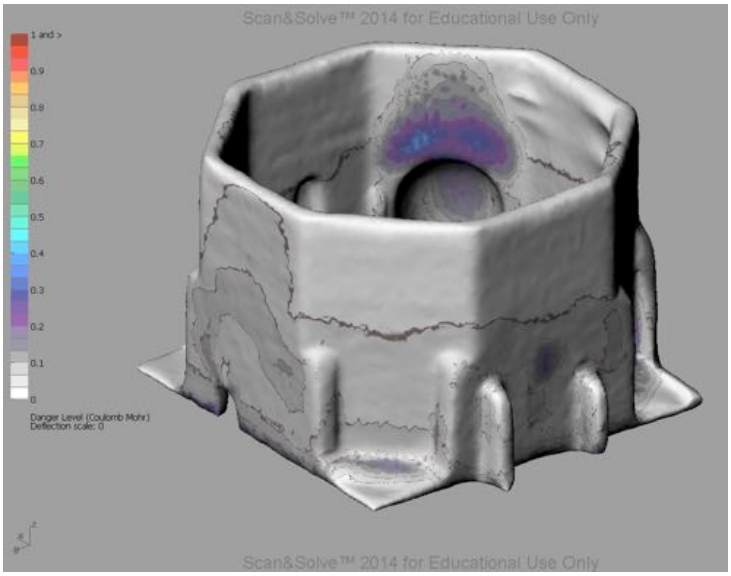

Table 5.53 – Verification of values with Coulomb-Mohr criterium.

From the previous figure, it is also possible to see that the most stressed part of the Baptistery is the wall over the vault of aps, congruently on what have been computed by LisaFEA and reported in sub paragraph 5.3.7. Focusing on the total displacement, it results, similarly to the previous case, that the maximum value, corresponding to 1,56 mm, is located exactly on the top of the vault of the aps. Also in this case, the major contribute of the displacement is given by the lowering long Z-axis. In this case, the maximum value is higher than the previous case of about the 28%, and also the trend of the values converges more quickly to the maximum value of the displacement, as it is possible to see in *Figure 5.54*. This is caused by the fact that the TLS 3D model, being more realistic, became more slender towards the upper part of the structure, while the simple 3D Model, conserving the same section all over its height, results more stubby and not deformable.

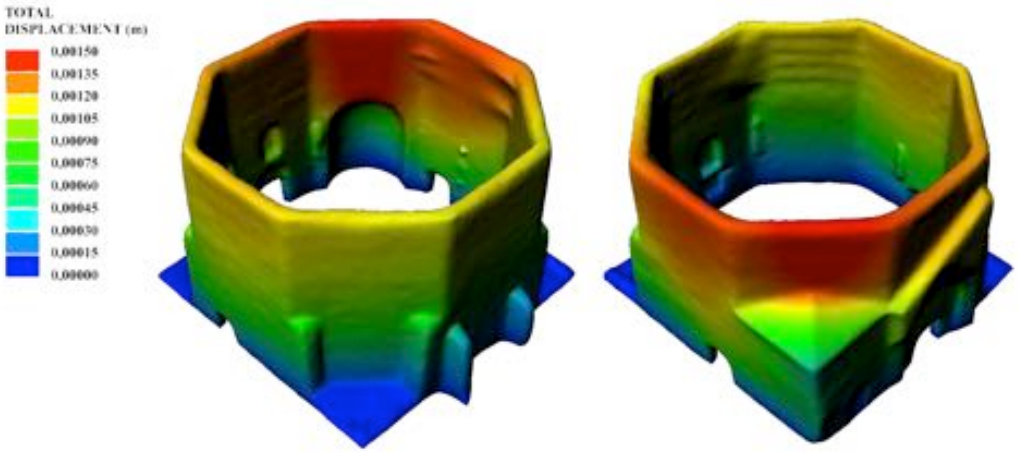

Figure 5.54 – Trend of the total displacement computed from the analysis held with Scan-and-Solve.

From the values of the displacement, through the equations introduced in sub paragraph 2.3.4, it is therefore possible to compute the remaining values of the structural characteristics.

5.4. Conclusions

In this chapter, the case of large size objects was studied, starting from a review of the current trends of the geomatic modelling techniques and finishing with a real case represented by the Baptistery of Aquileia. This building was surveyed and then, from the point cloud obtained, by following the pipeline of *Scheme 1.8*, it was obtained a 3D surface model. In order to proceed with the structural analysis, this mesh was further treated with the final purpose to obtain a 3D solid model, since this kind of feature is commonly importable in the most of the FEA software.

At the same time, in order to verify the results, a 3D simple solid model was created and verified as well. From the comparison between the geometry and the obtained results of the analysis, of the two models, it is clear that the TLS model highlight all the peculiarities of the real object, especially as refers to the thickness of the wall, to their slope and to the curvature of the vaults and that to these differences match other results for the structural analysis.

5.5. Bibliography

Brandt, O. (2009). Il battistero cromaziano. *Atti della XL Settimana di Studi Aquileiesi* (p. 323-375). Editreg.

Castagnetti, C., Bertacchini, E., Capra, A., & Dubbini, M. (2012). Terrestrial laser scanning for preserving cultural heritage: analysis of geometric anomalies for ancient structures. *Proceedings of the FIG Working Week.*

Castellazzi, G., D'Altri, A. M., Bitelli, G., Selvaggi, I., & Lambertini, A. (2015). Castellazzi, G., D'Altri, A. M., Bitelli, G., Selvaggi, I., & Lambertini, A. (2015). From laser scanning to finite element analysis of complex buildings by using a semi-automatic procedure. Sensors, 20, 2. *Sensors* (20), p. 2-20.

Guarnieri, A., Pirotti, F., Pontin, M., & Vettore, A. (2006). 3D Surveying for structural analysis applictions. *3rd IAG/ 12th FIG Symposium.* Baden.

Guerra, F., Balletti, C., Stevanin, C., & Vernier, P. (s.d.). "3D geometric analysis of the façades of gothic buildings in venice: examples of 3D modelling".

Istruzioni per l'applicazione delle Norme tecniche per le costruzioni di cui al D.M. 14 gennaio 2008 , Circolare n. 617 (Consiglio Superiore dei Lavori Pubblici febbraio 2, 2009).

Pieraccini, M., Dei, D., Betti, M., Bartoli, G., Tucci, G., & Guardini, N. (2014). Dynamic identification of historic masonry towers through an expeditious and no-contact approach: Application to the "Torre del Mangia" in Siena (Italy) . *Journal of Cultural Heritage* (15.3), p. 275-284.

Roca, P., & Lourenċo, P. B. (1998). *Experimental and numerical issues in the modelling of the mechanical behaviour of masonry.* Barcelona: CIMNE.

San José, J. I., Fernàndez MartIn, J. J., Pérez Moneo, J. D., Finat, J., & Martinez Rubio, J. (2007). Evaluation of structural damages from 3D Laser Scans. *XXI CIPA International Symposium: Anticipating the Future of the Cultural.* Athens.

Sternberg, H. (2006). Deformation measurements at historical buildings with the help of three-dimensional recording methods and two-dimensional surface evaluations. *3rd IAG/12th FIG Symposium.* Baden.

Tavano, S. (1972). Aquileia cristiana . *Antichità Altoadriatiche* (3).

Trimble Navigation. (1999). (©. 2. Limited, Produttore) Tratto il giorno 2015 da SketchUp: http://www.sketchup.com/it

6. EVALUATION OF THE DIFFERENT SIZE OBJECTS EXPERIMENTS

6.1. Introduction

The purpose of this research was to investigate what could be the actual contribution of geometric models obtained by Geomatics to structural analysis of cultural heritage. As already mentioned in the previous chapters of this thesis, geometry of objects belonging to the past are seldom regular, and software used for structural analysis have often a simplified modeller, therefore it results difficult, or even impossible, to reproduce correctly shape, dimensions, curvature, slope, or other geometric characteristics of these objects. Otherwise, at the same time, geometry assumes a decisive importance for the definition of the confidence factors and the level of knowledge, structural parameters specified in the regulations explained in the second chapter of this thesis.

As seen in the first chapter, beyond being in general worth willing for community, also various international charts and national standards recommend recording and documenting cultural heritage. Since geometry belongs to those data considered necessary to describe an object, often, complete surveying are available and, always more frequently, due to the high capability of the available geomatic techniques, the results of these geometrical surveying are fully detailed 3D models.

In this study, it was analysed how these accurate models can be used for structural purposes, analysing three different classes of objects, differentiating them by size, since for each one, different peculiarities have to be handed. The objects chosen for the analysis are together reported in *Table 6.1*, presented in a different order in the thesis, but here listed by dimension.

Typology	Object	Chapter
Small-size object	Statue of St. John Baptist	3
	Statue of Emperor Claudio	3
Medium-size object	Bollani Arch	4
Large-size object	Baptistery of Aquileia	5

Table 6.1 – Objects analysed in this thesis.

In this last chapter, all the results and the analysis obtained, from the study of these objects, have been collected and compared. Following the same pipeline of *Scheme 1.8*, all the phases are recalled and the most important values are listed, in order to have a clear framework of the research's results. The chapter is therefore organized by comparing:

- objects geometry and surveying (6.2);
- data registration, cleaning and resampling (6.3);
- meshing, mesh refinement and final 3D solid models (6.4);
- other models realized (6.5);
- structural analysis and obtained results (6.6).

6.2. Objects geometry and surveying

The main and most evident difference among the four objects is, of course, the size. Considering the minimum-bounding box, which is the virtual box with the smallest dimension within all points lie, principal values of width (W), depth (D), height (H) and resulting volume (V), are reported in *Table 6.2*. A quick visual comparison of the object can be seen in *Figure 6.3*, where they are figured in the same environment as already modelled.

Object	W (m)	D (m)	H (m)	V (m^3)
Statue of St. John Baptist	0,52	0,52	1,63	0,440
Statue of Emperor Claudio	0,77	0,55	2,10	0,889
Bollani Arch	7,74	2,76	8,24	176,026
Baptistery of Aquileia	17,91	16,05	10,92	3.139,014

Table 6.2 - Geometric characteristic: principal dimensions.

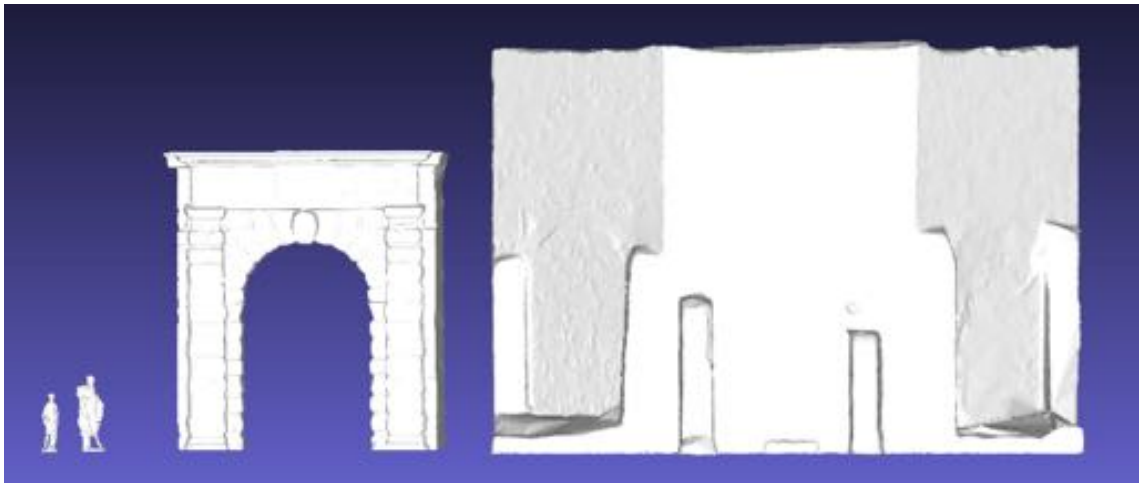

Figure 6.3 – The analysed objects compared in dimensions.

Of course, taking into account the bounding box, measures are referred to the largest parts of the object and specific sections must be considered to understand significant dimensions. Referring to the statues, which are the most complex elements, the fundamental dimension is of course height. Width and depth are determinate by protrusions or basement and, therefore, they result much wider than the real objects. In the case of the arch and of the building, the bounding box consider also the emptiness given by openings or open spaces. As it will be possible to see in paragraph 6.4, the real volumes of the objects are much more contained. In the further *Figure 6.4*, all the objects are represented in their quoted bounding box.

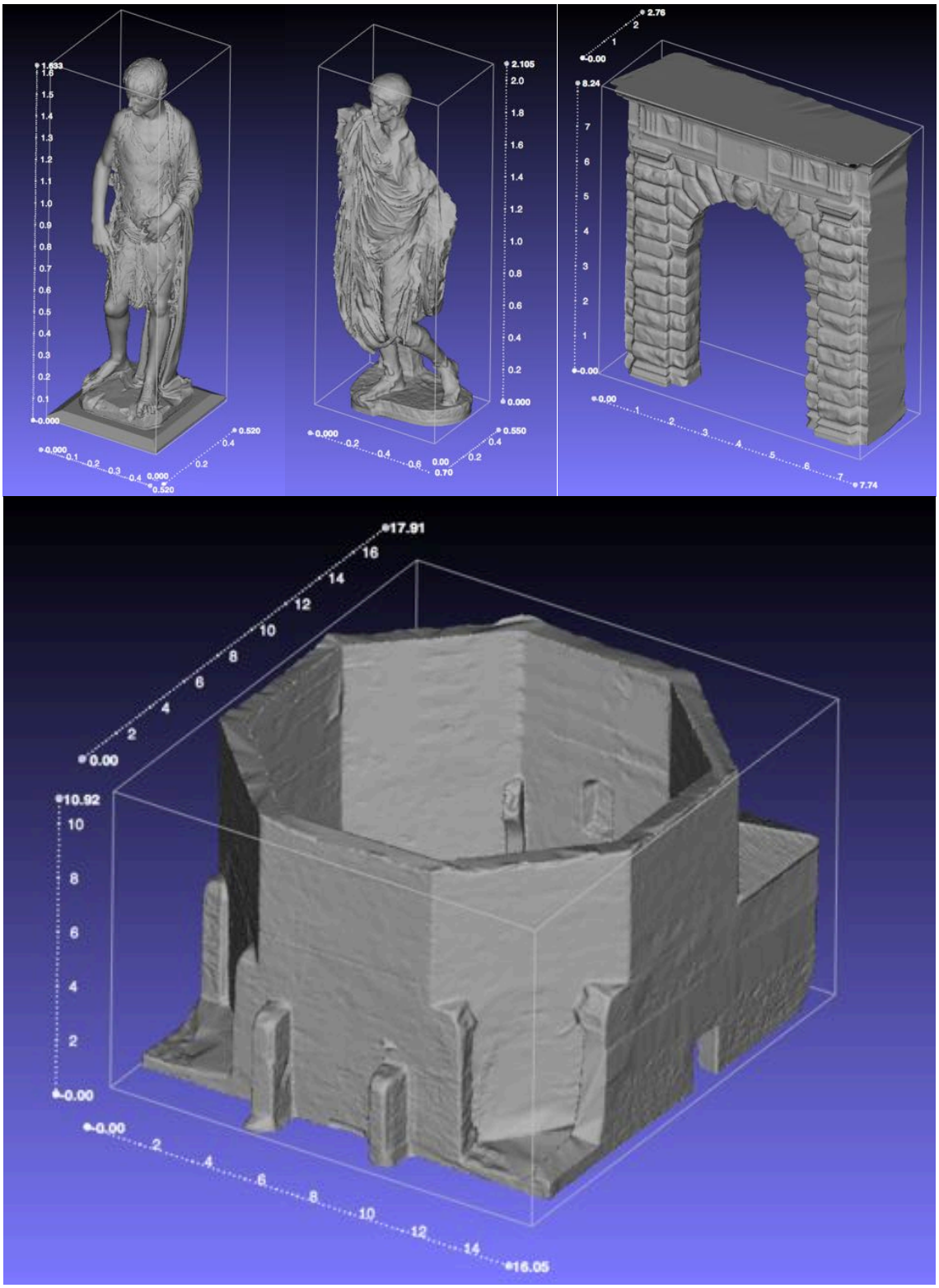

Figure 6.4 – The four objects represented in their quoted bounding box. From the top left, the Statue of St. John Baptist, the Statue of Emperor Claudio, the Bollani Arch and, on the bottom, the Baptistery.

Once summarized the dimensions of the objects, the different output data of the phases of *Scheme 1.8* of this thesis, can be analysed.

Phase 1 of acquisition of point clouds was held, for all the cases, with TLS surveying, except for the roof of the Baptistery, which was achieved by a photogrammetric surveying, for the reasons specified in 5.3.2. In *Table 6.5* are reported the instruments used for each surveying, the number of scans realized, the number of points acquired and the step angle used for the scans. For the photogrammetric surveys are reported instead the number of "stations" and the total number of acquired images.

Object		Instrument used	Scans (no.)	Points acquired (No.)	Step Angle (°)
Statue of St. John Baptist		ModelMaker MMDx/MMC Handheld	1	-	-
Statue of Emperor Claudio		TLS Faro Focus 3D S120	9	9.997.224	0,044
Bollani Arch		TLS Riegl Z390i	3	3.395.200	0,120
Baptistery of Aquileia	Ext.	TLS Riegl Z390i	9	3.219.815	0,120
	Int.	TLS Riegl Z400	16	23.751.491	0,080
	Ext.	CCD Canon EOS6D	(4) (77)	7.937.044	-
		Total		34.908.350	

Table 6.5 – Characteristic of four cases surveying.

Surveying was held obviously with different procedures, according to dimension and complexity of the objects. Among the considered cases, the one of the Statue of St. John Baptist, cannot be compared to the other, because of the different scanning system, which through one scan, with a handled device, allows to obtain directly the whole mesh surface.

Considering the three other objects, it is rather evident, only from a first glance to them, and referring only to shapes, that the statue is the most complex to survey. The statue of Emperor Claudio needed, in fact, the same number of scans of the exterior part of the Baptistery, even if the volume of the bounding box is about 1/3530. This is due to the presence of many occluded parts and geometry concavities, impossible to survey with only a frontal and a backside scans. On the other hand, the Baptistery has a very regular shape, therefore nine scans could be considered more than enough, considering one for each side of the octagonal shape, with also a minimum overlapping. In fact each scan was realized placing the instrument in front of each façade, except for those one covered by the Church of Pagans. Considering a

building, the distinction between "external" and "internal" surfaces arises, with geometrical and topological aspects to face. To this regard, the interior part of the Baptistery was more elaborate and challenging to survey because of the presence of decorations, of the hexagonal baptismal font, of the six columns and the recesses, therefore 16 scans were necessary, in order to cover the entire interior surface. Nevertheless, as already specified, it was indispensable to integrate the exterior TLS surveying with a photogrammetric one, in order to acquire also the points of the roof. The case of Bollani Arch resulted the simplest to survey, since only 3 scans were in fact sufficient to acquire all the surface of the object with a good LoD. It is interesting to focus also on the number of points acquired: for the same "medium LoD" of the statue were necessary a third of the points sufficient for describing an entire building and three times the number of points necessary for describing the arch.

6.3. Data registration, cleaning and resampling

The first block of *phase 2* of Scheme 1.8 refers to *Data Registration*. In order to achieve this result it was necessary, for each object, except for St. John Baptist with the already explained reasons, to place a certain number of targets all over the surfaces to acquire. As for the previous paragraph, the object with an inferior number of targets is the arch. For the case of the Statue, because of the many scans acquired, and therefore because of the extremely high overlapping, it was not necessary to place a lot of targets. The building case instead needed a lot of targets, for a total amount of 70 on the exterior part and 17 in the interior, and also 55 natural points. For the global registration of all the exterior and interior scans it was necessary to achieve a topographic network of ten vertexes, surveying with a EDM total station all the vertices and all the placed targets and natural points, evident protrusions identified on corners or edges.

As it refers to registration of scans, beside the St. John Baptist, and beside the Baptistery, which was registered thanks to topography, the other two models were, at first, registered with the software in use with the instrument, respectively Scene for Faro and RiSCAN for Riegl, and then the registration was refined through the ICP method. As it is possible to see in the *Table 6.6*, the final registration residual grows with the dimension of the object: as logical, an error of 3 mm dimension is influencing on a small size object, but is totally not perceptible on a large size object like a whole building.

Table 6.6 summarizes data on number and typologies of targets used, on the necessity to integrate the laser scanning surveying with a topographical one or with the use of natural points, and main results of registration of data.

Object	Topographic surveying		No. and typology target used	Natural points or features	Registration Residual (mm)	Final registration Residual (mm)
Statue of St. John Baptist	-		-	-	-	-
Statue of Emperor Claudio	-		6 spherical targets (Ø 14,5 cm) 18 checkerboards (10 x 10)	yes	3,2	1,8
Bollani Arch	-		14 cylindrical targets Ø 10 cm	yes	8,0	3,3
Baptistery of Aquileia	X	Ext.	17 targets 2 cm x 2 cm	yes	-	15,4
		Int.	15 cylindrical targets Ø 10 cm 55 disk Ø 5 cm	yes		
		Ext.	-	yes		

Table 6.6 – Registration of data reporting targets used and residuals.

Second block of *phase 2* of Scheme 1.8 refers to *Data Cleaning*. As already specified, this operation is necessary in order to eliminate those incorrect points due to noise of data and to the outlier points. In *Table 6.7* data after cleaning operations are reported.

Object		Points acquired (No.)	Points after Automatic Cleaning (No.)	Points after Manual Cleaning (No.)
Statue of St. John Baptist		-	-	-
Statue of Emperor Claudio		9.997.224	6.668.901	6.668.901
Bollani Arch		1.801.450	1.055.886	811.333
Baptistery of Aquileia	Ext.	3.219.815	2.000.832	1.684.137
	Int.	23.751.491	13.658.958	13.627.377
	Ext.	7.937.044	4.809.333	4.459.029
	Total	34.908.350	20.469.123	19.770.543

Table 6.7 – Data cleaning: number of points in the clouds before and after the operation of cleaning (automatically and manually).

Third and last block of *phase 2* of Scheme 1.8 refers to *Data Resampling* (*Table6.8*). This operation is necessary in order to arrange points on a grid, so homogenizing the various point clouds and also to have lighter clouds suitable for modeling. The statue of Emperor Claudio, since each scan was realized from very variable distance (from a minimum of 1 m to a maximum of 2 m), presented quite different resolutions (distance estimated between points 0,7 to 1,4 mm) and therefore resampling was necessary. For the same reason, it was performed also on the Bollani Arch. As it regards the Baptistery, beside the problem of different distance of scan stations, there was also a huge disparity between interior and exterior clouds, due to the different scanning settings and performance of the Riegl scanners Z390i and Z400.

Object		Points after Manual Cleaning (No.)	Points after Resampling (No.)
Statue of St. John Baptist		-	-
Statue of Emperor Claudio		6.668.901	4.848.532
Bollani Arch		811.333	811.333
Baptistery of Aquileia	Ext.	1.684.137	998.207
	Int.	13.627.377	3.237.531
	Ext.	4.459.029	1.547.648
	Total	19.770.543	5.783.386

Table 6.8 – Data Resampling: on the first column the original point clouds and on the last the data after resampling.

6.4. Meshing, mesh refinement and final 3D solid models

Phase 3 of the Scheme 1.8 refers to *meshing*: with this operation, carried out with different algorithms, surface models were obtained from point clouds, as it refers to Statue of St. John surface is the direct result of surveying, since the meshing is computed automatically by the software. As it is possible to see in *Table 6.9*, where are reported the number of triangles composing each mesh and the average surface of each triangle, this area grows with the size of the objects, while the number of triangles necessary for describing the objects decrease. This fact depends on the geometric LoD necessary for the different typologies. In the case of small size objects the surface of triangles is approximately millimetric: the Statue of St. John Baptist has an extraordinary high LoD, surely excessive for a structural analysis, while the Statue of Emperor Claudio has a low LoD, which is good enough for structural analysis, but not sufficient for 3D reprinting or advanced virtual reality. In the case of medium size objects, a centimetric surface of triangles is sufficient for a good LoD of the object and even excessive for a structural analysis. Finally, as it refers to large size objects, the dimension of triangles is decimetric: as in the previous case, this dimension offers a good LoD

Object		No. triangles	Average surface of triangles (mm^2)
Statue of St. John Baptist		5.178.132	0,40
Statue of Emperor Claudio		1.595.466	3,72
Bollani Arch		1.197.598	258
Baptistery of Aquileia	Int.	592.936	1.489
	Ext.	497.812	1.233
	Total	1.090.748	-

Table 6.9 – Feature of the surface models obtained.

In order to obtain 3D solid models different operation of mesh refinement were held on the different models, as expected by *phase 4* of Scheme 1.8. These operations included elimination of isolated vertexes, dangling edges, singular edges and vertexes, non-manifolds edges and triangles as well as the correction of orientation inconsistences, surface gaps and holes, self-intersections. Beside these operations, it was necessary to reconstruct the lacking parts in the boundary with connected structures, for the arch and the Baptistery, and merge the interior and exterior surfaces. The resulting 3D solid models have the characteristic reported in *Table 6.10*. Of course, referring to the statue of St. John Baptist the data are the same.

Object	No. triangles Surface model	No. triangles 3D solid model
Statue of St. John Baptist	5.178.132	5.178.132
Statue of Emperor Claudio	1.595.466	1.571.286
Bollani Arch	1.197.598	998.000
Baptistery of Aquileia	1.090.748	779.006

Table 6.10 – Feature of 3D solid models obtained.

Further interesting information are the ones related to surfaces and volumes of the objects, reported in *Table 6.11*:

Object	S (m^2)	V (m^3)
Statue of St. John Baptist	2,39	0,07
Statue of Emperor Claudio	4,36	0,23
Bollani Arch	309,53	131,79
Baptistery of Aquileia	1303,51	522,90

Table 6.11 - Geometric characteristic: surfaces and volumes.

The models so defined are directly structurally analysable, since they are 3D solid models with no incongruences and directly importable in Finite Element Analysis software. Otherwise, the geometrical LoD of these models resulted even excessive and therefore it was necessary to provide with a simplification of the mesh, except for the Statue of Emperor Claudio, where the starting LoD was already low.

6.5. Other models realized

Other models of the testing objects were realized, through the research, operating in three different ways, with various purposes:

1) building of hypothetical models, derived from the original one, and specifically the Statue of Emperor Claudio, but with a different conformation, in order to verify the possible contribute of certain parts of the artefacts or the behaviour of the statue with all the parts currently lacking;
2) realization of models with simplified methods, starting from measure derived by a direct surveying:. these models could be assimilated to the ones realized directly within the FEA software;
3) realization of models with a lower LoD, starting from the 3D solid models, in order to find the correct equilibrium among the opposite necessities to represent correctly the objects and the need of simplified models for computational analysis in FEA software.

Referring to first case, the argument was dealt in chapter 3 and refers only to the statue of Emperor Claudio. Beside the original model, two other models were realized: the first one without the back support and the second as a restoration of the statue, properly supposing its original shape (*Figure 6.12*).

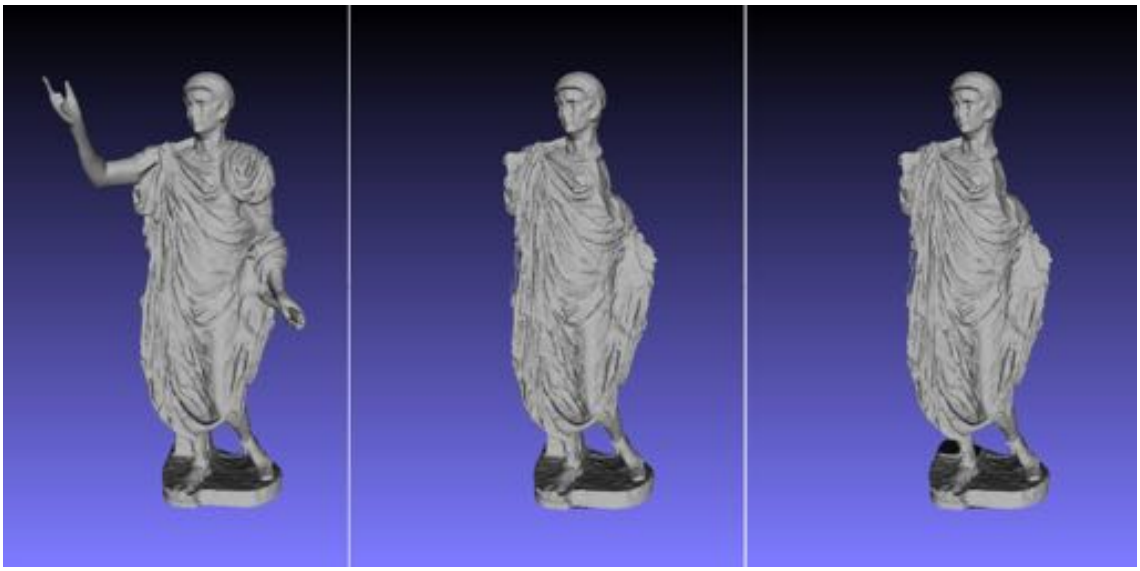

Figure 6.12 – The statue of Emperor Claudio. From the left the statue as it was supposed to be, the original model, the model without the back support.

Main data on these three models are reported in *Table 6.13*. Referring to the virtually restored model it is important to notice that, deriving it from the merging of two models, it needed further simplifications and therefore is made of a minor number of triangles.

Object	No. triangles	S (m^2)	V (m^3)
Statue of Emperor Claudio Restored model	649.826	4,68	0,252
Statue of Emperor Claudio Original model	1.571.286	4,36	0,231
Statue of Emperor Claudio No back support model	1.258.513	4,12	0,222

Table 6.13 - Geometric characteristic: surfaces and volumes.

Second purpose of realization of simplified models relates to the medium and large size objects. The first simplified model was realized within LisaFEA, starting from the measures derived from direct surveying (Figure 6.14), the second with SketchUp (*Figure 6.15*) starting from the measure of a previous plan, integrated with some measure of direct surveying (*Figure 6.16*).

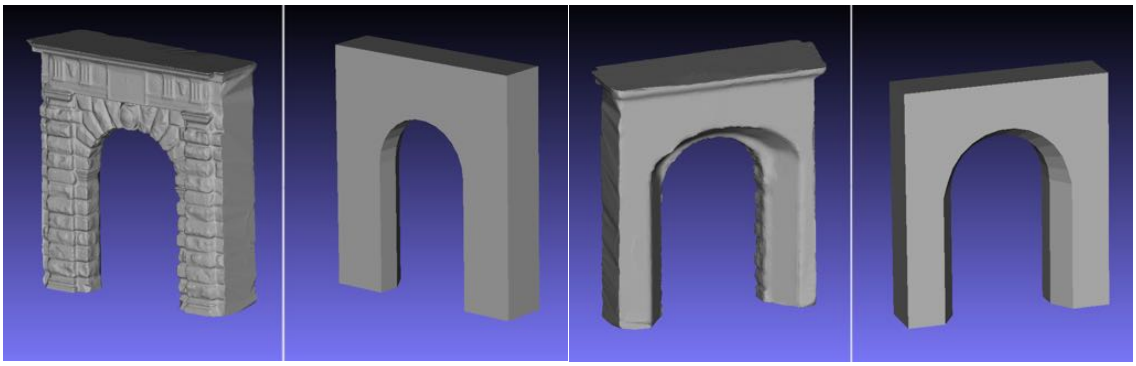

Table 6.14 – Front and back side of the Arch in its original model and in the simplified one.

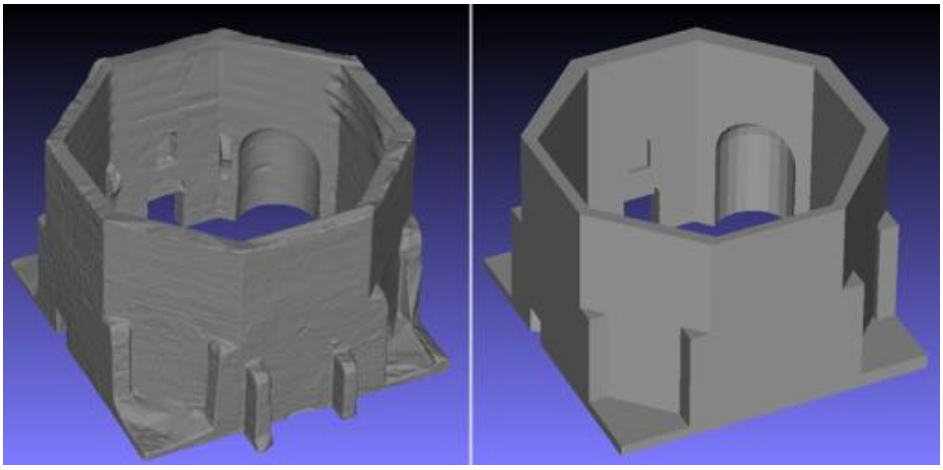

Table 6.15 - The Baptistery in its original model and in the simplified one.

In *Table 6.16* are reported the main differences, as it regards the number of triangles of the mesh and surfaces and the volumes values.

Object	Original model			Simplified model		
	No. triangles	S (m^2)	V (m^3)	No. triangles	S (m^2)	V (m^3)
Bollani Arch	998.000	162,38	66,082	432	142,792	60,027
Baptistery of Aquileia	779.006	1303,51	522,90	644	1255,22	470,307

Table 6.16 - Number of triangles composing the mesh and geometric characteristic (surfaces and volumes) of the original and the simplified models.

Finally last purpose refers to models with lower LoD realized starting from the original 3D solid model, and downstream simplified through processes of decimation. This procedure was widely described in sub paragraph 4.2.7, in the study of the Arch, but it was applied as well to the statue of St. John Baptist and to the Baptistery. Referring to the Arch several models (*Figure 6.17*) were built starting from the best LoD original one, at the end of the experiment it resulted that the ideal decimation is that one that reduces to the 90% the number of triangles (corresponding to 100.000 triangles) (*Table 6.18*). Applying this reduction to the geometry of the model, it resulted still realistic and the results of the structural analysis still very close to the ones obtained on the original model.

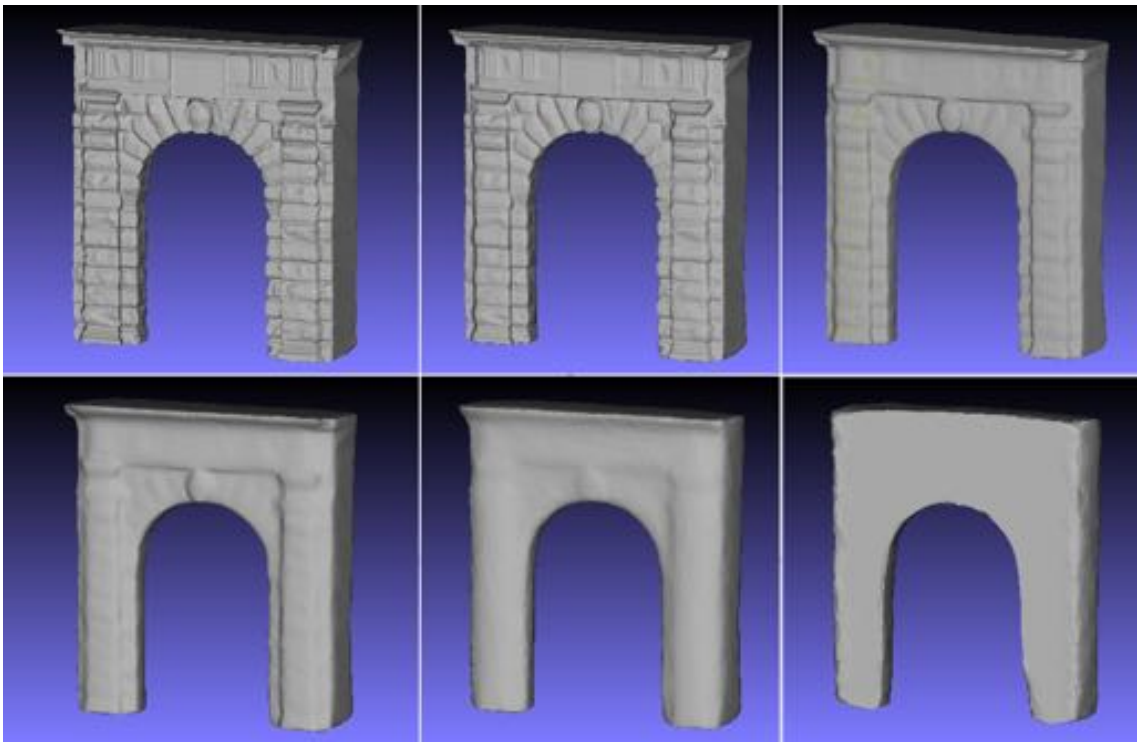

Figure 6.17 – The model of the arch simplified with 500.000 triangles, 200.000 triangles, 100.000 triangles, 50.000 triangles, 20.000 triangles and 10.000 triangles.

Object	Simplification (%)	No. triangles	S (m^2)	V (m^3)
Bollani Arch	0	998.000	162,38	66,082
	50	500.000	157,98	66,059
	80	200.000	151,42	65,716
	90	100.000	144,30	64,866
	95	50.000	138,88	63,793
	98	20.000	131,15	61,271
	99	10.000	120,61	53,919

Figure 6.18 – Values of surface and volume with 500.000 triangles, 200.000 triangles, 100.000 triangles, 50.000 triangles, 20.000 triangles and 10.000 triangles starting from the orignial 998.000 meshes.

Referring to the models of St. John Baptist, even a 97% a level decimation resulted appropriate for keeping a correct geometry (*Figure 6.19 and Table 6.20*) of the object and performing the structural analysis.

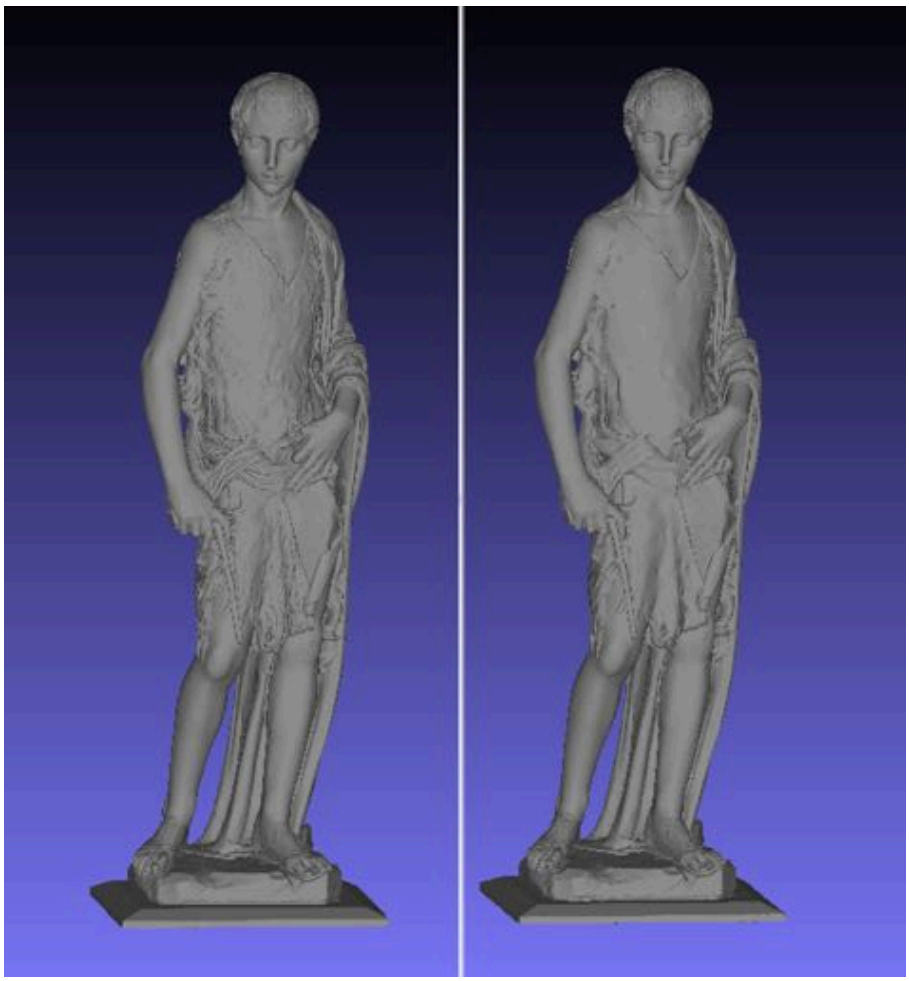

Figure 6.19 – The model of St. John Baptist before and after decimation.

Object	Simplification (%)	No. triangles	S (m^2)	V (m^3)
Statue of St. John Baptist	0	5.178.132	2,39	0,07
	97	157.173	2,38	0,07

Table 6.20 – Values of surface and volume of St. John Baptist model before and after decimation.

To the Baptistery it was sufficient to apply the 87% level of decimation (90%) (*Figure 6.21 and Table 6.22*) in order to have a model suitable for structural analysis.

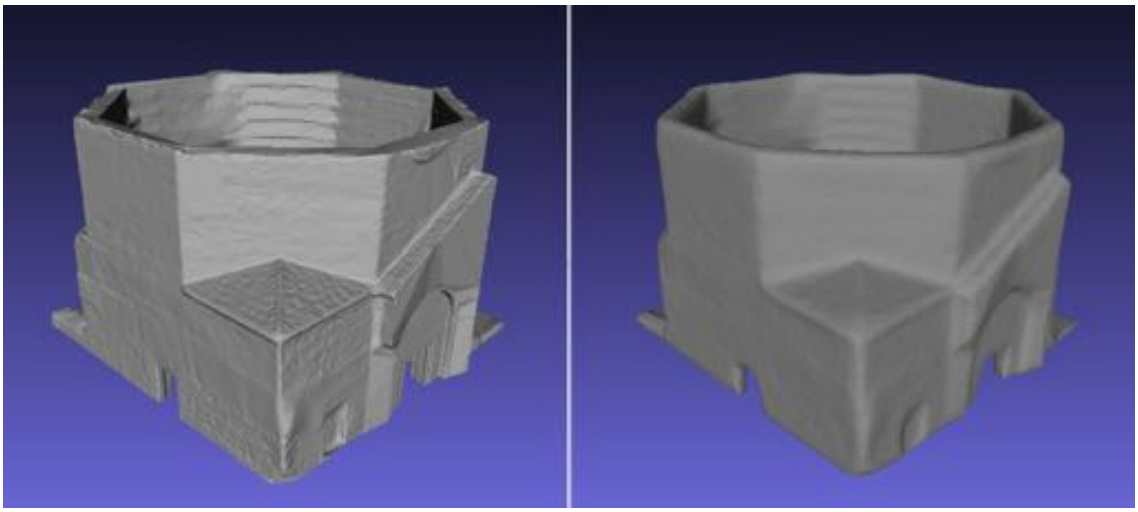

Figure 6.21 – The model of the Baptistery before and after decimation

Object	Simplification (%)	No. triangles	S (m^2)	V (m^3)
Baptistery of Aquileia	0	779.006	1303,51	522,900
	87	100.000	1201,29	509,194

Table 6.22 – Values of surface and volume of Baptistery model before and after decimation.

6.6. Structural analysis and obtained results

Once obtained the 3D solid models, suitable for FEA software, the structural analysis was held by means of the Rhinoceros plug-in Scan-and-Solve. For each model was therefore necessary to define:

- materials;
- restraints;
- forces acting;
- structural LoD.

Referring to the first topic of the list, of course, the characteristics of the materials used, for each object, were different, and therefore are reported in *Table 6.23*. The most resistant are the statue, which are monolithic pieces of marble, while the less resistant is the Baptistery, which is a composite material.

Object	Description	Density (kg/m^3)	Elastic modulus (Pa)	Poisson Ratio	Default failure Criterion	Ultimate tensile Strength (Pa)	Ultimate compressive strength (Pa)
Statue of St. John Baptist	Marble Low density	2370	6,00x10^{10}	0,25	Coulomb Mohr	7,00x10^6	6,89x10^7
Statue of Emperor Claudio	Marble Low density	2370	6,00x10^{10}	0,25	Coulomb Mohr	7,00x10^6	6,89x10^7
Bollani Arch	Brick Stone Composite	2700	2,70x10^9	0,25	Coulomb Mohr	1,72x10^6	7,00x10^6
Baptistery of Aquileia	2Leaves folded masonry	1900	8,70x10^8	0,20	Coulomb Mohr	1,05x10^5	1,40x10^6

Table 6.23 – Material properties for all the models.

Referring to restraints in all cases was adopted a fixed end for the base of the objects. This is a simplification that does not keep in consideration, especially for the Arch and for the Baptistery, the ground elasticity, and the behaviour of foundation. These parameters are anyway another discipline arguments and need also further survey or information, therefore, for testing results on the 3D models obtained the supposed restraints can be considered acceptable. For the case of the Arch and the Baptistery further restraints were assumed in considering other buildings, adopting links in this case.

As it regards the forces acting on the objects, in all the cases, except the statue of St. John Baptist, was considered only the gravity load. In the case of the St. John Baptist was supposed acting on the barycentre also one horizontal force, of the minimum value necessary to start an oscillatory movement, in order to verify if the collapsing is caused by over stresses or over turning.

As it concern the last topic of the previous list, and namely structural LoD, also this argument was studied for the medium size object in sub paragraph 4.2.8. Several model were tested in order to verify which is the most suitable structural LoD in order to preserve the correctness of results without having an excessive computational need. Models were therefore tested with a different numbers of cubes and it resulted that the ideal structural LoD is that one with cube dimensions as much possible similar to the medium dimensions of the geometric details of the object. Therefore the ideal LoD adopted for each object is reported in *Table 6.24*.

Object	Structural LoD adopted	Dimension of cube (mm)
Statue of St. John Baptist	10.000	22
Statue of Emperor Claudio	9.999	34
Bollani Arch	108.000	91
Baptistery of Aquileia	42.800	242

Table 6.24 – Structural LoD adopted for each model.

Once set the parameters above described it was possible to perform the structural analysis. Of course, referring to such different objects, as it concerns dimensions, applied loads and restraints, and even materials characteristic, it is illogical to compare values about resulting stresses and strains. In order to verify if the analysis are congruent to reality, the resulting total displacement of each object is reported in *Table 6.25*, along with the height of the building and the Elastic Module of the material. In order to verify data for the Statue of St. John Baptist, is reported only the value of total displacement due to gravity load.

Object	Height (m)	Elastic modulus (Pa)	Maximum total displacement (mm)
Statue of St. John Baptist	1,63	$6{,}00 \times 10^{10}$	0,01
Statue of Emperor Claudio	2,10	$6{,}00 \times 10^{10}$	0,03
Bollani Arch	8,24	$2{,}70 \times 10^{9}$	0,80
Baptistery of Aquileia	10,92	$8{,}70 \times 10^{8}$	1,56

Table 6.25 – Total displacement for each model, with Elastic modulus adopted and height of the objects.

Results appear to be congruent since the object less high and more stiff is the one with a lower total displacement, while the Baptistery, which is the higher object, but with lower material capability, is the one with a greater total displacement.

Referring to the two statues, it was not possible to compare the results with models obtained through other methodologies since so far, the only way to correctly reproduce shape of this complexity is by mean of Geomatic. The comparison between the models of the Roman statue as it was supposed to be, the original model and the model without the back support allowed understanding the importance of such support reducing nine times such displacement and also how cracks had origin. The main values of displacement are reported in *Table 6.26*. As it is possible to see from values the maximum total displacement is verified if the statue would be deprived of the back support, while in the case of the virtually restored statue, the total displacement is superior to the one of the original model because, as logical, if complete the statue is more heavy.

Object		Maximum total displacement (mm)	Height of most stressed section (cm)
Statue of Emperor Claudio	Original	0,03	45
	Virtually restored	0,08	37
	Without back support	0,28	30

Table 6.26 – Total displacement for the three models of Emperor Claudio and location of the section most stressed.

Referring to the Arch and to the Baptistery it was possible to verify results comparing the values obtained with the Scan-and-Solve analysis of the TLS 3D models to the ones achieved by the classic analysis of LisaFEA 3D simplified models.

Object	Original model		Simplified model		
	Maximum total displacement (mm)	V (m^3)	Maximum total displacement (mm)	V (m^3)	Difference (mm)
Bollani Arch	0,80	66,082	0,78	60,027	0,02
Baptistery of Aquileia	1,56	522,90	1,22	470,307	0,34

Table 6.27 - Total displacement for the original and simplified models of Bollani arch and Baptistery of Aquileia.

Regardings the displacements computed with different LoD models, even if difference is very small, as already specified in chapter 2, from the values of total displacement depends all the subsequence computation of other values of stresses and strain, therefore the correctness of it, even for infinitesimal values, is fundamental for structural analysis computations.

6.7. Conclusions

In this chapter were summarized all the obtained results and the conducted analysis and was performed a comparison among the various examples investigated. Referring to the main purpose of the thesis, and namely defining the contribute of geomatic models to Structural Engineering, it is possible to state that:

- DSM obtained through Geomatics are definitely too much detailed and it is convenient to reduce the geometrical LoD through decimation of the mesh;

- DSM obtained from TLS surveying, if suitably adapted, and transformed in 3D solid models, are directly usable by FEM software;
- in order to structurally analyse small objects, the only method assuring the correct geometry of the model is provided by Geomatic surveying techniques;
- in order to structurally analyse medium and large objects, appear convenient to use 3D solid models obtained from the processing of Geomatic models.

CONCLUSIONS

In my research path, during these three years, I had the opportunity to combine and implement my knowledge in Geomatics and apply them to a fundamental discipline of Engineering, and namely Structural Analysis.

My purpose was to verify if the 3D geometric models, obtained through Geomatics, could find use, not only in the traditional fields of artistic and architectural studies, but also for Structural purposes. It results in fact that, currently, the largest part of geometric data, available from a geomatic surveying, are not considered and 3D structural models are built upon few measures, available also from a direct surveying. This implies that, often, many peculiarities of the analysed objects are not correctly weighted.

The answer to the research effort done is for surely positive, since the advocated meeting point, between models realized through Geomatics and that ones used for Structural Analysis, was found.

The thesis dealt with three different typologies of objects, small, medium and large size, in order to test a common procedure for obtaining a 3D model, adaptable for Structural Analysis software. All the objects were surveyed by means of laser scanners and the sequence of data acquisition, data processing, meshing and meshing refinement, preparatory for achieving the 3D model, were thoroughly described.

To the first size belong two objects: the Statue of Emperor Claudio preserved in Aquileia and the Statue of St. John Baptist preserved in Florence. These two cases were developed differently, because for surveying two distinct systems were used and the output was a point cloud in the first case and already a mesh surface in the second one. The 3D solid models obtained were therefore structurally analysed. A geomatic method, as used in this research, is the only way possible for analysing a statue with its real geometry, since any other simplification adopted would conduct to an unrealistic model. The Level of Detail (LoD) for this typology of objects is definitely the highest: here the correctness of dimensions is crucial for performing properly the structural analysis since, it is obvious, that even small errors would conduct to uncorrected calculation values. As it refers the Statue of Emperor Claudio, beside the model obtained from surveying, also two virtually models were created, in order to verify what could have been the behaviour, of the statue if lacking of some parts, or if virtually restored. As it refers to the Statue of St. John Baptist, it was verified what could be the possible failure cause in presence of a horizontal force applied.

As second case, namely the medium size object, was considered the Bollani Arch in Udine. This one resulted the easiest object to analyse and, therefore, different tests were applied. Beside the methodologies adopted for obtaining the 3D model, the main study was related to the definition of the geometrical and the structural LoD. Several lower detailed geometrical models were generated, starting from the original highest one, decreasing the number of triangles on the mesh, through processes of decimation. The algorithms and the procedures adopted were tested and analysed. At the same time, these models were further diversified adopting different structural LoDs. All these models were then structurally analysed and the results demonstrate

that the correctness of displacements and stresses values depends much more from a realistic geometry than to an extreme structural modeling.

Third case dealt with an entire building and the chosen object was the Baptistery of Aquileia. Even if the geometry and the shape resulted quite regular, if compared to other largest and complex structures, its modelling was a not easy challenge. Beside the 3D model obtained from Geomatics, also another simple 3D model was realized, starting from measure of direct surveying. This last model well represents the standard geometrical LoD adopted generally for Structural Analysis. The two resulting geometries were compared identifying the main differences. Structural Analysis was held with two different software, comparing the obtained results.

At the end the following goals were therefore reached through this research:

- a "standard" procedure was defined for the creation of 3D solid models of objects belonging to cultural heritage, through a pipeline of operations;
- 3D solid models derived from Geomatics and suitable for structural analysis were obtained;
- the LoD necessary for a faithful representation of the objects, and appropriate Structural purposes, was defined;
- Structural Analysis was performed on the obtained models and the results were studied and valued.

Concluding, it can be assumed that correctness, accuracy and precision of geomatic surveying are necessary, and not excessive, in the study of structural behaviour of building and artefacts belonging to cultural heritage.

Some open questions on the current state of the research, and also some possibility or further development, are related to:

- the possibility to introduce different materials on the models, since, so far, only homogeneous objects were considered – this problem was not resolved, but could be implemented through the use of other software and through the collaboration with more specialized researcher of Structural Analysis;
- the opportunity to provide with a modelling of structures with a higher control on constraints conditions and on mechanical behaviour – as in the previous case also this problematic could find a solution creating a link with Structural engineers;
- the chance to provide with a texturing of the objects, in order to acquire, also from images, further information useful for the structural analysis, like the presence of cracks or the framework and the disposition of materials.

I strongly believe that all the models realized for documenting and data recording of cultural heritage could be used also for structural purposes, without throwing away precious data: maybe it is only necessary for Geomatics to promote the obtainable output and make it suitable for Structural Engineering inputs. What I have done is just a small step towards this goal.

BIBLIOGRAPHY

Chapter 1

3DSystem. (2014). *Geomagic*. Based on http://www.geomagic.com/it

Aicardi, I., Boccardo, P., Chiabrando, F., Donadio, E., Lingua, A., Maschio, P., et al. (2014). Rilievo metrico 3D multiscala per l'indagine e la rappresentazione architettonica e ambientale dell'area archeologica di Susa . *Convegno Nazionale ASITA 2014* (p. 27-34). Firenze: ASITA.

Attene, M., Campen, M., & Kobbelt, L. (2013). Polygon mesh repairing: An application perspective. *Journal ACM Computing Survey , 45* (15).

Balzani, M., Callieri, M., Caputo, G., Cignoni, P., Dellepiane, M., Montani, C., et al. Using multiple scanning technologies for the 3d acquisition of torcello's basilica. *In Int. Workshop 3D-ARCH*, (p. 22-24).

Barber, D., & Mills, J. (2011). *3D Laser Scanning for Heritage.* Swindon: English Heritage Publishing.

Bernardini, F., Rushmeier, H., Martin, I., Mittleman, J., & Taubin, G. (2002). Building a Digital Model of Michelangelo's Florentine Pietà. *IEEE Computer Graphics and Applications* , p. 59-67.

Bitelli, G. (2002). Moderne tecniche e strumentazioni per il rilievo dei beni culturali. *Atti 6a Conferenza Nazionale ASITA. IX-XXIV*. Perugia: ASITA.

Bonora, V., & Tucci, G. (2012). New technologies for cultural heritage documentation and conservation: the role of Geomatics. *Iconoarch - I Architectural and Technology International Congress*, (p. 444-451). Konya.

Cignoni, P., Callieri, M., Corsini, M., Dellepiane, M., Ganovelli, F., & Ranzuglia, G. (2008). MeshLab: an Open-Source Mesh Processing Tool . *Eurographics Italian Chapter Conference.* Salerno: V. Scarano, R. De Chiara, and U. Erra (Editors) .

Cioci, A., Spinetti, A., Atzeni, C., Cassani, C., & Lupus, A. (2005). Digital Three-Dimensional Modeling of Heritage by Frequency-Modulated Laser Radar: the case of Donatello's "David". *The 6th International Symposium on Virtual Reality, Archaeology and Cultural Heritage.* Vast: M. Mudge, N. Ryan, R. Scopigno (Editors).

Costantino, D., Angelini, M. G., & Caprino, G. (2010). Laser scanner survey of an archaeological site – Scala di Furno (Lecce, Italy). *ISPRS Commission V, Mid – Term Symposium "Close range image measurements techniques. XXXVIII Part 5.* , p. 178-183. Newcastle upon Tyne, United Kingdom: Editors: Mills, J. P., Barber, D. M., Miller, P.E. and Newton, I.. .

D'Agnano, F., Balletti, C., Guerra, F., & Vernier, P. (2015). Tooteko: a Case Study of Augmented Reality for an Accessible Cultural Heritage. Digitization, 3d Printing and Sensors for an Audio-Tactile Experience . *ISPRS-International Archives of the Photogrammetry, Remote Sensing and Spatial Information Sciences* (1), 207-213.

Erder, C. (1977). The Venice Charter Under Review. Ankara.

First International Congress of Architects and Technicians of Historic Monuments. (1931). The Athens Charter for the Restoration of Historic Monuments. Athens.

Georgopoulos, A., & Charalambos, I. (2004). Photogrammetric and Surveying Methods for the Geometric Recording of Archaeological Monuments . *FIG WORKING WEEK - Workshop - Archaeological Surveys* . Athens: FIG.

Girardeau-Montaut, D. (2015). *CloudCompare*. Based on http://www.cloudcompare.org/

Grün, A., Remondino, F., & Zhang, L. (2004). Photogrammetric Reconstruction of the Great Buddha of Bamiyan, Afghanistan. *The Photogrammetric Record , 19* (107), 177-199.

Guidi, G., Pieraccini, M., Ciofi, S., Damato, V., Beraldin, J. A., & Atzeni, C. (2001). Tridimensional digitizing of Donatello's Maddalena . *Ieee International Conference on Image Processing (ICIP 2001)*, (p. 578-581). Thessaloniki.

Guidi, G., Remondino, F., Russo, M., Menna, F., & Rizzi, A. (2008). 3D Modeling of Large and Complex Site Using Multi-sensor Integration and Multi-resolution Data. *VAST- The 9th International Symposium on Virtual Reality, Archaeology and Cultural Heritage* (p. 85-92). M. Ashley, S. Hermon, A. Proenca, and K. Rodriguez-Echavarria (Editors).

ICOMOS. (2015). *ICOMOS - International Council of Monuments and Sites*. Consulted on November 28, 2015 da www.icomos.org: http://www.icomos.org/

Ioannidis, M. T. (2003). Laser scanning and photogrammetry for the documentation of a large statue-experiences in the combined use. *Proceedings of CIPA XIX International Symposium*, (p. 517-523).

JCGM. (2012). VIM 2012. *International vocabulary of metrology 2012. Basic and general concepts and associated terms* . (J. C. Metrology, A cura di)

Letellier, R. (2007). *Recording, Documentation, and Information Management for the Conservation of Heritage Places - Guiding Principles.* Los Angeles: The Getty Conservation Institute.

Levoy, M., Pulli, K., Curless, B., Rusinkiewicz, S., Koller, D., Pereira, L., et al. (2000). The digital Michelangelo project: 3D scanning of large statues. *Proceedings of the SIGGRAPH '00 - 27th annual conference on Computer graphics and interactive techniques* (p. 131-144). New York: CM Press/Addison-Wesley Publishing Co.

Nobile, A. (2012). I sistemi a Scansione 3D per la documentazione metrica e lo studio diagnostico dei beni culturali. Firenze: Tesi di Dottorato.

Peloso, D. (2005). Tecniche laser scanner per il rilievo dei beni culturali. *Archeologia e Calcolatori , XVI*, 199-224.

Remondino, F., & Rizzi, A. (2010, September). Reality-based 3D documentation of natural and cultural heritage sites—techniques, problems, and examples. *APPLIED GEOMATICS* , 85-100.

Stanford Computer Graphics Laboratory. (1993). 3D Standford Bunny Model. *http://graphics.stanford.edu/data/3Dscanrep/* .

Stathopoulou, E. K., Lerma, J. L., & Georgopoulos, A. (2010). Geometric documentation of the Almoina door of the cathedral of Valencia. *EuroMed2010 - 3rd International Conference*

dedicated on Digital Heritage (p. 60-64). Limassol, Cyprus: M. Ioannides, D. Fellner, A. Georgopoulos, D. Hadjimitsis .

Tucci, G., Nobile, A., & Riemma, M. (2011). The Basilica della Madonna dell'Umiltà in Pistoia: Survey, Analysis and Documentation. *Proceedings of XXIII International CIPA Symposium*, (p. 1-8). Prague, Czech Rep.

UNESCO. (1972). Photogrammetry applied to the survey of Historic Monuments, of Sites and to Archaeology. UNESCO Editions.

UNESCO. (1954). *Unesco Portal*. (U. N. Organization, A cura di) Consulted on November 28, 2015 da http://unesdoc.unesco.org/images/0008/000824/082464mb.pdf#page=66

Visintini, D., Fico, B., & Spangher, A. (2006). Modellazione 3D dell'ambiente urbano mediante integrazione di scansioni laser aeree e terrestri: l'esempio del castello di Gorizia. *Proceedings of the Convegno SIFET 2006.*

Visual Computing Lab - ISTI CNR. (2014, April 02). Based on Meshlab: http://meshlab.sourceforge.net/

Chapter 2

Betti, M., Orlando, M., & Spinelli, P. (2015). La Rocca Strozzi a Campi Bisenzio: Analisi strutturali e proposte di interventi di consolidamento e miglioramento sismico. *Bollettino Ingegneri* (5), 3-24.

Binda, L., Cardani, G., & Saisi, A. (2005). *A classification of structures and masonries for the adequate choice of repair - International RILEM Workshop on Repair Mortars for Historic Masonry*, (p. 20-34). Delft.

Binda, L., Penazzi, D., & Saisi, A. (2003). Historic Masonry Buidings. Necessity of a Classification of Structures and Masonries for the Adequate Chioce of Analytical Models. *VI International Symposium Computer Methods in Structural Masonry* (p. 22-24). Rome: STRUMAS.

Chiarugi, A., Bartoli, G., & Bavetta, F. (1995). La meccanica della cupola. In *La cupola di Santa Maria del Fiore, il cantiere di restauro 1980-1995* (p. 47-62). Rome: Istituto Poligrafico e Zecca dello Stato.

Croci, G., D'Ayala, D., & Liburdi, R. (1995, 11/2). History, observation and mathematical models in the seismic analysis of the Valadier abutment area in the Colosseum. *Annali di Geofisica , XXXVIII* (5-6), p. 957-970.

Freytag, M., Shapiro, V., & Tsukanov, I. (2011, April 16). Finite element analysis in situ. *Finite element in Analysis and Design* , p. 957-969.

Giangreco, E. (2002). *Ingegneria delle strutture - Progettazione strutturale* (Vol. 3). Torino: UTET.

Gugliotta, A. (2002). *Elementi finiti* (Vol. 2). Torino: Otto Editore.

Intact Solutions, Inc. (2014). *Scan-and-Solve for Rhino*. Based on http://www.scan-and-solve.com/

Istruzioni per l'applicazione delle Norme tecniche per le costruzioni di cui al D.M. 14 gennaio 2008 , Circolare n. 617 (Consiglio Superiore dei Lavori Pubblici febbraio 2, 2009).

Linee Guida per la valutazione e riduzione del rischio sismico del patrimonio culturale, prot. n. 92 (Consiglio Superiore dei Lavori Pubblici luglio 23, 2010).

Lourenċo, P. B. (2002, 7 17). Computations on historic masonry structures. *Progress in Structural Engineering and Materials , 4* (3), p. 301-319.

Luft, B., Tsukanov, I., & Shapiro, V. (2008). Geometrically Adaptive Numerical Integration. *Proceedings of 2008 ACM Symposium on Solid and Physical Modeling* (p. 147-157). New York: Stony Brook.

Macchi, G., Ruggeri, G., Eusebio, M., & Moncecchi, M. (1993). Structural Assessment of the Leaning Tower of Pisa. *IABSE reports of the working commissions , 70* (351), p. 401-408.

Marques , R., & Lourenço, P. B. (2011). Possibilities and comparison of structural component models for the seismic assessment of modern unreinforced masonry buildings. . *Computers & Structures , 89* (21), p. 2079-2091.

Mola, F., & Vitaliani, R. (1995). Analysis, diagnosis and preservation of ancient monuments: the St. Mark's Basilica in Venice. In S. a. I. Barcelona, Spain: CIMNE.

Norme tecniche per le costruzioni (Decreto Ministeriale gennaio 14, 2008).

Pinto, P. E., & Franchin, P. (2008). Assessing existing buildings with Eurocode 8 part 3: a discussion with some proposal. *Eurocodes: background and application Workshop.* Brussels.

Quim, F., Lima, A., & Silva, N. (2012). Comparative analysis through semplified methods, plane frames and space frame for design of structural masonry buildings. *15th International Brick and Block Masonty Conference.* Florianopolis, Brazil.

Robert McNeel & Associates. (2014). *Rhinoceros*. Based on https://www.rhino3d.com/it/

Roca, P., Cervera, M., Gariup, G., & Pelà, L. (2010, 7 22). Structural Analysis of Masonry Historical Constructions. Classical and Advanced Approaches . *Archives of Computational Methods in Engineering* (17), p. 299-325.

Smoljanović, H., Živaljić, N., & Nikolić, Ž. (2013, 7 25). Overview of the methods for the modelling of historical masonry structures. *Građevinar , 65*, p. 603-618.

Sonnenhof Holdings. (2013). *Lisa FEA*. Based on http://lisafea.com/

Thrall, M. (2006). *3DWarehouse*. Based on

https://3dwarehouse.sketchup.com/model.html?id=b9ef29089cc807e5293cf63222c527f5

Trimble Navigation. (1999). (©. 2. Limited, Produttore) Tratto il giorno 2015 da SketchUp: http://www.sketchup.com/it

Visintini, D., & Spangher, A. (2013). Rilevamento laser scanning, modello della superficie (DSM) e modello per il metodo agli elementi finiti (FEM) di una struttura . *Atti 17a Conferenza Nazionale ASITA* (p. 1287-1294). Riva del Garda: ASITA.

Chapter 3

Attene, M., Campen, M., & Kobbelt, L. (2013). Polygon mesh repairing: An application perspective. *Journal ACM Computing Survey , 45* (15).

Augusti, G., & Ciampoli, M. (2000). *Vulnerabilità sismica degli oggetti esibiti nei musei: interventi per la sua riduzione.* (D. Liberatore, A cura di) Roma: Tipografia Esagrafica.

Betti, M., Orlando, M., & Spinelli, P. (2015). La Rocca Strozzi a Campi Bisenzio: Analisi strutturali e proposte di interventi di consolidamento e miglioramento sismico. *Bollettino Ingegneri* (5), 3-24.

Binda, L., Cardani, G., & Saisi, A. (2005). *A classification of structures and masonries for the adequate choice of repair - International RILEM Workshop on Repair Mortars for Historic Masonry*, (p. 20-34). Delft.

Binda, L., Penazzi, D., & Saisi, A. (2003). Historic Masonry Buidings. Necessity of a Classification of Structures and Masonries for the Adequate Chioce of Analytical Models. *VI International Symposium Computer Methods in Structural Masonry* (p. 22-24). Rome: STRUMAS.

Borri, A., Falletti, F., Fastellini, G., Grassi, S., Grazini, A., Marchetti, L., et al. (2005). *La stabilità delle grandi statue: il David di Michelangelo.* (A. Borri, A cura di) Roma: DEI s.r.l. Tipografia del Genio Civile.

Croci, G., D'Ayala, D., & Liburdi, R. (1995, 11/2). History, observation and mathematical models in the seismic analysis of the Valadier abutment area in the Colosseum. *Annali di Geofisica , XXXVIII* (5-6), p. 957-970.

De Canio, G. (2012). Marble devices for the Base isolation of the two Bronzes of Riace: a proposal for the David of Michelangelo. *The 15th World Conference on Earthquake Engineering.* Lisboa, Portugal.

De Nicola, Giacomo. (1913). Il San Giovannino Martelli di Donato. *Bollettino d'Arte , VII*, p. 277.

GECO. (2013). *Geomatica e conservazione*. Tratto il giorno 2015 da http://www.geomaticaeconservazione.it/: http://www.geomaticaeconservazione.it/

Giangreco, E. (2002). *Ingegneria delle strutture - Progettazione strutturale* (Vol. 3). Torino: UTET.

Grün, A., Remondino, F., & Zhang, L. (2004). Photogrammetric Reconstruction of the Great Buddha of Bamiyan, Afghanistan. *The Photogrammetric Record , 19* (107), 177-199.

Intact Solutions, LLC. (2009). Scan&Solve: FEA without meshing - White paper.

Istituto Regionale per il Patrimonio Culturale del Friuli Venezia Giulia. (2008). *http://www.sirpac-fvg.org/*. Tratto il giorno 2013 da Sistema informativo regionale del patrimonio culturale : http://46.137.91.31/web/catalogazione/search/SchedaDetail.aspx?TSK=RA&ID=15371&g=5

Istruzioni per l'applicazione delle Norme tecniche per le costruzioni di cui al D.M. 14 gennaio 2008 , Circolare n. 617 (Consiglio Superiore dei Lavori Pubblici febbraio 2, 2009).

Kazhdan, M., Bolitho, M., & Hoppe, H. (2006). Poisson Surface Reconstruction. *Eurographics Symposium on Geometry Processing* (p. 61-70). Aire-la-Ville: Dieter W. Fellner, Werner Hansmann, Werner Purgathofer, François Sillion Series Editors.

Levoy, M., Pulli, K., Curless, B., Rusinkiewicz, S., Koller, D., Pereira, L., et al. (2000). The digital Michelangelo project: 3D scanning of large statues. *Proceedings of the SIGGRAPH '00 -*

27th annual conference on Computer graphics and interactive techniques (p. 131-144). New York: CM Press/Addison-Wesley Publishing Co.

Limoncelli, M. (2012). *Il restauro virtuale in archeologia.* Roma: Carrocci editore.

Linee Guida per la valutazione e riduzione del rischio sismico del patrimonio culturale, prot. n. 92 (Consiglio Superiore dei Lavori Pubblici luglio 23, 2010).

Lolli, A. (2010). Monitoraggio per la diagnostica strutturale del David di Michelangelo. University of Bologna, Italy.

Lourenċo, P. B. (2002, 7 17). Computations on historic masonry structures. *Progress in Structural Engineering and Materials , 4* (3), p. 301-319.

Macchi, G., Ruggeri, G., Eusebio, M., & Moncecchi, M. (1993). Structural Assessment of the Leaning Tower of Pisa. *IABSE reports of the working commissions , 70* (351), p. 401-408.

Ministero dei beni e delle attività culturali e del turismo (MiBACT). (2013). *Museo di Casa Martelli - Firenze*. Tratto il giorno 2015 da museiditalia - musei digitali: http://www.culturaitalia.it/opencms/museid/viewItem.jsp?language=it&case=&id=oai%3Acultu raitalia.it%3Amuseiditalia-mus_8175

Nikon Corporation. (2013). *www.nikon.com*. Tratto il giorno 2014 da Nikon metrology.

Norme tecniche per le costruzioni (Decreto Ministeriale gennaio 14, 2008).

Pascale, G., Bastianini, F., & Carli, R. (2011). Monitoring marble cracking in the David by Michelangelo. (11), 21-24.

Pinto, P. E., & Franchin, P. (2008). Assessing existing buildings with Eurocode 8 part 3: a discussion with some proposal. *Eurocodes: background and application Workshop.* Brussels.

Riccardelli, C., Soultanian, J., Morris, M., Becker, L., Wheeler, G., & Street, R. (2014). The Treatment of Tullio Lombardo's Adam: A New Approach to the Conservation of Monumental Marble Sculpture. *Metropolitan Museum Journal* (49).

Roca, P., Cervera, M., Gariup, G., & Pelà, L. (2010, 7 22). Structural Analysis of Masonry Historical Constructions. Classical and Advanced Approaches . *Archives of Computational Methods in Engineering* (17), p. 299-325.

Santolaria, J., Guillomia, D., Cajac, C., Albajez, J. A., & Aguilar, J. J. (2009). Modeling and Calibration Technique of Laser Triangulation Sensors for Integration in Robot Arms and Articulated Arm Coordinate Measuring Machines. *Sensors , 9*, p. 7374-7396.

Smoljanović, H., Živaljić, N., & Nikolić, Ž. (2013, 7 25). Overview of the methods for the modeling of historical masonry structures. *Građevinar , 65*, p. 603-618.

Sorace, S., & Terenzi, G. (2015). Seismic performance assessment and base-isolated floor protection of statues exhibited in museum halls . *Bull Earthquake Eng* , 1873-1892.

Vasari, G. (1568). *Le vite de' più eccellenti pittori, scultori e architettori.* (M. Marini, A cura di) Roma, Italia: Newton Compton editori s.r.l.

Visintini, D., & Spangher, A. (2013). Rilevamento laser scanning, modello della superficie (DSM) e modello per il metodo agli elementi finiti (FEM) di una struttura . *Atti 17a Conferenza Nazionale ASITA* (p. 1287-1294). Riva del Garda: ASITA.

Chapter 4

Bertolini Cestari, C., Chiabrando, F., Invernizzi, S., Marzi, T., & Spanò, A. (2013). Terrestrial Laser Scanning and settled techniques: a support to detect pathologies and safety conditions of timber structures . *Advanced Materials Research , 778*, p. 350-357.

Cabaleiro, M., Riveiro, B., Arias, P., Caamano, J. C., & Vilan, J. A. (2014). Automatic 3D modeling of metal frame connections from LiDAR data for structural engineering purposes. *ISPRS Journal of Photogrammetry and Remote Sensing* (96), p. 47-56.

Cannella, M. (2015, 1 8-14). Digital Unwrapping and visualization of complex architectural surfaces for the documentation and the restoration. *DisegnareCon* (8).

Chiabrando, F., Donadio, E., Spanò, A., & Sammartano, G. (2015). La tecnologia laser scanning per la valutazione statica delle strutture storiche . *XIX Conferenza Nazionale ASITA* , (p. 253-261).

Di Sivo, M. (2004). *Atlante della pietra.* Torino, Italy: UTET.

Frangipane, A. (2007, 1). Natural stone portals of the town of Udine (Italy): their design, construction and materials between the 15th and 20th centuries. *Geological Society London Special Publication* (27), p. 33-42.

Visintini, D., & Spangher, A. (2013). Rilevamento laser scanning, modello della superficie (DSM) e modello per il metodo agli elementi finiti (FEM) di una struttura . *Atti 17a Conferenza Nazionale ASITA* (p. 1287-1294). Riva del Garda: ASITA.

Chapter 5

Brandt, O. (2009). Il battistero cromaziano. *Atti della XL Settimana di Studi Aquileiesi* (p. 323-375). Editreg.

Castagnetti, C., Bertacchini, E., Capra, A., & Dubbini, M. (2012). Terrestrial laser scanning for preserving cultural heritage: analysis of geometric anomalies for ancient structures. *Proceedings of the FIG Working Week.*

Castellazzi, G., D'Altri, A. M., Bitelli, G., Selvaggi, I., & Lambertini, A. (2015). Castellazzi, G., D'Altri, A. M., Bitelli, G., Selvaggi, I., & Lambertini, A. (2015). From laser scanning to finite element analysis of complex buildings by using a semi-automatic procedure. Sensors, 20, 2. *Sensors* (20), p. 2-20.

Guarnieri, A., Pirotti, F., Pontin, M., & Vettore, A. (2006). 3D Surveying for structural analysis applictions. *3rd IAG/ 12th FIG Symposium.* Baden.

Guerra, F., Balletti, C., Stevanin, C., & Vernier, P. (s.d.). "3D geometric analysis of the façades of gothic buildings in venice: examples of 3D modeling".

Istruzioni per l'applicazione delle Norme tecniche per le costruzioni di cui al D.M. 14 gennaio 2008 , Circolare n. 617 (Consiglio Superiore dei Lavori Pubblici febbraio 2, 2009).

Pieraccini, M., Dei, D., Betti, M., Bartoli, G., Tucci, G., & Guardini, N. (2014). Dynamic identification of historic masonry towers through an expeditious and no-contact approach: Application to the "Torre del Mangia" in Siena (Italy) . *Journal of Cultural Heritage* (15.3), p. 275-284.

Roca, P., & Lourenċo, P. B. (1998). *Experimental and numerical issues in the modeling of the mechanical behaviour of masonry.* Barcelona: CIMNE.

San José, J. I., Fernàndez MartIn, J. J., Pérez Moneo, J. D., Finat, J., & Martinez Rubio, J. (2007). Evaluation of structural damages from 3D Laser Scans. *XXI CIPA International Symposium: Anticipating the Future of the Cultural.* Athens.

Sternberg, H. (2006). Deformation measurements at historical buildings with the help of three-dimensional recording methods and two-dimensional surface evaluations. *3rd IAG/12th FIG Symposium.* Baden.

Tavano, S. (1972). Aquileia cristiana . *Antichità Altoadriatiche* (3).

Trimble Navigation. (1999). (©. 2. Limited, Produttore) Tratto il giorno 2015 da SketchUp: http://www.sketchup.com/it

In this last page of this thesis I want to say thanks to all the ones that made this my work possible.

First, and foremost I have to, and, at the same time, I want to, express my gratitude to professor Domenico Visintini. Beside being my tutor during this three years and the good teacher I already knew, he represented a guide and, at the same time, he have been able to raise my interest for Geomatics and its research, involving me in many activity and making me part of a team.

During these three years I had the opportunity, as well, to meet many people that contributed to make my knowledge growing, sharing their experiences and drawing me inspiration to new questions. I want to thank therefore all the staff of the Geomatics Laboratory for Conservation and Communication of Cultural Heritage of the University of Florence, for the many times they hosted me, and the staff of the Department of Civil, Chemical, Environmental and Materials Engineering of the University of Bologna, for the contribution in the study of the Aquileia Baptistery. I reserve a special thank also to the staff of Scan-and-Solve, and especially to Vadim Shapiro and Michael Freytag, for the licence of the software, for the interest in my research and for answering constantly to all my questions and doubts.

Of course I have to thank my Ph.D colleagues from the University of Bologna, Firenze, Torino and Genova: the constant interchange of data and experience grew as much as our friendship and I hope to keep in touch also in future.

I have to thank as well the Administration of the Municipality of Udine for allowing me to follow the Ph.D. courses and studies and for the flexibility I was granted in terms of job schedule and time off, especially during thesis period.

Finally I want to say thanks to all the ones that stood close to me: my friends for supporting, my family, for transmitting curiosity and thirst for knowledge and of course my husband, for being so patient, understanding and always loving. Thank you Giulio for supporting me everyday.